UNIVERSIDAD DE GRANADA

DEPARTAMENTO DE QUÍMICA INORGÁNICA

PROGRAMA OFICIAL DE DOCTORADO EN QUÍMICA

TESIS DOCTORAL

SÍNTESIS, CARACTERIZACIÓN Y PROPIEDADES DE NUEVOS MATERIALES BASADOS EN POLÍMEROS DE COORDINACIÓN MULTIDIMENSIONALES

ANTONIO JESÚS CALAHORRO CASANOVA

GRANADA, 2013

Editor: Editorial de la Universidad de Granada
Autor: Antonio Jesús Calahorro Casanova
D.L.: 388-2014
ISBN: 978-84-9028-785-9

SÍNTESIS, CARACTERIZACIÓN Y PROPIEDADES DE NUEVOS MATERIALES BASADOS EN POLÍMEROS DE COORDINACIÓN MULTIDIMENSIONALES

Memoria de Tesis Doctoral presentada por
Antonio Jesús Calahorro Casanova para aspirar al
Grado de Doctor por la Universidad de Granada

Fdo. Antonio Jesús Calahorro Casanova

LOS DIRECTORES DE LA TESIS:

Dr. Antonio Rodríguez Diéguez
Prof. Titular de Química Inorgánica
Universidad de Granada

Dra. Elisa Barea Martínez
Prof. Titular de Química Inorgánica
Universidad de Granada

Dr. Duane Choquesillo Lazarte
Investigador Postdoctoral
Instituto Andaluz de Ciencias de la Tierra (CSIC)

El doctorando Antonio Jesús Calahorro y los directores de la tesis Dr. Antonio Rodríguez Diéguez, Dra. Elisa Barea Martínez y Dr. Duane Choquesillo Lazarte, garantizamos, al firmar esta tesis doctoral, que el trabajo ha sido realizado por el doctorando bajo la dirección de los directores de la tesis y hasta donde nuestro conocimiento alcanza, en la realización del trabajo, se han respetado los derechos de otros autores a ser citados, cuando se han utilizado sus resultados o publicaciones.

Granada, 27 de junio de 2013

El Doctorando

Fdo.:Antonio Jesús Calahorro Casanova

Los Directores de la Tesis

Fdo.:Antonio Rodríguez Diéguez.

Profesor Titular de Química Inorgánica de la Universidad de Granada

Fdo.: Elisa Barea Martínez.

Profesora Titular de Química Inorgánica de la Universidad de Granada

Fdo.:Duane Choquesillo Lazarte.

Investigador Postdoctoral
Instituto Andaluz de Ciencias de la Tierra (CSIC)

A mi Abuelo

CONTENIDO Y ESTRUCTURA DE LA TESIS DOCTORAL

CONTENIDO Y ESTRUCTURA DE LA TESIS DOCTORAL

En esta Tesis Doctoral se estudia la síntesis y caracterización, así como las diferentes propiedades que presentan nuevos Metal-Organic Frameworks (MOFs) sintetizados mediante diferentes técnicas, principalmente métodos solvotermales, utilizando ligandos nitrogenados que posean grupos carboxilato. Los resultados experimentales obtenidos y la discusión de los mismos se presentan en esta Memoria divididos en 10 Capítulos.

En el **primer capítulo** se revisan los conceptos básicos del tema de investigación en el que se ha trabajado en la Tesis Doctoral, y la motivación del mismo en el contexto actual. Inicialmente, se describen las principales características estructurales de los Metal-Organic Frameworks, clases de redes existentes y algunas de las técnicas más relevantes con las que se suelen sintetizar estos materiales. Posteriormente se abordan las principales aplicaciones de los MOFs en el contexto de esta Tesis, mostrando algunos de los materiales más representativos que se han desarrollado con esos objetivos. Finalmente, se concluirá el capítulo con los objetivos que se han pretendido alcanzar en esta Tesis Doctoral.

En el **segundo capítulo** se muestra la estructura cristalina de un polímero de coordinación bidimensional de cadmio, de fórmula $[CdCl_2(PymNH_2)]$, sintetizado mediante técnicas solvotermales, empleando el ligando 2-aminopirimidina y cloruro de cadmio como reactivos precursores. Debido a la aromaticidad que presenta este ligando se han estudiado sus propiedades luminiscentes determinando tanto la longitud de onda de excitación como de emisión, así como sus tiempos de vida media.

En el **tercer capítulo** se desarrolla la síntesis de un nuevo MOF tridimensional de lantano y oxalato, formado como producto de la oxidación y descomposición del ligando 2-cianopirimidina, en el seno de una reacción hidrotermal a elevada temperatura. El hecho de generarse *in situ* en el seno de la reacción hidrotermal conlleva la formación de una estructura totalmente nueva y distinta a todas aquellas que existen en bibliografía. Al tratarse de una red tridimensional que presenta canales en las tres direcciones del espacio se estudió su capacidad de adsorción, así como de las propiedades luminiscentes del mismo.

En el **cuarto capítulo** se muestra la estructura cristalina del primer MOF tridimensional de cadmio compuesto por el ligando 4'-tetrazolato-4-bifenil carboxilato, $(TBPC)^{2-}$, ligando que ha sido sintetizado *in situ* en el seno de la reacción solvotermal basándose en la reacción de Demko para síntesis de tetrazoles a partir de los derivados cianurados. Además de la síntesis y la descripción estructural, se

han estudiado las propiedades luminiscentes que presenta dicho compuesto debido al más que prometedor comportamiento que ha de presentar por la extensa aromaticidad del linker orgánico empleado en la construcción de la red cristalina.

En el **quinto capítulo** se presentan dos novedosos MOFs de zinc, de fórmula $[Zn(1,3\text{-tzbaa})]_n$ y $[Zn(1,4\text{-tzbaa})]_n$ formados por dos ligandos generados por primera vez *in situ* en el seno de la reacción hidrotermal. Dichos ligandos, ácido 3-tetrazolatofenil acético y 4-tetrazolatofenil acético, poseen un grupo tetrazolato y un grupo carboxilato que favorecerán la formación de enlaces de coordinación a los centros metálicos. En estos casos se trata de estructuras tridimensionales muy complejas que presentan pequeñas cavidades en la dirección del eje *c* y *b*, respectivamente. Debido a la elevada conjugación del anillo bencénico con el grupo tetrazolato del ligando se han realizado estudios de la capacidad luminiscente de estos compuestos en estado sólido.

En el **sexto capítulo** aparece recogida la síntesis, caracterización y estudio de las propiedades de tres nuevos compuestos de cadmio con el ligando 4-piridintetrazolato y tres ligandos auxiliares diferentes de tipo carboxilato. En estos casos, el ligando de tipo tetrazolato se ha obtenido de dos formas, *in situ* en el seno de la reacción hidrotermal y partiendo de la sal sódica del mismo. A nivel sintético cabe resaltar que estos compuestos de fórmula $[Cd_2(ptz)(squarate)(OH)(H_2O)_2]_n$; $\{[Cd_2(ptz)(4\text{-carboxypyridine})(OH)_2]\cdot(H_2O)_2\}_n$ y $\{[Cd_5(ptz)_2(terephtalate)_4(H_2O)_2]\cdot(H_2O)_2\cdot(CH_3OH)_4\}_n$ han sido obtenidos mediante métodos solvotermales, destacando que en el segundo caso los ligandos han sido obtenido *in situ* durante reacción hidrotermal. Estos compuestos son MOFs tridimensionales que muestran unos canales en la dirección de los ejes *b, b* y a, respectivamente, por lo que se han llevado a cabo simulaciones moleculares para comprobar la capacidad de adsorción de estos compuestos, y realizar las pertinentes medidas experimentales. Además, debido a la elevada conjugación existente en los ligandos que forman estos compuestos, cabe esperar propiedades luminiscentes interesantes para estos tres materiales de cadmio.

En el **séptimo capítulo** se exponen dos nuevos MOFs tridimensionales de cadmio y cobalto, obtenidos mediante síntesis hidrotermal del ligando ácido 5-bromonicotínico con los respectivos cloruros metálicos y utilizando agua como disolvente. Estos materiales, de fórmula $[Cd(5\text{-BrNic})_2]_n$ y $[Co(5\text{-BrNic})_2(H_2O)]_n$, poseen canales en las direcciones de los ejes *c* de sus respectivas celdillas, de manera que se estudiaron las capacidades de adsorción de estos sistemas. Para ello se realizaron simulaciones moleculares de tipo Monte Carlo que nos dieron información sobre la distribución de tamaño de poro y la superficie accesible de estos materiales, así como de las isotermas de adsorción de distintos moléculas gaseosas, como H_2 y CH_4. Estos datos teóricos se corroboraron mediante las medidas

experimentales de las isotermas de adsorción. Además, debido a los puentes carboxilato existentes entre los centros metálicos en la estructura cristalina de cobalto, se realizaron medidas de susceptibilidad magnética frente a la temperatura para estudiar las propiedades magnéticas que presenta este compuesto de coordinación.

En el **octavo capítulo** se muestra la síntesis y el estudio de las propiedades magnéticas y luminiscentes de tres nuevos MOFs de cadmio, cobalto y zinc constituidos por el ligando ácido 5-(1H-tetrazol-5-il)isoftálico, obtenido mediante la cicloadición [2+3] del ligando cianurado en el seno de la reacción solvotermal. Los compuestos, $\{[Cd_4(TZI)_2(OH)_2(H_2O)_4](H_2O)_6\}_n$, $\{[Zn_2(TZI)(OH)(H_2O)_2](H_2O)\}_n$ y $\{[Co_8(TZI)_3(OH)_5((N_3)_2(H_2O)_8](H_2O)_8\}_n$, son estructuras tridimensionales en las que el ligando de tipo dicarboxi-tetrazolato exhibe distintos y nuevos modos de coordinación distintos a los conocidos hasta el momento en función del centro metálico al que se coordine. Debido a la elevada aromaticidad del ligando es de esperar que estos compuestos muestren unas propiedades luminiscentes muy interesantes para los compuestos de cadmio y zinc. Asimismo, para el compuesto de cobalto se estudiarán sus propiedades magnéticas debido a los múltiples puentes entre centros metálicos existentes en la estructura, resaltando especialmente la presencia de un triple puente azida-carboxilato-tetrazolato existente en algunos dímeros de cobalto. Cabe resaltar que, en química de la coordinación, es la primera vez que se observa dicho triple puente así como la existencia de una subunidad octanuclear de cobalto que conforma el MOF tridimensional.

En el **noveno capítulo** se aborda la síntesis y caracterización de un nuevo ligando orgánico de esqueleto dibenceno-tetrazínico (ácido 3,3'-(1,2,4,5-tetrazina-3,6-diil)dibenzoico). La caracterización se ha llevado a cabo mediante ^{1}H-RMN, ^{13}C-RMN, Análisis Elemental, Espectroscopia de Infrarrojo y Difracción de Rayos-X de monocristal. Se ha evaluado la citotoxicidad de este nuevo ligando mediante la exposición a células HEK293 en distintas concentraciones y periodos de incubación con el objetivo de utilizar dicho linker en la construcción de bio-MOFs para la liberación controlada de fármacos con aplicación biomédica. Además se presenta la síntesis y caracterización estructural de los primeros polímeros de coordinación con este ligando, $[Zn(dbtz)(H_2O)]_n$, y $\{[La_2(dbtz)_3(H_2O)_2](H_2O)_6\}_n$. Se han estudiado las propiedades luminiscentes de estos MOFs multidimensionales ya que son unos excelentes candidatos para mostrar fluorescencia en estado sólido debido a la extendida aromaticidad que presenta el ligando ácido 3,3'-(1,2,4,5-tetrazina-3,6-diil)dibenzoico.

En el **décimo capítulo** se expone un nuevo MOF tridimensional de cobre obtenido mediante síntesis convencional de fórmula $[Cu_2(glu)_2(\mu\text{-bpp})]\cdot 2H_2O$ formado por dímeros de cobre que se enlazan a través de los ligandos ácido

glutárico y 1,3-bis(4-piridil)propano para dar lugar a una red tridimensional con forma de panal de abeja con canales en la dirección del eje *c*, en cuyo interior se alojan moléculas de agua de cristalización. Para este material se han realizado simulaciones moleculares de tipo Monte Carlo que dieron información sobre la distribución de tamaño de poro y la superficie accesible de estos materiales, así como de las isotermas de adsorción de distintos moléculas gaseosas, como H_2, CO_2 y CH_4. Estos datos teóricos se corroboraron mediante las medidas experimentales de las isotermas de adsorción elucidando que este nuevo material es no poroso a metano mientras que es capaz de adsorber CO_2 mostrando una isoterma de tipo III no vista hasta el momento en compuestos microporosos. Además, se ha comparado este nuevo MOF con otro existente en biliografía, $[\{Cu_2(glu)_2(\mu\text{-bpp})\}\cdot(C_3H_6O)]_n$, que presenta una diferentes propiedades de adsorción de gases debido, fundamentalmente, al distinto empaquetamiento del ligando piridínico en la red tridimensional. Además, se han realizado estudios de difracción de rayos-X de monocristal en presión con el objetivo de estudiar y esclarecer el mecanismo de acción de dicho polímero corroborando la flexibilidad de dicha red.

Finalmente, en el **capítulo de conclusiones** se muestran las principales aportaciones que se han conseguido con estas líneas de investigación, y sus perspectivas futuras.

Los resultados del trabajo de investigación realizado durante el desarrollo de esta Tesis Doctoral se recogen en los siguientes artículos publicados que, aparecen ordenados cronológicamente según la fecha de publicación:

- Salinas-Castillo, Alfonso; Calahorro, A. J.; Choquesillo-Lazarte, Duane; Seco, Jose M.; Rodriguez-Dieguez, Antonio (2011). *A new 2D cadmium chloride network with 2-aminopyrimidine displaying long lifetime photoluminescence emission.* Polyhedron. 30. 1295-1298.

- Antonio J. Calahorro, Marta E. López-Viseras, Alfonso Salinas-Castillo, David Fairen-Jimenez, Enrique Colacio, Joan Cano and Antonio Rodríguez-Diéguez *(2012) Novel metal–organic frameworks based on 5-bromonicotinic acid: Multifunctional materials with H 2 purification capabilities.* Crystal Engeneering Communication 14. 6390-6393.

- A. J. Calahorro, Antonio Peñas-Sanjuan, Manuel Melguizo, David Fairen-Jimenez, Guillermo Zaragoza, Belén Fernández, Alfonso Salinas-Castillo and A. Rodríguez-Diéguez. (2013) *First Examples of Metal–Organic Frameworks with the Novel 3,3′-(1,2,4,5-Tetrazine-3,6-diyl)dibenzoic Spacer. Luminescence and Adsorption Properties.* Inorganic Chemistry 52. 546-548.

- Antonio J. Calahorro, David Fairen-Jiménez, Alfonso Salinas-Castillo, Marta E. López-Viseras, Antonio Rodríguez-Diéguez.(2013) *Novel 3D lanthanum oxalate metal-organic-framework: Synthetic, structural, luminescence and adsorption properties.* Crystal Engeneering Communication 52. 315-320.

- Antonio J. Calahorro, Alfonso Salinas-Castillo, José Manuel Seco, Javier Zuñiga, Enrique Colacio and Antonio Rodríguez-Diéguez. (2013) *Luminescence and Magnetic Properties of Three Metal-Organic Frameworks Based on 5-(1H-Tetrazol-5-yl)Isophthalic Acid Ligand.* DOI: 10.1039/C3CE40869H.

Además de estos, también se han incluido otros resultados procedentes de artículos que se encuentran en fase de revisión por las revistas a las que han sido enviadas. Estos artículos son los siguientes:

- Antonio J. Calahorro, Guillermo Zaragoza, Alfonso Salinas-Castillo, Jose M. Seco and Antonio Rodríguez-Diéguez. (2013) *Unique Metal-Organic-Framework with Based on 4'-Tetrazolate-4-Biphenyl Carboxylate Spacer: Blue-Green Photoluminescence.* Enviado a European Journal of Inorganic Chemistry

- Antonio J. Calahorro, Alfonso Salinas-Castillo, David Fairen-Jimenez, Jose M. Seco, Claudio Mendicute-Fierro, Santiago Gómez-Ruiz, Marta E. López-Viseras and Antonio Rodríguez-Diéguez. (2013) *Blue-green long lifetime photoluminescence emission of 3D cadmium metal-organic frameworks Based on the 5-(4-pyridyl)tetrazole ligand* Enviado a European Journal of Inorganic Chemistry

- Antonio J. Calahorro, Piero Macchi, Alfonso Salinas-Castillo and Antonio Rodríguez-Diéguez (2013) *Blue-Green Photoluminescence of the First Examples of Metal-Organic-Frameworks with Two Novel Tetrazolatephenyl Acetic Acid Derivatives.* Enviado a Dalton Transactions

- José M. Seco, David Fairen-Jimenez, Antonio J. Calahorro, Laura Méndez-Liñán, Manuel Pérez-Mendoza, Nicola Casati, Enrique Colacio and Antonio Rodríguez-Diéguez. (2013*) Modular Structure of a Microporous MOF based on Cu2 paddle-wheels with high CO_2 Selectivity* Enviado a Chemical Communications


CAROLVS·RO·IMP·SEMPER·AVG·HISPANN·REX·FUNDATOR·VNIVERSITATIS·GRANATENSIS

ÍNDICE

ÍNDICE

CAPÍTULO 1.

INTRODUCCIÓN

1.1. VISIÓN GENERAL

La Química de Coordinación constituye uno de los campos más importantes de la Química Inorgánica. Este área tiene como objetivo el estudio de los compuestos (moléculas neutras o iones) en los que un grupo de moléculas, átomos o iones denominados ligandos se enlazan a un ion o átomo central que, generalmente, es un metal. Esta definición es muy amplia e incluye un gran número de sustancias tradicionalmente no consideradas como complejos.

Con el paso del tiempo, la Química de la Coordinación ha ido evolucionando en el desarrollo de su campo teórico, en los métodos de síntesis y, más importante aún, en el campo de las aplicaciones de estos compuestos.

Durante las últimas décadas, dentro de este área, se han desarrollado una gran variedad de compuestos englobados en el término polímero de coordinación. La primera vez que se usó el término polímero fue en el año 1833 cuando J.J. Berzelius definió polímero como cualquier compuesto que pudiera ser descrito como múltiples unidades de un *building block* básico.[1] Años después, en el año 1916,[2] se empleó el término polímero de coordinación para describir dímeros y trímeros de cobalto (II), y, así, fue empleado continuamente por los científicos, llegando a publicarse la primera revisión bibliográfica en 1964.[3]

Posteriormente, en la década de los 90 surgen con fuerza, debido al interés en estos materiales y sus aplicaciones, dos conceptos muy empleados y utilizados hasta la actualidad: Polímeros de Coordinación (PCs) y Redes Metalorgánicas (del inglés, Metal-Organic Frameworks, MOFs), siendo el investigador O. M. Yaghi el primero en emplear el término MOF en el año 1995 al conseguir sintetizar un compuesto tridimensional de cobre[4] formado por redes interpenetradas de fórmula $Cu(4,4'\text{-bpy})_{1.5}NO_3(H_2O)_{1.25}$.

La coexistencia de estos términos ha supuesto bastantes discusiones entre la comunidad científica, puesto que algunos autores defendían su similitud y otros consideraban que no eran lo mismo. Tanto es así que, en el año 2009, la IUPAC encargó un proyecto titulado *Polímeros de Coordinación y Metal-Organic Frameworks: terminología y nomenclatura*, con el fin de esclarecer esa cuestión.[5] Como resultado de este proyecto, el 30 de abril de 2013 la IUPAC publicó la recomendación provisional[5c] en la que se considera que los Polímeros de Coordinación son aquellos compuestos de coordinación que se extienden en 1, 2 ó 3 dimensiones a través de enlaces de coordinación. Asimismo, se define Red de Coordinación como un compuesto de coordinación que se extiende, en 1 dimensión, pero con entrecruzamiento con dos o más cadenas individuales, bucles, o enlaces en

espiral o bien como un compuesto de coordinación que se extiende en 2 ó 3 dimensiones a través de enlaces de coordinación. El término Red Metalorgánica se reserva para los Polímeros de Coordinación o Redes de Coordinación que poseen un esqueleto abierto que contiene potencialmente huecos. También, se acepta el uso de otros términos cuando se quiere enfatizar alguna característica concreta del polímero de coordinación o de la red metalorgánica en cuestión. Este es el caso de "Polímero de Coordinación Poroso" (PCP) (especifica el hecho de que el PC sea un material poroso), "dia-MOF" (indica el tipo de topología de la red, en este caso, de tipo diamante) o "MOF-carboxilato" (destaca los constituyentes). En el esquema 1.1, se puede ver una clasificación estructurada de la definición y nomenclatura de los diversos compuestos de coordinación que nos podemos encontrar surgida de ese proyecto.

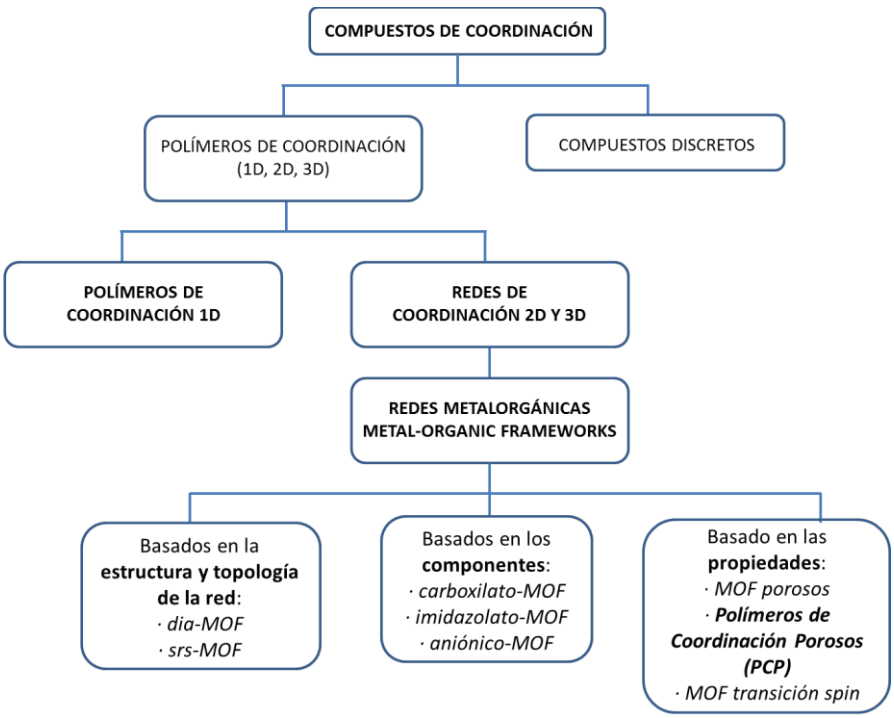

Esquema 1.1. *Esquema de la nomenclatura de los polímeros de coordinación y de las redes metalorgánicas según las recomendaciones de la IUPAC. Los códigos de tres letras indican la topología de la red tridimensional, basándose en el artículo de O'Keeffe y col.*[6] *(dia-MOF hace referencia a redes de tipo diamante y srs-MOF hace referencia a redes triplemente conectadas)-*

Como se ha mencionado anteriormente, el interés despertado por estos materiales se debe a sus múltiples aplicaciones en campos tan diferentes, como en el almacenamiento,[7] separación y purificación de gases,[8] catálisis heterogénea,[9] biomedicina,[10] y/o nanomateriales.[11] Estos sistemas poseen algunas características que mejoran las propiedades que presentan los materiales inorgánicos porosos clásicos (carbones activos y zeolitas), tales como: *i)* estructuras porosas bien ordenadas que muestran comportamientos dinámicos y flexibles en respuesta a moléculas huésped;[12] *ii)* el carácter funcionalizable de la superficie de los poros, lo que origina propiedades catalíticas selectivas[13] y *iii)* un esqueleto estructural que, al igual que en sólidos densos, es responsable de propiedades magnéticas, eléctricas y ópticas.[14,15] Debe destacarse que el desarrollo de este campo de investigación se ha intensificado en los últimos años, lo que se refleja en el número de publicaciones de carácter científico que cada año salen a la luz. En la figura 1.1, se observa que el número de publicaciones crece de manera exponencial, corroborando el interés de la comunidad científica por estos materiales.

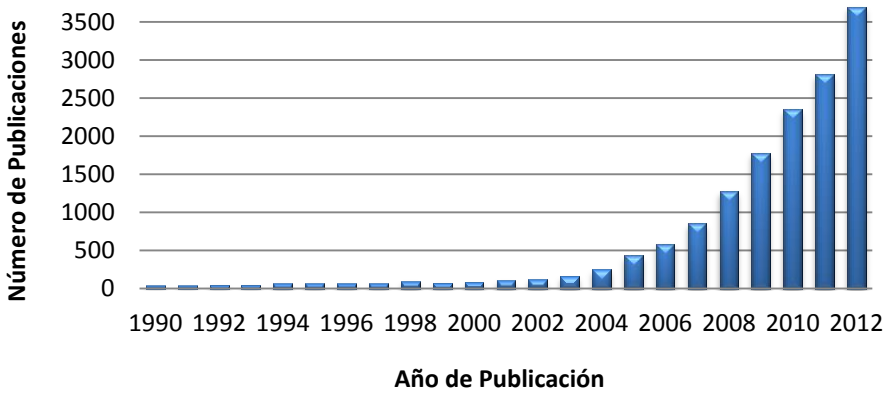

Figura 1.1. *Número de artículos publicados en los últimos años que contienen el concepto Metal-Organic Framework. Fuente: SciFinder Database.*

1.2. DISEÑO Y SÍNTESIS DE MOFS

1.2.1. LIGANDOS ORGÁNICOS. BUILDING BLOCKS

El diseño de estos materiales dependerá de la elección de los centros metálicos y de los ligandos orgánicos conectores.[16]

En relación a los centros metálicos, los iones más empleados suelen ser los metales de transición debido a su versatilidad. Dependiendo de su estado de oxidación, el número de coordinación puede variar entre 2 y 6, dando lugar a diferentes geometría de coordinación posibles: lineal, en forma de Y o T, tetraédrica, plano cuadrada, pirámide de base cuadrada, bipirámide trigonal, octaédrica, prisma trigonal, y sus correspondientes formas distorsionadas. También, se emplean frecuentemente iones lantánidos, que poseen un número de coordinación más elevado, entre 7 y 11, generando nuevas e inusuales topologías en las redes cristalinas. Además, los iones lantánidos dan lugar fácilmente a la formación de centros de coordinación insaturados, es decir, que poseen posiciones de coordinación libres que pueden ser ocupadas por ligandos orgánicos o por otras moléculas de disolvente.

Los espaciadores orgánicos que se pueden emplear como ligandos son muy variados. Estos ligandos pueden ser simples, como haluros, aniones CN^- o SCN^-, y otros más complejos y de mayor tamaño que posean grupos carboxilatos o azolato, entre otros. De la misma manera que con los metales, los ligandos empleados también van a condicionar la topología final de la red cristalina. Por ejemplo, para ligandos lineales, como la 4,4'-bipiridina, la topología de la red la marcará el entorno de coordinación y geometría del ion metálico, pero si se trata de otro tipo de ligandos más complejos, la topología resultante será una combinación de la geometría del metal y del ligando.

Por lo tanto, la combinación de centros metálicos y de ligandos orgánicos es infinita lo que proporcionará una gran diversidad de redes con propiedades físico-químicas diferentes. Debe destacarse que la estabilidad térmica/química del MOF resultante dependerá fundamentalmente de la robustez de los enlaces de coordinación entre los iones metálicos y los ligandos orgánicos que la forman. Normalmente, los enlaces de coordinación de tipo M-O (metal de transición-ligandos de tipo carboxilato) dan lugar a MOFs menos estables térmica y, sobre todo, químicamente que aquellos basados en enlaces de coordinación más robustos M-N (metal de transición-ligandos de tipo azolato). En este sentido, se han descrito MOFs altamente sensibles a la hidrólisis incluso en presencia de humedad ambiental, como por ejemplo el MOF-5,[17] así como otros que han mostrado tener una elevada estabilidad tanto térmica como química incluso en condiciones químicas extremas (disolventes orgánicos a reflujo, agua, disoluciones ácidas o básicas, etc.).

Este es el caso del ZIF-11,[18] un material de la familia de los ZIF (estructuras de tipo zeolítico formadas por metales Zn(II) y Co(II) y con ligandos de tipo imidazol) en este formado por Zn(II) y fenilimidazol. Para comprobar su estabilidad química y térmica, este material es sometido a distintos disolventes y a diferentes temperaturas, comprobando mediante difracción de rayos X en polvo (DRXP) si la

estructura se ha visto afectada. En la figura 1.2 se representa los difractogramas en polvo de la muestra cuando se somete a MeOH a 65° durante distintos periodos de tiempo, corroborando la estabilidad química de la estructura También, mediante un análisis termogravimétrico se comprobó la estabilidad térmica de este material, observando una pérdida de peso del 22.8% desde temperatura ambiente hasta 250°, correspondiente a moléculas de dietilformamida (DEF) alojadas en los poros, manteniéndose estable hasta 550° aproximadamente.

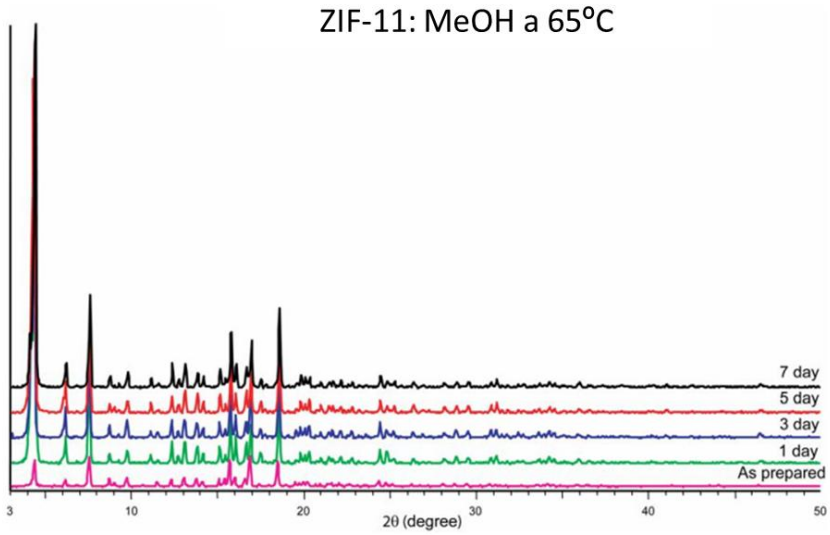

Figura 1.2. *Difractogramas en polvo del ZIF-11 en MeOH a 65°.*

1.2.2. CONDICIONES DE SÍNTESIS

Cuando el investigador se enfrenta al desafío de sintetizar nuevos MOFs, son muchas las variables o parámetros experimentales que ha de tener en cuenta y controlar para obtener el resultado deseado. La modificación en alguno de estos parámetros puede tener una influencia decisiva en la arquitectura del nuevo material. Estos parámetros se pueden dividir en dos tipos: procedimentales y químicos.

Procedimentales

- **Método de síntesis**: existe una amplia variedad de metodologías sintéticas para obtener los MOFs, que van desde la síntesis convencional

hasta métodos que emplean reacciones solvotermales en reactores de teflón, síntesis asistida por microondas, en estado sólido o síntesis electro- y mecanoquímica.

- **Temperatura**: el rango de temperatura dependerá del tipo de método que se emplee en la síntesis de estos materiales. Se pueden emplear temperaturas tan bajas como la del nitrógeno líquido hasta temperaturas de varios cientos de grados, aunque el límite de temperatura lo marca la temperatura de descomposición del ligando. El hecho de que algunas reacciones se realicen en autoclaves (ej. reacciones solvotermales) se debe a que la temperatura junto con la presión autógena generada por el disolvente hacen que se alcancen condiciones, en algunos casos supercríticas, en las que se favorece la disolución de los reactivos.

- **Tiempo de reacción**: Los tiempos de reacción pueden ser desde muy cortos (pocos minutos o pocas horas) hasta tiempos muy largos (varios días o incluso semanas).

-

Químicos

- **Concentración de reactivos**: la relación entre el metal y el ligando, así como la dilución de la mezcla con el disolvente debe ser controlada. En algunos casos, se pueden obtener diferentes materiales solamente cambiando la concentración de los reactivos.

- **Sales metálicas**: existe un amplio abanico de sales metálicas que se pueden emplear: cloruros, nitratos, sulfatos, percloratos, acetatos, bromuros, óxidos, etc. Normalmente, se usan sales de aquellos aniones que presenten menos capacidad coordinante para favorecer el desarrollo de estructuras poliméricas. Además, se debe de tener en cuenta que algunos aniones pueden influir en el pH del medio, como por ejemplo el acetato.

- **Disolvente**: Se suelen emplear disolventes orgánicos (etanol, metanol, acetonitrilo, etc.) y agua, para sintetizar los MOFs. El uso de disolventes con un alto punto de ebullición (DMSO, DMF,…) es bastante común ya a que a menudo se necesitan altas temperaturas para romper y formar enlaces en la estructura. Además de los disolventes puros, se suelen emplear mezclas de los mismos para favorecer la cristalización del material. En cualquier caso, es deseable el empleo de disolventes respetuosos con el medio ambiente.

- **pH**: la variación de pH de una reacción nos permite controlar la desprotonación parcial o total de los ligandos orgánicos empleados. Además, a veces se puede añadir ácido o base para modular la cinética del proceso.

1.2.3. TÉCNICAS EMPLEADAS EN LA FORMACIÓN DE MOFS

Como se ha desarrollado anteriormente, existen un gran número de técnicas y métodos para conseguir con éxito la síntesis de nuevos materiales multidimensionales. Tradicionalmente, se han empleado y siguen empleando métodos convencionales en los que las especies de partida se disolvían en un disolvente y se obtenía el compuesto deseado como fruto de la reacción entre los reactivos puestos en juego. Cada vez más, se han ido utilizando otras técnicas que permiten solventar ciertos problemas que los métodos convencionales presentan, tales como la insolubilidad de algunas especies o la formación de compuestos secundarios no deseados. Estos nuevos métodos solucionan, a veces, estos problemas permitiéndonos alcanzar la formación de nuevos materiales. Algunas de estas técnicas cada vez más empleadas en la síntesis de MOFs son los métodos solvotermales,[7b,19] sonoquímicos,[20] mecanoquímicos[21] y la síntesis en microondas.[7b,22]

1.2.3.1. Métodos Solvotermales

Sin duda alguna, la técnica más empleada en la síntesis de MOFs son los **métodos solvotermales** que han sido utilizados en gran medida en esta Tesis Doctoral (véase 8 de los 10 capítulos de los que consta esta Tesis Doctoral). Estos métodos permiten obtener estructuras poliméricas que mediante métodos convencionales serían casi imposibles de lograr, debido a las condiciones de presión-temperatura que sólo se alcanzan en las síntesis de este tipo.[23] La síntesis solvotermal se podría definir como un método de síntesis de materiales en el que una disolución se calienta por encima de su punto de ebullición, generando una presión superior a la atmosférica. Cuando el disolvente empleado es agua, esta técnica recibe el nombre de síntesis hidrotermal.

Esta técnica se ha empleado durante muchos años en la síntesis de compuestos inorgánicos, tanto así que ya se empleaba en los años 30 para sintetizar algunos materiales de cobre y calcio,[24] aunque fue hace dos décadas cuando se empezaron a emplear para la síntesis de MOFs

En estos métodos, el crecimiento cristalino se lleva a cabo en una autoclave que, normalmente, está compuesta por un vaso de teflón, capaz de soportar las altas presiones y temperaturas de reacción, y un reactor de acero que contiene dicho vaso (Figura 1.3). La temperatura máxima aconsejada de utilización continua del vaso de teflón es de unos 250 °C. En el caso de tener que utilizar temperaturas superiores, se recomienda emplear otras metodologías. Otro aspecto importante que se debe tener en cuenta en este tipo de síntesis es controlar si la temperatura y la presión autógena generada por el disolvente sobrepasa o no el denominado punto supercrítico (374.1 °C y 218.3 atm para el agua). Por encima de dicho punto, el disolvente se encontrará en condiciones supercríticas y el aumento de la presión con la temperatura será exponencial. En general, la síntesis solvotermal en condiciones subcríticas dará lugar a sólidos con estructuras más abiertas (tipo zeolitas), mientras que en condiciones supercríticas, el gran aumento de la presión producirá estructuras más compactas (tipo perovskitas).

***Figura 1.3**. Autoclaves utilizadas en síntesis hidrotermal.*

Empleando condiciones subcríticas, el investigador O. Yaghi y colaboradores desarrollaron una serie de MOFS muy estudiada denominada IRMOF,[25] (IsoReticular MOFs) los cuales se sintetizaron a partir del esqueleto del MOF-5 (IRMOF-1), sustituyendo el ligando orgánico en condiciones subcríticas, empleando DEF (dietilformamida) como disolvente y un rango de temperaturas entre 85 y 105°. Estos materiales presentan gran tamaño de poro, considerándose algunos materiales mesoporosos (tamaño de poro > 20 Å), y tienen una gran estabilidad termal, mostrando unas muy buenas capacidades de adsorción para distintos gases.

Por otra parte, debe destacarse que las altas temperaturas y presiones que se generan en el seno de una reacción solvotermal pueden favorecer la transformación de los reactivos (por ejemplo, el ligando) en otros diferentes generándose nuevas especies *in situ* que reaccionan para dar lugar a estructuras totalmente distintas e inesperadas a las que se obtendrían por métodos convencionales. Dentro de las reacciones que se pueden producir en estos procesos se encuentran la formación de enlaces carbono-carbono,[26] hidroxilación, [27]formación de tetrazoles mediante cicloadición de cianuros y azida,[28] formación de triazoles mediante cicloadición [2+2+1] de cianuros y azida, alquilación,[29] hidrólisis,[30] oxidación-hidrólisis,[31] acilación[32] y/o descarboxilación[33] de los reactivos iniciales.

Un ejemplo de las múltiples reacciones que se pueden realizar en una reacción hidrotermal es la síntesis del MOF $[Cd(pymc)_2]\cdot 7H_2O$ (RHO-ZMOF).[34] Este material está constituido por el ligando 2-pirimidincarboxilato (figura 1.4), el cual se ha formado por hidrólisis del ligando de partida 2-pirimidincarbonitrilo, de manera que se forma un MOF tridimensional poroso de tipo zeolítico con volumen accesible de 15583 $Å^3$.

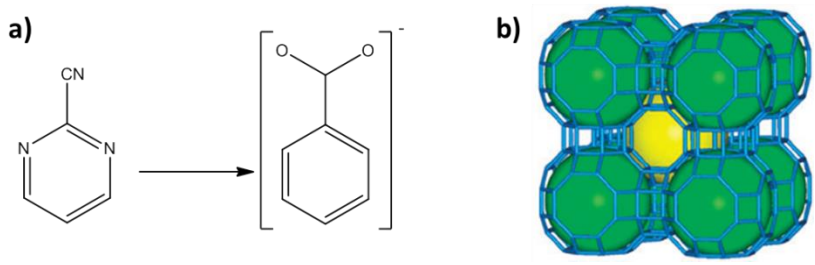

Figura 1.4. *Reacción de hidrólisis del ligando 2-pirimidincarbonitrilo (a); estructura 3D del compuesto RHO-ZMOF (b)*

1.2.3.2. Síntesis mediante Microondas

Un método que se están empleando cada vez más en la creación de MOFs es la **síntesis** mediante **microondas**, constituyendo un método rápido, fácil y relativamente barato en el que la única diferencia con los métodos solvotermales es el uso de radiación electromagnética de microondas como fuente de energía. La principal ventaja de esta técnica respecto a los métodos solvotermales es la rapidez con que se alcanzan elevadas temperaturas, favoreciendo las reacciones químicas. Además, presenta otras ventajas como la rápida cristalización de los materiales, la obtención de fases cristalinas de mayor pureza con tamaños de cristal más pequeños que los obtenidos mediante métodos solvotermales. Sin embargo, para esta técnica

no se ha descrito un mecanismo que sea capaz de describir y justificar la mejora en la velocidad, existiendo solo hipótesis de la misma.

Uno de los primeros MOFs sintetizados con esta técnica lo desarrollaron los investigadores Zheng Ni y Richard Masel,[35] quienes fueron capaces de obtener nanocristales de los materiales IRMOF-1, IRMOF-2 y IRMOF-3 empleando esta técnica. Como se ha mencionada, una de las principales ventajas de esta técnica es su rapidez, la cual quedó demostrada en esta síntesis, ya que mediante métodos solvotermales tiene un tiempo de reacción de 48 horas, mientras que empleando esta técnica el tiempo total es de unos 30 minutos.

1.2.3.3. Síntesis mediante métodos Mecanoquímicos

Otra técnica empleada es el **método mecanoquímico**. Se trata de un método en el que los reactivos empleados (sales metálicas y ligandos orgánicos) se molturan en un molino de bolas para obtener el material deseado. Se trata de una técnica de la llamada *química verde* en la que no se emplea disolventes orgánicos, obteniéndose materiales de alta calidad y con un rendimiento casi cuantitativo. El inconveniente de este método es que no es posible obtener estructuras cristalinas, obteniéndose polvos que serán caracterizados mediante difracción de rayos X en polvo. Este es el caso de los MOFs HKUST-1 ($Cu_3(BTC)_2$, BTC = 1,3,5-benzenetricarboxilato) y su análogo MOF-14 ($Cu_3(BTB)_2$, BTB = 4,4',4''-benzenetribenzoato) los cuales fueron sintetizados mediante esta técnica y caracterizados por DRXP,[36] observando como las características estructurales (área superficial) y propiedades de adsorción eran muy parecidas para los compuestos sintetizados mediante distintas técnicas.

1.2.3.4. Síntesis mediante métodos sonoquímicos

Los **métodos sonoquímicos** favorecen una nucleación homogénea y una reducción sustancial en el tiempo de cristalización si se compara con un calentamiento convencional. La principal característica de esta técnica es la creación, formación de unas burbujas en el fluido (disolvente), las cuales cuando alcanzan un determinado tamaño se hacen inestables, colapsándose por un fenómeno de cavitación, generando unas temperaturas y presiones extremadamente altas (temperaturas del orden de 5000 K y presiones superiores a los 1000 bar). Para estas técnicas se emplean disolventes que no sean muy volátiles, ya que su elevada presión de vapor reduce la intensidad del colapso de las burbujas formadas por el proceso de cavitación, reduciendo las temperaturas y presiones obtenidas.

Un ejemplo es el del MOF-5 sintetizado mediante esta técnica por A. Wha-Seung y colaboradores,[37] consiguiendo obtener unos microcristales de este MOF, los cuales fueron comparados con los obtenidos mediante técnicas solvotermales. Como se expuso, una de las principales ventajas era la reducción de tiempo de síntesis. Esto se manifestó en este MOF, ya que el tiempo de reacción empleando métodos sonoquímicos fue de 90 minutos, mientras que para obtener cristales de buena calidad mediante métodos solvotermales se necesitaron 24 horas de reacción. Ambos materiales fueron caracterizados y comparados por sus propiedades de adsorción y se comprobó que la similitud de los materiales era casi total, poniendo de relieve la eficiencia de estos métodos en la síntesis de MOFs.

1.2.4. DISEÑO RETICULAR DE MOFS

Un aspecto importante en la síntesis de MOFs es conocer qué estructura se quiere sintetizar para escoger de manera adecuada los linkers o *building blocks* que sean necesarios para llevar a cabo dicha síntesis. Para ello se puede partir de *building blocks* rígidos para mantener su integridad estructural en el proceso de síntesis, o bien formarlos *in situ* en las condiciones adecuadas. En este contexto se define la síntesis reticular.

La síntesis reticular se puede definir como el proceso de ensamblaje lógico de distintos *building blocks* con el fin de construir estructuras ordenadas que han sido predeterminadas (redes) Éstas se mantienen a través de enlaces fuertes, difiriendo de la retrosíntesis de moléculas orgánicas en la rigidez e integridad inalterada de los linkers durante el proceso de síntesis. Simplificando un poco, la síntesis (o química) reticular es la síntesis de materiales robustos de una manera lógica con *building blocks,* estructuras y propiedades predeterminadas.

Es importante resaltar que no es fácil conseguir la síntesis de estructuras robustas de esta manera, ya que se deben superar problemas como la falta de direccionalidad de los ligandos, o que en los MOFs basados en enlaces M-N en cuyos vértices hay un átomo solo tienen tendencia a colapsar después de eliminar las moléculas huésped que se alojen en su interior.

Este concepto surgió con fuerza de la mano de O. Yaghi y colaboradores cuando sintetizaron la serie conocida como IRMOFs,[25] la cual la lograron a partir del MOF-5, con el que fueron modificando el ligando orgánico dicarboxílico, funcionalizándolo y aumentando el tamaño, hasta conseguir la serie inicial de 16 MOFs, por la cual se representa en la figura 1.5.

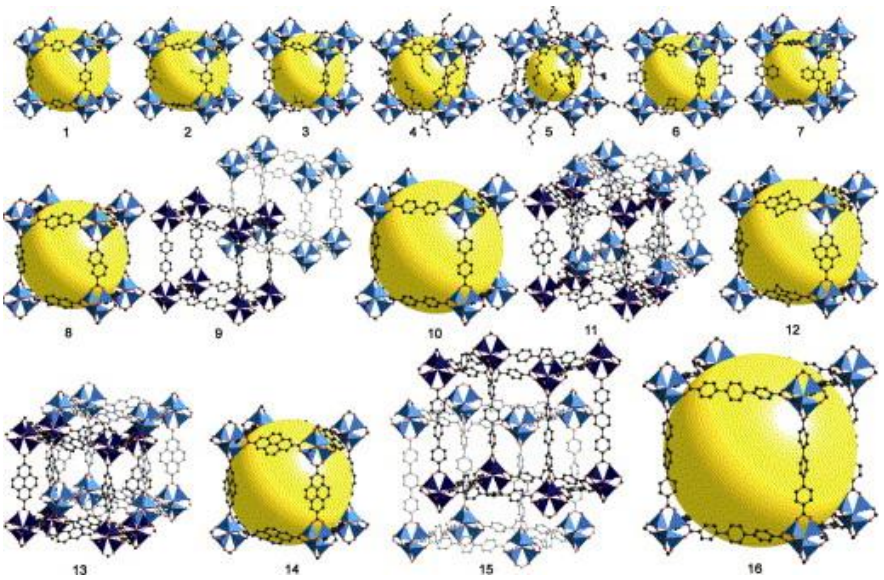

***Figura 1.5**. Representación esquemática de los MOFs pertenecientes a la serie IRMOF.*

1.2.5. ESTABILIDAD Y FLEXIBILIDAD DE MOFS

En el año 1998, el investigador S. Kitagawa[38] propuso una clasificación para los polímeros de coordinación porosos dividida en tres categorías basadas en la respuesta de estos materiales frente a la pérdida de las moléculas huésped que se alojan en su interior: primera, segunda y tercera generación (Figura 1.6).

Los MOFs de primera generación, entre los que se encuentra un amplio abanico de estructuras porosas, son aquellos que pierden completamente su orden cristalino después de eliminar las moléculas de disolvente que se encuentran en el interior de las cavidades. Dicho de otra manera, la estructura colapsa irreversiblemente y los materiales son incapaces de mostrar porosidad permanente y/o cristalinidad. Esto es lo que le ocurre a un MOF poroso de níquel de fórmula $Ni_3(btc)_2(py)_6(1,2\text{-pd})_3\cdot[(1,2\text{-pd})_{11}(H_2O)_8]$ (btc = ácido 1,3,5-benzenetricarboxílico; py = piridina; 1,2-pd = 1,2-propanodiol),[39] el cual tras ser sometido al tratamiento para eliminar las moléculas de disolvente, se transformaba en un material amorfo

Los MOFs de segunda generación poseen una estructura robusta y estable, perdiendo y readsorbiendo las especies huésped reversiblemente sin que ello suponga un cambio en la morfología del material. Por este motivo, estos materiales se han utilizado tradicionalmente como adsobentes, considerándolos análogos a las

zeolitas. Un claro ejemplo es el MOF Zn(BDC)·(DMF)(H_2O) (BDC = ácido 1,4-benzenedicarboxílico; DMF = N,N'-dimetilformamida),[40] el cual tras ser sometido a un tratamiento para eliminar las moléculas de DMF, mantenía la cristalinidad del MOF, observado mediante medidas de difracción de rayos X en polvo.

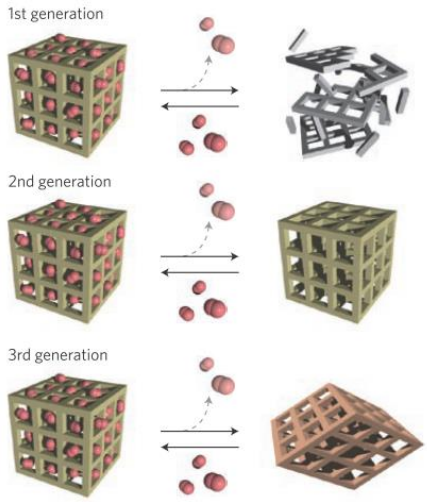

***Figura 1.6**. Representación esquemática de la clasificación de los Polímeros de Coordinación Porosos dada por Kitagawa.*[38]

Los MOFs de tercera generación (*Soft Porous Crystals*) son aquellos que muestran estructuras flexibles con comportamientos dinámicos, es decir, aquellos que modifican su estructura porosa reversiblemente como respuesta a un estímulo externo, ya sea químico (presencia de moléculas huésped) o físico (temperatura, presión, campo magnético, etc.). El estudio sobre este tipo de MOFs ha aumentado de manera considerable en los últimos años, puesto que la flexibilidad de sus estructuras permite obtener materiales con propiedades adsorbentes y catalíticas selectivas. La naturaleza dinámica de estos MOFs facilitará la incorporación de ciertas moléculas huésped y su naturaleza adaptable favorecerá la formación de determinados productos de reacción con un tamaño y forma específicos.[41]

Un ejemplo icónico de estos materiales es el MIL-53,[42] cuya fórmula es (Cr^{III}(OH)·{1,4-bdc}·{1,4-H_2bdc}$_{0.75}$ (1,4-H_2bdc = ácido bencendicarboxílico). Este material cambia su estructura de forma reversible cuando se adsorben y desorben

moléculas de agua en el interior de sus poros, modificando la forma de este material, como puede apreciarse en la figura 1.7.

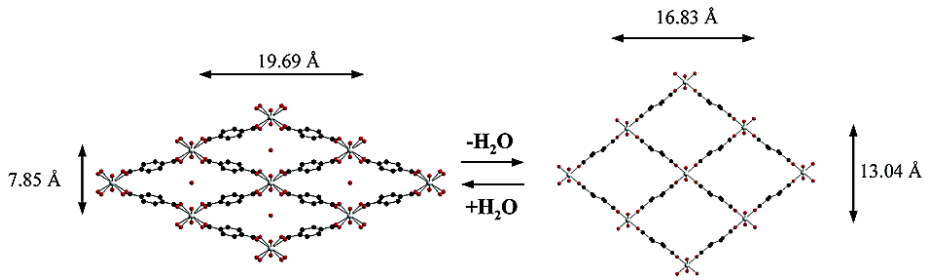

***Figura 1.7**. Representación esquemática del proceso de hidratación-deshidratación del MOF MIL-53*

1.2.6. SIMULACIONES MOLECULARES

La simulación molecular ha jugado un papel importante y creciente en un amplio conjunto de áreas científicas, abarcando desde el estudio de las propiedades termodinámicas de la materia al diseño de nuevos materiales o la síntesis de nuevos fármacos. Esta técnica es de gran importancia debido a la dificultad de alcanzar en algunas ocasiones las condiciones de interés, como temperaturas y presiones extremas. Además, la simulación molecular ofrece la posibilidad de poder estudiar un elevado número de sistemas y condiciones de una manera rápida y sencilla.

Conocer la relación adsorbente-adsorbato es fundamental para poder identificar qué materiales son interesantes para una aplicación específica. En este sentido, la simulación molecular facilita la conexión entre los fenómenos de adsorción a nivel molecular y el comportamiento de un material a escala macroscópica similar a cualquier experimento. Generalmente, estos experimentos son isotermas de adsorción, es decir, el estudio de la cantidad adsorbida de gas (masa o volumen) conforme aumenta la presión. La simulación molecular es capaz de predecir de manera cuantitativa cuál es la capacidad de adsorción de un material o, en caso de mezclas, es capaz de predecir la selectividad de un compuesto frente a los otros. Además, la simulación permite observar en qué regiones del material existe mayor interacción con una molécula de gas y así, dónde se produce la adsorción. Esta estrategia permite estudiar en detalle cómo influye la estructura de MOFs existentes o hipotéticos en su comportamiento durante la adsorción. Para ello se emplean las simulaciones Monte Carlo, ya que son el método más utilizado para predecir las isotermas de adsorción.

El método Monte Carlo es una técnica estocástica, es decir, se basa en el uso de números aleatorios y el estudio de la probabilidad para investigar problemas reales. El método más general para estudiar los procesos de adsorción en equilibrio es a través de la simulación Monte Carlo y el colectivo gran canónico (GCMC, de sus siglas en inglés).[43] Esto significa que tanto el potencial químico, el volumen y la temperatura del sistema se mantienen fijos, permitiendo que el número de moléculas de gas fluctúe hasta alcanzar el equilibrio, tal y como ocurre en un experimento de adsorción clásico. Cada simulación Monte Carlo consiste en millones de movimientos aleatorios: inserción de una molécula, eliminación, rotación o traslación a través de la porosidad, de los cuales solo algunos serán aceptados cuando ese movimiento suponga la estabilización energética del sistema.

Para poder realizar la simulación de un proceso de adsorción en compuestos cristalinos es necesario contar con un modelo estructural tanto del adsorbente como del gas a estudiar. El modelo de un material se obtiene a partir de sus coordenadas cristalográficas mediante difracción de rayos-X. En la mayoría de los casos se asume que el material está totalmente activado, por lo que no tiene restos de disolvente ni precursores en el interior de la estructura y que no presenta ningún tipo de defecto cristalino. Además, se suele admitir que la estructura es rígida y no presenta ningún tipo de flexibilidad, una idea válida para un gran número de MOFs.

Un ejemplo de la validez de las simulaciones en los estudios de adsorción se produce cuando se comparan los cálculos teóricos con las medidas experimentales del IRMOF-1.[44] En la figura 1.8 se representan las isotermas de adsorción de CO_2 para este material a diferentes temperaturas, corroborando como los modelos teóricos se ajustan a las medidas experimentales.

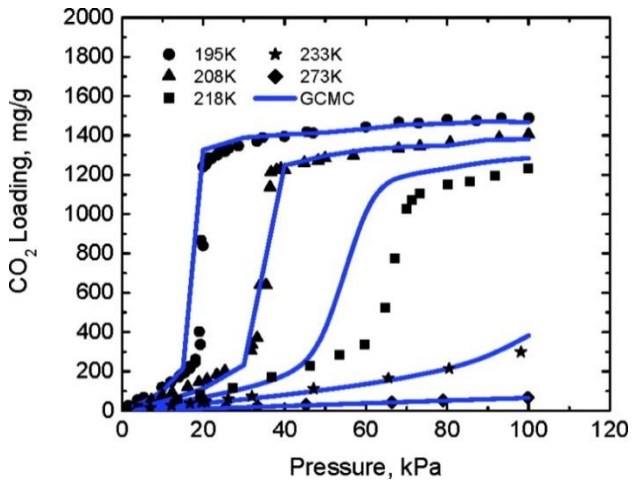

***Figura 1.8**. Comparación entre las simulaciones GCMC y las isotermas experimentales de adsorción de CO_2 para el IRMOF-1*

1.3. APLICACIONES Y PROPIEDADES DE LOS MOFS

Si por algo destacan los MOFs es por sus múltiples propiedades y potenciales aplicaciones en diversos campos de gran interés (adsorción, catálisis, luminiscencia, magnetismo, biomedicina, nanotecnología, etc.). A continuación, se detallan algunas de las propiedades y aplicaciones de estos materiales, que han sido objeto de estudio en esta Tesis Doctoral, así como algunos ejemplos de los MOFs más destacados en estos campos.

1.3.1. ADSORCIÓN DE GASES

La adsorción de gases en MOFs ha sido una de las propiedades más estudiadas dentro de esta clase de materiales. Concretamente, en relación con esta propiedad, algunas de las aplicaciones más interesantes son el almacenamiento, la separación y purificación de gases.

1.3.1.1. Almacenamiento de gases

Como se ha comentado anteriormente, los MOFs son un nuevo tipo de materiales cristalinos, sintéticos constituidos por iones metálicos conectados a través de ligandos orgánicos,[45] de forma que se genere una red abierta accesible a moléculas huésped. En general, los MOFs poseen estructuras porosas con áreas superficiales elevadas, lo que hace que sean materiales muy atractivos para su empleo en la adsorción de gases (Figura 1.9). Hasta la fecha se han sintetizado algunos MOFs con áreas superficiales incluso por encima de los 6000 m^2/g,[46] que exhiben una capacidad excepcional de almacenamiento de gases.

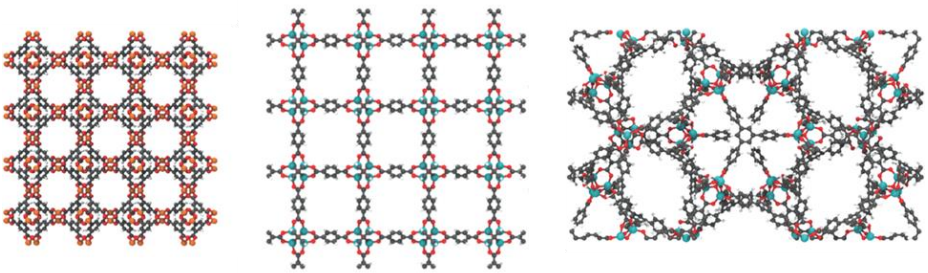

Figura 1.9. Tres de los MOFs más conocidos por sus propiedades de adsorción de gases: HKUST-1 (izquierda), IRMOF-1 (centro), y MOF-177 (derecha).

A lo largo de estos años, muchos investigadores han intentado mejorar la capacidad de almacenamiento de gases en MOFs modulando las interacciones de los mismos con la red polimérica. Esto se puede conseguir a través de: *i)* la presencia de centros metálicos con posiciones de coordinación insaturadas[47] y *ii)* la incorporación de grupos funcionales apropiados en los ligandos orgánicos o en los centros metálicos con posiciones de coordinación insaturadas mediante funcionalizaciones pre-sintéticas o post-sintéticas.[48]

La mayoría de los estudios sobre la capacidad de los MOFs para el almacenamiento de gases se han centrado en el metano, hidrógeno y dióxido de carbono. El porqué de este mayor interés en el almacenamiento de estas sustancias se debe a los siguientes factores:

- El gas metano es un combustible más limpio que la gasolina y tiene una proporción hidrógeno/carbono (H/C) mayor que cualquier otro hidrocarburo combustible fósil.
- El hidrógeno es un combustible muy atractivo debido a su alta densidad energética, no es tóxico y su producto de oxidación es el agua (no contaminante). Además, el descenso en la reserva de combustibles fósiles disponibles, hacen que el hidrógeno se considere uno de los vectores energéticos con mayor posibilidad de sustituir a los actuales combustibles basados en el carbón. Actualmente, la mayor dificultad tecnológica para conseguir el uso del hidrógeno como combustible tanto en aplicaciones estacionarias como, sobre todo, en aplicaciones móviles es su almacenamiento de una forma eficiente y segura. Por tanto, el desarrollo de nuevos materiales capaces de almacenar este gas supone más que un desafío, una necesidad.
- Las emisiones de CO_2 producidas de manera antropogénica han aumentado considerablemente en los últimos años, por lo que su captura, así como una drástica reducción de las emisiones industriales, constituyen uno de los mayores retos medioambientales a los que la civilización se enfrenta.

Almacenamiento de hidrógeno

Ante el agotamiento de los combustibles fósiles, nace la gran necesidad de buscar nuevos recursos energéticos como por ejemplo la energía solar y eólica. En este contexto, surge el hidrógeno como fuente de energía alternativa. El hidrógeno tiene una densidad energética excepcionalmente alta (123 MJ/kg), que es casi tres veces mayor que el valor equivalente para hidrocarburos líquidos (47 MJ/kg). Además, el hidrógeno se puede considerar un portador de energía respetuoso con el medioambiente porque sólo produce vapor de agua como producto de combustión.

A pesar de esto, el mayor obstáculo para su aplicación práctica reside en la falta de sistemas de almacenamiento eficientes (compactos, ligeros), seguros y que sean capaces de liberar la cantidad de hidrógeno gaseoso necesaria, al ritmo deseado y a temperatura y presión ambiente.

El Departamento de Energía de Estados Unidos (DOE) ha fijado los objetivos que tiene que cumplir cualquier material para su aplicación en el almacenamiento de hidrógeno en aplicaciones móviles. Según el DOE, para el año 2015, estos materiales deben alcanzar una capacidad de adsorción gravimétrica superior al 5.5 % y una capacidad de adsorción volumétrica mayor de 0.040 Kg de H_2/L. Por ahora, ninguno de los MOFs desarrollados hasta la fecha alcanza estos objetivos.

A continuación se describirán algunos de los materiales más representativos logrados hasta el momento con el fin de almacenar hidrógeno, diferenciando los grupos funcionales que presenten los ligandos orgánicos empleados: ligandos de tipo carboxílicos y de tipo azolato.

Los ligandos que presentan grupos carboxílicos en su estructura han sido bastante empleados en la síntesis de MOFs. La gran variedad de ligandos y de iones metálicos empleados han proporcionado un amplísimo abanico de redes tridimensionales. El empleo de ligandos rígidos con grupos carboxilato en la síntesis de MOFs ofrecen la posibilidad de crear estructuras porosas con unas propiedades de robustez excepcionales, y muchas de ellas no colapsan incluso después de haber eliminado las moléculas de disolventes que se alojan en ellas durante el proceso de síntesis. Entre los metales más empleados en la síntesis se encuentran Zn, Cu, Mn, Co, Cd, Ni e iones lantánidos. Algunos de los MOFs, en particular los de Zn, son conocidos por ser sensibles al aire, es decir, su capacidad de adsorción de hidrógeno disminuye al ser expuestos a condiciones atmosféricas.

Dentro de la amplia variedad de ligandos con grupos carboxilato existentes, los ligandos di- y tricarboxílicos han sido los más empleados debido a la gran variedad de modos de coordinación que pueden presentar.

Un referente es el MOF-5.[25] A partir de él, se obtuvieron una serie de MOFs isoreticulares (IRMOF) empleando diversos ácidos dicarboxílicos.[25,49] Las estructuras generadas son unas redes cúbicas tridimensionales en las que los clusters Zn_4O forman unas unidades octaédricas, las cuales se enlazan a 6 ligandos de tipo carboxilato generando redes cúbicas. La mayoría de estos IRMOFs tienen un área superficial elevada y un volumen de poro bastante alto. El MOF-5 (IRMOF-1) tiene una superficie BET de 3800 m^2g^{-1} con una capacidad de adsorción de un 7.1 wt% a una presión de 40 bares y una temperatura de 77K (figura 1.10), y es considerado todavía como uno de los mejores materiales en lo que a almacenamiento de hidrógeno se refiere.[17]

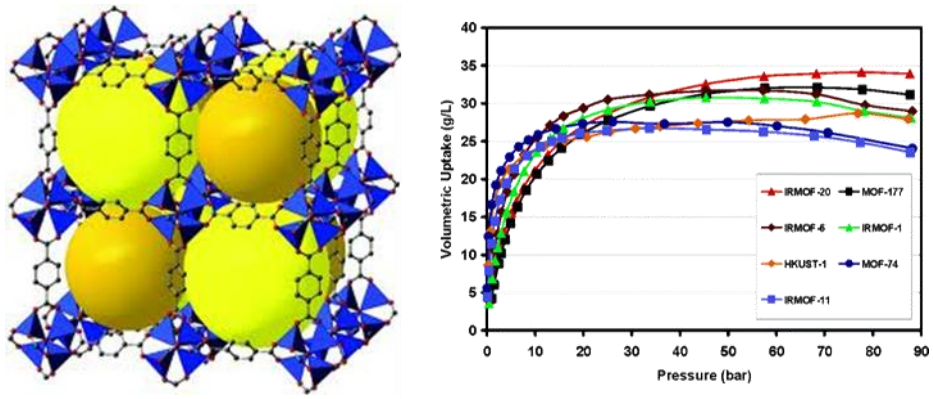

Figura 1.10. *Estructura del MOF-5 (izq) y representación de las isotermas de H_2 realizadas a alta presión y a 77K para diferentes MOFs en unidades volumétricas (g/L).*

Otro gran grupo de MOFs lo constituyen aquel formado por ligandos tricarboxílicos y clusters Zn_4O como unidades secundarias. El conocido MOF-177 se encuentra formado por estos clusters Zn_4O y ligando 4,4',4''-benceno-1,3,5-triyltribenzoato (BTB), donde cada unidad [Zn_4O] se encuentra conectada a seis grupos carboxilato y cada ligando tricarboxilato se une a tres unidades [Zn_4O] generando así una red de tipo (6,3) (figura 1.11). Este MOF-177 posee un área de superficie BET de 4750 m^2g^{-1} y un volumen de poro de 1.59 cm^3g^{-1}, haciendo de este material uno de los MOFs más porosos que se conocen[49c,50] teniendo una capacidad de adsorción de 7.5 wt% a 77K y una presión de 70 bares.[49c]

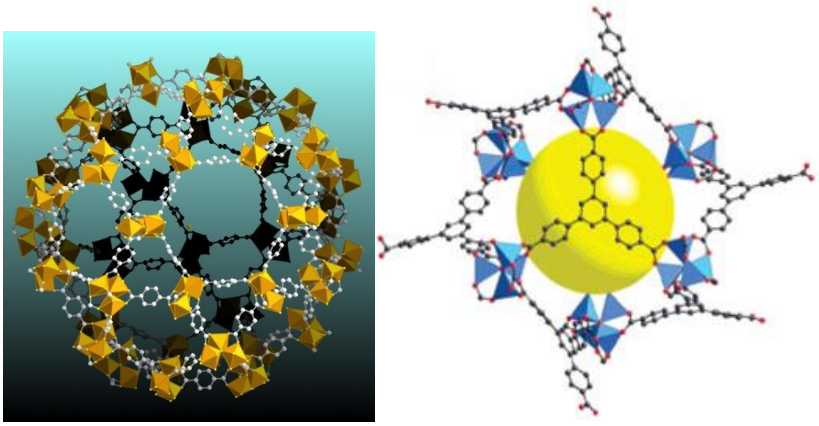

Figura 1.11. *Visión de la red cristalina del MOF MIL-101 (izquierda).Estructura del MOF-177 (derecha).*

Otra serie muy representativa la constituye la formada por los materiales MIL (MIL: Material from Institute Lavoisier), la cual está formada por unidades triméricas de cromo (III) y ligandos di- y tricarboxílicos.[51] Estos MOFs presentan elevada porosidad y estabilidad química. Por ejemplo, el MOF MIL-101 (figura 1.8, derecha) tiene una capacidad de adsorción de H_2 de 6.1 wt% a 77K y 80 bares.

Por otra parte, existen una gran variedad de MOFS formados por ligandos de tipo azolato. En estos MOFs los ligandos que se emplean como building blocks son heterociclos como imidazoles, pirazoles, triazoles y tetrazoles.

Las redes con imidazoles de tipo zeolítico (ZIFs) son redes neutras formadas por iones Zn^{II} y Co^{II} coordinados tetraédricamente y ligandos de tipo imidazol (Figura 1.12). El ángulo de enlace M-IM-M (M=metal; IM=imidazol) es muy similar al que presentan las zeolitas, con un valor de ángulo de enlace Si-O-Si de 145° Estas estructuras presentan una topología de tipo zeolítico con una elevada estabilidad química y térmica.

Una de las estructuras más destacables es el ZIF-8 (figura 1.11), que emplea como ligando el metilimidazol, que posee una capacidad de adsorción de H_2 de 3.3 wt% a 77K y 30 bar de presión, lo que hasta la fecha es la mayor capacidad de adsorción de H_2 publicada para este tipo de estructuras.

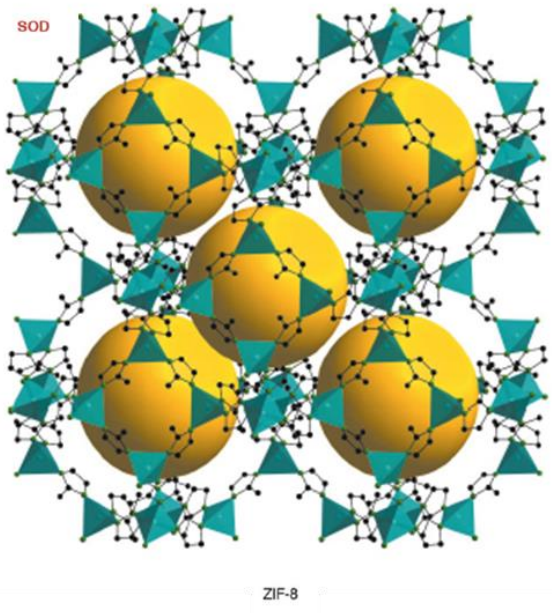

Figura 1.12. *Estructura cristalina del ZIF-8 (la topología de la red aparece con tres letras rosas). Los centros metálicos están representados con poliedros azul para ZnN_4 y los ligandos como bolas y sticks. La bola amarilla representa el espacio en la cavidad.*

Los grupos tetrazolatos son similares a los ácidos carboxílicos en lo que a capacidad de actuar como ácido se refiere, con un valor de pKa alrededor de 4.9. La presencia de múltiples átomos de N dadores aumenta el número de modos de coordinación del ligando con el centro metálico generando un amplio abanico de posibilidades que desembocan en fascinantes estructuras.

Pese a los resultados mostrados, no existe todavía un material que satisfaga las objetivos propuestos por la DOE para el almacenamiento de H_2 a temperatura ambiente, ya que se ha observado que la capacidad de adsorción de los MOFs disminuye conforme aumenta la temperatura, es decir, a temperaturas muy bajas (criogenización) sí se han desarrollado estos materiales, pero ninguna llega al reto que supone alcanzar buenas propiedades de adsorción a temperatura ambiente. Por lo tanto, la obtención de estos materiales supone uno de los grandes retos de la ingeniería cristalina.

Adsorción de CO_2

Las emisiones de dióxido de carbono procedentes de procesos industriales contibuyen al calentamiento global, al aumento del nivel del mar y a un aumento irreversible de los niveles de acidez de los océanos con un impacto medioambiental terrible. Estas amenazas han llevado a los científicos a proponer soluciones para reducir los niveles de gases de efecto invernadero, especialmente de CO_2.

Para reducir el número de emisiones y capturar el CO_2 existen medios convencionales como emplear especies básicas, tales como amoníaco o sólidos con aminas funcionalizadas. Sin embargo, empleando materiales en los que se den procesos de fisisorción entre las moléculas de CO_2 y el adsorbente, obtenemos un método para eliminar el dióxido de carbono de una manera energéticamente más beneficiosa que los métodos convencionales anteriormente descritos.[52]

En este sentido, ya se ha investigado con algunos materiales como los carbones activados, tamices moleculares y zeolitas como adsorbentes de CO_2,[53] aunque estos materiales presentan graves problemas de capacidad de almacenamiento y regeneración de los mismos.

Por esta razón, la síntesis de MOFs con buenas capacidades de almacenamiento de CO_2 constituye uno de las áreas de investigación más activas, desarrollando materiales que presenten una elevada selectividad a este gas. Esta selectividad la podemos conseguir modificando dos parámetros: a) un factor

cinético, en el que la característica principal de la estructura sea el tamaño de poro, el cual rige qué moléculas pueden ser adsorbidas por el material dado su diámetro; b) un factor termodinámico, en la que la diferencia de afinidad de los gases por ser adsorbidos en la superficie del material es el factor determinante. Se debe tener en cuenta que si se produce una elevada interacción entre la molécula de CO_2 y el adsorbente el proceso de desorción será energéticamente muy caro; y por otra parte, si la interacción es débil, el material no adsorberá la cantidad adecuada de CO_2. A la vista de lo anterior, la búsqueda de un equilibrio entre estos dos factores constituye un reto a alcanzar en la síntesis de MOFs.

Hace unos años, los investigadores Millward y Yaghi[54] publicaron un trabajo pionero en la adsorción de CO_2 en el que mostraban las diferentes isotermas de adsorción de CO_2 a una presión de 42 bares, tal y como se representa en la figura 1.13. De todas ellas, destaca la del MOF-177, que presenta para una temperatura de 298 K y 42 bares de presión, una capacidad de adsorción de CO_2 de 33.5 mol kg^{-1}.

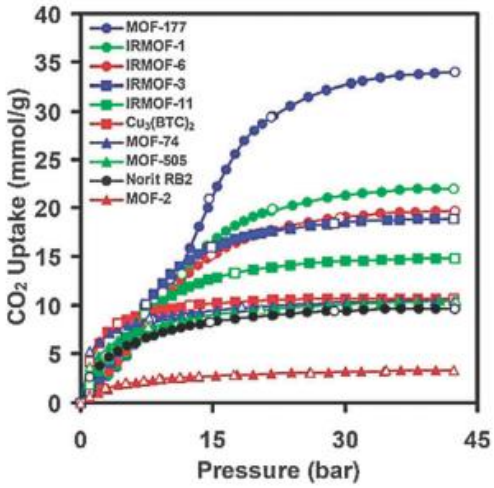

Figura 1.13. *Comparación de la adsorción de CO_2 para varios MOFs (y el carbón activado NORIT como referencia) determinadas a temperatura ambiente y una presión de 42 bar.*

Además de estos materiales, existen una gran cantidad de estructuras porosas a las que se han estudiado sus capacidades de adsorción de CO_2.[55] Una de ellas es el MOF MIL-53, que presenta dos formas isoestructurales, una con aluminio y otra con cromo como centro metálico.[55b] En esta estructura existen moléculas de

agua en el interior de los poros que modifican la forma de los mismos, debido a las interacciones de tipo puente de hidrógeno establecidas entre los átomos de hidrógeno de las moléculas de agua y de los átomos de oxígeno de los grupos carboxilato de los ligandos que forman el MOF. En este caso nos encontramos ante un material que presenta una capacidad de adsorción de CO_2 similar a la que tienen los materiales carbonosos microporosos, con un valor de adsorción de 10.4 mol kg^{-1}.

Obviamente, cuanto más extensos sean los linkers orgánicos empleados, en principio, mayor área superficial va a poseer la estructura resultante y mayor va a ser su capacidad de almacenamiento (figura 1.14).

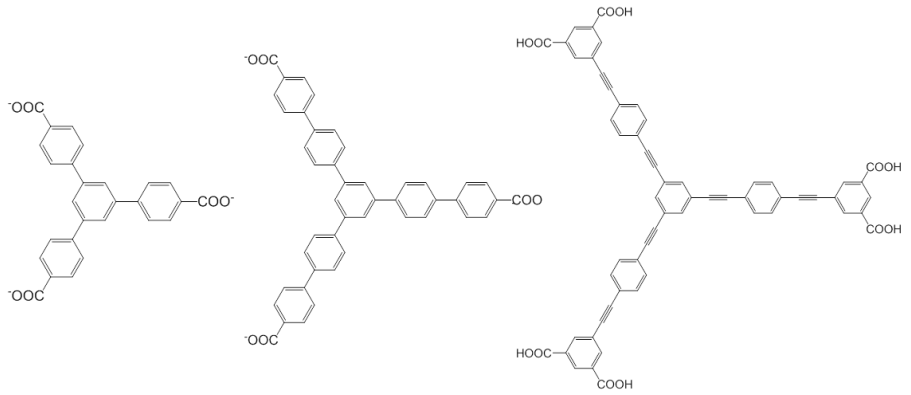

Figura 1.14. *Linkers usados para sintetizar MOFs aumentando su área superficial y tamaño de poro. 4,4',4'-Benzeno-1,3,5-triyltribenzoato (BTB) se emplea para sintetizar el MOF-177, mientras que 4,4',4''-(benzene-1,3,5-triyl-tris (benzeno-4,1-diyl))tribenzoato (BBC) se usa para sintetizar el MOF-200; LH_6 se usa para sintizar NU-100*

El ligando LH_6 se ha empleado para la síntesis del MOF NU-100,[46a] un material con una superfice BET bastante elevada (6143 m^2g^{-1}) y una elevada capacidad de adsorción de CO_2 (46.4 mol kg^{-1}), mientras que el ligando BBC se ha utilizado para sintetizar el MOF-210,[46b] el cual presenta una altísima superficie BET (6240 m^2g^{-1}) y una excelente capacidad de adsorción de 54.5 mol kg^{-1}, a una temperatura de 298 K y una presión de 50 bares. Este dato constituye, hasta el momento, el mejor resultado de un MOF (es el mismo que para el MOF-200) en lo que a capacidad de adsorción de CO_2 se refiere (tabla 1).

Tabla 1. *Datos de adsorción de CO_2 para una serie de relevantes MOFs.*

Muestra	Área superficial ($m^2\ g^{-1}$) BET	Langmuir	Volumen poro ($cc\ g^{-1}$)	Adsorción CO_2 ($mol\ kg^{-1}$)	Temperatura (K)	Presión (bar)
HKUST-1	1270	-	0.71	17.5	308	300
MOF-5	2833	-	-	21.7	298	35
IRMOF-3	2160	-	-	18.7	298	35
IRMOF-6	2516	-	-	19.5	298	35
IRMOF-11	2096	-	-	14.7	298	35
MIL-53 (Cr)	-	1500	-	10.0	304	25
MIL-100 (Cr)	1900	-	1.1	18	304	50
MIL-101 (Cr)[a]	4230	-	2.2	40	304	50
MIL-102 (Cr)	-	-	-	3.1	304	30
MOF-177	4508	-	-	33.5	298	35
MOF-200	4530	10400	3.59	54.5	298	50
MOF-205	4460	6170	2.16	38.1	298	50
MOF-210	6240	10400	3.60	54.5	298	50
NU-100	6143	-	-	46.4	298	40
UMCM-1	4100	-	2.14	23.5	298	24

[a] Activado con etanol y NH_4F

Si tenemos en cuenta la capacidad de adsorción de estos materiales y los objetivos propuestos, los MOFs actuales están mejor preparados para la adsorción y captura de CO_2 que de H_2, aunque sin alcanzar los objetivos marcados. Es por ello que se debe seguir trabajando en el desarrollo de estos materiales, reduciendo costes y mejorando la estabilidad de los MOFs.

1.3.1.2. Separación de Gases

Los procesos de separación juegan un papel muy importante en la industria, con una aplicación directa en la vida diaria por su uso en industrias como la alimentaria o la electrónica. Tradicionalmente, en el proceso de separación y purificación se han utilizado bases para eliminar sulfuro de hidrógeno y dióxido de carbono, así como procesos de oxidación, conversión termal y catalítica de impurezas, empleo de tamices moleculares y de membranas permeables.[56] Debido a la importancia de estos procesos, su aplicación se ha visto incrementada en los últimos tiempos.

Dentro de los materiales porosos inorgánicos se incluyen una amplia variedad de adsorbentes como geles de sílice, carbones activados, tamices moleculares y zeolitas. Son precisamente este último grupo el que despertó un gran

interés por sus propiedades, para que actualmente se desarrollen MOFs con el objetivo de ser aplicados en este campo, sintetizando materiales que posean una capacidad de adsorción elevada, buena selectividad referente a las moléculas que se pretenden adsorber, cinética de adsorción favorable, regenerabilidad y estabilidad química y termal

Estos procesos de separación se pueden dar por efectos estéricos, cinéticos y de equilibrio. Los primeros hacen referencia al tamaño de la molécula frente al tamaño del poro del material, de manera que una molécula difundirá en un material si el tamaño de poro lo permite. La selectividad cinética viene dada por la diferencia entre el proceso de adsorción y desorción que muestre la mezcla de los componentes; por ejemplo, el oxígeno difunde 30 veces más rápido que el nitrógeno. Los procesos de equilibrio se basan en interacciones adsorbato-adsorbente, las cuales vienen determinadas por las propiedades de la molécula que se pretenda adsorber y de la superficie del adsorbente, por lo que para escoger el material adecuado es importante conocer las propiedades fisicoquímicas del adsorbato, tales como la susceptibilidad magnética, la naturaleza ácido-base o la polarizabilidad.

El fundamento de los procesos de separación es el responsable de las distintas aplicaciones que pueden tener los MOFs en el campo de la separación de gases. Por ejemplo, cuando estos materiales actúan como tamices moleculares, el factor más decisivo en la separación selectiva de gases es el tamaño de poro del MOF, siendo más relevante cuando el objetivo es separar moléculas de pequeño tamaño (H_2, N_2, O_2, CO, CO_2, CH_4), ya que para moléculas de mayor tamaño como hidrocarburos, además del tamaño de poro, la naturaleza química del MOF tendrá un papel importante.

En general, uno de los casos más frecuentes es la separación y captura selectiva de CO_2 por su gran importancia en los procesos industriales. Un ejemplo es el compuesto $Mn(HCO_2)_2$,[57] el cual es una estructura porosa con unas cavidades de 4.5 Å de diámetro. Este MOF apenas sí presentaba adsorción de N_2 y Ar a 78 K pero sí una importante capacidad de adsorción de CO_2 a 178 K (figura 1.15), atribuyendo este comportamiento al tamaño de poro, ya que el pequeño tamaño que presenta este material dificulta la difusión de moléculas de N_2 y Ar en las condiciones observadas.

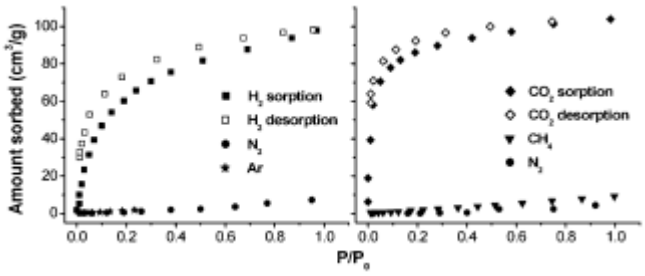

Figura 1.15. *Isotermas de adsorción y desorción de H_2, Ar, N_2, CH_4 y CO_2 para el MOF $Mn(HCO_2)_2$*

Sin embargo cuando tenemos materiales con un tamaño de poro elevado, el factor estérico pierde importancia en favor de las interacciones adsorbato-adsorbente. Este comportamiento se manifiesta en las separaciones de H_2 y CO_2, en las que el elevado momento cuadrupolar y lo altamente polarizable que es el la mólecula de CO_2 favorecen las interacciones con la superficie de los MOFs. Un caso es el del MOF $CoNa_2(1,3\text{-bdc})_2$ (1,3-bdc = ácido 1,3-benzendicarboxílico),[58] en el que tras realizar las isotermas de adsorción de H_2 y CO_2 (figura 1.16)se observa como las moléculas de CO_2 son las que difunden en los poros del material por las interacciones entre las moléculas de gas y la superficie de la estructura tridimensional, mientras que el H_2 no es capaz de ser adsorbido.

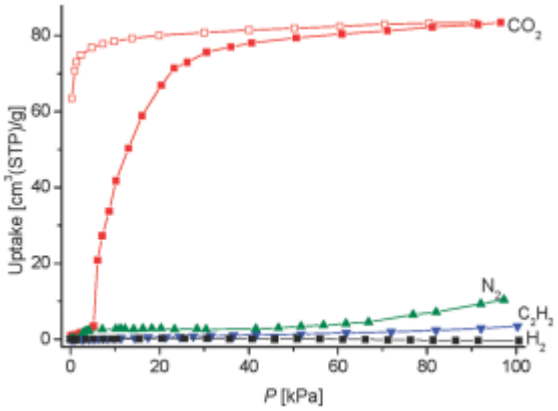

Figura 1.16. *Isotermas de adsorción de H_2, N_2, C_2H_2 y CO_2 para el MOF $CoNa_2(1,3\text{-bdc})_2$*

La separación y captura selectiva de CO_2 es una de las aplicaciones más estudiadas, aunque existen algunos estudios sobre la adsorción selectiva de otras moléculas como H_2 y N_2. Quizás el caso del H_2 sea el más destacado por su interés como posible alternativa a los tradicionales combustibles fósiles.

El hidrógeno empleado en celdas de combustible deriva de una mezcla que contiene H_2, CH_4 y N_2, por lo que el proceso de separación es muy importante. Con este fin, el Investigador J. Long[59] estudió la capacidad de adsorción selectiva de una serie de materiales en unas condiciones de 313 K y 40 bar, condiciones cercanas a las que se dan en los procesos de purificación de H_2. En ellos se observa un comportamiento de adsorción de CO_2, lo que permite capturarlo y obtener H_2 puro. En la figura 1.17 se representan las diferentes isotermas de adsorción de estos materiales.

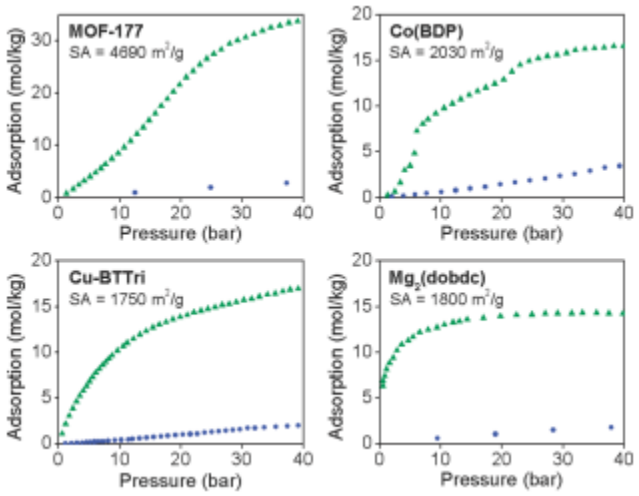

Figura 1.17. *Isotermas de adsorción de H_2 (círculos azules) CO_2 (triángulos verdes) para los MOFs MOF-177, Co(BDP), Cu-BTTri y Mg_2(dobdc).*

Además de la adsorción de estos gases, existe un campo de aplicación muy importante que involucra la adsorción y separación de gases contaminantes como H_2S, NO_x, NH_3, SO_2, Cl_2, CO, entre otros. La mayoría de estos gases son liberados como residuos durante procesos industriales, por lo que la captura efectiva de estos gases es muy importante para proteger el medio ambiente. Para ello, el investigador O. Yaghi y colaboradores[60] comprobaron la capacidad de adsorción y separación de algunos MOFs (MOF-199, MOF-5, MOF-74, MOF-177, IRMOF-3 e IRMOF-62) frente a

diversos gases nocivos como SO_2, NH_3 y Cl_2, y comparados frente a un carbón comercial (BPL), observando que la funcionalización de los poros juega un papel fundamental en la adsorción de estos gases, como aparece reflejado en la figura 1.x. Por ejemplo, para el caso del MOF-74, se observan unas muy buenas curvas de adsorción de SO_2 y NH_3 (figura 1.19), debido a la presencia de centros metálicos activos y de grupos oxo reactivos en la estructura.

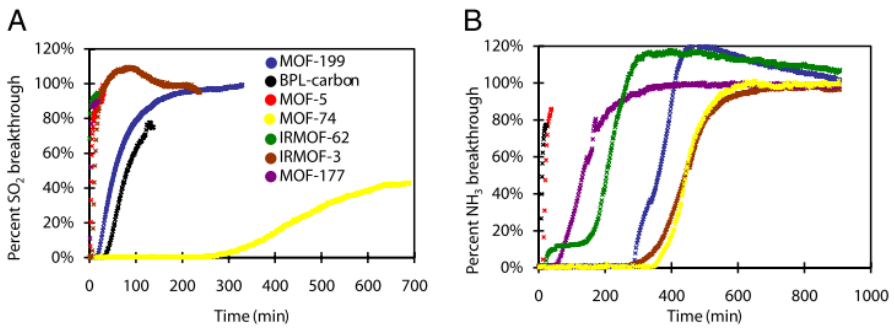

Figura 1.19. *Curvas de ruptura de los contaminantes gaseosos SO_2 (A) y NH_3 (B) para los MOFs mencionados anteriormente.*

1.3.2. APLICACIONES EN MAGNETISMO

Una de las líneas de investigación que provocan mayor interés es la preparación de materiales que combinen dos o más propiedades de interés. De las múltiples posibilidades, la combinación de magnetismo y porosidad ha conseguido la atención de los investigadores en la pasada década, consiguiendo así materiales que pueden ser empleados como sensores magnéticos, imanes moleculares o como medio para llevar a cabo separaciones magnéticas.

Las propiedades magnéticas, tales como ferromagnetismo, antiferromagnetismo, y ferrimagnetismo en sistemas polimetálicos se deben a interacciones de intercambio cooperativo entre iones metálicos paramagnéticos (primera serie de transición y lantánidos) y/o radicales orgánicos diamagnéticos que actúan de puente, por lo que de esta manera, el comportamiento magnético de un MOF dependerá de la naturaleza intríseca del metal y del ligando orgánico, así como de la interacción entre ambos. Así pues, el ligando empleado en la formación del MOF es crucial para organizar los centro metálicos paramagnéticos en una determinada topología y para transmitir eficientemente las interacciones entre los iones metálicos de la manera deseada.

Los estudios de MOFS magnéticos están focalizados en el área de los imanes moleculares y en el diseño de materiales magnéticos monoméricos o monodimensionales, sensores magnéticos y materiales multifuncionales. Es por ello que se persiguen estructuras con ligandos orgánicos que favorezcan acoplamientos entre los centro metálicos, siendo usuales el empleo de linkers que puedan presentar puentes oxo, ciano o azida.[19e,61]

Seguidamente veremos algunos ejemplos de MOFs que presentan propiedades magnéticas.

1.3.2.1. Propiedades Ferromagnéticas

Hasta la fecha no existen muchos MOFs que presenten propiedades ferromagnéticas. Uno de ellos es el MOF TTTA·$Cu(hfac)_2$ (TTTA: ácido 2,2',2''-[1,3,5-triazina-2,4,6-triiltris(sulfanediil)]triacético, hfac: hexafluoroacetilacetona),[62], el cual se puede definir como un aducto de un complejo metálico y un radical orgánico libre. En esta estructura el ligando TTTA actúa de puente entre los iones Cu^{2+} obteniendo unas cadenas en zigzag a lo largo del eje b, las cuales se unen a través de short contacts entre el átomo de S del anillo ditiazólico del ligando y los átomos de O de $Cu(hfac)_2$ para dar lugar a unas capas bidimensionales (figura 1.20a)

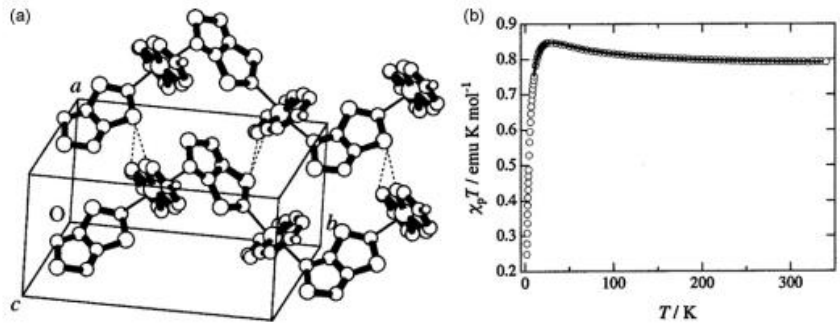

Figura 1.20 *a) Vista de la estructura TTTA·$Cu(hfac)_2$, en las que los grupos CF3 han sido omitidos por claridas. Las líneas punteadas son los enlaces entre las cadenas. b) Dependencia de la temperatura con $\chi_p T$*

Las medidas magnéticas mostraban un acoplamiento ferromagnético atribuible a los enlaces de coordinación entre $Cu(hfac)_2$ y el ligando TTTA, además de un débil acoplamiento antiferromagnético a baja tempeartura como consecuencia de la débil interacción entre $Cu(hfac)_2$ y el ligando TTTA y/o de las interacciones entre las cadenas que forman el compuesto. Así pues, las propiedades magnéticas de esta estructura se pueden interpretar como un dímero ferromagnético con una débil interacción antiferromagnética entre los dímeros.

1.3.2.2. Propiedades Antiferromagnéticas

Muchos compuestos presentan propiedades antiferromagnéticas debido al acoplamiento antiparalelo de los espines de los iones metálicos. Un ejemplo de esto lo constituye el MOF $Mn_2(tzc)_2(bpea)$ (Htzc=ácido tetrazólico, bpea= 1,2-bis(4-piridil)etano)),[63] el cual está constituido por capas que presentan dobles puentes μ_3-tzc y carboxilato, las cuales se unen a través del ligando espaciador bpea para generar una estructura tridimensional que presenta acoplamiento antiferromagnético entre los iones Mn^{2+}(figura 1.21a y 1.21b).

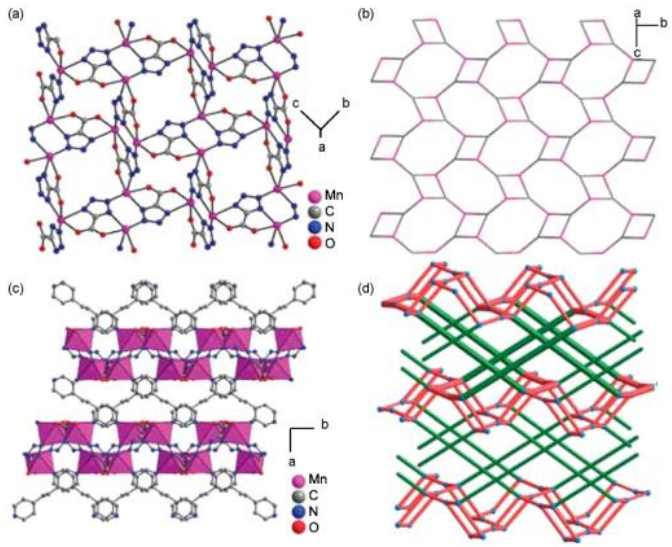

Figura 1.21. *Estructura del MOF $Mn_2(tzc)_2(bpea)$. a) Capa 2D con puentes μ3-tzc y carboxilato. b) topología 2D de la estructura. c) estructura 3D. d) topología 3D mostrando la interpenetración en líneas verdes oscuras.*

Otro ejemplo lo constituye el MOF $Co_3(TATB)_2(H_2O)_2{\cdot}2DMA{\cdot}3H_2O$ (TATB = 4,4′,4′′-s-triazine-2,4,6-triyl-tribenzoato; DMA = dimetilacetamida)formado por clusters trimetálicos en forma de reloj de arena unidos por el ligando orgánico, siendo el cluster el responsable de las propiedades magnéticas del MOF.[64] En la estructura cada par de ligandos se unen a tres clusters de Co^{2+} y cada cluster se enlaza a tres pares de ligandos, de forma que se construye una red tridimensional con canales en la dirección del eje *c* (figura 1.22a). Las medidas de susceptibilidad magnética indican que en este MOF existe acoplamiento antiferromagnético entre los átomos de Co^{2+} dentro del rango de temperatura medido (2-300K) (figura 1.21b).

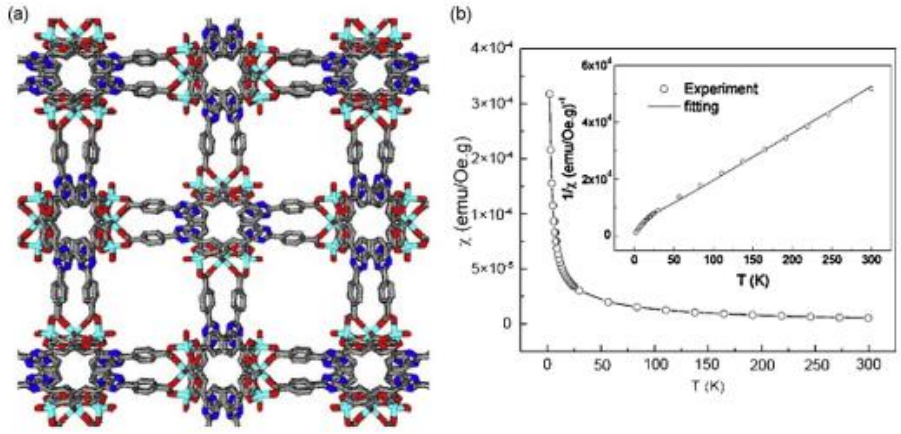

Figura 1.22. *a) Estructura 3D del compuesto $Co_3(TATB)_2(H_2O)_2{\cdot}2DMA{\cdot}3H_2O$. b) Representación de la susceptibilidad en función de la temperatura (en el interior se muestra la curva 1/ χ frente a T con un ajuste teórico)*

1.3.2.3.Propiedades Ferrimagnéticas

Normalmente los sistemas ferrimagnéticos presentan dos tipos de portadores de spin que alternan regularmente e interactúan antiferromagnéticamente. Sin embargo, existen sistemas ferrimagnéticos con un tipo de spin que solo poseen un tipo de portador de spin, en los que a pesar del acoplamiento antiferromagnético, se consigue la no cancelación de espines como consecuencia de un ordenamiento particular de los mismos. Un ejemplo de esto es el MOF $Cu_3(L)_2(VO_3)_4$ (L = (5-pirimidin-2-il)tetrazolato);[65] en esta estructura existen dos centros de Cu^{2+} cristalográficamente independientes que son los responsables de este comportamiento ferrimagnético, con T_N=10K (figura 1.23).

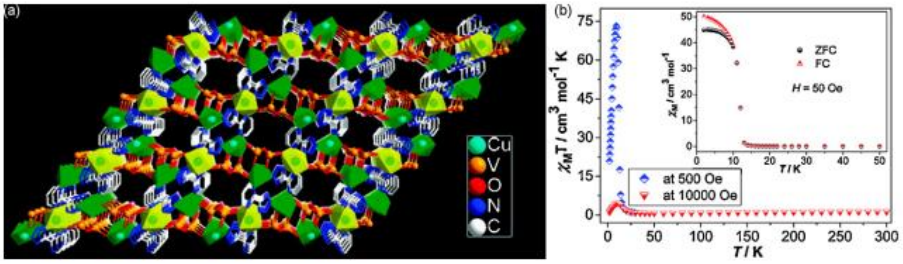

Figura 1.23. *a) Estructura 3D del compuesto $Cu_3(L)_2(VO_3)_4$. b) Representación de $\chi_m T$ frente a T a diferentes campos y representación en el interior de la susceptibilidad a campo cero.*

1.3.2.4. Frustación y spin canting

Los materiales magnéticamente frustrados han sido centro de atención en los últimos tiempos debido a que en estos materiales las interacciones competitivas suprimen o reducen significativamente el ordenamiento magnético. La frustración magnética se observa en redes con forma de plaquetas triangulares o tetraédricas.[66] Ejemplo de ello es el compuesto $Mn[Mn_3(\mu_3\text{-}F)(bta)_3(H_2O)_6]_2$,[67] (bta= bis(5-tetrazol)amine) que es una capa bidimensional que alternan centros de tres átomos de Mn^{2+} y otros mononucleares. Este compuesto a bajas temperaturas se comporta antiferromagnéticamente (figura 1.24). La estequiometría y la forma de conectarse las entidades mono- y trinucleares de Mn^{2+} en la capas permiten generar un momento de spin sin compensar, motivo de la frustración magnética.

Al contrario que el ferrimagnetismo, el spin residual proveniente de la perturbación de un acoplamiento paralelo o antiparalelo puede inducir spin canting. El origen de este comportamiento magnético reside en interacciones asimétricas de intercambio y en anisotropía magnética del ion y que se manifiesta con un momento magnético distinto a cero a la temperatura de 0 K.

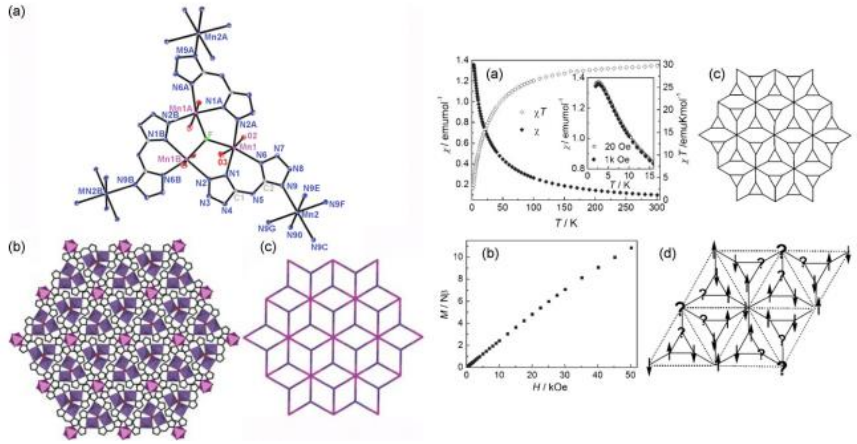

Figura 1.24. *Izq: vistas de las estructuras mostrando a) entorno de coordinación del metal y del ligando, b) capa 2D, red de tipo 6-3. Derecha: a) dependencia de la susceptibilidad del compuesto, b) representación de la magnetización dependiente del campo, c) topología de la red 2D, d) ilustración de la frustración en un segmento trinuclear de* Mn^{2+}.

Bastantes MOFs han presentado este comportamiento, como el MOF de Co^{II}, $Co_2(L)_2(H_2O)_2$ (L = 2,1,3-tiadiazol-4,5-carboxilato),[68] en cual presenta dos únicos centros de Co^{II} en la unidad asimétrica, y estos átomos se unen a los ligandos para generar la estructura tridimensional. Los centros de Co^{II} son los responsables de las propiedades magnéticas que se muestran en la figura 1.24, con un comportamiento ferromagnético entre los átomos de Co^{2+}, existiendo acoplamientos Co1-Co2, Co1-Co1 y Co2-Co2 que son antiferromagnéticos (figura 1.25). Por lo que la causa de este ordenamiento magnético se debe a un ordenamiento magnético débil, llamado canting.

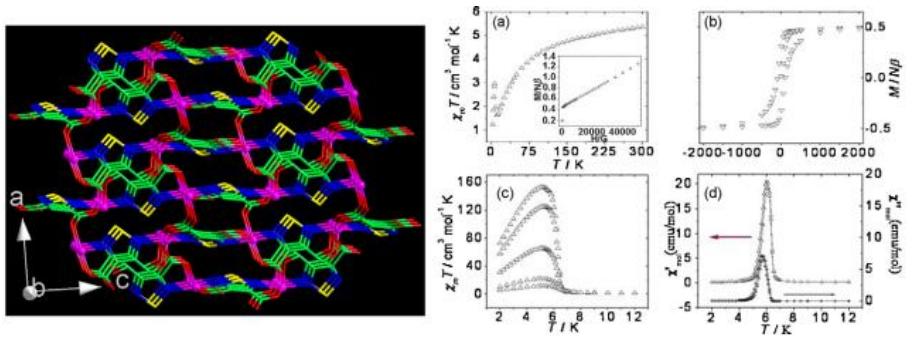

Figura 1.25. *Izq: vista de la estructura 3D del MOF (átomos de oxígeno sin coordinar y moléculas de agua han sido omitidas por claridad). Der: a) representación de de $\chi_m T$ frente a T (en el interior se representa la magnetización a 2K), b) ciclo de histéresis, c) representación de de $\chi_m T$ frente a T a diferentes campos (desde 1000 hasta 50G) y a baja temperatura, d) representación de la susceptibilidad ac*

1.3.2.5. Cambio Magnético Inducido en MOFs

Entre los esfuerzos para introducir funciones específicas en los MOFs, la incorporación de centros electrónicamente activos (switching) es una aplicación muy interesante para crear materiales magnéticamente activos. Cuando hablamos de centros electrónicamente activos nos referimos a metales de transición d^4-d^7 que pueden cambiar entre los estados de alto y bajo spin como respuesta a la variación de temperatura, presión o irradiación.[69]

Un ejemplo de este comportamiento es observado en el MOF nanoporoso $[Fe_2(azpy)_4(NCS)_4 \cdot (disolvente)]$[70], que se puede definir como unas dobles capas interpenetradas formadas por los centros activos Fe2+, formando una estructura que posee canales en los que se alojan las moléculas de disolvente que son adsorbidas y desorbidas de manera reversible (figura 1.26)

La flexibilidad que presenta esta red permite la adsorción y posterior liberación de las moléculas de disolvente , lo que causa unos cambios sustanciales en la geometría de los centros metálicos de Fe^{2+}, que afectaran a sus propiedades magnéticas. Como se puede apreciar en la figura 1.26 el MOF que contiene EtOH en el interior de los canales muestra un momento magnético efectivo de 5.3 mB en el rango de temperatura entre 300 y 150 K. Por debajo de esta temperatura el valor decrece hasta un valor constante de 3.65 mB, mientras que para el caso del material que no presenta molécula de disolvente el momento magnético presenta un valor constante de 5.1 mB, indicando que la fase con disolvente, la fase adsorbida

presenta spin-crossover, mientras que la fase desorbida no muestra un comportamiento de spin-crossover

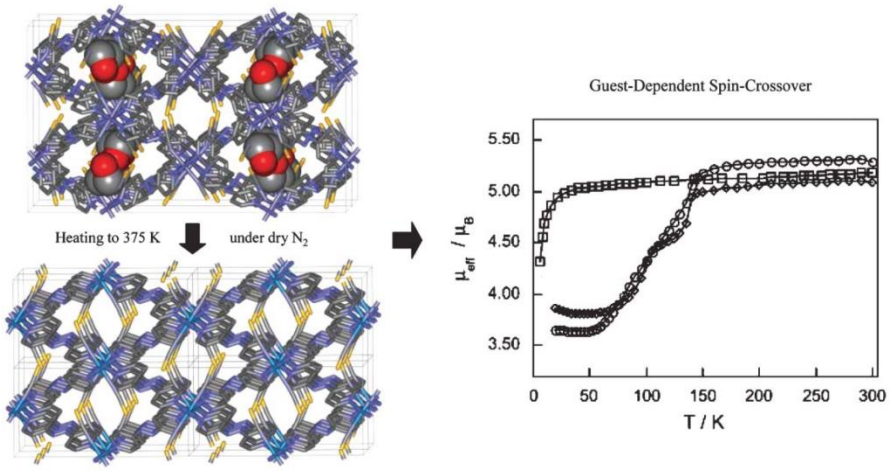

Figura 1.26. *(Izq) Representación de la estructura $[Fe_2(azpy)_4(NCS)_4 \cdot (EtOH)]$ a 150 y 375 K. (Der) Representación del momento magnético dependiendo de la temperatura de (O) el MOF $[Fe_2(azpy)_4(NCS)_4 \cdot (EtOH)]$, (□) el MOF sin el disolvente $[Fe_2(azpy)_4(NCS)_4]$ y (◊) el MOF $[Fe_2(azpy)_4(NCS)_4 \cdot (1\text{-}PrOH)]$ resultante de exponer la red sin disolvente a 1-Propanol.*

1.3.3. APLICACIONES EN LUMINISCENCIA

Los materiales tradicionales luminiscentes inorgánicos y orgánicos han sido ampliamente estudiados y empleados en diversas aplicaciones tales como en dispositivos luminosos, ópticos o sensores[71]. De hecho, algunos de estos materiales luminiscentes, como $BaMgAl_{10}O_{17}:Eu^{2+}$ y $GdMgB_5O_{10}:Tb^{3+}$, han sido comercializados y empleados como lámparas luminiscentes azul y verde, respectivamente. Estas propiedades luminiscentes se deben a un gran número de factores, tales como estructura atómica, homogeneidad de la composición, tamaño de partícula, defectos estructurales y/o microestructura. El interés en la luminiscencia de materiales orgánicos se inició a principios de la década de los 80 por sus aplicaciones en diodos orgánicos emisores de luz (OLEDs).[72] En este sentido, la combinación de componentes inorgánicos y orgánicos originaron una gran variedad de estructuras con propiedades luminiscentes muy interesantes[4,10a,73]

La luminiscencia es el fenómeno por el cual la luz se emite debido a una absorción de energía previa. La luminiscencia presenta dos formas básicas: fluorescencia y fosforescencia (figura 1.27), dependiendo de la multiplicidad de spin

de los estados de energía durante el proceso de relajación. La fluorescencia ocurre entre estados que presentan la misma multiplicidad de spin, con un tiempo de vida medio no superior a 10 nanosegundos, mientras que la fosoforescencia se refiere al proceso de emisión que tiene lugar entre estados con diferente multiplicidad de spin, y la duración del proceso se encuentra entre microsegundos y segundos, es decir, la fosforescencia conlleva una emisión más prolongada que en la fluorescencia.

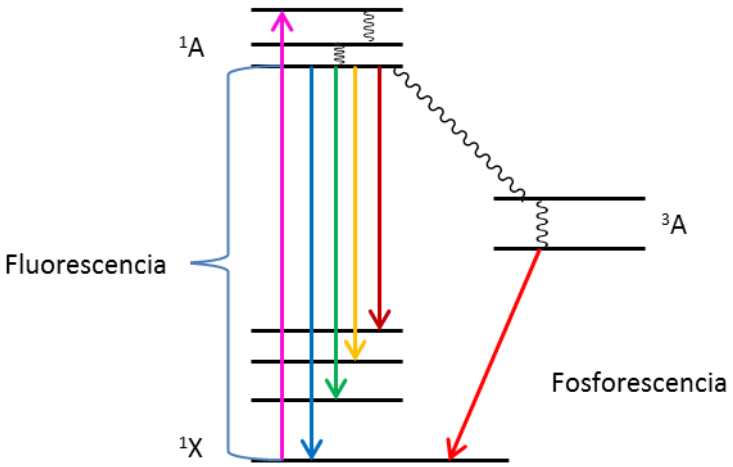

Figura 1.27. *Diagrama de Jablonski que muestra la disposición de los estados electrónicos que participan en el fenómeno dela luminiscencia.*

La luminiscencia en este tipo de estructuras se puede producir debido a diversos factores como el ligando orgánico empleado (especialmente aquellos que poseen elevada conjugación), el centro metálico (ampliamente observado en los MOF que poseen lantánidos, a través de lo que se conoce como efecto antena), transferencia de carga desde el ligando al metal (LMTC) o desde el metal al ligando (MLTC) y, por último, se puede producir debido a las moléculas huésped que se alojan en los MOFs.

Con todo esto no resulta extraño que el número de MOF que se han investigado y publicado con propiedades luminiscentes sea muy elevado. A continuación se van a mostrar distintos ejemplos de MOFs que muestran propiedades luminiscentes basadas en los factores mencionados con anterioridad.

1.3.3.1.Luminiscencia basada en el ligando

En los MOFs se suele utilizar un amplio abanico de ligandos, empleándose comúnmente aquellos que son π-conjugados debido a su rigidez y a que la mayoría presenta un esqueleto rígido y funcionalizado con varios grupos coordinantes (carboxilatos y/o heterociclos). Generalmente, la emisión de un ligando orgánico corresponde con la transición desde el estado excitado singlete de menor energía al estado fundamental singlete; sin embargo, en un MOF la emisión que ofrece un ligando es diferente a la que tiene como molécula libre, debido a que el ligando se estabiliza en el entramado reticular que forma el MOF, permitiendo incrementar la intensidad de fluorescencia y su tiempo de vida medio.

Un ejemplo de ello es el MOF $Zn_3(\mu_5\text{-pta})_2(\mu_2\text{-}H_2O)_2$ (pta = 2,4,6-piridintricarboxilato).[74] El ligando *pta* libre ofrece una longitud de onda de emisión de 415nm cuando se excita a 338nm a temperatura ambiente, aumentando esa longitud de onda de emisión hasta los 467nm cuando forma el MOF de Zn (figura 1.28). Este incremento se atribuye a la formación de la estructura, ya que se ha reforzado la rigidez del esqueleto aromático y se han maximizado las interacciones intra- e intermoleculares entre los linkers orgánicos, disminuyendo la barrera energética entre los orbitales HOMO-LUMO.

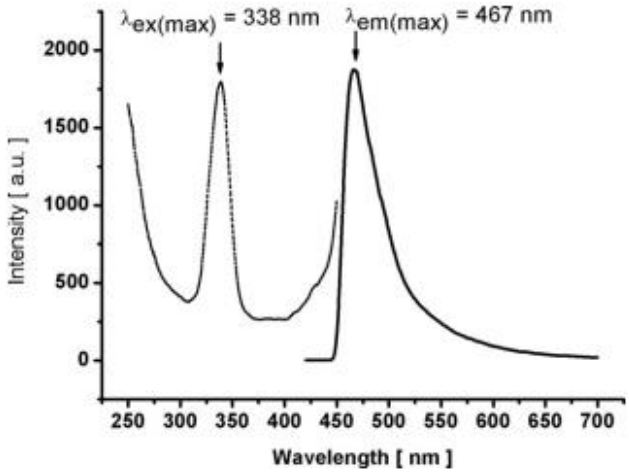

***Figura 1.28**. Espectro de emisión para el MOF $Zn_3(\mu_5\text{-pta})_2(\mu_2\text{-}H_2O)_2$*

1.3.3.2. Luminiscencia basada en lantánidos

Los iones lantánidos (Ln3+) se caracterizan por una ocupación de sus orbitales 4f, desde el $4f^0$ (La^{3+}) hasta el $4f^{14}$ (Lu^{3+}), de forma que se generan una gran variedad de niveles energéticos electrónicos.[75] Los iones lantánidos más empleados son Eu^{3+} y Tb^{3+}, debido a que presentan fuertes y características transiciones que hacen que sus propiedades luminiscentes sean muy interesantes. En los complejos que tienen Eu^{3+} las transiciones que se observan son $^5D_0$ -> $^7F_1$, y $^5D_0$ -> $^7F_2$, mientras que para las estructuras con Tb^{3+}, las transiciones que ofrecen mejor luminiscencia son las $^5D_5$ -> ^7F_J, con J=2,4 y 6.[76]

Sin embargo, los lantánidos poseen una absorción de luz débil debido a las transiciones f-f prohibidas, por lo que para aumentar este proceso se necesitan especies que se acoplen y puedan participar en los procesos de transferencia de energía, dando lugar a lo que se conoce como efecto antena.[71a,75,77] En este mecanismo la luz es absorbida por los ligandos que hay alrededor del centro metálico, se transfiere a los iones lantánidos y la luminiscencia se genera por los lantánidos (figura 1.29). Debido a este proceso de transferencia de energía la luminiscencia del ligando no se observa, aunque si ese proceso no es muy eficiente se puede observar luminiscencia por parte del ligando y del centro metálico.

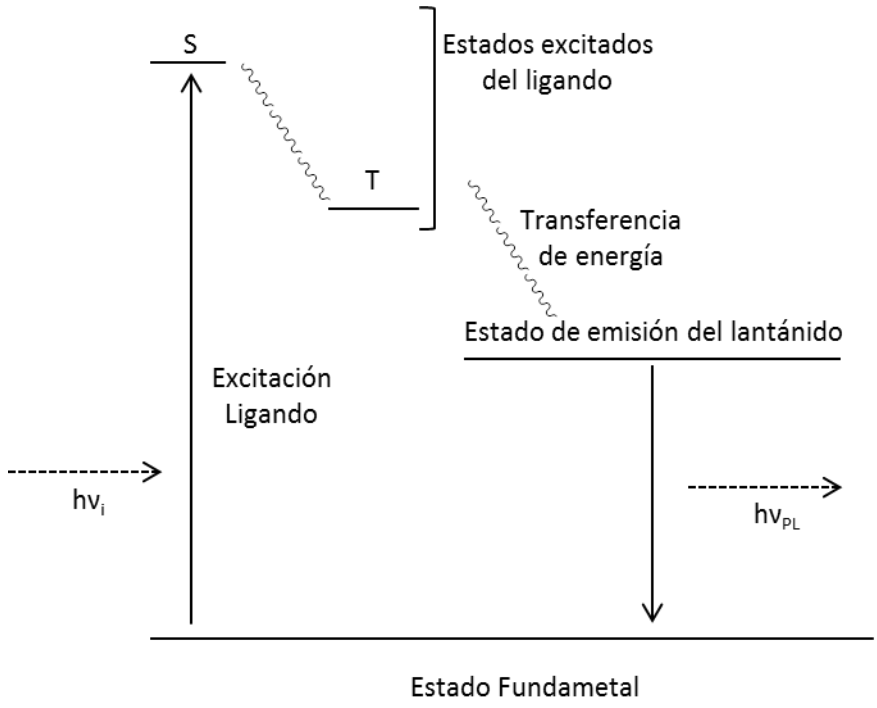

Figura 1.29. *Representación esquemática del efecto antena*

Además, este efecto antena no sólo puede ofrecerlo el ligando orgánico que forma la estructura, sino que también lo puede ofrecer, si existen, las molécula huésped que posea el MOF. Un ejemplo de esto lo constituye el MOF [Eu_2(ácido adípico)$_3$(H_2O)$_2$·4,4'-dipirina, en el que el ligando 4,4'-dipiridina actúa como molécula huésped.[78] Cuando la estructura se excita a una longitud de 236nm, que coincide con el máximo de absorción del ligando, en el espectro de emisión se observan dos picos característicos a 595 y 615 nm atribuidos, respectivamente, a las transiciones del átomo de Eu^{3+} $^5D_0$ -> $^7F_1$, y $^5D_0$ -> $^7F_2$ (figura 1.30).

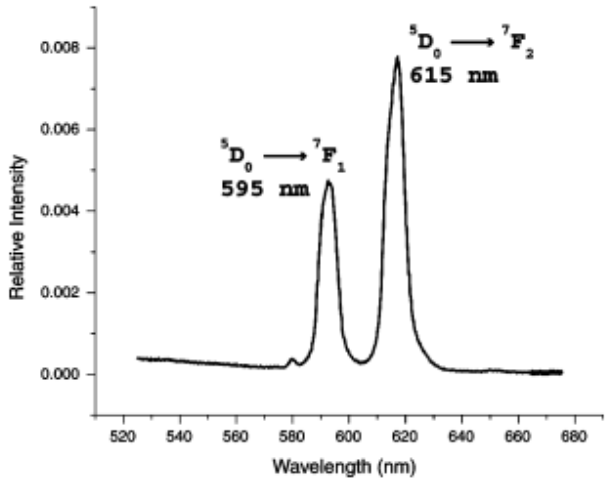

Figura 1.30. *Espectro de fluorescencia para el MOF [Eu_2(ácido adípico)$_3$(H_2O)$_2$·4,4'-dipirina*

1.3.3.3. Luminiscencia basada en procesos de transferencia de carga

La luminiscencia por transferencia de carga en los MOFs se genera gracias a las transiciones permitidas de un estado excitado a su estado fundamental pudiendo ser de dos tipos: transferencia desde el ligando al metal (LMCT) o desde el metal al ligando (MLCT). La LMCT implica transiciones electrónicas desde un orbital del ligando hasta un orbital del metal, mientras que para la MLCT ocurre el proceso contrario, la transferencia tiene lugar desde un orbital del metal hacia un orbital del ligando.

Este tipo de luminiscencia es frecuente en los MOFs basados en los centros metálicos d^{10}, como por ejemplo, en el MOF $Cu_3(C_7H_2NO_3)_2·3H_2O$ ($C_7H_2NO_3$ = ácido 4-hidroxipiridina-2,6-dicarboxílico) fluorescencia a 398 y 478 nm (figura 1.29), siendo

esta luminiscencia originada por la transferencia desde el orbital 3d del átomo de Cu^{2+} hacia los orbitales O-2p y N-2p del ligando.[78b]

Un ejemplo de luminiscencia originada por LMCT lo constituye el MOF [Cd(2,3-pydc)(bpp)(H_2O)]·3H_2O (H_2pydc = ácido piridina-2,3-dicarboxílico)[79] que muestra emisión de fluorescencia intensa a 438 nm cuando se le excita a una longitud de onda de 370 nm (figura 1.31), cuando a este valor de λ el ligando muestra una señal muy débil, debiéndose la fluorescencia a un proceso de transferencia de carga.

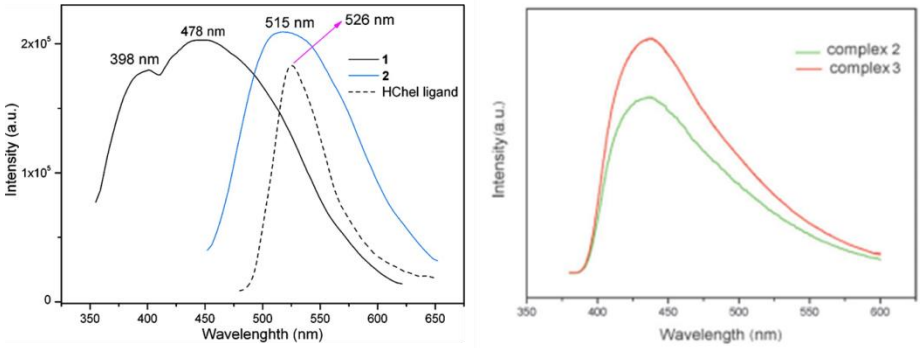

Figura 1.31 *(Izq) Espectro de emisión en estado sólido para el MOF $Cu_3(C_7H_2NO_3)_2·3H_2O$ (1). (Der) Espectro de emisión fluorescente para el MOF [Cd(2,3-pydc)(bpp)(H_2O)]·3H_2O (3).*

1.3.3.4. Luminiscencia inducida por las moléculas huésped

Debido al control del tamaño de poro que se puede desarrollar en los MOFs, se pueden encapsular diferentes especies, como iones lantánidos o pigmentos fluorescentes, para mejorar las propiedades luminiscentes de estos compuestos. Es lo que ocurre con el bio-MOF-1, que fue dopado con diferentes iones lantánidos (Tb^{3+}, Sm^{3+}, Eu^{3+}, Yb^{3+}) obteniendo una serie nueva (@bio-MOF-1) de MOFs.[80] En ellos, cuando se excita a 365 nm, los MOFs dopados emiten colores distintivos (Eu^{3+}, rojo; Tb^{3+}, verde; Sm^{3+}, naranja-rosa) (figura 1.32)

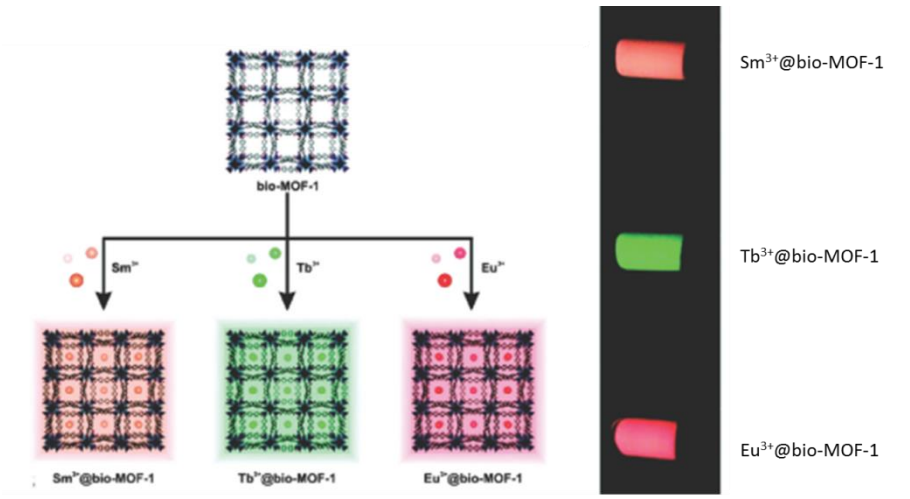

Figura 1.32. *Luminiscencia de los distintos @bio-MOF-1 dopados con lantánidos.*

Como se ha mencionado anteriormente, el número de MOFs que presentan propiedades luminiscentes es muy amplio ya que, como hemos visto, esta luminiscencia puede provenir de muchos y diferentes factores, haciendo que las aplicaciones de estos materiales luminiscentes también sean muy variadas.

Los MOFs porosos y luminiscentes se suelen emplear como sensores de iones (cationes y aniones),[81] ya que las propiedades luminiscentes de los MOFs cambian al adsorber esos iones. También son empleados como sensores de moléculas pequeñas (tolueno, acetona o agua)[82], así como de gases o vapores(oxígeno y nitrógeno)[83], además de explosivos en fase gaseosa como DNT o DMNB.[84]

Otro de sus usos más extendidos es el empleo de estos materiales como dispositivos emisores de luz debido a su diversidad estructural y luminiscencia modificable, ya sea como emisores de luz blanca[85] o emisores en la franja del infrarrojo cercano[86] (sistemas de iluminación-nocturna, sistemas ópticos de telecomunicación).

Por último, hay que destacar su uso en un tema tan apasionante y esperanzador como es el de la biomedicina. Estos MOFs con propiedades luminiscentes y porosas se pueden emplear como transportadores de agentes anticancerígenos, como adsorbentes de NO (molécula de elevada importancia en diversos procesos biológicos) y/o como agentes de contraste, obteniendo hasta el momento unos resultados muy prometedores.[80,87]

1.4 NUESTRA INVESTIGACIÓN

Con lo expuesto anteriormente, queda claro que la síntesis de MOFs multifuncionales constituye un campo de investigación muy abierto, interesante y con gran aplicabilidad. En este sentido, en nuestro grupo de investigación se había trabajado en sistemas que presentaran propiedades magnéticas relevantes;[88] además, con ese propósito, habían comenzado a utilizar los métodos solvotermales,[89] siendo uno de los primeros grupos en utilizarlos a nivel nacional en el campo de la Química de la Coordinación.

Por ello, con la experiencia adquirida en estas técnicas, se decidió como tema fundamental de esta Tesis Doctoral el diseño, síntesis y caracterización de nuevos materiales bi- o tridimensionales que presentaran diferentes propiedades, especialmente propiedades de adsorción, magnéticas y/o luminiscentes.

Para ello se han utilizado sales de metales de transición como cadmio, cobalto, cobre, níquel y zinc, así como de diversos iones lantánidos. El átomo de cobre tiene una esfera de coordinación octaédrica muy plástica que favorece la formación de diversas estructuras con él. El hecho de emplear sales de cadmio y zinc deriva de su capacidad como elementos d^{10} para formar compuestos con propiedades luminiscentes, que serán favorecidas por el empleo de ligandos con elevada aromaticidad. Asimismo, es de esperar que al utilizar sales de cobalto y níquel, los compuestos resultantes presenten unas interesantes propiedades magnéticas.

Para construir los nuevos materiales que se presentan en esta Tesis Doctoral se han empleado ligandos comerciales y ligandos que han sido sintetizados por primera vez con este fin, ya sea por métodos tradicionales o, aprovechando las ventajas de los métodos solvotermales, sintetizándolos *in situ* en el seno de la reacción solvotermal.

Se han escogido ligandos de carácter carboxílico por la labilidad de los enlaces metal-oxígeno, así como la cierta direccionalidad que ofrecen los grupos carboxilato, lo que presumiblemente, favorecerá la formación de estructuras tridimensionales escogiendo los átomos metálicos adecuados. Además, la presencia de anillos aromáticos en buena parte de los ligandos escogidos contribuirá a la presencia de propiedades luminiscentes en los materiales que se obtengan A continuación, en el esquema 1.2, se exponen los ligandos comerciales usados en esta Tesis Doctoral

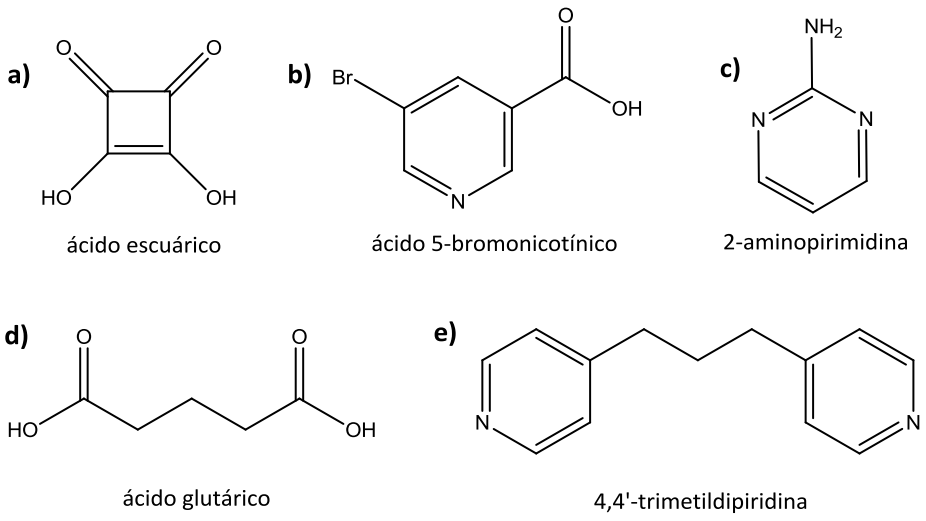

Esquema 1.2. *Ligandos comerciales empleados en esta Tesis Doctoral en la síntesis de MOFs*

Como se ha mencionado anteriormente, una de las ventajas de los métodos solvotermales es la síntesis *in situ* de los ligandos que forman la estructura de los materiales que se obtienen. En este aspecto, una de las reacciones más interesantes es la síntesis de tetrazoles a partir de grupos carbonitrilo en disolución acuosa (reacción de Demko y Sharpless).

El hecho de usar ligandos grupos tetrazolatos es porque son similares a los ácidos carboxílicos en lo que a capacidad de actuar como ácido se refiere, con un valor de pKa alrededor de 4.9. Además, la presencia de múltiples átomos de N dadores aumenta el número de modos de coordinación del ligando con el centro metálico generando un amplio abanico de posibilidades que desembocan en fascinantes estructuras.

Los ligandos sintetizados *in situ* empleados en esta Tesis Doctoral son los que aparecen en el esquema 1.3

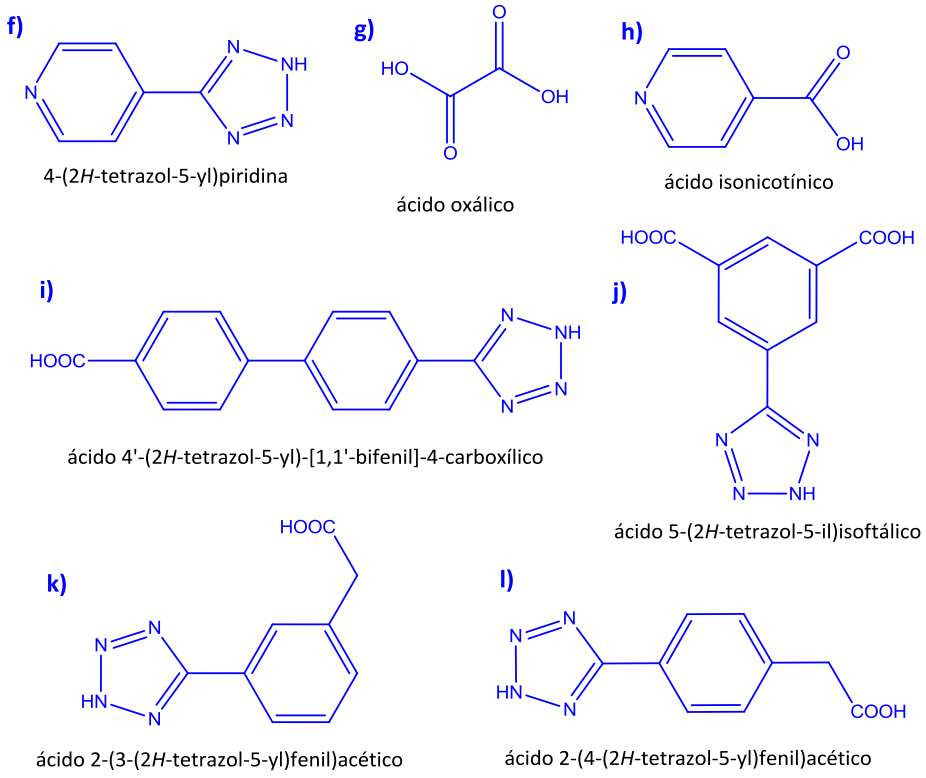

Esquema 1.3. *Ligandos empleados en esta Tesis Doctoral obtenidos in situ en reacciones solvotermales en la síntesis de MOFs*

También se han conseguido sintetizar, en colaboración con el profesor D. Manuel Melguizo del Departamento de Química Inorgánica y Orgánica de la Universidad de Jaén, un nuevo ligando orgánicos con un esqueleto tetrazínico (esquema 1.4), con los que se han sintetizado algunos materiales como primer paso en el empleo de estos ligandos para la síntesis de MOFs.

m)

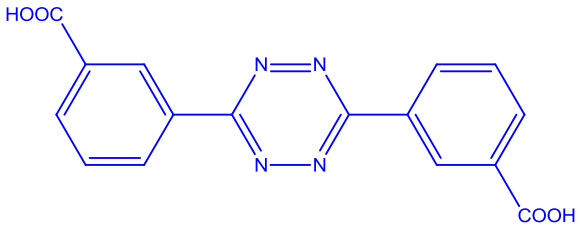

ácido 3,3'-(1,2,4,5-tetrazina-3,6-diyl)dibenzoico

Esquema 1.4. *Ligandos con el esqueleto tetrazínico obtenidos en esta Tesis Doctoral.*

Empleando estos ligandos, hemos sido capaces de sintetizar una gran cantidad de compuestos multidimensionales, presentando en esta Tesis Doctoral un total de 32 nuevas estructuras, las cuales se irán describiendo en los siguientes capítulos.

1.5. OBJETIVOS

Una de las áreas de investigación más activas en el campo de la Química de Coordinación es la que se dedica al estudio de nuevos MOFs multifuncionales. Es por ello que esta Tesis Doctoral se encuadra en ese campo y tiene como objetivo fundamental el diseño, síntesis, caracterización estructural y estudio de las propiedades de adsorción, luminiscentes y magnéticas que presenten nuevos materiales multidimensionales sintetizados a partir de diferentes técnicas.

Los objetivos concretos que se persiguen son:

1. Obtener mediante técnicas solvotermales compuestos bi- y tridimensionales de iones metálicos divalentes, así como de iones lantánidos con ligandos, principalmente, de carácter carboxílico y tetrazolato.

2. Sintetizar mediante técnicas solvotermales compuestos tridimensionales constituidos por ligandos formados *in situ* en el seno de la reacción solvotermal; para ello se emplearán principalmente ligandos que posean grupos cianuro que son susceptibles de reaccionar en presencia de azida sódica para dar grupos tetrazolatos (reacción Demko-Sharpless) tal y como se muestra en el esquema 1.x.. Estos

grupos tetrazolato han sido empleados ampliamente en síntesis de compuestos multidimensionales debido a los múltiples modos de coordinación que presentan.

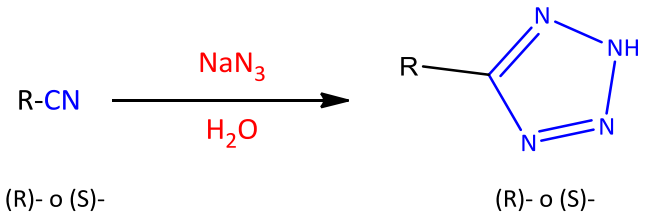

Esquema 1.x. *Representación de la reacción de Demko y Sharpless*

3. Diseñar y sintetizar mediante diferentes métodos MOFs tridimensionales y porosos, empleando para ello iones divalentes que puedan presentar geometrías de coordinación octaédricas (Cd^{2+}, Cu^{2+}), y ligandos dicarboxílicos.

4. Caracterizar estructuralmente todos los materiales aislados mediante las siguientes técnicas instrumentales: análisis elemental (AE), espectroscopía de infrarrojo (IR), análisis térmico (TG y DSC) y difracción de rayos X monocristal (DRX). En caso de no conseguir aislar cristales de algún MOF se caracterizará por difracción de rayos X en polvo (DRXP).

5. Estudiar las propiedades de adsorción, luminiscentes y/o magnéticas que pudieran presentar los materiales aislados. Para ello se realizarán las correspondientes isotermas de adsorción, medidas en espectroscopía ultravioleta-visible y/o medidas de susceptibilidad magnética.

BIBLIOGRAFÍA

(1) Ihde, A. J. *The Development of Modern Chemistry*; Dover Publications: New York, 1964.

(2) Shibata, Y. *Journal of the College of Science, Imperial University of Tokyo* **1916**, *37*, 1.

(3) Bailar, J. C., Jr. *Preparative Inorg. Reactions* **1964**, *1*, 1.

(4) Yaghi, O. M.; Li, H. *Journal of the American Chemical Society* **1995**, *117*, 10401.

(5) (a) Coordination Polymers and Metal Organic Frameworks: Terminology and Nomenclature Guidelines, http://www.iupac.org/web/ins/2009-012-2-200; (b) Öhrström, L.; in Chemistry International, IUPAC, 2010, January–February, 23

(6) O'Keeffe, M.; Peskov, M. A.; Ramsden, S. J.; Yaghi, O. M. *Accounts of Chemical Research* **2008**, *41*, 1782.

(7) (a) Kanoo, P.; Matsuda, R.; Higuchi, M.; Kitagawa, S.; Maji, T. K. *Chemistry of Materials* **2009**, *21*, 5860(b) McDonald, T. M.; Lee, W. R.; Mason, J. A.; Wiers, B. M.; Hong, C. S.; Long, J. R. *Journal of the American Chemical Society* **2012**, *134*, 7056(c) Mu, B.; Li, F.; Huang, Y.; Walton, K. S. *Journal of Materials Chemistry* **2012**, *22*, 10172(d) Qian, J.; Jiang, F.; Yuan, D.; Wu, M.; Zhang, S.; Zhang, L.; Hong, M. *Chemical Communications (Cambridge, United Kingdom)* **2012**, *48*, 9696(e) Zhang, F.; Zou, X.; Gao, X.; Fan, S.; Sun, F.; Ren, H.; Zhu, G. *Advanced Functional Materials* **2012**, *22*, 3583.

(8) (a) Borjigin, T.; Sun, F.; Zhang, J.; Cai, K.; Ren, H.; Zhu, G. *Chemical Communications (Cambridge, United Kingdom)* **2012**, *48*, 7613(b) Das, M. C.; Guo, Q.; He, Y.; Kim, J.; Zhao, C.-G.; Hong, K.; Xiang, S.; Zhang, Z.; Thomas, K. M.; Krishna, R.; Chen, B. *Journal of the American Chemical Society* **2012**, *134*, 8703.

(9) (a) Cirujano, F. G.; Llabres i Xamena, F. X.; Corma, A. *Dalton Transactions* **2012**, *41*, 4249(b) Harding, J. L.; Reynolds, M. M. *Journal of the American Chemical Society* **2012**, *134*, 3330(c) Li, B.; Zhang, Y.; Ma, D.; Li, L.; Li, G.; Li, G.; Shi, Z.; Feng, S. *Chemical Communications (Cambridge, United Kingdom)* **2012**, *48*, 6151.

(10) (a) Meek Scott, T.; Greathouse Jeffery, A.; Allendorf Mark, D. *Advanced materials (Deerfield Beach, Fla.)* **2011**, *23*, 249(b) Qin, J.-S.; Du, D.-Y.; Li, W.-L.; Zhang, J.-P.; Li, S.-L.; Su, Z.-M.; Wang, X.-L.; Xu, Q.; Shao, K.-Z.; Lan, Y.-Q. *Chemical Science* **2012**, *3*, 2114(c) Wang, H.-N.; Meng, X.; Yang, G.-S.; Wang, X.-L.; Shao, K.-Z.; Su, Z.-M.; Wang, C.-G. *Chemical Communications (Cambridge, United Kingdom)* **2011**, *47*, 7128.

(11) (a) Della Rocca, J.; Liu, D.; Lin, W. *Accounts of Chemical Research* **2011**, *44*, 957(b) Xu, H.; Rao, X.; Gao, J.; Yu, J.; Wang, Z.; Dou, Z.; Cui, Y.; Yang, Y.; Chen, B.; Qian, G. *Chemical Communications (Cambridge, United Kingdom)* **2012**, *48*, 7377(c) Zhang, J.; Sun, L.; Xu, F.; Li, F.; Zhou, H.-Y.; Liu, Y.-L.; Gabelica, Z.; Schick, C. *Chemical Communications (Cambridge, United Kingdom)* **2012**, *48*, 759.

(12) Fukushima, T.; Horike, S.; Inubushi, Y.; Nakagawa, K.; Kubota, Y.; Takata, M.; Kitagawa, S. *Angewandte Chemie, International Edition* **2010**, *49*, 4820.

(13) (a) Dan-Hardi, M.; Serre, C.; Frot, T.; Rozes, L.; Maurin, G.; Sanchez, C.; Ferey, G. *Journal of the American Chemical Society* **2009**, *131*, 10857(b) Rieter, W. J.; Pott, K. M.; Taylor, K. M. L.; Lin, W. *Journal of the American Chemical Society* **2008**, *130*, 11584.

(14) (a) Liu, C. B.; Ferreira, R. A. S.; Almeida Paz, F. A.; Cadiau, A.; Carlos, L. D.; Fu, L. S.; Rocha, J.; Shi, F. N. *Chemical Communications (Cambridge, United Kingdom)* **2012**, *48*, 7964(b) Niu, D.; Yang, J.; Guo, J.; Kan, W.-Q.; Song, S.-Y.; Du, P.; Ma, J.-F. *Crystal Growth & Design* **2012**, *12*, 2397(c) Cui, Y.; Xu, H.; Yue, Y.; Guo, Z.; Yu, J.; Chen, Z.; Gao, J.; Yang, Y.; Qian, G.; Chen, B. *Journal of the American Chemical Society* **2012**, *134*, 3979(d) Yan, C.; Li, K.; Wei, S.-C.; Wang, H.-P.; Fu, L.; Pan, M.; Su, C.-Y. *Journal of Materials Chemistry* **2012**, *22*, 9846.

(15) (a) Yan, Z.; Li, M.; Gao, H.-L.; Huang, X.-C.; Li, D. *Chemical Communications (Cambridge, United Kingdom)* **2012**, *48*, 3960(b) Chuang, Y.-C.; Liu, C.-T.; Sheu, C.-F.; Ho, W.-L.; Lee, G.-H.; Wang, C.-C.; Wang, Y. *Inorganic Chemistry (Washington, DC, United States)* **2012**, *51*, 4663(c) Sarma, D.; Mahata, P.; Natarajan, S.; Panissod, P.; Rogez, G.; Drillon, M. *Inorganic Chemistry (Washington, DC, United States)* **2012**, *51*, 4495(d) Ferrando-Soria, J.; Serra-Crespo, P.; de Lange, M.; Gascon, J.; Kapteijn, F.; Julve, M.; Cano, J.; Lloret, F.; Pasan, J.; Ruiz-Perez, C.; Journaux, Y.; Pardo, E. *Journal of the American Chemical Society* **2012**, *134*, 15301(e) Coronado, E.; Gimenez-Marques, M.; Espallargas, G. M.; Brammer, L. *Nature Communications* **2012**, *3*, 1827/1.

(16) S. Kitagawa, R. Kitaura, S. Noro, Angew. Chem. Int. Ed. 2004, 43, 2334

(17) Kaye, S. S.; Dailly, A.; Yaghi, O. M.; Long, J. R. *Journal of the American Chemical Society* **2007**, *129*, 14176.

(18) Park, K. S.; Ni, Z.; Cote, A. P.; Choi, J. Y.; Huang, R.; Uribe-Romo, F. J.; Chae, H. K.; O'Keeffe, M.; Yaghi, O. M. *Proceedings of the National Academy of Sciences of the United States of America* **2006**, *103*, 10186.

(19) (a) Cai, Y.; Zhang, Y.; Huang, Y.; Marder, S. R.; Walton, K. S. *Crystal Growth & Design* **2012**, *12*, 3709(b) Das, S.; Kim, H.; Kim, K. *Journal of the American Chemical Society* **2009**, *131*, 3814(c) Guillerm, V.; Ragon, F.; Dan-Hardi, M.; Devic, T.; Vishnuvarthan, M.; Campo, B.; Vimont, A.; Clet, G.; Yang, Q.; Maurin, G.; Ferey, G.; Vittadini, A.; Gross, S.; Serre, C. *Angewandte Chemie, International Edition* **2012**, *51*, 9267(d) He, J.; Yu, J.; Zhang, Y.; Pan, Q.; Xu, R.

Inorg. Chem. **2005**, *44*, 9279(e) Li, H.; Shi, W.; Zhao, K.; Li, H.; Bing, Y.; Cheng, P. *Inorg. Chem.* **2012**, *51*, 9200(f) Luo, F.; Zheng, J.-m.; Batten, S. R. *Chemical Communications (Cambridge, United Kingdom)* **2007**, 3744(g) Ma, L.; Jin, A.; Xie, Z.; Lin, W. *Angewandte Chemie, International Edition* **2009**, *48*, 9905(h) Qin, L.; Hu, J.-S.; Zhang, M.-D.; Li, Y.-Z.; Zheng, H.-G. *CrystEngComm* **2012**, *14*, 8274(i) Wang, X.-J.; Li, P.-Z.; Liu, L.; Zhang, Q.; Borah, P.; Wong, J. D.; Chan, X. X.; Rakesh, G.; Li, Y.; Zhao, Y. *Chemical Communications (Cambridge, United Kingdom)* **2012**, *48*, 10286(j) Zhang, J.; Wojtas, L.; Larsen, R. W.; Eddaoudi, M.; Zaworotko, M. J. *Journal of the American Chemical Society* **2009**, *131*, 17040(k) Zhao, T.; Jing, X.; Wang, J.; Wang, D.; Li, G.; Huo, Q.; Liu, Y. *Crystal Growth & Design* **2012**, *12*, 5456.

(20) (a) Carson, C. G.; Brown, A. J.; Sholl, D. S.; Nair, S. *Crystal Growth & Design* **2011**, *11*, 4505(b) Huh, S.; Jung, S.; Kim, Y.; Kim, S.-J.; Park, S. *Dalton Transactions* **2010**, *39*, 1261(c) Li, Z.-Q.; Qiu, L.-G.; Xu, T.; Wu, Y.; Wang, W.; Wu, Z.-Y.; Jiang, X. *Materials Letters* **2008**, *63*, 78(d) Loera-Serna, S.; Oliver-Tolentino, M. A.; Lopez-Nunez, M. d. L.; Santana-Cruz, A.; Guzman-Vargas, A.; Cabrera-Sierra, R.; Beltran, H. I.; Flores, J. *Journal of Alloys and Compounds* **2012**, *540*, 113(e) Luo, G.-G.; Wu, D.-L.; Liu, L.; Wu, S.-H.; Li, D.-X.; Xiao, Z.-J.; Dai, J.-C. *Journal of Molecular Structure* **2012**, *1014*, 92(f) Sun, D.; Li, Y.-H.; Wu, S.-T.; Hao, H.-J.; Liu, F.-J.; Huang, R.-B.; Zheng, L.-S. *CrystEngComm* **2011**, *13*, 7311(g) Tahmasian, A.; Morsali, A. *Inorganica Chimica Acta* **2012**, *387*, 327(h) Yan, Y.; Zhang, G.-x.; Zhang, X. *Huaxue Gongchengshi* **2012**, *26*, 13.

(21) (a) Beldon, P. J.; Fabian, L.; Stein, R. S.; Thirumurugan, A.; Cheetham, A. K.; Friscic, T. *Angewandte Chemie, International Edition* **2010**, *49*, 9640(b) Klimakow, M.; Klobes, P.; Rademann, K.; Emmerling, F. *Microporous and Mesoporous Materials* **2012**, *154*, 113(c) Singh, N. K.; Hardi, M.; Balema, V. P. *Chemical Communications (Cambridge, United Kingdom)* **2013**, *49*, 972(d) Yan, D.; Gao, R.; Wei, M.; Li, S.; Lu, J.; Evans, D. G.; Duan, X. *Journal of Materials Chemistry C: Materials for Optical and Electronic Devices* **2013**, *1*, 997.

(22) (a) Cho, H.-Y.; Yang, D.-A.; Kim, J.; Jeong, S.-Y.; Ahn, W.-S. *Catalysis Today* **2012**, *185*, 35(b) Haque, E.; Khan, N. A.; Kim, C. M.; Jhung, S. H. *Crystal Growth & Design* **2011**, *11*, 4413(c) Klinowski, J.; Almeida Paz, F. A.; Silva, P.; Rocha, J. *Dalton Transactions* **2011**, *40*, 321(d) Lin, Z.-J.; Yang, Z.; Liu, T.-F.; Huang, Y.-B.; Cao, R. *Inorg. Chem.* **2012**, *51*, 1813(e) Liu, Y.-Y.; Couck, S.; Vandichel, M.; Grzywa, M.; Leus, K.; Biswas, S.; Volkmer, D.; Gascon, J.; Kapteijn, F.; Denayer, J. F. M.; Waroquier, M.; Van Speybroeck, V.; Van Der Voort, P. *Inorg. Chem.* **2013**, *52*, 113(f) Maniam, P.; Stock, N. *Inorg. Chem.* **2011**, *50*, 5085(g) Yang, W.; Feng, J.; Song, S.; Zhang, H. *ChemPhysChem* **2012**, *13*, 2734.

(23) (a) Devic, T.; Serre, C.; Audebrand, N.; Marrot, J.; Ferey, G. *Journal of the American Chemical Society* **2005**, *127*, 12788(b) Su, C.-Y.; Goforth, A. M.; Smith, M. D.; Pellechia, P. J.; zur Loye, H.-C. *Journal of the American Chemical Society* **2004**, *126*, 3576.

(24) (a) Noll, W. *Nachr. Ges. Wiss. Gottingen, Math.-physik. Klasse.* **1932**, 122(b) Nagai, S. *Zeitschrift fuer Anorganische und Allgemeine Chemie* **1932**, *207*, 313(c) Park, C. F., Jr. *Economic Geology and the Bulletin of the Society of Economic Geologists* **1931**, *26*, 857.

(25) Eddaoudi, M.; Kim, J.; Rosi, N.; Vodak, D.; Wachter, J.; O'Keeffe, M.; Yaghi, O. M. *Science (Washington, DC, United States)* **2002**, *295*, 469.

(26) (a) Liu, C. M.; Gao, S.; Kou, H. Z. *Chemical communications (Cambridge, England)* **2001**, 1670(b) Xiao, D.; Hou, Y.; Wang, E.; Lu, J.; Li, Y.; Xu, L.; Hu, C. *Inorganic Chemistry Communications* **2004**, *7*, 437.

(27) (a) Tao, J.; Zhang, Y.; Tong, M.-L.; Chen, X.-M.; Tan, Y.; Lin, C. L.; Huang, X.; Li, J. *Chemical Communications (Cambridge, United Kingdom)* **2002**, 1342(b) Zhang, X.-M.; Tong, M.-L.; Chen, X.-M. *Angewandte Chemie, International Edition* **2002**, *41*, 1029(c) Xiao, D.; Hou, Y.; Wang, E.; Wang, S.; Li, Y.; De, G.; Xu, L.; Hu, C. *Journal of Molecular Structure* **2003**, *659*, 13.

(28) (a) Xiong, R.-G.; Xue, X.; Zhao, H.; You, X.-Z.; Abrahams, B. F.; Xue, Z. *Angewandte Chemie, International Edition* **2002**, *41*, 3800(b) Xue, X.; Abrahams, B. F.; Xiong, R.-G.; You, X.-Z. *Australian Journal of Chemistry* **2002**, *55*, 495(c) Xue, X.; Wang, X.-S.; Wang, L.-Z.; Xiong, R.-G.; Abrahams, B. F.; You, X.-Z.; Xue, Z.-L.; Che, C.-M. *Inorg. Chem.* **2002**, *41*, 6544(d) Qu, Z.-R.; Zhao, H.; Wang, X.-S.; Li, Y.-H.; Song, Y.-M.; Liu, Y.-J.; Ye, Q.; Xiong, R.-G.; Abrahams, B. F.; Xue, Z.-L.; You, X.-Z. *Inorg. Chem.* **2003**, *42*, 7710.

(29) Cheng, J.-K.; Yao, Y.-G.; Zhang, J.; Li, Z.-J.; Cai, Z.-W.; Zhang, X.-Y.; Chen, Z.-N.; Chen, Y.-B.; Kang, Y.; Qin, Y.-Y.; Wen, Y.-H. *Journal of the American Chemical Society* **2004**, *126*, 7796.

(30) (a) Lin, W.; Ma, L.; Evans, O. R. *Chemical Communications (Cambridge)* **2000**, 2263(b) Evans, O. R.; Lin, W. *Chemistry of Materials* **2001**, *13*, 3009(c) Evans, O. R.; Lin, W. *Chemistry of Materials* **2001**, *13*, 2705.

(31) (a) Li, X.; Cao, R.; Sun, D.; Shi, Q.; Bi, W.; Hong, M. *Inorganic Chemistry Communications* **2003**, *6*, 815(b) Zhang, X.-M.; Wu, H.-S.; Chen, X.-M. *European Journal of Inorganic Chemistry* **2003**, 2959.

(32) (a) Hu, X.-X.; Pan, C.-L.; Xu, J.-Q.; Cui, X.-B.; Yang, G.-D.; Wang, T.-G. *European Journal of Inorganic Chemistry* **2004**, 1566(b) Hu, X.-X.; Xu, J.-Q.; Cheng, P.; Chen, X.-Y.; Cui, X.-B.; Song, J.-F.; Yang, G.-D.; Wang, T.-G. *Inorg. Chem.* **2004**, *43*, 2261(c) Liu, F.; Duan, L.; Li, Y.; Wang, E.; Wang, X.; Hu, C.; Xu, L. *Inorganica Chimica Acta* **2004**, *357*, 1355.

(33) Yan, Y.; Wu, C.-D.; Lu, C.-Z. *Zeitschrift fuer Anorganische und Allgemeine Chemie* **2003**, *629*, 1991.

(34) Zhang, J.-Y.; Cheng, A.-L.; Yue, Q.; Sun, W.-W.; Gao, E.-Q. *Chemical Communications (Cambridge, United Kingdom)* **2008**, 847.

(35) Ni, Z.; Masel, R. I. *Journal of the American Chemical Society* **2006**, *128*, 12394.

(36) Klimakow, M.; Klobes, P.; Thuenemann, A. F.; Rademann, K.; Emmerling, F. *Chemistry of Materials* **2010**, *22*, 5216.

(37) Son, W.-J.; Kim, J.; Kim, J.; Ahn, W.-S. *Chemical Communications (Cambridge, United Kingdom)* **2008**, 6336.

(38) Kitagawa, S.; Kondo, M. *Bulletin of the Chemical Society of Japan* **1998**, *71*, 1739.

(39) Bradshaw, D.; Prior, T. J.; Cussen, E. J.; Claridge, J. B.; Rosseinsky, M. J. *Journal of the American Chemical Society* **2004**, *126*, 6106.

(40) Li, H.; Eddaoudi, M.; Groy, T. L.; Yaghi, O. M. *Journal of the American Chemical Society* **1998**, *120*, 8571.

(41) Horike, S.; Shimomura, S.; Kitagawa, S. *Nature Chemistry* **2009**, *1*, 695.

(42) Serre, C.; Millange, F.; Thouvenot, C.; Nogues, M.; Marsolier, G.; Loueer, D.; Ferey, G. *Journal of the American Chemical Society* **2002**, *124*, 13519.

(43) Frenkel, D.; Smit, B.; Editors *Understanding Molecular Simulation: From Algorithms to Applications*, 1996.

(44) Walton, K. S.; Millward, A. R.; Dubbeldam, D.; Frost, H.; Low, J. J.; Yaghi, O. M.; Snurr, R. Q. *Journal of the American Chemical Society* **2008**, *130*, 406.

(45) Eddaoudi, M.; Moler, D. B.; Li, H.; Chen, B.; Reineke, T. M.; O'Keeffe, M.; Yaghi, O. M. *Accounts of Chemical Research* **2001**, *34*, 319.

(46) (a) Farha, O. K.; Oezguer Yazaydin, A.; Eryazici, I.; Malliakas, C. D.; Hauser, B. G.; Kanatzidis, M. G.; Nguyen, S.-B. T.; Snurr, R. Q.; Hupp, J. T. *Nature Chemistry* **2010**, *2*, 944(b) Furukawa, H.; Ko, N.; Go, Y. B.; Aratani, N.; Choi, S. B.; Choi, E.; Yazaydin, A. O.; Snurr, R. Q.; O'Keeffe, M.; Kim, J.; Yaghi, O. M. *Science (Washington, DC, United States)* **2010**, *329*, 424.

(47) (a) Chen, B.; Ockwig, N. W.; Millward, A. R.; Contreras, D. S.; Yaghi, O. M. *Angewandte Chemie, International Edition* **2005**, *44*, 4745(b) Dinca, M.; Dailly, A.; Liu, Y.; Brown, C. M.; Neumann, D. A.; Long, J. R. *Journal of the American Chemical Society* **2006**, *128*, 16876(c) Dinca, M.; Long, J. R. *Angewandte Chemie, International Edition* **2008**, *47*, 6766.

(48) (a) Himsl, D.; Wallacher, D.; Hartmann, M. *Angewandte Chemie, International Edition* **2009**, *48*, 4639(b) Mulfort, K. L.; Farha, O. K.; Stern, C. L.; Sarjeant, A. A.;

Hupp, J. T. *Journal of the American Chemical Society* **2009**, *131*, 3866(c) Montoro, C.; Garcia, E.; Calero, S.; Perez-Fernandez, M. A.; Lopez, A. L.; Barea, E.; Navarro, J. A. R. *Journal of Materials Chemistry* **2012**, *22*, 10155.

(49) (a) Rowsell, J. L. C.; Millward, A. R.; Park, K. S.; Yaghi, O. M. *Journal of the American Chemical Society* **2004**, *126*, 5666(b) Rowsell, J. L. C.; Yaghi, O. M. *Journal of the American Chemical Society* **2006**, *128*, 1304(c) Wong-Foy, A. G.; Matzger, A. J.; Yaghi, O. M. *Journal of the American Chemical Society* **2006**, *128*, 3494.

(50) Chae, H. K.; Siberio-Perez, D. Y.; Kim, J.; Go, Y. B.; Eddaoudi, M.; Matzger, A. J.; O'Keeffe, M.; Yaghi, O. M. *Nature (London, United Kingdom)* **2004**, *427*, 523.

(51) (a) Ferey, G.; Mellot-Draznieks, C.; Serre, C.; Millange, F.; Dutour, J.; Surble, S.; Margiolaki, I. *Science (New York, N.Y.)* **2005**, *309*, 2040(b) Ferey, G.; Serre, C.; Mellot-Draznieks, C.; Millange, F.; Surble, S.; Dutour, J.; Margiolaki, I. *Angewandte Chemie, International Edition* **2004**, *43*, 6296(c) Latroche, M.; Suble, S.; Serre, C.; Mellot-Draznieks, C.; Llewellyn, P. L.; Lee, J.-H.; Chang, J.-S.; Jhung, S. H.; Ferey, G. *Angewandte Chemie, International Edition* **2006**, *45*, 8227.

(52) (a) Hsu, C.-J.; Tang, S.-W.; Wang, J.-S.; Wang, W.-J. *Molecular Crystals and Liquid Crystals* **2006**, *456*, 201(b) Bakkali, H.; Marie, C.; Ly, A.; Thobie-Gautier, C.; Graton, J.; Pipelier, M.; Sengmany, S.; Leonel, E.; Nedelec, J.-Y.; Evain, M.; Dubreuil, D. *European Journal of Organic Chemistry* **2008**, 2156(c) Kodama, T.; Matsui, M.; (Toyota Motor Corp., Japan). Application: JP 2008.

(53) (a) Johnston, M. R.; Latter, M. J.; Warrener, R. N. *Org. Lett.* **2002**, *4*, 2165(b) Zhang, J. *Acta Crystallographica, Section E: Structure Reports Online* **2010**, *E66*, m1480(c) Gombosuren, N.; Novak, Z.; Kotschy, A.; Mincsovics, E.; Dibo, G. *Journal of Biochemical and Biophysical Methods* **2007**, *69*, 239.

(54) Kodama, T.; (Toyota Motor Corp., Japan). Application: JP 2008.

(55) (a) Warrener, R. N. *e-EROS Encyclopedia of Reagents for Organic Synthesis* **2001**, No pp given(b) Bourrelly, S.; Llewellyn, P. L.; Serre, C.; Millange, F.; Loiseau, T.; Ferey, G. *Journal of the American Chemical Society* **2005**, *127*, 13519(c) Loiseau, T.; Serre, C.; Huguenard, C.; Fink, G.; Taulelle, F.; Henry, M.; Bataille, T.; Ferey, G. *Chemistry--A European Journal* **2004**, *10*, 1373(d) Dinolfo, P. H.; Williams, M. E.; Stern, C. L.; Hupp, J. T. *Journal of the American Chemical Society* **2004**, *126*, 12989(e) Oxtoby, N. S.; Blake, A. J.; Champness, N. R.; Wilson, C. *CrystEngComm* **2003**, *5*, 82.

(56) Kohl, A.; Nielsen, R. *Gas Purification, 5th Edition*, 1997.

(57) Dybtsev, D. N.; Chun, H.; Yoon, S. H.; Kim, D.; Kim, K. *Journal of the American Chemical Society* **2004**, *126*, 32.

(58) Zhang, J.-P.; Ghosh, S. K.; Lin, J.-B.; Kitagawa, S. *Inorg. Chem.* **2009**, *48*, 7970.

(59) Herm, Z. R.; Swisher, J. A.; Smit, B.; Krishna, R.; Long, J. R. *Journal of the American Chemical Society* **2011**, *133*, 5664.

(60) Britt, D.; Tranchemontagne, D.; Yaghi, O. M. *Proceedings of the National Academy of Sciences of the United States of America* **2008**, *105*, 11623.

(61) Forster, R. J.; Keyes, T. E.; Bond, A. M. *Journal of Physical Chemistry B* **2000**, *104*, 6389.

(62) Fujita, W.; Awaga, K. *J Am Chem Soc* **2001**, *123*, 3601.

(63) Jia, Q.-X.; Wang, Y.-Q.; Yue, Q.; Wang, Q.-L.; Gao, E.-Q. *Chemical Communications (Cambridge, United Kingdom)* **2008**, 4894.

(64) Yu, C.; Ma, S.; Pechan, M. J.; Zhou, H.-c. *Journal of Applied Physics* **2007**, *101*, 09E108/1.

(65) Li, J.-R.; Yu, Q.; Sanudo, E. C.; Tao, Y.; Song, W.-C.; Bu, X.-H. *Chemistry of Materials* **2008**, *20*, 1218.

(66) (a) Bartlett, B. M.; Nocera, D. G. *Journal of the American Chemical Society* **2005**, *127*, 8985(b) Paul, G.; Choudhury, A.; Sampathkumaran, E. V.; Rao, C. N. R. *Angewandte Chemie, International Edition* **2002**, *41*, 4297.

(67) Gao, E.-Q.; Liu, N.; Cheng, A.-L.; Gao, S. *Chemical Communications (Cambridge, United Kingdom)* **2007**, 2470.

(68) Li, J.-R.; Yu, Q.; Tao, Y.; Bu, X.-H.; Ribas, J.; Batten, S. R. *Chemical Communications (Cambridge, United Kingdom)* **2007**, 2290.

(69) (a) Guetlich, P.; Goodwin, H. A. *Topics in Current Chemistry* **2004**, *233*, 1(b) Guetlich, P.; Goodwin, H. A. *Comprehensive Coordination Chemistry II* **2004**, *2*, 421.

(70) Halder Gregory, J.; Kepert Cameron, J.; Moubaraki, B.; Murray Keith, S.; Cashion John, D. *Science (New York, N.Y.)* **2002**, *298*, 1762.

(71) (a) Binnemans, K. *Chemical Reviews (Washington, DC, United States)* **2009**, *109*, 4283(b) Carlos, L. D.; Ferreira, R. A. S.; Bermudez, V. d. Z.; Julian-Lopez, B.; Escribano, P. *Chemical Society Reviews* **2011**, *40*, 536(c) Eliseeva, S. V.; Bunzli, J.-C. G. *Chemical Society Reviews* **2010**, *39*, 189(d) Hwang, S.-H.; Moorefield, C. N.; Newkome, G. R. *Chemical Society Reviews* **2008**, *37*, 2543.

(72) (a) Grimsdale, A. C.; Leok Chan, K.; Martin, R. E.; Jokisz, P. G.; Holmes, A. B. *Chemical Reviews (Washington, DC, United States)* **2009**, *109*, 897(b) Lo, S.-C.; Burn, P. L. *Chemical Reviews (Washington, DC, United States)* **2007**, *107*,

1097(c) Veinot, J. G. C.; Marks, T. J. *Accounts of Chemical Research* **2005**, *38*, 632.

(73) (a) Allendorf, M. D.; Bauer, C. A.; Bhakta, R. K.; Houk, R. J. T. *Chemical Society Reviews* **2009**, *38*, 1330(b) Cahill, C. L.; de Lill, D. T.; Frisch, M. *CrystEngComm* **2007**, *9*, 15(c) Janiak, C. *Dalton Transactions* **2003**, 2781(d) Kitagawa, S.; Kitaura, R.; Noro, S.-i. *Angewandte Chemie, International Edition* **2004**, *43*, 2334(e) Silva, C. G.; Corma, A.; Garcia, H. *Journal of Materials Chemistry* **2010**, *20*, 3141.

(74) Li, X.; Wang, X.-W.; Zhang, Y.-H. *Inorganic Chemistry Communications* **2008**, *11*, 832.

(75) Moore, E. G.; Samuel, A. P. S.; Raymond, K. N. *Accounts of Chemical Research* **2009**, *42*, 542.

(76) Richardson, F. S. *Chem. Rev.* **1982**, *82*, 541.

(77) (a) Sabbatini, N.; Guardigli, M.; Lehn, J. M. *Coordination Chemistry Reviews* **1993**, *123*, 201(b) Weissman, S. I. *Journal of Chemical Physics* **1942**, *10*, 214.

(78) (a) de Lill, D. T.; Gunning, N. S.; Cahill, C. L. *Inorg. Chem.* **2005**, *44*, 258(b) Zou, J.-P.; Peng, Q.; Wen, Z.; Zeng, G.-S.; Xing, Q.-J.; Guo, G.-C. *Crystal Growth & Design* **2010**, *10*, 2613.

(79) Wang, G.-H.; Li, Z.-G.; Jia, H.-Q.; Hu, N.-H.; Xu, J.-W. *CrystEngComm* **2009**, *11*, 292.

(80) An, J.; Shade, C. M.; Chengelis-Czegan, D. A.; Petoud, S.; Rosi, N. L. *Journal of the American Chemical Society* **2011**, *133*, 1220.

(81) (a) Zhao, B.; Chen, X.-Y.; Cheng, P.; Liao, D.-Z.; Yan, S.-P.; Jiang, Z.-H. *Journal of the American Chemical Society* **2004**, *126*, 15394(b) Liu, W.; Jiao, T.; Li, Y.; Liu, Q.; Tan, M.; Wang, H.; Wang, L. *Journal of the American Chemical Society* **2004**, *126*, 2280(c) Kozlowski, H.; Janicka-Klos, A.; Brasun, J.; Gaggelli, E.; Valensin, D.; Valensin, G. *Coordination Chemistry Reviews* **2009**, *253*, 2665(d) Que, E. L.; Domaille, D. W.; Chang, C. J. *Chemical Reviews (Washington, DC, United States)* **2008**, *108*, 1517.

(82) (a) Gu, X.; Xue, D. *CrystEngComm* **2007**, *9*, 471(b) Chen, B.; Yang, Y.; Zapata, F.; Lin, G.; Qian, G.; Lobkovsky, E. B. *Advanced Materials (Weinheim, Germany)* **2007**, *19*, 1693.

(83) (a) Habibagahi, A.; Mebarki, Y.; Sultan, Y.; Yap, G. P. A.; Crutchley, R. J. *ACS Applied Materials & Interfaces* **2009**, *1*, 1785(b) Katz, M. J.; Ramnial, T.; Yu, H.-Z.; Leznoff, D. B. *Journal of the American Chemical Society* **2008**, *130*, 10662.

(84) Lan, A.; Han, L.; Yuan, D.; Jiang, F.; Hong, M. *Inorganic Chemistry Communications* **2007**, *10*, 993.

(85) Guo, H.; Zhu, Y.; Qiu, S.; Lercher, J. A.; Zhang, H. *Advanced Materials (Weinheim, Germany)* **2010**, *22*, 4190.

(86) (a) Kim, J. H.; Holloway, P. H. *Advanced Materials (Weinheim, Germany)* **2005**, *17*, 91(b) Zhang, J.; Shade, C. M.; Chengelis, D. A.; Petoud, S. *Journal of the American Chemical Society* **2007**, *129*, 14834.

(87) (a) Rowe, M. D.; Thamm, D. H.; Kraft, S. L.; Boyes, S. G. *Biomacromolecules* **2009**, *10*, 983(b) Taylor-Pashow Kathryn, M. L.; Della Rocca, J.; Xie, Z.; Tran, S.; Lin, W. *J Am Chem Soc* **2009**, *131*, 14261(c) An, J.; Farha, O. K.; Hupp, J. T.; Pohl, E.; Yeh, J. I.; Rosi, N. L. *Nature Communications* **2012**, *3*, 1618/1(d) An, J.; Geib, S. J.; Rosi, N. L. *Journal of the American Chemical Society* **2010**, *132*, 38(e) Atci, E.; Erucar, I.; Keskin, S. *Journal of Physical Chemistry C* **2011**, *115*, 6833(f) Bohrman, J. A.; Carreon, M. A. *Chemical Communications (Cambridge, United Kingdom)* **2012**, *48*, 5130(g) Ferey, G.; Millange, F.; Morcrette, M.; Serrem, C.; Doublet, M.-L.; Grenech, J.-M.; Tarascon, J.-M. *Angewandte Chemie, International Edition* **2007**, *46*, 3259(h) Munoz, B.; Ramila, A.; Perez-Pariente, J.; Diaz, I.; Vallet-Regi, M. *Chemistry of Materials* **2003**, *15*, 500(i) Vallet-Regi, M.; Ramila, A.; del Real, R. P.; Perez-Pariente, J. *Chemistry of Materials* **2001**, *13*, 308(j) Xiao, B.; Wheatley, P. S.; Zhao, X.; Fletcher, A. J.; Fox, S.; Rossi, A. G.; Megson, I. L.; Bordiga, S.; Regli, L.; Thomas, K. M.; Morris, R. E. *Journal of the American Chemical Society* **2007**, *129*, 1203(k) Horcajada, P.; Chalati, T.; Serre, C.; Gillet, B.; Sebrie, C.; Baati, T.; Eubank, J. F.; Heurtaux, D.; Clayette, P.; Kreuz, C.; Chang, J.-S.; Hwang, Y. K.; Marsaud, V.; Bories, P.-N.; Cynober, L.; Gil, S.; Ferey, G.; Couvreur, P.; Gref, R. *Nature Materials* **2010**, *9*, 172(l) Harbuzaru, B. V.; Corma, A.; Rey, F.; Jorda, J. L.; Ananias, D.; Carlos, L. D.; Rocha, J. *Angewandte Chemie, International Edition* **2009**, *48*, 6476.

(88) (a) Colacio, E.; Maimoun, I. B.; Lloret, F.; Suarez-Varela, J. *Inorg. Chem.* **2005**, *44*, 3771(b) Colacio, E.; Palacios, M. A.; Rodriguez-Dieguez, A.; Mota, A. J.; Herrera, J. M.; Choquesillo-Lazarte, D.; Clerac, R. *Inorg. Chem.* **2010**, *49*, 1826(c) Colacio, E.; Ruiz-Sanchez, J.; White, F. J.; Brechin, E. K. *Inorg. Chem.* **2011**, *50*, 7268(d) Mota, A. J.; Rodriguez-Dieguez, A.; Palacios, M. A.; Herrera, J. M.; Luneau, D.; Colacio, E. *Inorg. Chem.* **2010**, *49*, 8986(e) Palacios, M. A.; Rodriguez-Dieguez, A.; Sironi, A.; Herrera, J. M.; Mota, A. J.; Cano, J.; Colacio, E. *Dalton Transactions* **2009**, 8538.

(89) (a) Rodriguez, A.; Kivekaes, R.; Colacio, E. *Chemical Communications (Cambridge, United Kingdom)* **2005**, 5228(b) Rodriguez, A.; Sakiyama, H.; Masciocchi, N.; Galli, S.; Galvez, N.; Lloret, F.; Colacio, E. *Inorg. Chem.* **2005**, *44*, 8399(c) Rodriguez-Dieguez, A.; Cano, J.; Kivekaes, R.; Debdoubi, A.; Colacio, E. *Inorg. Chem.* **2007**, *46*, 2503(d) Rodriguez-Dieguez, A.; Kivekaes, R.; Sakiyama, H.; Debdoubi, A.; Colacio, E. *Dalton Transactions* **2007**, 2145(e) Rodriguez-Dieguez, A.; Mota, A. J.; Cano, J.; Ruiz, J.; Choquesillo-Lazarte, D.; Colacio, E. *Dalton Transactions* **2009**, 6335(f) Rodriguez-Dieguez, A.; Mota, A. J.; Seco, J.

M.; Palacios, M. A.; Romerosa, A.; Colacio, E. *Dalton Transactions* **2009**, 9578(g) Rodriguez-Dieguez, A.; Palacios, M. A.; Sironi, A.; Colacio, E. *Dalton Transactions* **2008**, 2887.

CAPÍTULO 2.

A NEW 2D CADMIUM CHLORIDE NETWORK WITH 2-AMINOPYRIMIDINE DISPLAYING LONG LIFETIME PHOTOLUMINESCENCE EMISSION

ARTICLE: *A NEW 2D CADMIUM CHLORIDE NETWORK WITH 2-AMINOPYRIMIDINE DISPLAYING LONG LIFETIME PHOTOLUMINESCENCE EMISSION.*


Contents lists available at ScienceDirect

Polyhedron

journal homepage: www.elsevier.com/locate/poly

A new 2D cadmium chloride network with 2-aminopyrimidine displaying long lifetime photoluminescence emission

Alfonso Salinas-Castillo [a], A.J. Calahorro [b], Duane Choquesillo-Lazarte [c], José M. Seco [d], Antonio Rodríguez-Diéguez [b,*]

[a] Instituto de Biología Molecular y Celular, Universidad Miguel Hernández, 03202 Elche, Alicante, Spain
[b] Departamento de Química Inorgánica, Universidad de Granada, 18071 Granada, Spain
[c] Laboratorio de Estudios Cristalográficos, IACT-CSIC, E-18100 Granada, Spain
[d] Departamento de Química Aplicada, Facultad de Química de San Sebastián, Universidad del País Vasco, Paseo Manuel Lardizábal, 20008 San Sebastián, Spain

ABSTRACT

The hydrothermal reaction of $CdCl_2$ with 2-aminopyrimidine in water yields a 2D metal-organic coordination framework $[CdCl_2(PymNH_2)]$ (1) ($PymNH_2$ = 2-aminopyrimidine). This compound consists of $Cd_2(\mu\text{-}Cl)_2$ corner-sharing chains bridged by $PymNH_2$ through the endocyclic ring nitrogen atoms. Interestingly, this polymer exhibits long lifetime photoluminescence emission at room temperature in the solid state with long lifetimes decay.

1. INTRODUCTION

In recent years, there has been increasing research interest in the design and synthesis of extended coordination frameworks as potential zeolitic, magnetic, conducting, nonlinear optical materials, etc.[1] Although most of these systems have been synthesized by controlled mixing of suitable soluble molecular components, solvothermal conditions have provided increasing success in alternative pathways to the preparation of single-crystalline supramolecular solids, including metal–organic

coordination networks and hydrogen-bonded systems. 2-substituted-pyrimidine ligands have been shown to be excellent and versatile building blocks, with charge and multi-connectivity abilities, to produce under conventional and hydrothermal conditions multidimensional coordination polymers with interesting properties.[2] Moreover, many six- or seven-coordinated and some five- or eight-coordinated Cd(II) coordination polymers[3] have recently received attention because of their excellent photoluminescence properties, well beyond the interest raised by their new structural features. Although some studies on the luminescent properties of 2-aminopyrimidine have been reported so far,[4] however, no examples of Cd(II) coordination polymers containing this ligand and exhibiting luminescence properties exist. Recently, we have designed and prepared novel coordination polymers with different pyrimidine derivative ligands, with interesting luminescent properties.[5] In this context, and as a part of our continuing studies in this field, we present here the synthesis, structural aspects and luminiscence properties of $[CdCl_2(PymNH_2)]$.

2. EXPERIMENTAL

2.1. General.

All analytical reagents were purchased from commercial sources and used without further purification.

2.2. Preparation of $[CdCl_2(PymNH_2)]$.

A mixture of $CdCl_2 \cdot 2.5H_2O$ (0.080 g, 0.350 mmol), $PymNH_2$ (0.097 g, 0.350 mmol) and distilled water (10 mL) was sealed in a Teflon-lined acid digestion autoclave and heated at 160 ºC under autogenous pressure. After 12 h of heating, the reaction vessel was slowly cooled down to room temperature during a period of about 4 h. Colourless crystals of the compound under study were obtained. Yield: 64 %, based on Cd. Anal. Calcd. for $C_4H_5CdCl_2N_3$: C, 17.26; H, 1.81; N, 15.09. Found: C, 17.35; H, 1.91; N, 15.24.

2.3. Physical measurements

Elemental analyses were carried out at the "Centro de Instrumentación Científica" (University of Granada) on a Fisons-Carlo Erba analyser model EA 1108. The IR spectra on powdered samples were recorded with a ThermoNicolet IR200FTIR by using KBr pellets.

2.4. Single-Crystal Structure Determination.

Suitable crystal of $[CdCl_2(PymNH_2]$ was mounted on glass fiber and used for data collection. Data were collected with Bruker X8 Proteum diffractometers at 296(2) K. From the 782 measured reflections, 782 were independent and used to refine 46 parameters with zero restraints. Bruker X8 Kappa ApexII diffractometer ($2.8 < 2\Theta < 26.3º$). Final *R* [$I < 2\sigma(I)$], *R*1 = 0.0350, *wR*2 = 0.0758, final *R* (all data), *R*1 = 0.0599, *wR*2 = 0.0805. Max./min. residual electron density 0.883/-0.843 e $Å^{-3}$. The data were processed with APEX2[6] and corrected for absorption using SADABS.[7] The structures were solved by direct methods using SIR97,[8] revealing positions of all non-hydrogen atoms. These atoms were refined on F^2 by a full matrix least-squares procedure using anisotropic displacement parameters.[9]

2.5. Luminescence measurement

A Varian Cary-Eclipse Fluorescence Spectrofluorimeter solid sample holder accessory was used to obtain the fluorescence spectra. The spectrofluorimeter was equipped with a xenon discharge lamp (peak power equivalent to 75 kW), Czerny-Turner monochromators, R-928 photomultiplier tube which is red sensitive (even 900 nm) with manual or automatic voltage controlled using the Cary Eclipse software for Windows 95/98/NT system. The photomultiplier detector voltage was 800 V and the instrument excitation and emission slits were set at 10 and 10 nm, respectively.

3. Results and Discussion

3.1. Structure and crystallographic results

Colourless crystals of the compound under study were obtained by hydrothermal reaction of $CdCl_2$ and 2-aminopyrimidine in 1:1 molar ratio. This compound crystallizes in the monoclinic space group $P2_1/m$. The coordination environment around the metal atom is shown in Figure 1. The cadmium(II) ion, which lies on an inversion centre, exhibits a compressed octahedral geometry with a N_2Cl_4 donor set. In this description, four symmetry-related μ_2-chlorine bridging atoms are located in equatorial positions [Cd1-Cl1 2.611(2) Å], whereas two symmetry-related nitrogen atoms belonging to two μ_2-$PymNH_2$ bridging ligands occupy the axial positions [Cd1-N3 2.417(4) Å].

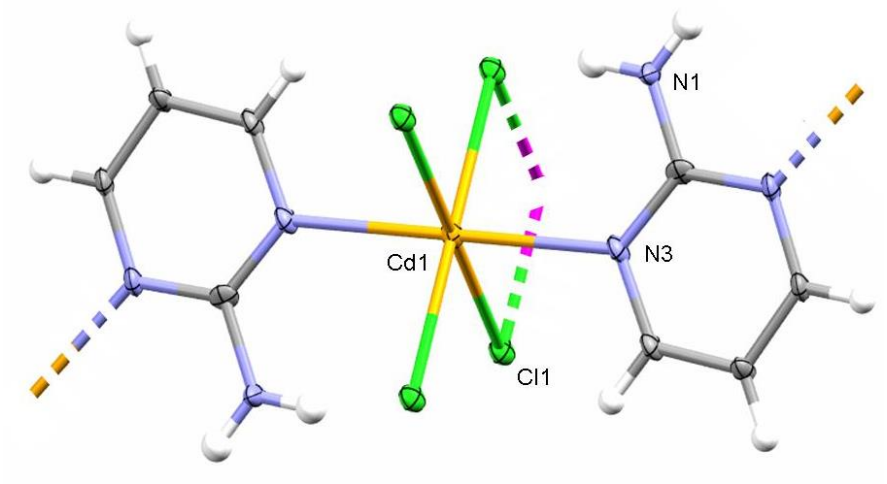

Figure 1. *Coordination environment of cadmium(II) in compound **1**. Symmetry codes: i) x,y,z; ii) -x,-y,1-z; iii) 1+x,y,z; vi) 1-x,-y,1-z; v) x,1/2-y,z. Thermal ellipsoids are drawn at the 50 % probability level.*

Table 1. *Crystallographic Data and Structural Refinement Details.*

compound	**$[CdCl_2(PymNH_2)]$**
CCDC	717413
chemical formula	$C_4H_5CdCl_2N_3$
M/gmol^{-1}	278.41
T (K)	296(2)
λ/Å	1.54178
cryst syst	monoclinic
space group	$P2_1/m$
a/ Å	3.7645(14)
b/ Å	13.636(9)
c/ Å	7.266(5)
α/deg	90
β/deg	96.66(3)
γ/deg	90
V/ Å^3	370.5(4)
Z	2
ρ(g cm-3)	2.496
μ(mm-1)	3.58
Unique reflections	782
R(int)	0.069
GOF on F^2	0.987
R1[a] [I > 2σ(*I*)]	0.035
wR2[a] [I > 2σ(*I*)]	0.076

[a] $R(F) = \sum||F_o| - |F_c||/\sum|F_o|$, $wR(F^2) = [\sum w(F_o^2 - F_c^2)^2/\sum wF^4]^{1/2}$

Owing to the inversion centre located on each cadmium(II) ion, the μ_2-$PymNH_2$ ligands are coordinated in *trans* positions resulting in a linear chain $[Cd(PymNH_2)]_n^{n+}$ with the aromatic ring displaying a zigzag distribution along the *b* axis. Similar *trans*-axial arrangements have been reported in *trans*-$[MX_4(PymNH_3)_2]$ (M = Co, Ni; X = Cl, Br)[10] and *trans*-$[MX_4(PymNH_3)_2]$ (M = Cu, X = Br).[11] Chloride anions act as bridges between neighbouring metal centres [Cd-Cl-Cd 91.47(6)°, Cd···Cd separation of 3.764 Å] connecting neighbouring 2-amino-pyrimidine-

cadmium chains, which result in a 2D undulating layered network parallel to the *ab* plane (Figure 2). A cobalt(II) complex with similar crystal structure have been reported previously by Pike *et al* (*Cmcm* Space group; a=3.6139(2), b=14.3170(7), c=12.9986(7); bond distances, Co-Cl = 2.4668(6)Å and Co-N = 2.228(3)Å)[12]. Multi π,π-stacking interactions between pyrimidine rings of $PymNH_2$ ligands (centroid-centroid distance 3.764 Å) and N-H···Cl hydrogen bonding (3.277 Å, 255.0°) reinforce the 2D layer.

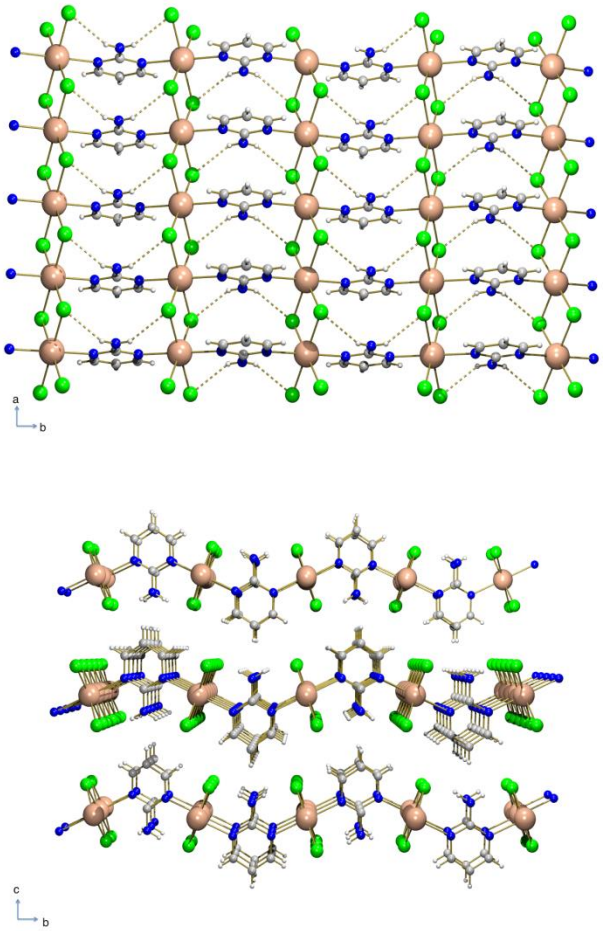

Figure 2. *View of the 2D layer structure of* ***1*** *in the ab plane (top). View down of the a axis showing undulated layers stacked along c axis (bottom).*

3.2. Luminescence Properties

Among the most studied properties of materials containing aromatic molecules, in molecular crystals, organic polymers, coordination compounds or even donor–acceptor pairs, luminescence occupies a special ranking, due to the potential applications of visible light emitters[13] in a number of technologically advanced fields. Thanks to its extended aromaticity and to the presence of hexa-atomic rings, 2-aminopyrimidine is a good candidate for enhanced emissive properties. The excitation and emission spectrum of $[CdCl_2(PymNH_2)]$ in the solid state at room temperature is shown in Figure. 3.

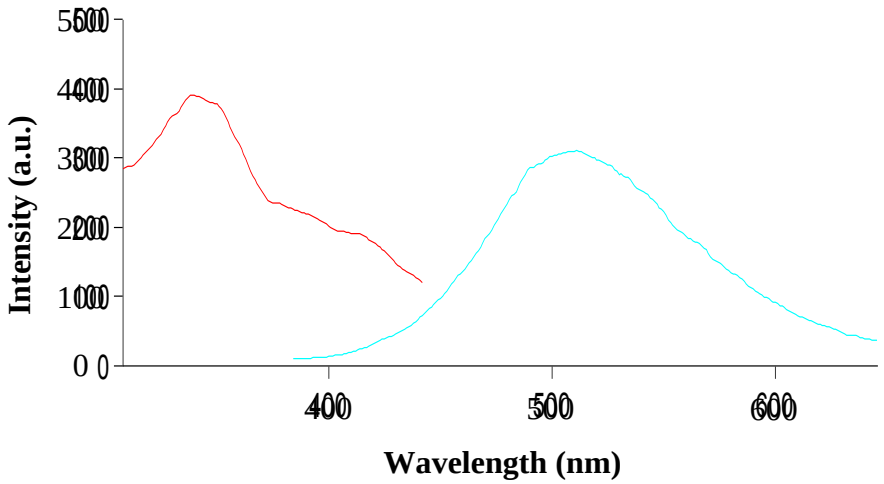

Figure. 3. *Excitation (red) and emission (blue) spectra of compound $[CdCl_2(PymNH_2)]$ at room temperature in the solid state. Horizontal axis: wavelength (nm); vertical axis: intensity (a.u.).*

Using a 340 nm incident radiation, intense emission band at 510 was observed. Previous reports, about analogous cadmium complexes with azolate ligands, show similar intense bands, which were attributed to ligand-to-ligand electronic transitions.[14]

These analogous compounds are multidimensional cadmium complexes with other N-heterocyclic ligand. For 2D [Cd(pmtz)$_2$] when excited at 340 nm present one very intense (and broad) emission band at 416 nm.[5] For 2,6-bis[(4-methylphenylimino)ethyl]pyridine $CdCl_2$ CH_3CN and 2,6-bis[1-(2,6-diethylphenylimino)ethyl]pyridine $CdCl_2 \cdot 0.5CH_3CN$, using a 330 nm incident radiations, intense emission bands at 495 and 489 nm were observed.[14b] These values are similar to those found in our compound. We have assigned this band to an intraligand transition, which is affected by the coordination of the ligand to the Cd(II) atom.

The luminescence decay curve of the compound was obtained at room temperature. We try to fit the data to a mono exponential function but these data were impossible to fitted, for this reason the decay curve was fitted to double exponential fuction: $I = I_0 + A_1 \exp(-t/\tau_1) + A_2 \exp(-t/\tau_2)$, where I and I_0 are the luminescent intensities at time t and 0, τ_1 and τ_2 are defined as the luminescent lifetimes. For this function, the best fit of the experimental luminescence intensities to the above equation led to the lifetimes of 0.12 ms and 2.89 ms for τ_1 and τ_2 respectively, thus indicating phosphorescence. Photoluminescence in the ultraviolet-visible comprises two similar phenomena: fluorescence and phosphorescence. The large separation between excitation and emission luminescence (typically phosphorescence occurs at longer wavelength than fluorescence) together with such long lifetimes (the average lifetime of the electron in the excited state in fluorescent is only 10^{-5}-10^{-8} s and the average lifetime for phosphorescence ranges from 10^{-4} to 10^4 s) might indicate phosphorescence rather than fluorescence in [$CdCl_2(PymNH_2)$]. Nevertheless, because we have no other experimental results supporting phosphorescence in this compound and because the phosphorescence emission is sometimes accompanied with fluorescence emission, we prefer to describe the observed photoluminescence as long lifetime photoluminescence emission. Few coordination polymers shown decay with two values of τ, however, some mono-dimensional examples have been reported.[15] Recently, one two-dimensional compound that shows phosphorescence properties with two values of τ (177 and 464.1μs) has been reported by L. Zhao et *al*.[16]

To the best of our knowledge, there is no previously reported coordination polymers synthesized with 2-aminopyrimidine that show phosphorescent properties.

4. CONCLUSIONS

In this work we have shown that new polymers with interesting properties can be synthesized by using old ligands such as $PymNH_2$ (2-aminopyrimidine). We present a 2D metal-organic coordination framework $[CdCl_2(PymNH_2)]$ which is made of $Cd_2(\mu\text{-}Cl)_2$ corner-sharing chains bridged by $PymNH_2$ through the endocyclic ring nitrogen atoms. It is of interest that this compound exhibits long lifetime photoluminescence emission at room temperature in the solid state and it represents one of the few examples of polymeric compounds with two lifetime decay values. This result opens the door toward the preparation of new coordination polymers with interesting luminescent properties synthesized with 2-aminopyrimidine and other related ligands. Work along this line is in progress in our laboratory.

5. REFERENCES

[1] (a) B. Moulton and M. J. Zaworotko, Chem. Rev. 101 (2001) 1629; (b) A. Oxtoby and N. R. Champness, Coord. Chem. Rev. 246 (2003) 145; (c) C. Janiak, Dalton Trans. (2003) 2781; (d) S. Kitagawa, R. Kitaura and S.-I. Noro, *Angew*. Chem., Int. Ed. 43 (2004) 2334; (e) M. Eddaoudi, D. B. Moler, H.-L. Li, B. Chen, T. M. Reineke, M. O'Keeffe and O.M. Yaghi, Acc. Chem. Res. 34 (2001) 319; (f) S. Kitagawa and K. Uemura, Chem. Soc. Rev. 34 (2005) 109; (g) G. Férey, C. Mellot-Draznieks, C. Serre and F. Millange, Acc. Chem. Res. 38 (2005) 217; (h) S. R. Batten, Curr. Opin. Solid State Mater. Sci. 5 (2001) 107; (i) O. R. Evans andW. Lin, Acc. Chem. Res. 35 (2002)

511; (j) Y. García, V. Niel, M. C. Muñoz and J. A. Real, Top. Curr. Chem. 233 (2004) 229; (k) M. Yoshizawa, T. Kusukawa, M. Kawano, T. Ohhara, I. Tanaka, K. Kurihara, N. Niimura andM. Fujita, J. Am. Chem. Soc. 127 (2005) 2798; (l) B. Kesanli and W. B. Lin, Coord. Chem. Rev. 246 (2003) 305; (m) Magnetism: Molecules to Materials, ed. J. S. Miller And M. Drillon, volumes I–V, VCH,Weinheim, 2001–2005; (n) E. Coronado and P. Day, Chem. Rev. 104 (2004) 5419.

[2] (a) J.A.R. Navarro, B. Lippert, Coord. Chem. Rev. 185 (1999) 653. (b) J.A.R. Navarro, E. Barea, M.A. Galindo, J.M. Salas, M.A. Romero, M. Quirós, N. Masciocchi, S. Galli, A. Sironi, B. Lippert, Journal of Solid State Chemistry 178 (2005) 2436. (c) A. Rodríguez-Diéguez, J. Cano, R. Kivekäs, A. Debdoubi, E. Colacio, Inorg. Chem. 46 (2007) 2503. (d) A. Rodríguez-Diéguez, H. Aouryaghal, A.J. Mota, E. Colacio, Acta Cryst. E64 (2008) m618/1. (e) J. Suárez-Varela, A.J. Mota, H. Aouryaghal, J. Cano, A. Rodríguez-Diéguez, D. Luneau, E. Colacio, Inorg. Chem. 47 (2008) 8143.

[3] (a) J. C. Dai, X. T. Wu, Z. Y. Fu, S. M. Hu, W. X. Du, C. P. Cui, L. M. Wu, H. H. Zhang and R. Q. Sun, Chem. Commun. (2002) 12; (b) J. Fan, H. F. Zhu, T. Okamura, W. Y. Sun, W. X. Tang and N. Ueyamab, New J. Chem. 27 (2003) 1409; (c) J. Tao, X. Yin, Z. B. Wei, R. B. Huang and L. S. Zheng, Eur. J. Inorg. Chem. (2004) 125; (d) X. Shi, G. S. Zhu, Q. R. Fang, G.Wu, G. Tian, R.W.Wang, D. L. Zhang, M. Xue and S. L. Qiu, Eur. J. Inorg. Chem. (2004) 185; (e) S. Skoulika, P. Dallas, M. G. Siskos, Y. Deligiannakis and A. Michaelides, Chem. Mater. 15 (2003) 4576; (f) J. Luo,M. C. Hong, R. H.Wang, R. Cao, L. Han and Z. Z. Lin, Eur. J. Inorg. Chem. (2003) 2705; (g) S. L. Zheng, J. H. Yang, X.-L. Yu, X.M. Chen and W. T.Wong, Inorg. Chem. 43 (2004) 830; (h) D. D. Wu and T. C.W.Mak, Inorg. Chim. Acta 253 (1996) 15; (i) Z. F. Chen, R. G. Xiong, B. F. Abrahams, X. Z. You and C. M. J. Che, J. Chem. Soc., Dalton Trans. (2001) 2453.

[4] N. Nishi and M. Kinoshita, Chemical Physics Letters 27 (1974) 342.

[5] A Rodríguez-Diéguez, A. Salinas-Castillo, S. Galli, N. Masciocchi, J. M. Gutiérrez-Zorrilla, P. Vitoria and E. Colacio, Dalton Trans. (2007) 1821.

[6] Bruker Apex2, Bruker AXS Inc, Madison, Wisconsin, USA, 2004.

[7] Sheldrick, G.M., SADABS, Program for empirical adsorption correction, Institute for Inorganic Chemistry, University of Göttingen, Germany, 1996.

[8] A.. Altomare, M. C. Burla, M. Camilla, G.L. Cascarano, C. Giacovazzo, A. Guagliardi, A. G. G. Moliterni, G. Polidori, R. Spagna. J. Appl. Crystallogr. 32 (1999) 115.

[9] Sheldrick, G. M., SHELX 97, Program for crystal structure refinement, University of Göttingen, Göttingen, Germany, 1997.
[10] M.E. Masaki, B.J. Prince, M.M. Turnbull, J. Coord. Chem.55 (2002) 1337.

[11] G. Pon, R.D. Willett, W.T. Robinson, M.M. Turnbull, Inorg. Chim. Acta 255 (1997) 325.

[12] R.D. Pike, M.J. Lim, E.A.L. Willcor, T.A. Tronic, J. Chem. Crystallogr. 36 (2006) 781.

[13] U. H. F. Bunz, Chem. Rev. 100 (2000) 1605.

[14] (a) X. S. Wang, Y. Z. Tang, X. F. Huang, Z. R. Qu, C. M. Che, P. W. H. Chang and R. G. Xiong, Inorg. Chem. 44 (2005) 5278; (b) R.-Q. Fan, H. Chen, P. Wang, Y.-L. Yang, Y.-B. Yin and W. Hasi, Journal of Coordination Chemistry 9 (2010) 1514.

[15] E.J. Fernández, A. Laguna, J.M. López-de-Luzuriaga, M. Montiel, M.E. Olmos, J. Pérez, Inorganica Chimica Acta 358 (2005) 4293.

[16] L. Zhao, Y. Chen, H. Zhang, C. Li, R. Sun, Q. Yang, Journal of Molecular Structure 920 (2009) 441.

CAPÍTULO 3.

NOVEL 3D LANTHANUM OXALATE METAL-ORGANIC-FRAMEWORK: SYNTHETIC, STRUCTURAL, LUMINESCENCE AND ADSORPTION PROPERTIES

ARTICLE: *NOVEL 3D LANTHANUM OXALATE METAL-ORGANIC-FRAMEWORK: SYNTHETIC, STRUCTURAL, LUMINESCENCE AND ADSORPTION PROPERTIES.*

Contents lists available at SciVerse ScienceDirect

Polyhedron

journal homepage: www.elsevier.com/locate/poly

Novel 3D lanthanum oxalate metal-organic-framework: Synthetic, structural, luminescence and adsorption properties

Antonio J. Calahorro [a], David Fairen-Jiménez [b], Anfonso Salinas-Castillo [c], Marta E. López-Viseras [a], Antonio Rodríguez-Diéguez [a,*]

[a] Departamento de Química Inorgánica, Universidad de Granada, 18071 Granada, Spain
[b] Institute for Materials and Processes, School of Engineering, The University of Edinburgh, United Kingdom
[c] Departamento de Química Analítica, Universidad de Granada, 18071 Granada, Spain

ABSTRACT

The hydrothermal reaction of $La(NO_3)_3$ with 2-pyrimidinecarbonitrile in water yields a 3D Metal-Organic Coordination Framework $[La_2(ox)_3(H_2ox)(H_2O)_2](H_2O)_8$ (**1**) (ox = oxalate). This compound has channels with hosted water molecules inside and shows an intense photoluminescence emission at room temperature in the solid state. Due to the great channels that this compounds possess we have analyzed the experimental and simulated adsorption properties. This is one of the few examples of three-dimensional lanthanum polymers based only on oxalate ligand.

1. INTRODUCTION

In recent years, a great deal of attention has been paid to metal-organic frameworks (MOFs) due to their intrinsic properties.[1] Although most of these systems have been synthesized by controlled mixing of suitable soluble molecular components, solvothermal conditions have provided increasing success in

alternative pathways to the preparation of single-crystalline supramolecular solids, including metal–organic coordination networks and hydrogen-bonded systems.

Among others, the design and study of Ln-based MOF has evolved enormously[2] because of their interesting structures and potential applications in fields such as magnetism,[3] luminescence,[4] gas adsorption,[5] sensing and optical storage[6]. Three-dimensional coordination compounds have been commonly prepared through a bottom-up approach, connecting lanthanide ions with the appropriate bridging ligands. In this way, there is still a great interest in the search for bridging ligands, which can produce new materials with intriguing structures and physical properties. Oxalate anion ($C_2O_4^{2-}$, ox) has been extensively used as bridging ligand to construct a great variety of multidimensional polynuclear complexes that exhibit interesting structures and physical properties (magnetic, magneto-optical, magnetic conductor, superconductor, etc).[7] Although numerous examples of 2D and 3D oxalate-bridged metal complexes exist, only a few of them are three-dimensional lanthanum systems based only on oxalate.[8]

On the other hand, we have recently demonstrated the use of hydrothemal syntheses to generate *in situ* new ligands.[9] A similar process has been shown to occur for pyrimidine-2-carboxamide-oxime,[10] 5-pyrimidyltetrazole[11], pyrimidine-4,6-dicarboxylate ligand[12] and pyridine-2-carboxylic acid[13] species, which react with metal ions under hydrothermal conditions to afford oxalate-bridged polymeric complexes. In this context, drastic hydrothermal conditions have been employed to obtain novel metal-organic frameworks containing oxalate bridges generated *in situ* from the decomposition and oxidation of 2-pyrimidinecarbonitrile with the aim of studying the physical properties of the isolated species.

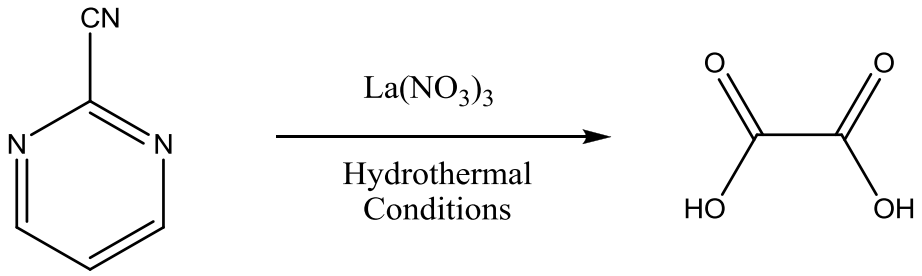

Scheme I. *"In situ" formation of oxalate ligand in compound* ***1*** *by hydrothermal routes.*

As a contribution to this field, we report herein on the synthetic, structural, luminescence and adsorption properties of this novel 3D-polymer of formula: $[La_2(ox)_3(H_2ox)(H_2O)_2](H_2O)_8$. The compound shows intense photoluminescence at room temperature in solid state. Experimental adsorption studies, backed up by grand canonical Monte Carlo simulations, have been realized to study its porous properties.

2. EXPERIMENTAL AND SIMULATION PROCEDURES

2.1. General.

All analytical reagents were purchased from commercial sources and used without further purification.

2.2. Preparation of $[La_2(ox)_3(H_2ox)(H_2O)_2](H_2O)_8$.

A mixture of $La(NO_3)_3{\cdot}xH2O$ (0.097 g, 0.300 mmol), 2-pyrimidinecarbonitrile (0.054 g, 0.450 mmol) and distilled water (10 mL) was sealed in a Teflon-lined acid digestion autoclave and heated at 160 ^{o}C under autogenous pressure. After 24 h of heating, the reaction vessel was slowly cooled down to room temperature during a period of about 4 h. Colourless powder and yellow crystals of the compound under study were obtained. Yield: 64 %, based on La. Anal. Calcd. for $C_8H_{22}O_{26}La_2$: C, 11.83;

H, 2.73. Found: C, 12.05; H, 2.81. IR data (KBr pellet /cm-1): 442(m), 660(w), 826(m), 1404(s), 1580(m), 1633(s), 3064(w), 3213(s).

2.3. Elemental analysis

Elemental analysis was carried out on a Fisons-Carlo Erba analyser model EA 1108. The IR spectra on powdered samples were recorded with a ThermoNicolet IR200FTIR by using KBr pellets.

2.4. Single-Crystal Structure Determination

Suitable crystal of $[La_2(ox)_3(H_2ox)(H_2O)_2](H_2O)_8$ (**1**) was mounted on glass fiber and used for data collection. Data was collected using a Bruker AXS APEX CCD area detector equipped with graphite monochromated Mo Kα radiation (λ = 0.71073 Å) by applying the ω-scan method. The data was processed with APEX2[14] and corrected for absorption using SADABS.[15] The structure was solved by direct methods using SIR97,[16] revealing positions of all non-hydrogen atoms. These atoms were refined on *F*2 by a full matrix least-squares procedure using anisotropic displacement parameters (excluding C1B, C2B and O2B atoms).[17] Hydrogen atoms pertaining to protonated oxalate (B) were located. Hydrogen atoms bonded to water molecules could not be reliably positioned. Attempts to identify the solvent molecules (water) failed. Instead, a new set of *F*2 (*hkl*) values with the contribution from solvent molecules was obtained by the SQUEEZE procedure implemented in PLATON-94.[18] Refinement reduced *R*1 to 0.046. It should be noted that all crystals undergo a very fast degradation when they are removed from the mother liquor which has a high impact on the quality of the data. Several crystals of compound were measured and the structures were solved from the best data we were able to collect. Final *R(F)*, *wR(F^2)* and goodness of fit agreement factors, details on the data collection and analysis can be found in Table 1. Crystallographic data (excluding structure factors) for the reported structure have been deposited with the Cambridge Crystallographic Data Centre as supplementary publication No. CCDC 884936. Copies of the data can be obtained free of charge upon application to CCDC, 12 Union Road, Cambridge CB2 1EZ, U.K. (fax, (+44)1223 336-033; e-mail, deposit@ ccdc.cam.ac.uk).

2.5. Luminescence measurements

A Varian Cary-Eclipse Fluorescence Spectrofluorimeter solid sample holder accessory was used to obtain the fluorescence spectrum. The spectrofluorimeter was equipped with a xenon discharge lamp (peak power equivalent to 75 kW), Czerny-Turner monochromators, R-928 photomultiplier tube which is red sensitive (even 900 nm) with manual or automatic voltage controlled using the Cary Eclipse software for Windows 95/98/NT system. The photomultiplier detector voltage was 800 V and the instrument excitation and emission slits were set at 10 and 10 nm, respectively.

2.6 Gas adsorption procedures

N2 adsorption isotherm was recorded at 77 K using a Micromeritics ASAP 2020 instrument. Prior to the measurements, the sample was degassed at 383 K using a heating rate of 5 K min-1 for 18 h.

The adsorption of N_2 was also investigated using grand canonical Monte Carlo (GCMC) simulations.[19] We used an atomistic model for structure **1**, in which the framework atoms were kept fixed at the crystallographic positions. We used the standard Lennard-Jones (LJ) 12-6 potential to model the interatomic interactions between the framework and N_2. Apart from the LJ, we included electrostatic interactions between N_2 molecules. The parameters for the framework atoms were obtained from the UFF force field.[20] N_2 was modeled using the TraPPE potential with charges placed on each atom and at the center of mass.[21] The Lorentz-Berthelot mixing rules were employed to calculate fluid/solid parameters. Interactions beyond 18 Å were neglected. 10^7 Monte Carlo steps were performed, the first 40% of which were used for equilibration, and the remaining steps were used to calculate the ensemble averages. To calculate the gas-phase fugacity we used the Peng-Robinson equation of state.[22]

3. Results and Discussion

3.1 Structure and crystallographic results.

Yellow crystals of compound **1** were obtained by hydrothermal reaction of $La(NO_3)_3$ with 2-pyrimidinecarbonitrile in 2:3 molar ratio. This compound crystallizes in the triclinic space group *P-1*. The crystal structure was determined by single-crystal X-ray crystallography (Table 1) and consists of a three-dimensional metal–organic framework with channels that propagate along the *a*, *b* and *c* crystallographic axes and hosted water molecules inside the channels. This complex is built up from the connection of lanthanum atoms with bischelating oxalate ligands (Figure 1).

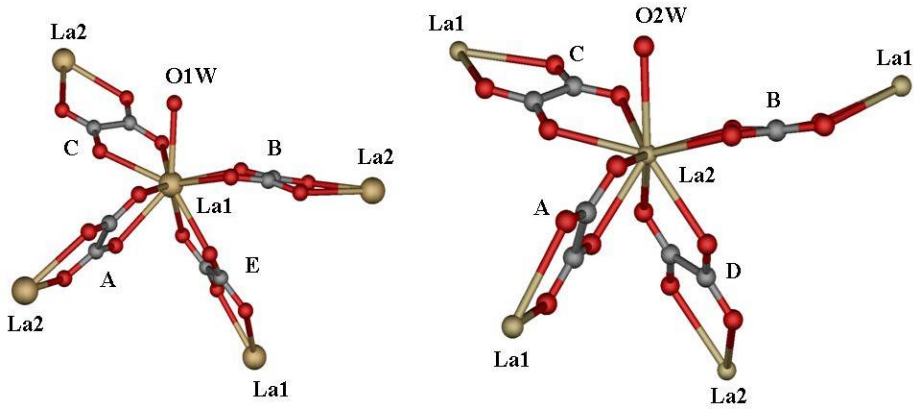

Figure 1. *Coordination environments of different lanthanum(III) ions in compound **1**. Metal centers are connected by different oxalate ligands (A, B, C, D and E).*

This oxalate anion can be obtained by conventional routes but, in this case, it has been synthesized from 2-pyrimidinecarbonitrile.[9c] The asymmetric unit has two different La^{3+} ions, three oxalate ligands, two half oxalates, two coordination water molecules, and eight crystallization water molecules. The La^{3+} ions exhibit an unsymmetrical LaO9 coordination environment which is made of eight oxygen atoms from four oxalate ligands and one oxygen atom pertaining to one coordination water molecule. The coordination environments around the metal atoms are shown in Figure 1. The La–O_{ox} bond distances are in the range 2.436(12)-2.553(11) Å and 2.454(12)-2.546(12) Å for La1 and La2, respectively. The La–O_{water} distances are

2.515(11) and 2.578(10) for La1 and La2, respectively. Bond distances and bond angles in the coordination sphere of La1 and La2 are listed in Tables 2 and 3, respectively.

Table 1. Crystallographic Data and Structural Refinement Details

compound	**1**
chemical formula	$C_8H_{22}La_2O_{26}$
CCDC	884936
M/gmol^{-1}	812.08
T (K)	293
λ/Å	0.71073
cryst syst	triclinic
space group	*P-1*
a/ Å	10.016(2)
b/ Å	11.380(3)
c/ Å	12.821(3)
α/deg	80.39(3)
β/deg	80.65(3)
γ/deg	66.34(3)
V/ Å^3	1312.3(5)
Z	2
ρ(g cm-3)	2.055
μ(mm-1)	3.315
Unique reflections	6323
R(*int*)	0.085
GOF on F^2	0.830
R1 [$I > 2\sigma(I)$]	0.046
wR2 [$I > 2\sigma(I)$]	0.096

[a] $R(F) = \Sigma||F_o| - |F_c||/\Sigma|F_o|$,
$wR(F^2) = [\Sigma w(F_o^2 - F_c^2)^2/\Sigma wF^4]^{1/2}$

The LaO9 coordination sphere is unsymmetrical and can be considered as intermediate between several nine-vertex polyhedra.[23] The coordination polyhedron of the lanthanum atom is a distorted mono-capped square antiprism, with O3A and O2W, the longer distances from the lanthanum, occupying the cap position with 2.553(11) and 2.578(10) Å, respectively. It should be noted that similar LaO9

coordination environments have been previously reported for the compound $[La(H_2O)(C_2O_4)_2]\cdot(CN_3H_6)$.[24] The structure can be described of honey-comb layers bridged by oxalate ligands, parallel to the *ab* plane, constructed from alternately fused 6 metalmembered rings, in which metal centers are bridged by oxalate groups in a bisdidentate mode (Figure 2). In these 2D layers, each lanthanum ion is coordinated to others three lanthanum ions by three oxalate-bridged ligands. In turn, these 2D layers are bridged by other oxalate in the *c* axis direction generating a three-dimensional polymer.

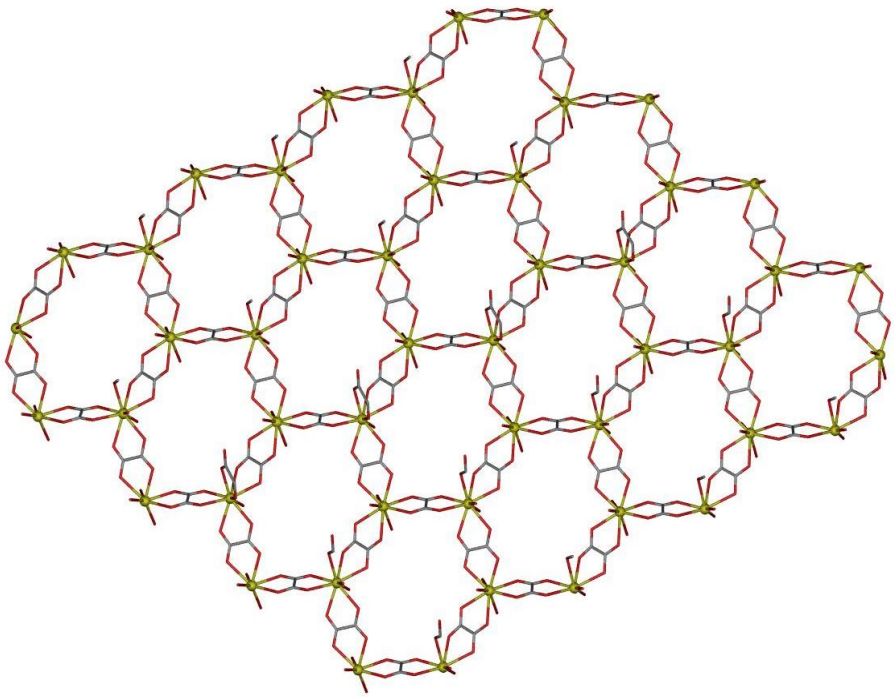

Figure 2. *View down the c axis of a layer of* ***1*** *and 6 metalmembered rings insides of two-dimensional sheets.*

This compound has channels with hosted water molecules. These disorder water molecules generate a complicated hydrogen bond network in the channels (figures 4 and 5). There is a great structural disorder in the compound with these

crystallization water molecules. Figure 3 shows the channels generated in the *a*, *b* and *c* crystallographic axes, accounting for the 44% of the cell volume.

Table 2. Bond Distances for La1 and La2 (Å)

La1 O2A	2.436(12)
La1 O2B	2.472(9)
La1 O1C	2.484(10)
La1 O1E	2.495(11)
La1 O2E	2.500(11)
La1 O1W	2.515(11)
La1 O3B	2.521(12)
La1 O4C	2.536(11)
La1 O3A	2.553(11)
La2 O2D	2.454(12)
La2 O4A	2.483(11)
La2 O2C	2.488(11)
La2 O3C	2.504(10)
La2 O1A	2.511(12)
La2 O4B	2.537(11)
La2 O1D	2.545(11)
La2 O1B	2.546(12)
La2 O2W	2.578(10)

Table 3. Bond Angles for La1 and La2 (º)

O2A La1 O2B 74.2(4)	O2D La2 O4A 135.7(4)
O2A La1 O1C 141.1(4)	O2D La2 O2C 93.6(4)
O2B La1 O1C 126.3(3)	O4A La2 O2C 77.6(4)
O2A La1 O1E 82.8(4)	O2D La2 O3C 70.0(4)
O2B La1 O1E 62.8(3)	O4A La2 O3C 136.5(3)
O1C La1 O1E 134.8(4)	O2C La2 O3C 64.6(4)
O2A La1 O2E 132.4(4)	O2D La2 O1A 71.7(4)
O2B La1 O2E 115.6(3)	O4A La2 O1A 64.4(4)
O1C La1 O2E 73.2(4)	O2C La2 O1A 70.7(4)
O1E La1 O2E 65.3(4)	O3C La2 O1A 117.5(4)
O2A La1 O1W 82.0(4)	O2D La2 O4B 126.8(4)
O2B La1 O1W 71.7(3)	O4A La2 O4B 72.5(4)
O1C La1 O1W 76.0(4)	O2C La2 O4B 139.7(4)
O1E La1 O1W 134.4(4)	O3C La2 O4B 125.2(4)
O2E La1 O1W 145.5(4)	O1A La2 O4B 117.2(4)
O2A La1 O3B 136.7(4)	O2D La2 O1D 64.6(4)
O2B La1 O3B 62.6(4)	O4A La2 O1D 94.0(4)
O1C La1 O3B 72.8(3)	O2C La2 O1D 138.9(4)
O1E La1 O3B 77.7(4)	O3C La2 O1D 128.5(4)
O2E La1 O3B 71.6(4)	O1A La2 O1D 69.5(4)
O1W La1 O3B 84.7(4)	O4B La2 O1D 70.5(4)
O2A La1 O4C 79.5(4)	O2D La2 O1B 75.7(4)
O2B La1 O4C 138.0(3)	O4A La2 O1B 136.9(4)
O1C La1 O4C 63.6(4)	O2C La2 O1B 138.4(4)
O1E La1 O4C 144.7(4)	O3C La2 O1B 74.0(4)
O2E La1 O4C 106.3(4)	O1A La2 O1B 137.6(4)
O1W La1 O4C 72.7(4)	O4B La2 O1B 64.4(4)
O3B La1 O4C 134.4(4)	O1D La2 O1B 72.4(4)
O2A La1 O3A 64.7(4)	O2D La2 O2W 141.9(4)
O2B La1 O3A 123.1(3)	O4A La2 O2W 78.6(4)
O1C La1 O3A 110.3(4)	O2C La2 O2W 76.4(4)
O1E La1 O3A 74.2(4)	O3C La2 O2W 72.5(4)
O2E La1 O3A 72.9(4)	O1A La2 O2W 134.4(4)
O1W La1 O3A 133.9(4)	O4B La2 O2W 71.7(4)
O3B La1 O3A 141.4(4)	O1D La2 O2W 142.0(4)
O4C La1 O3A 70.6(4)	O1B La2 O2W 87.7(4)

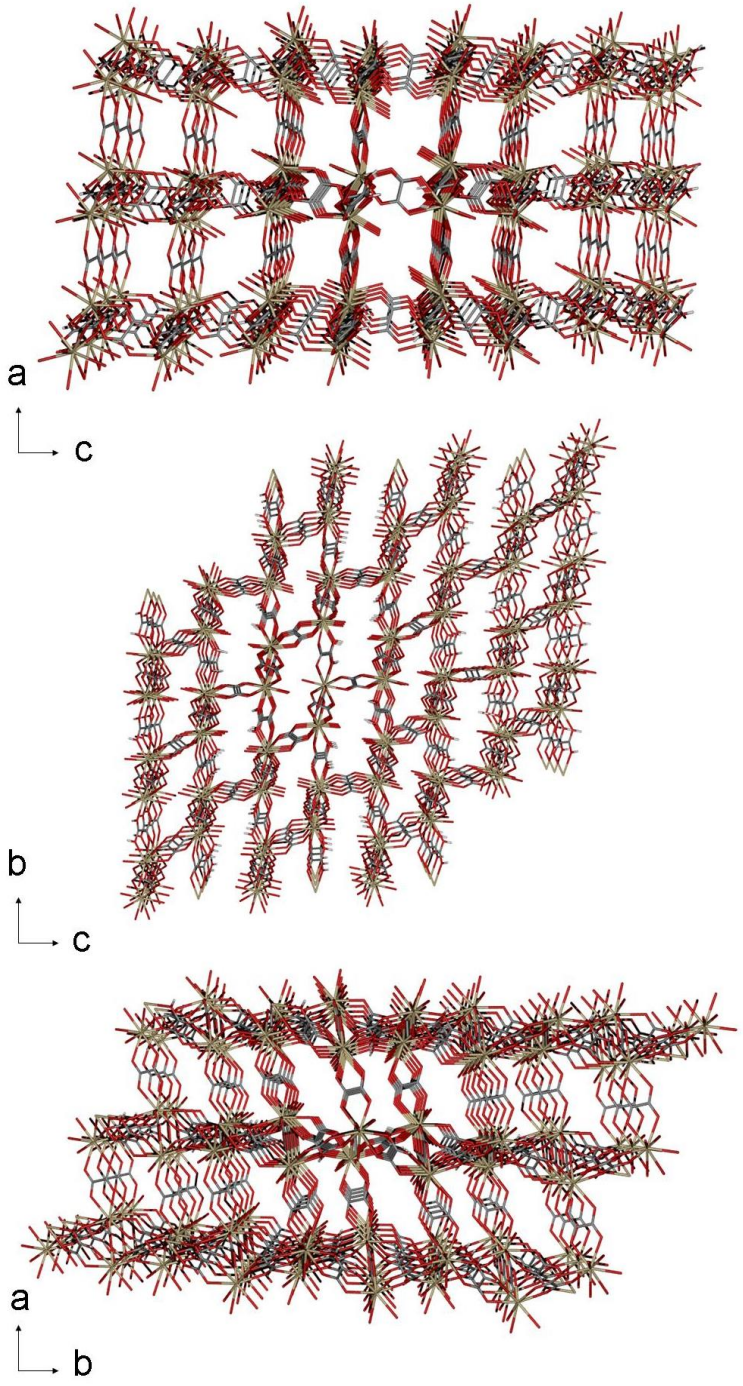

Figure 3. *View of the channels pertaining to 3D network of* ***1*** *in the ac (top), bc (middle) and ab (bottom) planes.*

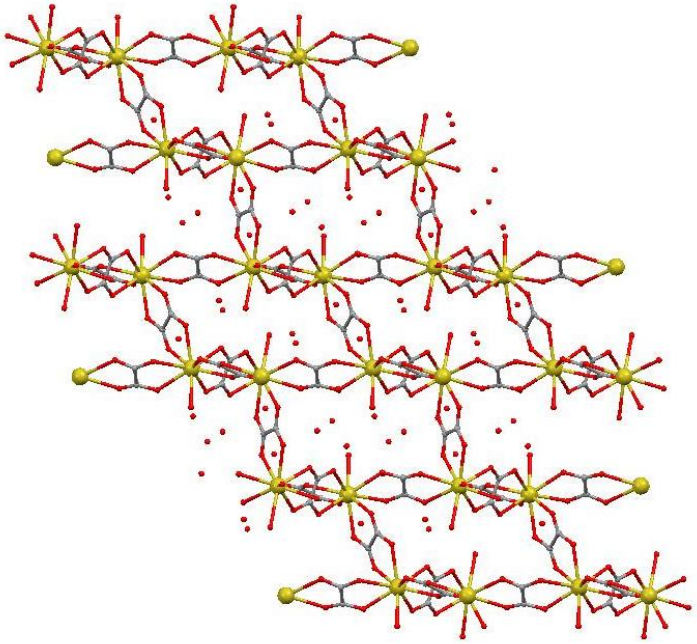

Figure 4. *View along a axis of the water molecules in the channels pertaining to 3D network of* ***1***.

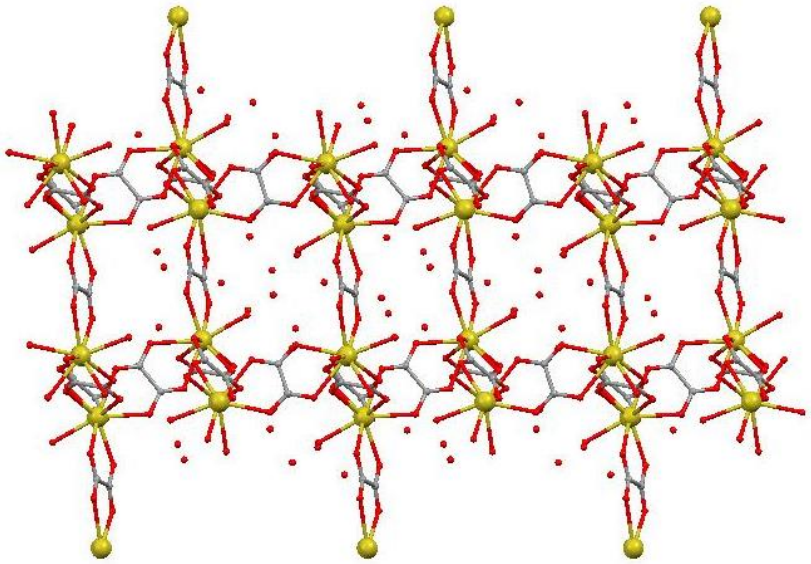

Figure 5. *View along b axis of the water molecules in the channels pertaining to 3D network of* ***1***.

3.2. Luminescence Properties

The emission spectrum of the compound **1** (Figure 6) at room temperature in solid state displays strong blue fluorescent emission band at 450 nm under excitation at 330 nm. [25] The ox ligand exhibited no emission spectra when excited at 330 nm, which probably indicates that it is neither Metal-to-Ligand Charge Transfer nor Ligand-to-Metal Charge Transfer. As is well-known, the characteristic luminescence of La^{3+} should not lie at 450 nm.[26] So the observed emission at 450 nm may be connected with the oxide-to-La(III) absorption band (charge-transfer spin transition).[27] The high-dimensional condensed polymeric structure leads to significant enhancement of fluorescence intensity.[28]

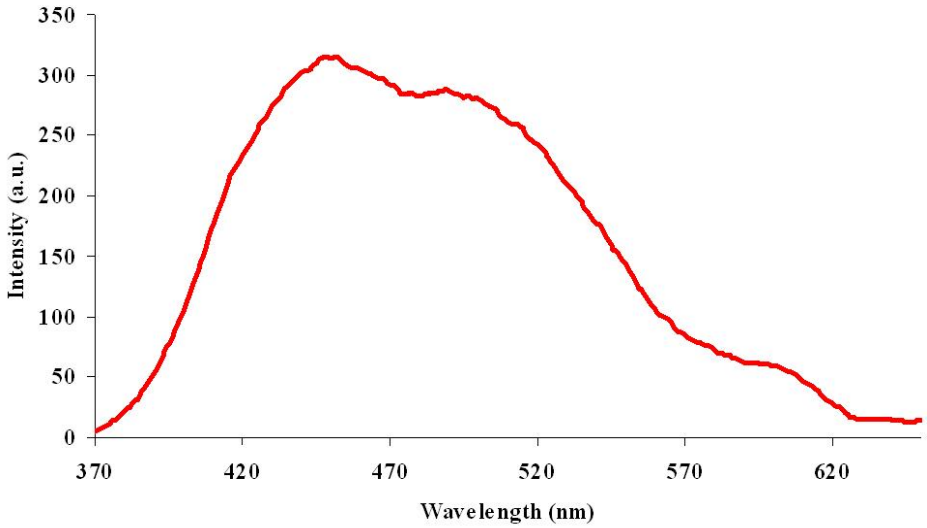

Figure 6. *Emission spectrum of compound $[La_2(ox)_3(H_2ox)(H_2O)_2](H_2O)_8$ at room temperature in the solid state. Horizontal axis: wavelength (nm); vertical axis: intensity (a.u.), λ_{ex} = 330nm.*

3.3. Adsorption Properties

The porosity of structure **1** after solvent removal by heating under vacuum was determined by N_2 adsorption at 77 K (Figure 7). Structure **1** presents a porous structure with a maximum uptake of 5.11 mmol/g. Grand canonical Monte Carlo

(GCMC) simulation[18] of N_2 adsorption isotherm correctly describes the shape of the isotherm but slightly overpredicts the experimental capacity. The description of the experimental adsorption process is improved after applying a scaling factor (Φ) of 0.84, calculated as the ratio of the experimental and simulated maximum amounts adsorbed, on the simulated curve. The over-prediction in the simulations, performed on a perfect structure devoid of any porous defect, is generally explained by the existence of structural defects in the experimental sample that limits the micropore volume and the maximum capacity of the real solid.[29] Calculated BET surface areas on the experimental and simulated N_2 isotherms, using the consistency criteria suggested in the literature, correspond to 420 and 492 m^2/g, respectively (Table S1).

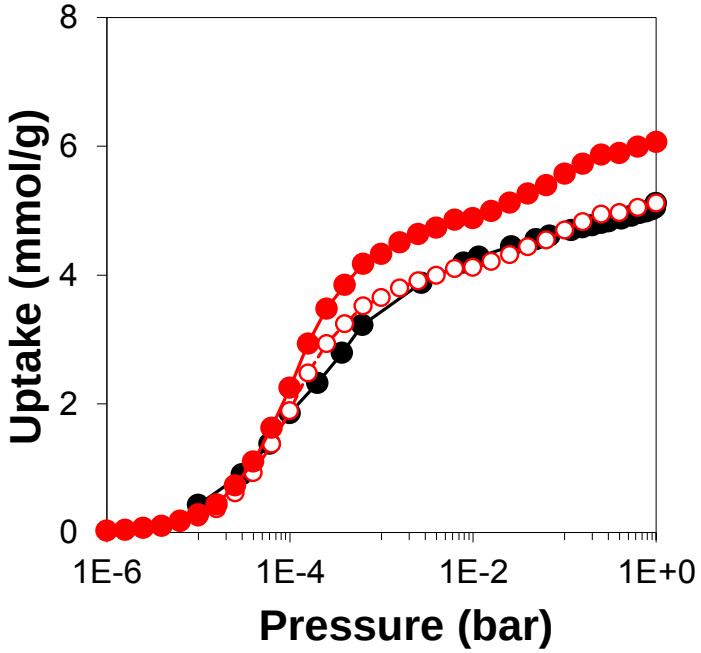

***Figure 7**. Experimental, black closed circles, and simulated, red closed circles, N_2 isotherms at 77 K on **1**. Scaled (Φ = 0.85) simulated isotherms, red open circles. Note the semilog scale in the representation.*

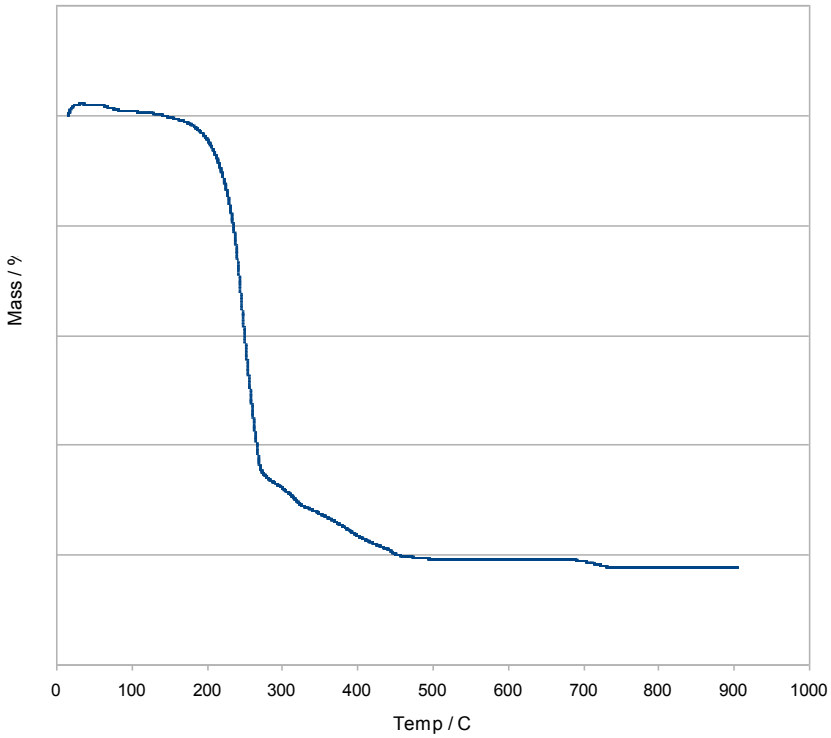

Figure 8. *Thermogravimetric graphic of compound* ***1****.*

Besides the N_2 adsorption isotherms, the geometric pore size distribution was calculated using a Monte Carlo technique which determines the diameter of the largest sphere that can fit into the cavities without overlapping with any of the framework atoms.[30] Figure 9 shows that the maximum is localized around 4.8 Å of diameter.

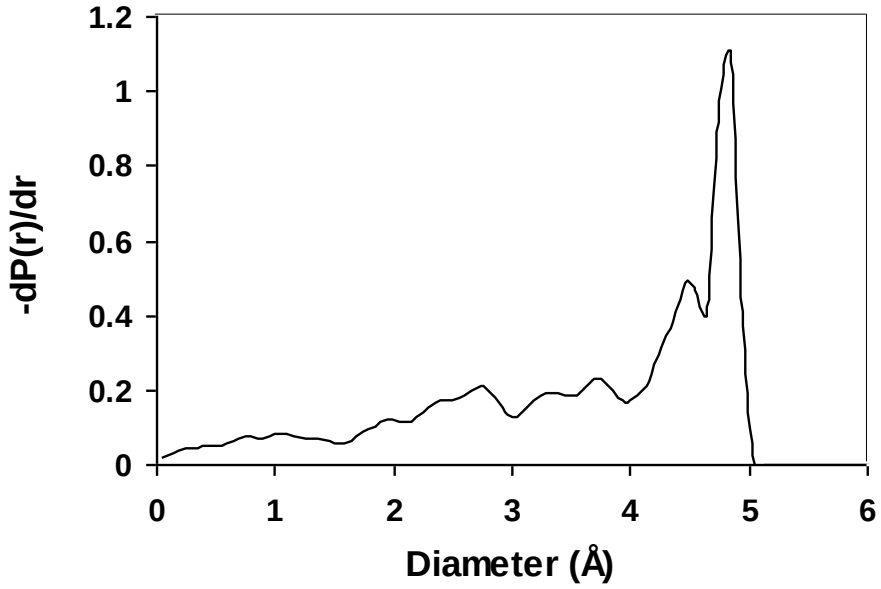

***Figure 9**. Geometric pore size distribution of **1**.*

4. CONCLUSIONS

We have succeeded in obtaining, via an hydrothermal method, a 3D channelled lanthanum MOF containing oxalate bridging ligand, the latter being generated in situ in the course of the hydrothermal reaction. This oxalate anion can be used by conventional routes but, in this case, it has been synthesized from 2-pyrimidinecarbonitrile. This MOF exhibits an intense blue photoluminescence emission at room temperature in the solid state and it represents one of the few examples of three-dimensional polymeric compounds based only on oxalate ligand. Calculated BET surface areas on the experimental and simulated N_2 isotherms, correspond to 420 and 492 m^2/g, respectively.

5. REFERENCES

[1] (a) A.C. Sudik, A.P. Cote, A.G. Wong-Foy, M. O'Keeffe, O.M. Yaghi, Angew. Chem., Int. Ed. 45 (2006) 2528; (b) A. Kondo, H. Noguchi, H. Kajiro, L. Carlucci, P. Mercandelli, D.M. Proserpio, H. Tanaka, K. Kaneko, H. Kanoh, J. Phys. Chem. B, 110 (2006) 25565; (c) J.L.C. Rowsell, O.M. Yaghi, J. Am. Chem. Soc. 128 (2006) 1304: (d) S.H. Jhung, J.-H. Lee, A.K. Cheetham, G. Ferey, J.S. Chang, J. Catal. 239 (2006) 97; (e) M. Hong, Cryst. Growth Des. 7 (2007) 10; (f) A. Vertova, I Cucchi, P. Fermo, F. Porta, D.M. Proserpio, S. Rondinini, Electrochim. Acta 52 (2007) 2603; (g) C. Janiak, Dalton Trans. 14 (2003) 2781; (h) D. Braga, M. Polito, D. D'Addario, F. Grepioni, Cryst. Growth Des. 4 (2004) 1109; (i) S.T. Hyde, O. Delgado-Friedrichs, S.J. Ramsden, V. Robins, Solid State Sci. (2006) 740.

[2] (a) F.A. Almeida Paz, J. Klinowski, Chem. Commun. (2003) 1484; (b) D. Sun, R. Cao, Y. Liang, Q. Shi, M.J. Hong, Chem. Soc. Dalton Trans. (2002) 1847; (c) D.-L. Long, A.J. Blake, N.R. Champness, C. Wilson, M. Schröder, Angew. Chem. Int. Ed. 40 (2001) 2444; (d) L.G. Westin, M. Kritikos, A. Caneschi, Chem. Commun. (2003) 1012; (e) C.-D. Wu, C.-Z. Lu, H.-H. Zhuang, J.-S. Hang, J. Am. Chem. Soc. 124 (2002) 3836; (f) B.-Q. Ma, D.-S. Zhang, S. Gao, T.-Z. Jin, C.-H. Yan, G.-X. Xu, Angew. Chem. Int. Ed. 39 (2000) 3644.

[3] (a) A.H. Morrish, The Physical Principles of Magnetism; Wiley: New York (1965); (b) Z. Chen, B. Zhao, Y. Zhang, W. Shi and P. Cheng, Cryst. Growth Des., 8 (2008) 229.

[4] (a) D.T. de Lill, A. de Bettencourt-Dias, C.L. Cahill, Inorg. Chem. 46 (2007) 3960; (b) K. Lunstroot, K. Driesen, P. Nockemann, C. Gorller-Walrand, K. Binnemans, S. Bellayer, J. Le Bideau, A. Vioux, Chem. Mater. 18 (2006) 5711; (c) R. Shunmugam, G.N. Tew, J. Am. Chem. Soc., 2005, 127, 13567. (d) N.L. Rosi, J. Kim, M. Eddaoudi, B.L. Chen, M. O'Keeffe, O.M. Yaghi, J. Am. Chem. Soc. 127 (2005)

1504. (e) W.S. Liu, T.Q. Jiao, Y.Z. Li, Q.Z. Liu, M.Y. Tan, H. Wang, L.F. Wang, J. Am. Chem. Soc. 126 (2004) 2280.

[5] L. Pan, K.M. Adams, H.E. Hernandez, X. Wang, C. Zheng, Y. Hattori, K. Kaneko, J. Am. Chem. Soc. 125 (2003) 3062.

[6] (a) K. Kuriki, Y. Koike, Y. Okamoto, Chem. Rev. 102 (2002) 2347; (b) C.L. Cahill, D.T. de Lill, M. Frisch, Cryst. Eng. Comm. 9 (2007) 15; (c) O. Guillou, C. Daiguebonne, Handbook on the Physics and Chemistry of Rare Earths; Elsevier: Amsterdam, The Netherlands, 34 (2005) 5; (d) R.J. Hill, D.L. Long, P. Hubberstey, M. Schroder, N.R.J. Champness, Solid State Chem. 178 2005 2414; (e) J.C.G. Bünzli, C. Piguet, Chem. Soc. Rev. 34 (2005) 1048; (f) A.Y. Robin, K.M. Fromm, Coord. Chem. Rev. 250 (2006) 2127; (g) S. Faulkner, J.L. Matthews, Comprehensive Coordination Chemistry II; Elsevier: Oxford, U.K. 9 (2004) 913; (h) C. Piguet, J.-C.G. Bünzli, Chem. Soc. Rev. 28 (1999) 347; (i) R. Gheorghe, P. Cucos, M. Andruh, J.P. Costes, B. Donnadieu, S. Shova, Chem. Eur. J. 12 (2005) 187.

[7] (a) S. Decurtins, R. Pellaux, A. Hauser, M. E. Von Arx in Magnetism: A Supramolecular Function (Ed.: O. Kahn), Kluwer, Dordrecht, (1996) 487 (b) M. Pilkington, S. Decurtins in Comprehensive Coordination Chemistry II. From Biology to Nanaotechnology, Vol. 7 (Eds.: J. A. MacCleverty, T. J. Meyer), Elsevier, Amsterdam (2004) 177; (c) M. Pilkington, S. Decurtins, Perspectives Supramol. Chem. 7 (2003) 275; (d) R. Clément, S. Decurtins, M. Gruselle, C. Train, Monastsh. Chem. 134 (2003) 117 and references therein; (e) H. Tamaki, Z. J. Zhong, N. Matsumoto, S. Kida, M. Koikawa, N. Achiwa, I. Hashimoto, H. Okawa, J. Am. Chem .Soc. 114 (1992) 6974; (f) P. J. Day, J. Chem. Soc., Dalton Trans. (1997) 701; (g) E. Coronado, J. R. Galán-Mascarós, C. Martí- Gastaldo, Inorg. Chem. 45 (2006) 1882; (h) E. Coronado, J. R. Galán-Mascarós, C. J. Gómez-García, V. Laukhin, Nature 408 (2000) 447; (i) D. Armentano, G. D. Munno, T. F. Mastroprieto, M. Julve, F. Lloret, J. Am. Chem. Soc. 127 (2005) 10778; (j) E.

Cariati, R. Macchi, D. Roberto, R. Ugo, S. Galli, N. Casati, P. Macchi, A. Sironi, L. Bogani, A. Caneschi, D. Gatteschi, J. Am. Chem. Soc. 129 (2007) 9410.

[8] S.-H. Huang, G.-D. Zhou, T.C.W..Mak, J.Crystallogr.Spectrosc.Res. 21 (1991) 127.

[9] (a) A. Rodríguez-Diéguez, J. Cano, R. Kivekäs, A. Debdoubi, E. Colacio, Inorg. Chem. 46 (2007) 2503; (b) A. Rodríguez-Diéguez, A. Salinas-Castillo, A. Sironi, J.M. Seco and E. Colacio, CrystEngComm, 12 (2010) 1876; (c) A. Rodríguez-Diéguez, J. Seco and E. Colacio, Eur.J.Inorg.Chem. (2012) 203;

[10] A. Rodriguez-Dieguez, R. Kivekäs, H. Sakiyama, A. Debdoubi, E. Colacio, Dalton Trans. (2007) 2145.

[11] A. Rodríguez-Diéguez, E. Colacio, Chem. Commun. (2006) 4140.

[12] J. Cepeda, R. Balda, G. Beobide, O. Castillo, J. Fernández, A. Luque, S. Pérez-Yáñez, P. Román, D. Vallejo-Sánchez, Inorg Chem., 50 (2001) 8437-51.

[13] J. Y. Lu, J. Macías, J. Lu, J. E. Cmaidalka, Cryst. Growth Des. 2 (2002) 485.

[14] Bruker Apex2, Bruker AXS Inc, Madison, Wisconsin, USA (2004).

[15] G. M. Sheldrick, SADABS, Program for Empirical Adsorption Correction, Institute for Inorganic Chemistry, University of Göttingen, Germany (1996).

[16] A. Altomare, M. C. Burla, M. Camilla, G. L. Cascarano, C. Giacovazzo, A. Guagliardi, A. G. G. Moliterni, G. Polidori and R. Spagna, J. Appl. Crystallogr. 32 (1999) 115.

[17] G. M. Sheldrick, SHELX97, Program for Crystal Structure Refinement, University of Göttingen, Göttingen, Germany (1997).

[18] A. L. Spek, PLATON-94 (V-101094),AMultipurposeCrystallographic Tool, University of Utrecht, The Netherlands, (1994).

[19] Frenkel, D.; Smit, B., Understanding Molecular Simulations: From Algorithms to Applications. 2th ed.; Academic Press: San Diego, (2002).

[20] Rappé, A. K.; Casewit, C. J.; Colwell, K. S.; Goddard, W. A.; Skiff, W. M. J. Am. Chem. Soc. 114 (1992) 10024.

[21] Potoff, J. J.; Siepmann, J. I. AIChE Journal 47 (2001) 1676.

[22] Reid, R. C.; Pausnitz, J. M.; Poling, B. E., The properties of gases & liquids. 4th ed.; McGraw-Hill Companies: New York, (1987).

[23] A. Ruiz-Martínez, D. Casanova, S. Álvarez, Chem. Eur. J. 14 (2008) 1291.

[24] Fabrice Fourcade-Cavillou, Jean-Christian Trombe, Solid State Sciences 4 (2002) 1199.

[25] P. Mahata, S. Natarajan, Inorg. Chem. 46 (2007) 1250; S.M. Ying, J.G. Mao, Cryst. Growth Des. 6 (2006) 964.

[26] P. Mahata, S. Natarajan, Inorg. Chem. 46 (2007) 1250.

[27] Li. Zhang, W. Gu, B. Li, X. Liu, D.Z. Liao, Inorg. Chem. 46 (2007), 622.

[28] (a) D. Rendell, Fluorescence and Phosphorescence, Wiley, New York, 1987; (b) C. M. Che, C. W. Wan, K. Y. Ho and Z. Y. Zhou, New J. Chem., 2001, 25, 63; (c) L.-Z. Zhang, Y. Xiong, P. Cheng, G.-Q. Tang, L.-J. Wang and D.-Z. Liao, J. Mater. Chem. 11 (2001) 2903; (d) Z.-P. Deng, S. Gao and L.-H. Huo, Appl. Organomet. Chem. 21 (2007)

978; (e) Z.-P. Deng, S. Gao, Z.-B. Zhu and L.-H. Huo, Z. Anorg. Allg. Chem. 634 (2008) 593.

[29] A. Rossin, D. Fairen-Jimenez, T. Düren, G. Giambastiani, M. Peruzzini and J. G. Vitillo, Langmuir 27 (2011) 10124.

[30] L. D. Gelb and K. E. Gubbins, Langmuir 15 (1998) 305.

CAPÍTULO 4.

UNIQUE METAL-ORGANIC-FRAMEWORK WITH BASED ON 4'-TETRAZOLATE-4-BIPHENYL CARBOXYLATE SPACER: BLUE-GREEN PHOTOLUMINESCENCE

ARTICLE: UNIQUE METAL-ORGANIC-FRAMEWORK WITH BASED ON 4'-TETRAZOLATE-4-BIPHENYL CARBOXYLATE SPACER: BLUE-GREEN PHOTOLUMINESCENCE.

ABSTRACT

We have been successful in the synthesis of the first Metal-Organic-Frameworks with the novel 4'-tetrazolate-4-biphenyl carboxylate spacer. We report the formation *in situ* of cadmium MOF by hydrothermal routes. The compound is a three-dimensional structure with small channels that shows an intense blue-green photoluminescence emission at room temperature in the solid state. To the best our knowledge, this is the first time that a coordination compound has been synthesized with this ligand

1. INTRODUCTION

The growth of Metal-Organic Framework materials is an area of intense current interest owing to the need not only to develop various functional materials but also to elucidate the topologies as a consequence of their potential uses in many applications.[1] Recently, the design and study of Cd-based MOF has evolved enormously[2] because of their interesting structures and potential applications in areas such as luminescence,[3] gas adsorption,[4] sensing, and optical storage.[5]

These materials are commonly prepared through a bottom-up approach, using solvothermal methods, connecting ions with the appropriate bridging ligands. Still, there is a great interest in the design of new bridging ligands that will allow the preparation of novel MOFs. In the last years, we have designed and prepared novel coordination polymers with different pyrimidine derivates ligands, with interesting luminescent properties[6] synthesized by in-situ Demko-Sharpless [2+3] cycloaddition reactions of organonitriles and sodium azide. [7]

Moreover, we have demonstrated the use of hydrothemal syntheses to generate *in situ* new ligands. [8] Following our work, we have designed and synthesized, by hydrothermal routes, a new multidentate bridging dianionic ligand derivative of 4-tetrazolyl benzene carboxylate and p-mesitylphenyltetrazole, which contain one carboxylate group and one tetrazolate ring with two benzene rings in the middle of the spacer. Thanks to its extended aromaticity and to the presence of poly-heterosubstituded penta- and hexa-atomic rings, 4'-tetrazolate-4-biphenyl carboxylate spacer $(TBPC)^{2-}$ is a good candidate for enhanced emissive properties, tunable, in principle, by coordination to different metals or environments. Here, we report the synthetical, structural and luminescence properties of the first example of 3D-MOFs $[Cd(TBPC)(H_2O)]_n$ (**1**) with the new multidentate $(TBPC)^{2-}$, shown in scheme I, demonstrating the potential of this new linker to construct novel MOFs. To the best of our knowledge, this is the first example of MOFs with this ligand due to it´s the first time that this ligand is synthesized and studied. There are some studies about the 4-tetrazolyl benzene carboxylate and p-mesitylphenyltetrazole in which ligand show fascinating luminescence properties and interesting applications (ie OLEDs). [9]

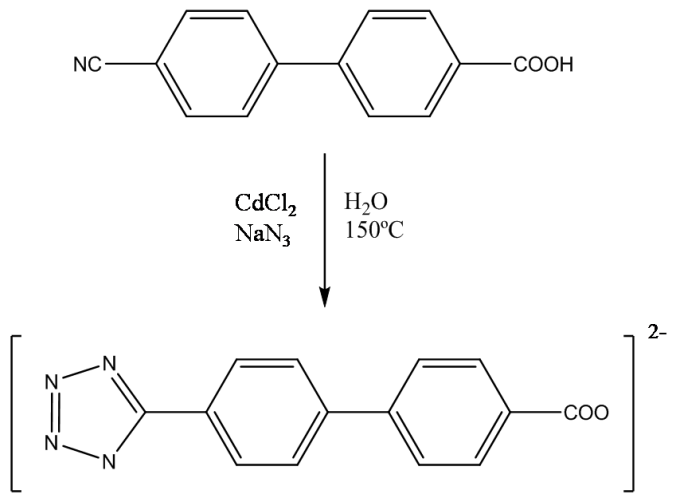

Scheme I. *Preparation in situ of the anionic* $(TBPC)^{2-}$ *ligand by hydrothermal routes.*

2. Experimental Section

2.1. Materials: All analytical reagents were purchased from commercial sources and used without further purification.

2.2. Physical Measurements: Elemental analyses were carried out at the "Centro de Instrumentación Científica" (University of Granada) on a Fisons-Carlo Erba analyzer model EA 1108. The IR spectra on powdered samples were recorded with a ThermoNicolet IR200FTIR instrument by using KBr pellets.

2.3. Single-Crystal Structures Determination.

Suitable crystals of **1** was mounted on glass fiber and used for data collection. Data were collected with a Bruker AXS APEX CCD area detector equipped with graphite monochromated Mo Kα radiation (λ = 0.71073 Å) by applying the ω-scan method. The data were processed with APEX2[14] and corrected for absorption using SADABS.[15] The structures were solved by direct methods using SIR97,[16] revealing positions of all non-hydrogen atoms. These atoms were refined on F^2 by a full matrix least-squares procedure using anisotropic displacement parameters.[17] All hydrogen atoms were located in difference Fourier maps and included as fixed contributions riding on attached atoms with isotropic thermal displacement parameters 1.2 times those of the respective atom. Crystallographic data (excluding structure factors) for the reported structure have been deposited with the Cambridge Crystallographic Data Centre as supplementary publication No. CCDC 926617. Copies of the data can be obtained free of charge upon application to CCDC, 12 Union Road, Cambridge CB2 1EZ, U.K. (fax, (+44)1223 336-033; e-mail, deposit@ ccdc.cam.ac.uk).

2.4. *Preparation of [Cd(TBPC)(H_2O)]$_n$ (1).*

A mixture of $CdCl_2$ (0.183 g, 1 mmol), 4'-cyano-4-biphenyl carboxylic acid (0.223 g, 1 mmol), sodium azide (0.195 mg, 3 mmol) and distilled water (10 mL) was sealed in a Teflon-lined acid digestion autoclave and heated at 150 ^oC under autogenous pressure. After 12 h of heating, the reaction vessel was slowly cooled down to room temperature during a period of about 3 h. Colourless crystals of the compound under study were obtained. Yield: 65%, based on Cd. Anal. calcd $C_{14}H_{10}N_4O_3Cd$: C 42.61, H 2.51, N 14.20. Found: C 42.78, H 2.71, N 14.09. IR/cm^{-1}: 3403 (m), 3132 (s), 1587 (m), 1526 (m), 1458 (w), 1399 (s), 1251 (w), 832 (m), 785 (m), 689 (m).

2.5. Luminescence measurement

A Varian Cary-Eclipse Fluorescence Spectrofluorimeter solid sample holder accessory was used to obtain the fluorescence spectra. The spectrofluorimeter was equipped with a xenon discharge lamp (peak power equivalent to 75 kW), Czerny-Turner monochromators, R-928 photomultiplier tube which is red sensitive (even 900 nm) with manual or automatic voltage controlled using the Cary Eclipse software for Windows 95/98/NT system. The photomultiplier detector voltage was 800 V and the instrument excitation and emission slits were set at 10 and 10 nm, respectively.

3. Results and Discussion

3.1. Structure and crystallographic results

Hydrothermal reaction of cadmium chloride (1 mmol) with the appropriate 4'-cyano-4-biphenyl carboxylic acid (1 mmol) and sodium azide (3 mmol) in water (10 ml) at 150 ^oC for 12 h followed by cooling to room temperature over 3 h yields prismatic colourless crystals of **1** (in 65% yield). The crystal structure was determined by single crystal X-ray crystallography. [10] Compound **1** crystallizes in the monoclinic space group $P2_1/c$. The 3D-MOF structure can be described as ditetrazolate doble-

bridged Cd(II) dimers connected by $(TBPC)^{2-}$ ligands (Figure 1).

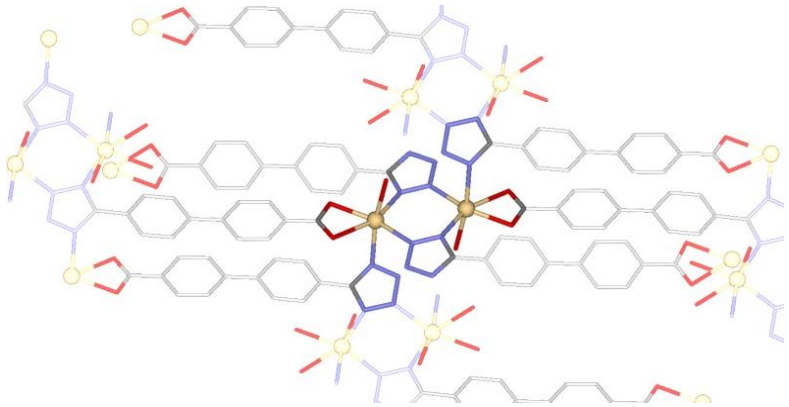

Figure 1. *View of the metal environment and coordination mode of the tetrazolate group for* ***1****. Hydrogen atoms have been omitted for clarity. Colour code N = blue, O = red, C = grey, Cd = yellow.*

These dimers are formed by two cadmium atoms bridged through nitrogen atoms N3 and N4 from tetrazolate group, and are united to others dimers through N1 atom of the same tetrazolate ring. Dimers form a dihedral angle of 87.68º and generate cationic (4,4) layers formed by square units (Figure 2).

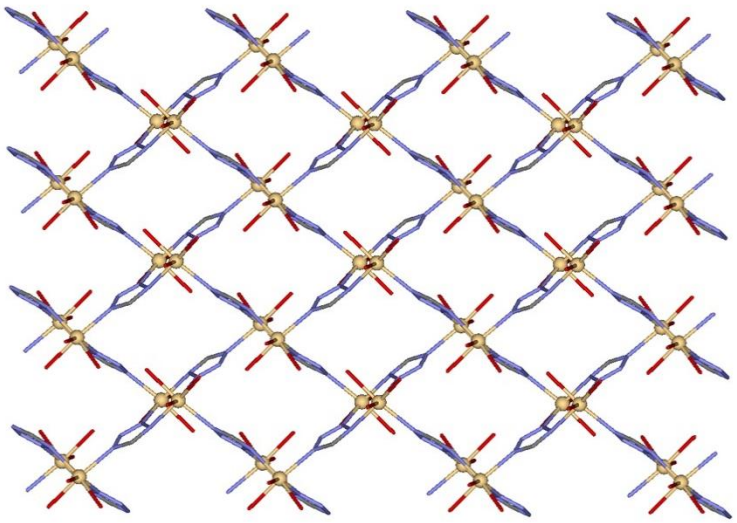

Figure 2. *View down the bc plane of cationic (4,4) layers in compound* ***1****. Hydrogen atoms have been omitted for clarity.*

Within the dinuclear Cd_2 units, each cadmium atom adopts a very distorted octahedral coordination geometry in which has a CdN_3O_3 environment in *fac* disposition. The distortion of the Cd^{II} coordination polyhedron is mainly due to the small bite angle of the carboxylate group pertaining to $(TBPC)^{2-}$ ligand. The Cd atom is coordinated to three nitrogen atoms pertaining to three different tetrazolate groups (N1, N3 and N4), two oxygen atoms (O1 and O2) belonging to one carboxylate group from $(TBPC)^{2-}$ ligand and one water molecule. Cd-N distances are in the ranges 2.292(8)-2.365(7) Å, whereas Cd-O distances have values of 2.187(6), 2.515(6) and 2.314(7) Å, for O1, O2 and O3, respectively. *cis* and *trans* angles of metal environment are in the ranges 55.5(2)-104.7(3)º and 150.1(2)-169.8(2), respectively, highlighting the small bite angle of the carboxylate group (55.5(2)º) and *cis* N–M–N angles are in the ranges 87.2(3)-104.7(3).

Within the sheets formed by dimers, the intradimer Cd···Cd separation through the tetrazolate ring (N3 and N4) is 4.138(3) Å, whereas the interdimer shortest Cd···Cd distances through the N1 are 6.354 (3) and 6.755(3) Å. Within these square-grid-like sheets parallel to *bc* plane, the Cd···Cd distances through the diagonal are 7.329 and 10.799 Å. These sheets are bridged by $(TBPC)^{2-}$ linker and this distance is 12.906 Å. With respect to $(TBPC)^{2-}$ spacer, whereas the carboxylate group and the two benzenes are almost coplanar (dihedral angle of 3.77 and 5.42^{o}), the dihedral angle between the tetrazolate group and the adjacent benzene ring is 66.68º. It should be noted that a similar tetra-chelating bridging mode in which tetrazolate ring coordinates through N1, N3 and N4 atoms and the two oxygen atoms pertaining to one carboxylate group coordinates to one metal atom has been only previously reported for the compound [Cd(cptta)(H_2O)] (H_2cptta = 5-(4´-carboxy-phenyl)tetrazole) with a shorter different ligand.[11]

As above, the structure can be described as sheets, formed by ditetrazolate doble-bridged Cd(II) dimers, propagating along *bc* plane, and are bridged by the aromatic skeleton of the $(TBPC)^{2-}$ linker in *a* direction generating a interesting 3D-MOF (Figure 3).

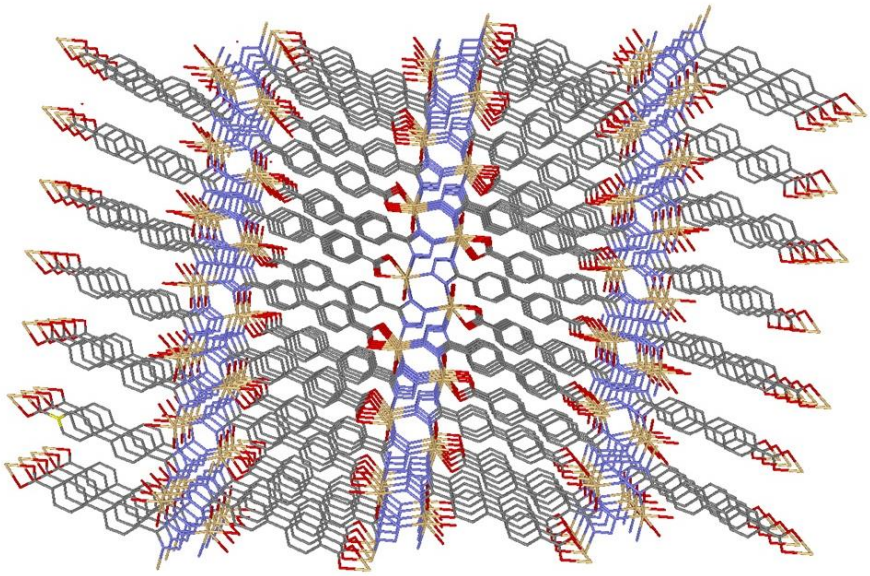

Figure 3. *View down the b axis of the structure in the three-dimensional network. Hydrogen atoms have been omitted for clarity.*

3.2. Luminiscence properties

Luminescence properties occupies a special ranking among the most studied properties of materials containing aromatic molecules, in molecular crystals, organic polymers, coordination compounds or even donor–acceptor pairs, due to the potential applications of visible light emitters[12] in a number of technologically advanced fields. Thanks to its extended aromaticity and to the presence of polyheterosubstituded hexa- and penta-atomic rings, $(TBPC)^{2-}$ is a good candidate for enhanced emissive properties, tunable, in principle, by coordination to different metals or environments.

The excitation and emission spectra of compound **1** in solid state at room temperature are shown in in Figure 4. The emission spectrum of **1** exhibited broad intense emission bands centred about 405, 420 and 447 nm, respectively, upon excitation at 315 nm. The emission in complex **1** is assigned to intraligand □□□□

transitions.

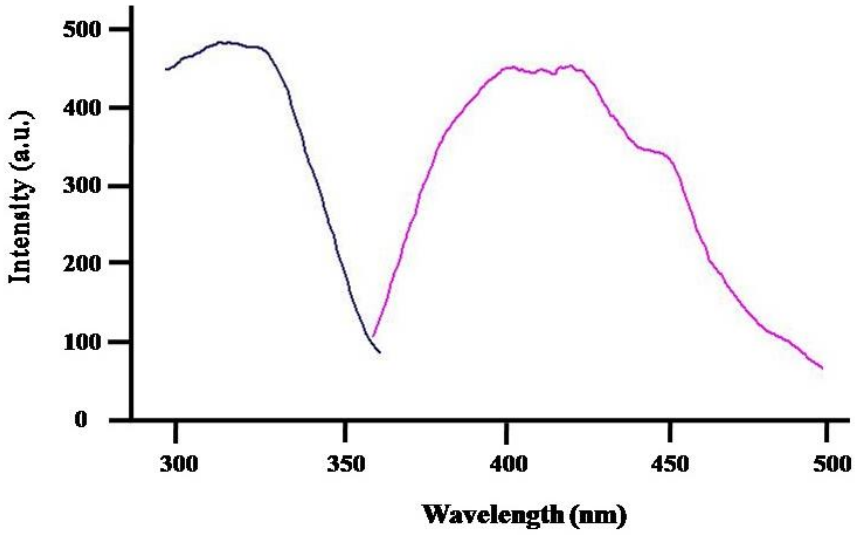

Figure 4. *Excitation (blue) and emission (pink) spectra of compound **1** at room temperature in the solid state. Horizontal axis: wavelength (nm); vertical axis: intensity (a.u.).*

The similarity of emissions for **1** to other compounds[13] is in agreement with the explanation, which indicates that ligand-centered π-π* excitation is responsible for emissions. In contrast with Cd complexes of 5-aliphatic tetrazolates that usually show emissions in the range of 420–530 nm,[14] lower energetic emissions in **1** possibly come from the conjugation of tetrazolate and phenyl-carboxylate groups.

4. Conclusions

Therefore, we have been successful in the synthesis of the first metal-organic-framework with the novel 4'-tetrazolate-4-biphenyl carboxylate spacer. This compound shows an interesting structure with intense blue-green photoluminescence emission at room temperature in the solid state. To the best our

knowledge, this is the first time that a coordination compound has been synthesized with this new multidentate ligand.

5. REFERENCES

[1] (a) A. C. Sudik, A. P. Cote, A. G. Wong-Foy, M. O'Keeffe, O.M. Yaghi, *Angew. Chem. Int. Ed.* **2006**, *45*, 2528-2533; (b) A. Kondo, H. Noguchi, H. Kajiro, L. Carlucci, P. Mercandelli, D. M. Proserpio, H. Tanaka, K. Kaneko, H. Kanoh, *J. Phys. Chem. B* **2006**, *110*, 25565-25567; (c) J. L. C. Rowsell, O. M. Yaghi, *J. Am. Chem. Soc.* **2006**, *128*, 1304-1315; (d) S. H. Jhung, J. H. Lee, A. K. Cheetham, G. Ferey, J. S. Chang, *J. Catal.* **2006**, *239*, 97-104; (e) M. Hong, *Cryst. Growth & Design* **2007**, *7*, 10-14; (f) A. *Vertova, I* Cucchi, P. Fermo, F. Porta, D. M. Proserpio, S. Rondinini, *Electrochim. Acta* **2007**, *52*, 2603-2611; (g) C. Janiak, *Dalton Trans.* **2003**, *14*, 2781-2804; (h) D. Braga, M. Polito, D. D'Addario, F. Grepioni, *Cryst. Growth & Design* **2004**, *4*, 1109-1112.

[2] (a) Q. R. Fang, D. Q. Yuan, J. Sculley, W. G. Lu, H. C. Zhou, *Chem.Commun.* **2012**, *48*, 254-256; (b) E. J. Kyprianidou, G. S. Papaefstathiou, M. J. Manos, A. J. Tasiopoulos, *CrystEngComm.* 2012, *14*, 8368-8373; (c) D. Sun, Z. H. Yan, Y. K. Deng, S. Yuan, L. Wang, D. F. Sun, *CrystEngComm.* **2012**, *14*, 7856-7860; (d) N. Wang, J. G. Ma,W. Shi, P. Cheng, *CrystEngComm.* **2012**, *14*, 5198-5202; (e) M. D. Zhang, C. M. Di, L. Qin, Q. X. Yang, Y. Z. Li, Z. J. Guo, H. G. Zheng, *CrystEngComm.* **2013**, *15*, 227-230; (f) Z. Zhang, L. Zhang, L. Wojtas, P. Nugent, M. Eddaoudi, M. J. Zaworotko, *J. Am. Chem. Soc.* **2012**, *134*, 924-927; (g) T. Zhao, X. Jing, J. Wang, D. Wang, G. Li, Q. Huo, Y. Liu, *Cryst. Growth & Design* **2012**, *12*, 5456-5461; (h) D. C. Zhong, W. X. Zhang, F. L. Cao, L. Jiang, T. B. Lu, *ChemComm.* **2011**, *47*, 1204-1206; (i) D. F. Sava, T. B. Kravtsov, F. Nouar, L. Wojtas, J. F. Eubank, M. Eddaoudi, *J. Am. Chem. Soc.* **2008**, *130*, 3768-3770.

[3] (a) C. X. Chen, Q. K. Liu, J. P. Ma, Y. B. Dong, *Journal of Materials Chemistry* **2012**, *22*, 9027; (b) F. Guo, F. Wang, H. Yang, X. Zhang, J. Zhang, *Inorg.Chem.* **2012**, *51*, 9677; (c) L. J. Li,X. L. Wang, K. Z. Shao, Z. M. Su, *Inorg.Chem.Comm.* **2012**, *26*, 42; (d) T. W. Tseng, T. T. Luo, S. Y. Chen, C. C. Su, K. M. Chi, K. L. Lu, *Crystal Growth & Design* **2013**, *13*, 510; (e) J. J. Wang, T. L. Hu, X. H. Bu, *CrystEngComm.* **2011**, *13*, 5152; (f) K. A. White, D. A. Chengelis, K. A. Gogick, J. Stehman, N. L. Rosi, S. Petoud, *J. Am. Chem. Soc.* **2009**, *131*, 18069; (g) Y. Yang, P. Du, J. F. Ma, W. Q. Kan, B. Liu, J. Yang, *Cryst. Growth & Design* **2011**, *11*, 5540; (h) X. Zhou, B. Li, G. Li, Z. Qi, Z. Shi, S. Feng, *CrystEngComm.* **2012**, *14*, 4664.

[4] (a) Q. R. Fang, D. Q. Yuan, J. Sculley, W. G. Lu, H. C. Zhou, *Chem. Commun.* **2012**, *48*, 254; (b) Q. R. Fang, G. S. Zhu, Z. Jin, M. Xue, X. Wei, D. J. Wang, S. L. Qiu, *Angew. Chem. Int. Ed.* **2006**, *45*, 6126; (c) L. Hu, P. Zhang, Q. Chen, H. Zhong, X. Hu, X. Zheng, Y. Wang, N. Yan, *Cryst. Growth & Design* **2012**, *12*, 2257; (d) D. F. Sava, V. C. Kravtsov, F. Nouar, L. Wojtas, J. F. Eubank, M. Eddaoudi, *J. Am. Chem. Soc.* **2008**, *130*, 3768; (e) M. Xue, G. Zhu, Y. Li, X. Zhao, Z. Jin, E. Kang, S. Qiu, *Cryst. Growth & Design* **2008**, *8*, 2478; (f) D. C. Zhong, W. X. Zhang, F. L. Cao, L. Jiang, T. B. Lu, *Chem. Commun.* **2011**, *47*, 1204.

[5] (a) S. M. Chen, T. T. Lian, *Inorg. Chem. Comm.* **2011**, *14*, 447; (b) Z. Jin, H. Zhao, D. Yang, X. Yao, G. Zhu, *Inorg. Chem. Comm.* **2012**, *25*, 74; (c) M. M. Wanderley, C. Wang, C. D. Wu, W. Lin, *J. Am. Chem. Soc.* **2012**, *134*, 9050.

[6] (a) A. Rodríguez-Diéguez, R. Kivekäs, E. Colacio, *Chem. Commun.* **2005**, 5228; (b) A. Rodríguez-Diéguez, E. Colacio, *Chem. Commun.* **2006**, 4140; (c) A Rodríguez-Diéguez, A. Salinas-Castillo, S. Galli, N. Masciocchi, J. M. Gutiérrez-Zorrilla, P. Vitoria, E. Colacio, *Dalton Trans*. **2007**, 1821; (d) A. Rodríguez-Diéguez, M. A. Palacios, E. Colacio, *Dalton Trans*. **2008**, 2887; (e) A. Rodríguez-Diéguez, J. Cano, R. Kivekäs, A. Debdoubi, E. Colacio, *Inorg. Chem.* **2007**, *46*, 2503; (f) J. Suárez-Varela, A. J. Mota, H. Aouryaghal, J. Cano, A. Rodríguez-Diéguez, D. Luneau, E. Colacio, *Inorg. Chem.* **2007**, *47*, 8143; (g) A. Rodríguez-Diéguez, A. Salinas-Castillo, J. M. Seco, E. Colacio, *CrystEngComm.* **2010**, *12*, 1876.

[7] (a) Z. P. Demko, K. B. Sharpless, *Angew. Chem. Int. Ed*. **2002**, *41*, 2110; (b) Z. P. Demko, K. B. Sharpless, *J. Org. Chem.* **2001**, *66*, 7945; (c) Z. P. Demko, K. B. Sharpless, *Angew. Chem. Int. Ed*. **2002**, *41*, 2113.

[8] (a) A. Rodríguez-Diéguez, J. M. Seco, E. Colacio, *Eur. J. Inorg. Chem*. **2012**, 203; (b) J. M. Seco, M. de Araujo-Farias, N. M. Bach, A. B. Caballero, A. Salinas-Castillo, A. Rodríguez-Diéguez, *Inorg.Chim. Acta* **2010**, *363*, 3194; (c) A. J. Calahorro, D. Fairen-Jiménez, A. Salinas-Castillo, M. E. López-Viseras, A. Rodríguez-Diéguez, *Polyhedron* 2013, *doi.org/10.1016/j.poly. 2012.09.018.*

[9] (a) L. Wang, J. Morales, T. Wu, X. Zhao, W. P. Beyermann, X. Bu, P. Feng, *Chem. Commun.* **2012**, *48*, 7498; (b) Q. Wei, D. Yang, T. E. Larson, T. L. Kinnibrugh, R. Zou, N. J. Henson, T. Timofeeva, H. Xu, Y. Zhao, B. R. Mattes, *J. Mater. Chem*. **2012**, *22*, 10166; (c) P. Venkatakrishnan, P. Natarajan, J. N. Moorthy, Z. Lin, T. J. Chow, *Tetrahedron* **2012**, *68*, 7502.

[10] Crystal Data. 1: $[CdC_{14}H_{10}N_4O_3]$, M = 394.66, monoclinic, space group *P21/c*, a = 16.246(3), b = 7.3291(15), c = 10.799(2) Å, β = 99.02(3), V = 1269.9(4) Å^3, Z = 4, ρ_{calcd} = 2.064 g cm^{-3}, μ(Mo-$K\alpha$) = 1.74 mm^{-1}, R_{int} = 0.0997, T = 100 K, $R1(F_o)$ = 0.0636, ($wR2(F_o^2)$ = 0.1309), GOF= 1.039. Data were collected by ω and ψ scans

on a Bruker APEXII diffractometer with graphite-monochromated MoK radiation (λ = 0.71073 Å). The structures were solved by direct methods and refined on F^2 by the SHELX-97 program. CCDC reference number is 926617.

[11] T. Jiang, Y. F. Zhao, X. M. Zhang, *Inog. Chem. Comm*. **2007**, *10*, 1194.

[12] U. H. F. Bunz, *Chem. Rev.* **2000**, *100*, 1605.

[13] D. C. Zhong, M. Meng, J. H. Deng, X. Z. Luo, Y. R. Xie, *Inog. Chem. Comm.* **2011**, *14*, 1952.

[14] (a) T. Hu, L. Liu, X. Lv, X. Chen, H. He, F. Dai, G. Zhang, D. Sun, *Polyhedron* **2010**, *29*, 296; (b) Y. Qiu, Y. Li, G. Peng, J. Cai, L. Jin, L. Ma, H. Deng, M. Zeller, S.R. Batten, *Cryst. Growth & Design* **2010**, *10*, 1332; (c) J. Tao, Z. J. Ma, R. B. Huang, L. S Zheng, *Inorg. Chem.* **2004**, *43*, 6133.

[15] *Bruker Apex2*, Bruker AXS Inc, Madison, Wisconsin, USA, 2004.

[16] G. M. Sheldrick, *SADABS, Program for Empirical Adsorption Correction*, Institute for Inorganic Chemistry, University of Gottingen, Germany, 1996.

[17] A. Altomare, M. C. Burla, M. Camilla, G. L. Cascarano, C. Giacovazzo, A. Guagliardi, A. G. G. Moliterni, G. Polidori and R. Spagna, *J. Appl. Crystallogr*, **1999**, *32*, 115.

[18] G. M. Sheldrick, *SHELX97, Program for Crystal Structure Refinement*, University of Göttingen, Göttingen, Germany, 1997.

CAPÍTULO 5.

BLUE-GREEN PHOTOLUMINESCENCE OF THE FIRST EXAMPLES OF METAL-ORGANIC-FRAMEWORKS WITH TWO NOVEL TETRAZOLATEPHENYL ACETIC ACID DERIVATIVES.

ARTICLE: *BLUE-GREEN PHOTOLUMINESCENCE OF THE FIRST EXAMPLES OF METAL-ORGANIC-FRAMEWORKS WITH TWO NOVEL TETRAZOLATEPHENYL ACETIC ACID DERIVATIVES.*

ABSTRACT

We report on the synthesis of two new Zn Metal-Organic-Frameworks with 1,3-tetrazolatephenyl-acetic and 1,4-tetrazolatephenyl-acetic spacers obtained *in situ* by hydrothermal routes. These three-dimensional structures exhibit an intense blue-green long lifetime photoluminescence emissions at room temperature in the solid state. To the best of our knowledge, this is the first time that coordination compounds have been synthesized with these ligands.

1. Introduction

Metal-Organic Framework materials currently represent an area of enormous interest owing not only to the need of developing new functional materials but also of elucidating their topologies and their potential applications.[1] Recently, the design and study of Zn-based MOF has evolved enormously[2] because of their interesting structures and in particular their potential applications in areas such as luminescence,[3] gas adsorption,[4] sensing, and optical storage.[5]

These materials are commonly prepared through a bottom-up approach, using solvothermal methods, connecting ions with the appropriate bridging ligands. Still, there is a great interest in the design of new bridging ligands that will allow the preparation of novel MOFs. In the last years, we and others have described different metal coordination polymers based on tetrazolate with interesting topologies synthesized by *in situ* Demko-Sharpless cycloaddition reactions of organonitriles and

sodium azide.[6]

Recently, we have designed and prepared novel coordination polymers with different pyrimidine derivative ligands, with interesting luminescent properties.[7] Moreover, we have shown the use of hydrothemal syntheses to generate *in situ* new ligands and construct novel three-dimensional coordination polymers.[8] Following our work, we have designed, by hydrothermal routes, two new multidentate bridging anionic ligands derivatives of tetrazol-phenyl-acetic acid (H_2tzbaa), 3-tetrazolatephenyl acetic and 4-tetrazolatephenyl acetic linkers, which contain one carboxylate group and one tetrazolate ring with a methylene-benzene group in the middle of the spacer. Thanks to its extended aromaticity and to the presence of poly-heterosubstituded penta- and hexa-atomic rings, H_2tzbaa is a good candidate for enhanced emissive properties, tunable, in principle, by coordination to different metals or environments

Here, we report on the synthesis, the crystal structure and the luminescence properties of the first examples of 3D-MOFs $[Zn(1,3\text{-tzbaa})]_n$ (**1**) and $[Zn(1,4\text{-tzbaa})]_n$ (**2**) with the new multidentate derivative anionic $tzbaa^{2-}$ ligands, shown in scheme I, demonstrating the potential of this new linkers to construct novel MOFs. To the best of our knowledge, these are the first examples of MOFs with these derivative ligands, investigated here for the first time. There is only one biological study on 1,4-H_2tzbaa, used as inhibitor for the Syk C-Terminal SH2 Domain in biomedical area.[9]

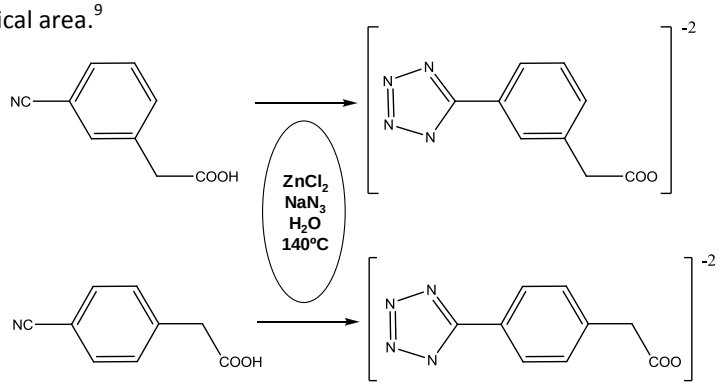

Scheme I. *Preparation of the anionic $(1,3\text{-tzbaa})^{2-}$ (up) and $(1,4\text{-tzbaa})^{2-}$ (down) ligands by hydrothermal routes.*

2. Experimental

2.1. General.

All analytical reagents were purchased from commercial sources and used without further purification.

2.2. Preparation of [Zn(1,3-tzbaa)]$_n$ (1) and [Zn(1,4-tzbaa)]$_n$ (2).

Preparation of [Zn(1,3-tzbaa)]$_n$ (1). A mixture of $ZnCl_2$ (0.136 g, 1 mmol), 3-cyanophenyl acetic acid (0.161 g, 1 mmol), sodium azide (0.195 mg, 3 mmol) and distilled water (10 mL) was sealed in a Teflon-lined acid digestion autoclave and heated at 160 ^oC under autogenous pressure. After 12 h of heating, the reaction vessel was slowly cooled down to room temperature during a period of about 3 h. Yellow crystals of the compound under study were obtained. Yield: 65%, based on Zn. Anal. calcd $C_9H_6N_4O_2Zn$: C 40.37, H 2.24, N 20.93. Found: C 40.78, H 2.81, N 21.29. IR/cm^{-1}: 3421 (s), 2921 (m), 2850 (w), 1536 (s), 1385 (s), 1209 (m), 1077 (m), 813 (m), 773 (m), 742 (s), 684 (s).

Preparation of [Zn(1,4-tzbaa)]$_n$ (2). A mixture of $ZnCl_2$ (0.136 g, 1 mmol), 4-cyanophenyl acetic acid (0.161 g, 1 mmol), sodium azide (0.195 mg, 3 mmol) and distilled water (10 mL) was sealed in a Teflon-lined acid digestion autoclave and heated at 160 ^oC under autogenous pressure. After 12 h of heating, the reaction vessel was slowly cooled down to room temperature during a period of about 3 h. Colourless crystals of the compound under study were obtained. Yield: 39%, based on Zn. Anal. calcd $C_9H_6N_4O_2Zn$: C 40.37, H 2.24, N 20.93. Found: C 40.49, H 2.92, N 21.11. IR/cm^{-1}: 3440 (m), 2957 (w), 2910 (w), 1541 (s), 1382 (s), 1212 (m), 1018 (m), 832 (m), 743 (m), 710 (m).

2.3. Physical measurements

Elemental analyses were carried out at the "Centro de Instrumentación Científica" (University of Granada) on a Fisons-Carlo Erba analyser model EA 1108. The IR spectra on powdered samples were recorded with a ThermoNicolet IR200FTIR by using KBr pellets.

2.4. Luminescence measurement

A Varian Cary-Eclipse Fluorescence Spectrofluorimeter solid sample holder accessory was used to obtain the fluorescence spectra. The spectrofluorimeter was equipped with a xenon discharge lamp (peak power equivalent to 75 kW), Czerny-Turner monochromators, R-928 photomultiplier tube which is red sensitive (even 900 nm) with manual or automatic voltage controlled using the Cary Eclipse software for Windows 95/98/NT system. The photomultiplier detector voltage was 800 V and the instrument excitation and emission slits were set at 10 and 10 nm, respectively.

3. RESULTS AND DISCUSSION

3.1. Structure and crystallographic results

Hydrothermal reactions of zinc chloride (1 mmol) with the appropriate 3-cyanophenyl acetic acid or 4-cyanophenyl acetic acid (1 mmol) and sodium azide (3 mmol) in water (10 ml) at 160 ^{o}C for 12 h followed by cooling to room temperature over 3 h yields prismatic yellow and colourless crystals of 1 (in 65% yield) and 2 (in 39% yield), respectively.[10] The crystal structures were determined by single crystal X-ray crystallography.[11]

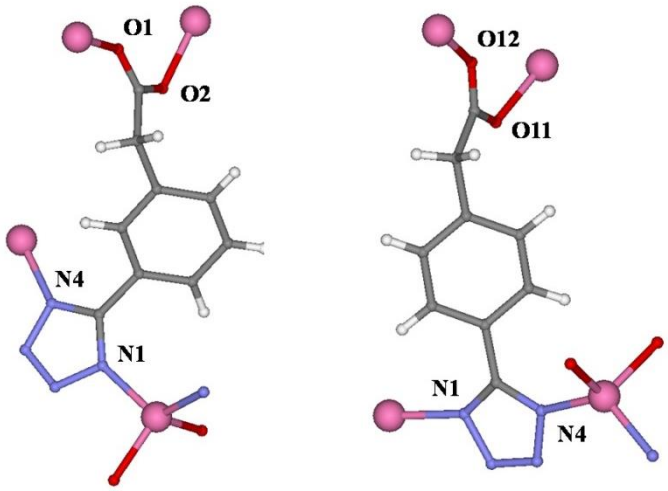

Figure 1. *A view of the coordination mode of the ligands (1,3-tzbaa)2- and (1,4-tzbaa)2- for 1(left) and 2 (right), respectively.*

Both MOFs crystallize in the orthorhombic system and crystal class mm2, though not in the same space group ($Pna2_1$ and $Pca2_1$ for **1** and **2**, respectively). Both structures are three-dimensional, built from tetrahedral Zn^{2+} connectors coordinated to four $(tzbaa)^{2-}$ linkers. The biding sites of $(tzbaa)^{2-}$ are two oxygen of the carboxylate group and two nitrogen atoms (N1 and N4) of the tetrazole ring. The two isomers produce different supramolecular structures, because **2** is characterized by large rings of 3 linkers and 3 connectors (Figure 2, right), producing apparent channels (in reality not available for guest molecules) along ***b*** and therefore perpendicular to the 2_1 helix. These rings are formed by two long edges (Zn-tetrazole-carboxylate-Zn) and a shorter one (Zn-tetrazole-Zn). The rings are interconnected forming 8 member rings (4 connectors and 4 linkers) perpendicular to ***a***, with shorter edges (Zn-tetrazole-Zn or Zn-carboxylate-Zn).

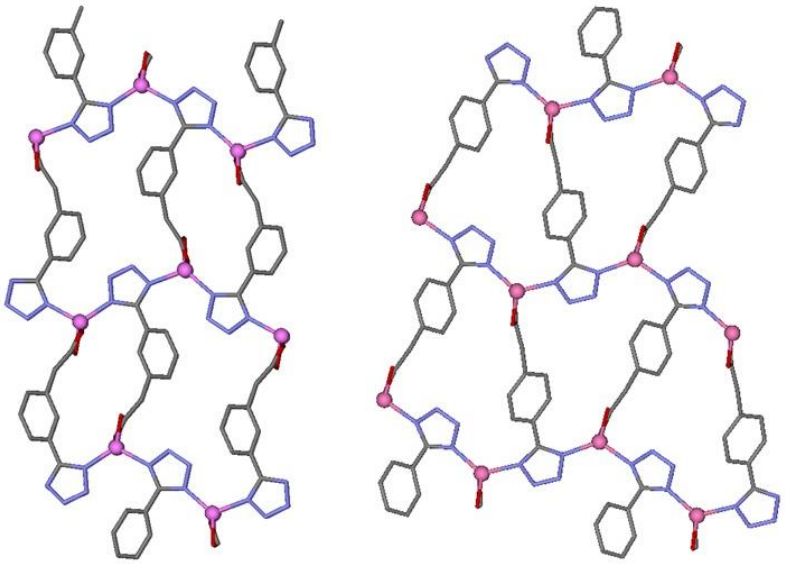

Figure 2. *A view of the rings formed in the structures for 1(left) and 2 (right), respectively.*

The structure of **1** instead is more complex (Figure 2, left), having two different cycles (4 connectors + 4 linkers and 2 connectors + 2 linkers respectively) which form apparent channels along the helical axis ***c***. This different structure is due to the more asymmetric shape of 1,3-tzbaa. 8-member rings similar to those of **2** are perpendicular to ***b*.** In Figure 3, the two packings are shown.

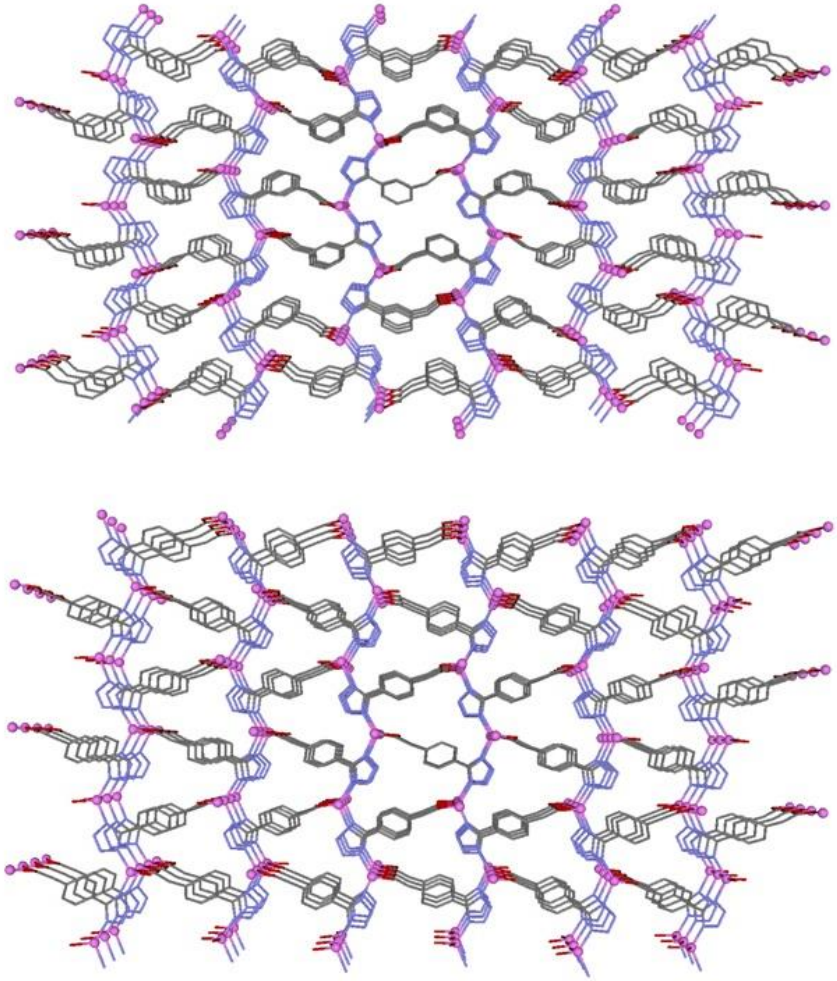

Figure 3. *Packings of 1 (top) and 2 (bottom) along c and b axes, respectively.*

3.2. Luminescence Properties

The emission spectra of **1** and **2** in the solid state at room temperature are shown in Figure 3. Broad intense emission bands are observed, centred about λ = 449 and 479 nm, respectively, upon excitation at λ = 350 nm. The emissions in complexes **1** and **2** are assigned to intraligand π→π* transitions.

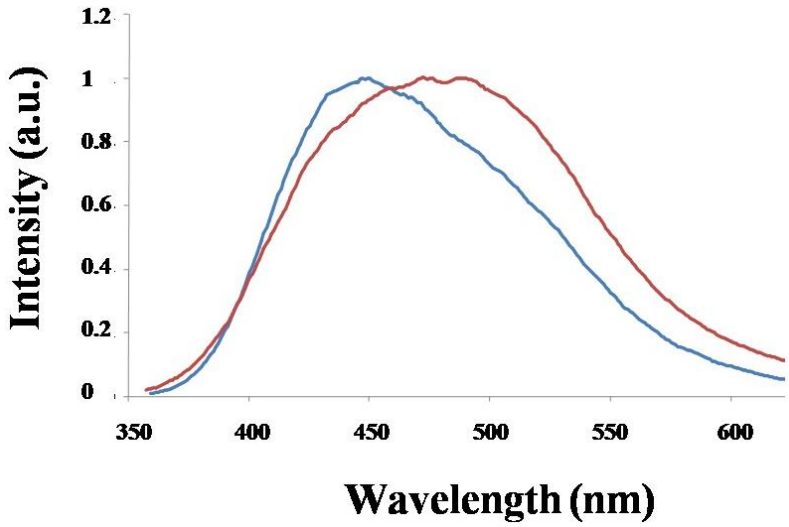

Figure 4. *The emission spectra of 1 (blue) and 2 (red) after excitation at 350 nm in solid state at room temperature.*

The similarity of emissions for **1** and **2** is in agreement with the explanation, which indicates that ligand-centered π-π* excitation is responsible for emissions. In contrast with Zn complexes of 5-aliphatic tetrazolates that usually show emissions in the range of 390–420 nm,[12] energetic emissions in **1** and **2** possibly come from the conjugation of tetrazolate and phenyl-carboxylate groups. The decay curves were fitted to mono exponential function: $I = I_0 + A_1 \exp(-t/\tau)$, where I and I_0 are the luminescent intensities at time t and 0, τ is defined as the luminescent lifetime. For this function, the best fit of the experimental luminescence intensities to the above equation led to the lifetimes of 0.084 ms and 0.098 ms for **1** and **2**, respectively.

4. CONCLUSIONS

We have succeeded in synthesising the first metal-organic-frameworks with the 1,3-tetrazolatephenyl-acetic and 1,4-tetrazolatephenyl-acetic spacer ligands.

These compounds show fascinating structures with intense blue-green photoluminescence emission at room temperature in the solid state. To the best of our knowledge, this is the first time that coordination compounds have been synthesized with these new multidentate ligands.

5. REFERENCES

[1].- (a) H. Xu, X. Rao, J. Gao, J. Yu, Z. Wang, Z. Dou, Y. Cui, Y. Yang, B. Chen and G. Qian, *Chem.Commun.*, 2012, **48**, 7377-7379. (b) J.L.C. Rowsell, O.M. Yaghi, *J. Am. Chem. Soc.* 2006, **128**, 1304. (c) S.H. Jhung, J.-H. Lee, A.K. Cheetham, G. Ferey, J.S. Chang, *J. Catal.* 2006, **239,** 97. (d) M. Hong, *Cryst. Growth Des.* 2007, **7,** 10. (e) A. Vertova, I Cucchi, P. Fermo, F. Porta, D.M. Proserpio, S. Rondinini, *Electrochim. Acta* 2007, **52,** 2603. (f) M. M. Wanderley, C. Wang, C.-D. Wu and W. Lin, *J. Am. Chem. Soc*, 2012, **134**, 9050-9053. (g) P. Kar, R. Haldar, C. J. Gomez-Garcia and A. Ghosh, *Inorg. Chem.*, 2012, **51**, 4265-4273. (h) S.T. Hyde, O. Delgado-Friedrichs, S.J. Ramsden, V. Robins, *Solid State,* 2006, 740.

[2].- (a) F.A. Almeida Paz, J. Klinowski, *Chem. Commun*., 2003, 1484. (b) V. Colombo, C. Montoro, A. Maspero, G. Palmisano, N. Masciocchi, S. Galli, E. Barea and J. A. R. Navarro, *J. Am. Chem. Soc*, 2012, **134**, 12830-12843 (c) D.-L. Long, A.J. Blake, N.R. Champness, C. Wilson, M. Schröder, *Angew. Chem. Int. Ed*., 2001, **40**, 2444. (d) L.G. Westin, M. Kritikos, A. Caneschi, *Chem. Commun*., 2003, 1012. (e) B.-Q. Ma, D.-S. Zhang, S. Gao, T.-Z. Jin, C.-H. Yan, G.-X. Xu, *Angew. Chem. Int. Ed.*, 2000, **39**, 3644. (f) J. Seo, C. Bonneau, R. Matsuda, M. Takata and S. Kitagawa, *J. Am. Chem. Soc*, 2011, **133**, 9005-9013.

[3].- (a) D.T. de Lill, A. de Bettencourt-Dias, C.L. Cahill, *Inorg. Chem*., 2007, **46**, 3960. (b) K. Lunstroot, K. Driesen, P. Nockemann, C. Gorller-Walrand, K. Binnemans, S. Bellayer, J. Le Bideau, A. Vioux, *Chem. Mater*., 2006, **18**, 5711. (c) R. Shunmugam, G.N. Tew, *J. Am. Chem. Soc*., 2005, **127**, 13567. (d) N.L. Rosi, J. Kim, M. Eddaoudi, B.L. Chen, M. O'Keeffe, O.M. Yaghi, *J. Am. Chem. Soc*., 2005, **127**, 1504. (e) M. Ji, X. Lan, Z. Han, C. Hao and J. Qiu, *Inorg. Chem.*, 2012, **51**, 12389-12394. (f) Y. Yang, P. Du, J.-F. Ma, W.-Q. Kan, B. Liu and J. Yang, *Crystal Growth & Design*, 2011, **11**, 5540-5553. (g) F. Tong, Z.-G. Sun, K. Chen, Y.-Y. Zhu, W.-N. Wang, C.-Q. Jiao, C.-L. Wang and C. Li, *Dalton Trans.*, 2011, **40**, 5059-5065.

[4].- (a) L. Pan, K.M. Adams, H.E. Hernandez, X. Wang, C. Zheng, Y. Hattori, K. Kaneko, *J. Am. Chem. Soc*., 2003, **125**, 3062. (b) Q.-G. Zhai, Q. Lin, T. Wu, L. Wang, S.-T. Zheng, X. Bu and P. Feng, *Chemistry of Materials*, 2012, **24**, 2624-2626. (c) W. Morris, N. He, K. G. Ray, P. Klonowski, H. Furukawa, I. N. Daniels, Y. A. Houndonougbo, M. Asta, O. M. Yaghi and B. B. Laird, *Journal of Physical Chemistry C*, 2012, **116**, 24084-24090 (d) P.-Q. Liao, D.-D. Zhou, A.-X. Zhu, L. Jiang, R.-B. Lin, J.-P. Zhang and X.-M. Chen, *J. Am. Chem. Soc*, 2012, **134**, 17380-

17383. (e) P. Cui, Y.-G. Ma, H.-H. Li, B. Zhao, J.-R. Li, P. Cheng, P. B. Balbuena and H.-C. Zhou, *J. Am. Chem. Soc*, 2012, **134**, 18892-18895.

[5].- (a) K. Kuriki, Y. Koike, Y. Okamoto, *Chem. Rev*., 2002, **102**, 2347. (b) C.L. Cahill, D.T. de Lill, M. Frisch, *Cryst. Eng. Comm.*, 2007, **9**, 15. (c) J.C.G. Bünzli, C. Piguet, *Chem. Soc. Rev*., 2005, **34**, 1048. (d) A.Y. Robin, K.M. Fromm, *Coord. Chem. Rev.*, 2006, **250**, 2127. (e) G. Lu and J. T. Hupp, *J. Am. Chem. Soc*, 2010, **132**, 7832-7833. (f) R. Gheorghe, P. Cucos, M. Andruh, J.P. Costes, B. Donnadieu, S. Shova, *Chem. Eur. J*., 2005, **12**, 187. (g) B. Gole, A. K. Bar and P. S. Mukherjee, *Chem Commun*, 2011, **47**, 12137-12139.

[6].- (a) A. Rodríguez-Diéguez, R. Kivekäs, E. Colacio, *ChemComm*, 2005, 5228; (b) A. Rodríguez-Diéguez and E. Colacio, *ChemComm*, 2006, 4140; (c) Z. P. Demko and K. B. Sharpless*, J. Org. Chem.*, 2001, **66**, 7945.

[7].- (a) A Rodríguez-Diéguez, A. Salinas-Castillo, S. Galli, N. Masciocchi, J. M. Gutiérrez-Zorrilla, P. Vitoria and E. Colacio, Dalton Trans. (2007) 1821. (b) J.M. Seco, M. de Araujo-Farias, N.M. Bach, A.B. Caballero, A. Salinas-Castillo and A. Rodríguez-Diéguez, *InorgChimActa*, 2010, 363, 3194.

[8].- (a) A. Rodríguez-Diéguez, J. Cano, R. Kivekäs, A. Debdoubi, E. Colacio, *Inorg. Chem.* 2007, **46**, 2503. A. Rodríguez-Diéguez, J.M. Seco and E. Colacio, *Eur.J.Inorg.Chem*., 2012, 203; (b) A. Rodríguez-Diéguez, A. Salinas-Castillo, A. Sironi, J.M. Seco and E. Colacio, *CrystEngComm*, 2010, **12**, 1876. ; (c) A.J. Calahorro, D. Fairen-Jiménez, A. Salinas-Castillo, M.E. López-Viseras and A. Rodríguez-Diéguez, *Polyhedron*, 2013, *doi.org/10.1016/j.poly. 2012.09.018.*

[9].- T. Niimi, M. Orita, M. Okazawa-Igarashi, H. Sakashita, K. Kikuchi, E. Ball, A. Ichikawa, Y. Yamagiwa, S. Sakamoto, A. Tanaka, S. Tsukamoto and S. Fujita, *J.Med.Chem*, **2001**, *44*, 4737-4740.

[11].- Crystal Data. **1**: $[C_9H_6N_4O_2Zn)]$, M = 267.55, orthorhombic, space group *Pna21, a* = 10.4858(3), b = 18.8309(6), c = 4.8130(2) Å, V = 950.36(6) Å^3, Z = 4, ρ_{calcd} = 1.87 g cm^{-3}, μ(Mo-$K\alpha$) = 2.572 mm^{-1}, R_{int} = 0.0303, T = 293 K, $R1(F_o)$ = 0.0319, ($wR2(F_o^2)$ = 0.0731) with a goodness-of-fit on F^2 1.08. **2**: $[C_9H_6N_4O_2Zn)]$, M = 267.55, orthorhombic, space group *Pca21*, a = 18.5081(5), b = 4.8230(1), c = 10.9635(4) Å, V = 978.65(5) Å^3, Z = 4, ρ_{calcd} = 1.816 g cm^{-3}, μ(Mo-$K\alpha$) = 2.498 mm^{-1}, R_{int} = 0.043, T = 293 K, $R1(F_o)$ = 0.0347, ($wR2(F_o^2)$ = 0.058) with a goodness-of-fit on F^2 1.049. Data were collected by *2Θ* scans (on a Bruker APEXII diffractometer with graphite-monochromated Mo-Kα radiation (λ = 0.71073 Å). The structures were solved by direct methods and refined on F2 by the SHELX-97 program. CCDC reference numbers are 930950 and 930951.

[12].- X.-S. Wang, Y.-Z. Tang, X.-F. Huang, Z.-R. Qu, C.-M. Che, P.W.H. Chan, R.-G. Xiong, *Inorg. Chem*., 2005, **44**, 5278.

CAPÍTULO 6.

BLUE-GREEN LONG LIFETIME PHOTOLUMINESCENCE EMISSION OF 3D CADMIUM METAL-ORGANIC FRAMEWORKS BASED ON THE 5-(4-PYRIDYL)TETRAZOLE LIGAND.

ARTICLE: *BLUE-GREEN LONG LIFETIME PHOTOLUMINESCENCE EMISSION OF 3D CADMIUM METAL-ORGANIC FRAMEWORKS BASED ON THE 5-(4-PYRIDYL)TETRAZOLE LIGAND.*

ABSTRACT

Three new metal-organic frameworks based on 5-(4-pyridyl)tetrazole have been synthesized by hydrothermal routes mixing this linker with cadmium(II) chloride in the presence of secondary ligands such as squaric acid, 4-carboxypyridine and terephtalic acid in water. Hydrothermal syntheses reveal new possibilities to rational formation on MOFs by mixtures of different linkers using the appropriate stoichiometry. These polymers exhibit blue-green long lifetime photoluminescence emission at room temperature in the solid state with long lifetime decays. Theoretical studies about pore size distribution and experimental gas adsorption studies have also been included.

1. INTRODUCTION

In recent years, there has been an increasing research interest in the design and synthesis of extended coordination frameworks as multi-functional materials.[1] Metal–organic frameworks (MOFs), are attracting increasing attention not only due to their fascinating topologies but also because of their interesting applications in areas such as gas adsorption, catalysis, magnetic behaviour, non-linear optical activity and electrical conductivity.[2] The major task for the synthesis of these MOFs is to choose appropriate metal-connecting nodes and bridging ligands to get the desired porous properties.

Amongst the most interesting ligands, multidentate N and O-donor bridging ligands have drawn extensive attention in the construction of these novel systems.[3] So far, considerable efforts have been devoted to the synthesis of unusual

coordination polymers based on carboxylate and pyridine-based ligands,[4] while there are also many examples of synthetic materials derived from polydentate aromatic nitrogen heterocyclic ligands, such as pyrazoles, imidazoles, triazoles and tetrazoles.[5] In recent years, solvothermal conditions have provided increasing success in alternative pathways to the preparation of single-crystalline supramolecular solids, including metal–organic coordination networks and hydrogen-bonded systems. Nitrogen-based ligands have been shown to be excellent and versatile building blocks, with charge and multi-connectivity ability, to produce multidimensional coordination polymers under conventional and hydrothermal conditions.[6]

Recently, we have designed and prepared novel MOFs with different pyrimidine derivate ligands showing interesting luminescent properties[7] as well as zeolitic imidazolate frameworks (ZIFs) with high pore volumes and extra-framework containing zinc imidazolate units on the internal surface.[8] On the other hand, many six- or seven-coordinated and some five- or eight-coordinated Cd(II) coordination polymers have recently received attention because of their excellent photoluminescence properties, [9] well beyond the interest raised by their new structural features. Moreover, the Cd(II) ion has a d^{10} configuration and the required softness that permits a wide variety of geometries and coordination numbers and that may allow the construction of non-interpenetrating high-dimensional structures with good thermal stability.

In this context, and as a part of our ongoing studies on nitrogen ligands, we present here the synthesis, structural aspects, adsorption, theoretical studies and luminescence properties of three novel metal-organic frameworks based on 5-(4-pyridyl)tetrazole (Hptz): $[Cd_2(ptz)(squarate)(OH)(H_2O)_2]_n$ **(1),** $\{[Cd_2(ptz)(4\text{-carboxypyridine})(OH)_2]\cdot(H_2O)_2\}_n$ **(2)** and **{**$[Cd_5(ptz)_2(terephtalate)_4(H_2O)_2]\cdot(H_2O)_2\cdot(CH_3OH)_4\}_n$ **(3)**. We have designed these 3D-MOFs by using of secondary ligands with carboxylate groups such as, squarate and terephthalic acid, and 4-carboxypyridine generated *"in situ"* using 4-cyanopyridine

by hydrothermal routes. We have chosen these tetrazolate/carboxylate derivative ligands because these building-blocks have aromatic rings and electron-donating N atoms inducing rich coordination modes and, in particular, are good candidates for enhanced emissive properties.

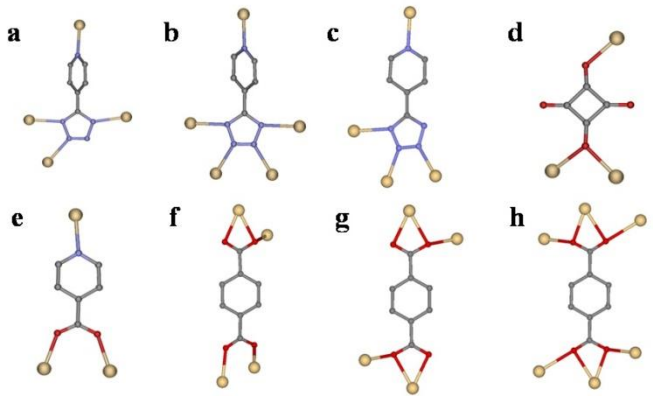

Scheme 1. *Observed coordination modes for the ligands pertaining to compounds* ***1*** *(a, b),* ***2*** *(c, d) and* ***3*** *(e, f, g, h). Colour code N = blue, O = red, C = grey and Cd = tan.*

2. Experimental.

2.1. General

Unless otherwise stated, all reactions were conducted by hydrothermal conditions, with the reagents purchased commercially and used without further purification.

*2.2. Preparation of complexes***.**

$[Cd_2(ptz)(squarate)(OH)(H_2O)_2]_n$ (1): A mixture of $CdCl_2$ (366 mg, 2 mmol), 5-(4-pyridyl)tetrazole sodium salt (Naptz) (169 mg, 1 mmol), squaric acid (114 mg, 1 mmol) and water (14 mL) was sealed in a Teflon-lined acid digestion autoclave and heated at 140 °C under autogenous pressure. After 12 h of heating, the reaction

vessel was cooled down to room temperature during a period of 2 h. Prismatic colorless crystals of **1** were obtained and were washed with H_2O. Yield: 41% based on Cd. Anal. Calcd for ($Cd_2C_{16}N_{10}O_7H_9$): C 28.20, H 1.33, N 20.57. Experimental: C 28.37, H 1.39, N 20.51. FT-IR (KBr pellet): 3425 (s), 1718 (w), 1605 (m), 1509 (s), 1466 (s), 771 (m), 735 (m) cm^{-1}.

{[Cd_2(ptz)(4-carboxypyridine)$(OH)_2$]·$(H_2O)_2$}$_n$ (2): A mixture of $CdCl_2$(366 mg, 2 mmol), 4-cyanopyridine (208 mg, 2 mmol), sodium azide (65 mg, 1 mmol) and water (14 mL) was sealed in a Teflon-lined acid digestion autoclave and heated at 140°C under autogenous pressure. After 12 h of heating, the reaction vessel was cooled down to room temperature during a period of 2 h. Prismatic colorless crystals of **2** were obtained and were washed with H_2O. Yield: 37% based on Cd. Anal. Calcd for ($Cd_2C_{12}N_6O_6H_{14}$): C 25.45, H 2.49, N 14.85. Experimental: C 25.35, H 2.41, N 14.97. FT-IR (KBr pellet): 3388 (s), 1622 (m), 1575 (s), 1450 (m), 1392 (s), 1244 (m), 1105 (w), 759 (m), 729 (m) cm^{-1}.

{[Cd_5(ptz)$_2$(terephtalate)$_4$$(H_2O)_2$]$(H_2O)_2$·$(CH_3OH)_4$}$_n$ (3): Compound 3 was prepared similar to that of compound **1**, but the terephthalic acid (166 mg, 1 mmol) was used instead of squaric acid. Prismatic colourless crystals of **3** were obtained and were washed with H_2O. Yield: 53% based on Cd. Anal. Calcd for ($Cd_5C_{48}N_{10}O_{23}H_{46}$): C 33.89, H 2.73, N 8.24. Experimental: C 33.99, H 2.76, N 8.21. FT-IR (KBr pellet): 3416 (m), 3128 (s), 1626 (m), 1544 (s), 1400 (s), 1219 (w), 1020 (m), 747 (m), 714 (m) cm^{-1}.

2.3. Physical measurements.

Elemental analyses were carried out at the "Centro de Instrumentación Científica" (University of Granada) on a Fisons-Carlo Erba analyser model EA 1108. IR spectra on powdered samples were recorded with a ThermoNicolet IR200FTIR using KBr pellets.

*2.4. Single-Crystal Structure Determination***.**

Suitable crystals of **1**-**3** were mounted on a glass fibre and used for data collection on a Bruker AXS APEX CCD area detector equipped with graphite monochromated Mo Kα radiation (λ = 0.71073 Å) by applying the ω-scan method. Lorentz-polarization and empirical absorption corrections were applied. The structures were solved by direct methods and refined with full-matrix least-squares calculations on F^2 using the program SHELXS97.[10] Anisotropic temperature factors were assigned to all atoms except for hydrogen atoms, which are riding their parent atoms with an isotropic temperature factor arbitrarily chosen as 1.2 times that of the respective parent. Attempts to identify the solvent molecules (water and methanol) failed in compounds **2** and **3**. Instead, a new set of F^2 (hkl) values with the contribution from solvent molecules withdrawn was obtained by the SQUEEZE procedure implemented in PLATON-94.[11] Refinement reduced R_1 to 0.026 and 0.059 for **2** and **3**, respectively. Several crystals of **2** and **3** were measured and the structure was solved from the best data we were able to collect. Final R(F), wR(F^2) and goodness of fit agreement factors, details on the data collection and analysis can be found in Table 1. Selected bond lengths and angles are given in Tables S1 and S2 (ESI). CCDC reference numbers for the structures of **1**-**3** were 930225-930227. Copies of the data can be obtained free of charge upon application to CCDC, 12 Union Road, Cambridge CB2 1EZ, U.K. (fax, (+44)1223 336-033; e-mail, deposit@ ccdc.cam.ac.uk).

*2.4. Luminescence measurements***.**

A Varian Cary-Eclipse Fluorescence Spectrofluorimeter was used to record the fluorescence spectra. The spectrofluorimeter was equipped with a xenon discharge lamp (peak power equivalent to 75 kW), Czerny-Turner monochromators, R-928 photomultiplier tube which is red sensitive (even 900 nm) with manual or automatic voltage controlled using the Cary Eclipse software for Windows 95/98/NT system. The photomultiplier detector voltage was 700 V and the instrument excitation and emission slits were set at 5 and 5 nm, respectively.

2.6. Computational Details.

The material was characterized geometrically, starting from the crystallographic coordinates. The pore size distributions were calculated using the method of Gelb and Gubbins, where the largest sphere that can fit in a random point within a structure without overlapping the van der Waals surface of the framework is recorded for a large number of random points.[12]

2.7. N_2 Adsorption-Desorption Isotherm

N_2 gas adsorption-desorption isotherm was performed using a Micromeritics ASAP 2020 analyzer degassing the sample at 90^{o}C during 6 hours prior to the adpsortion experiments

3. Results and Discussion.

Hydrothermal reactions of cadmium chloride (2 mmol) with Naptz (1 mmol) and a secondary ligand (1 mmol) in water (14 ml) at 140 ^{o}C for 12 h followed by cooling down to room temperature over 2 h, yield prismatic colourless crystals of **1** (40% yield) and **3** (50% yield), respectively. Compound **2** was obtained *in situ* by hydrothermal reaction of cadmium chloride (2 mmol) with 4-cyanopyridine (2 mmol) and sodium azide (1 mmol) in water (14 ml) at 140 ^{o}C for 12 h. Colourless crystals of **2** (35% yield) were obtained. Crystal structures were determined by single crystal X-ray diffraction methods and found that both compounds exhibit fascinating and different 3D-MOF structures. Selected bond lengths and angles of the studied structures are given in Tables S1 and S2.

3.1. Description of the structures.

The crystal structure of **1** consists of a three-dimensional coordination polymer in which the asymmetric unit includes two crystallographically independent Cd^{2+} centers, one squarate anion (Scheme 1, *d* coordination), one ptz^- ligand, one OH-bridge anion and two coordination water molecules (Figure 1). Each cadmium atom adopts a very distorted octahedral coordination geometry.

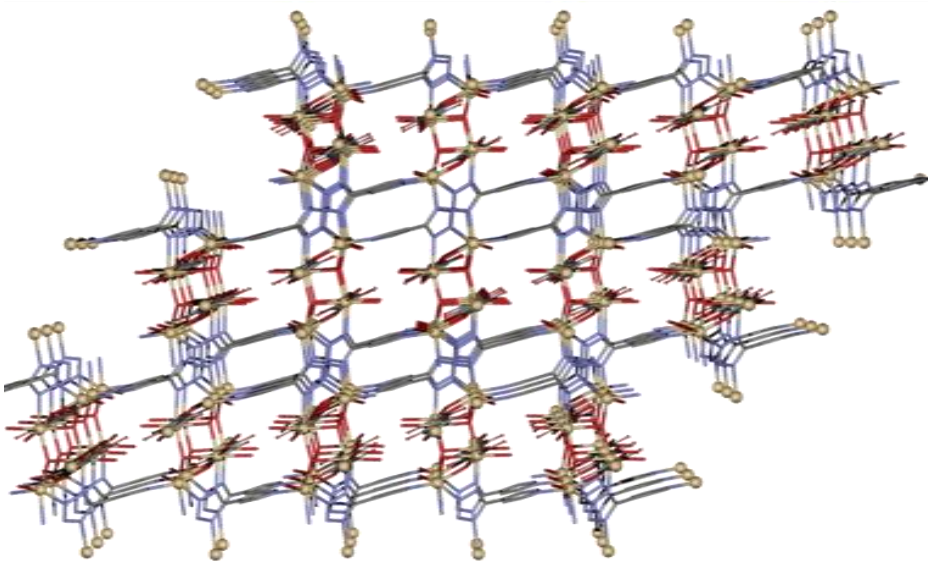

Figure 1. *View of the 3D network of* ***1*** *in the ac plane.*

The Cd1 atom has a CdN_3O_3 environment in *fac* disposition which is coordinated with one oxygen atom pertaining to one squarate dianion, three nitrogen atoms from three different tetrazolate groups (N2A, N4A and N9A), one oxygen atom (O1) from a OH^- anion and one water molecule. The Cd2 atom has a $CdNO_5$ environment and is coordinated to one N atom (N1A) of a tetrazolate group, two O atoms from two different squarate ligands in *trans* positions, two O1 atoms from two OH^- anions in *cis* positions and one water molecule (Figure 2). Although the ptz^- ligand has five N donors, only three N donors from the tetrazole ring and one N

donor from the pyridyl ring bind to four Cd^{2+} centers (Scheme 1, *a* coordination). This coordination mode of the ligand has been shown only in compounds such as $[Cu_2(ptz)CN]_n$ and $\{Ag[\mu_4\text{-}(ptz)]\}_n$.[13]

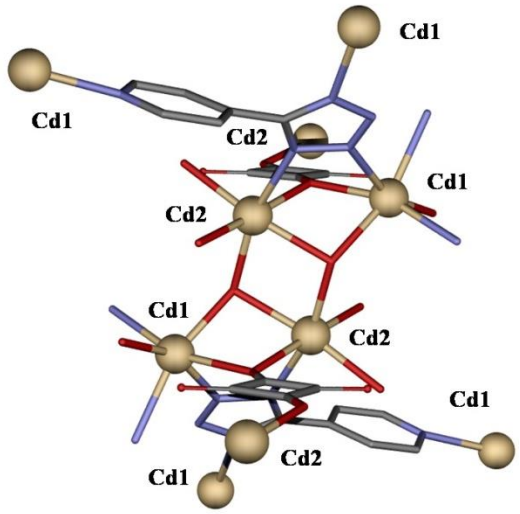

Figure 2. *A view of the metal environment and coordination mode of the ligands for* ***1****.*

Compound **2** is a three-dimensional coordination polymer (Figure 3) in which the asymmetric unit is formed by two different cadmium atoms with distorted octahedral fashion, one ptz^- ligand with a pentadentate-bridging coordination mode (Scheme 1, *b* coordination), one monodeprotonated tridentate-bridging 2-carboxypyridine (Scheme 1, *e*), one bridging-OH^- anion and one coordinated OH^- anion.

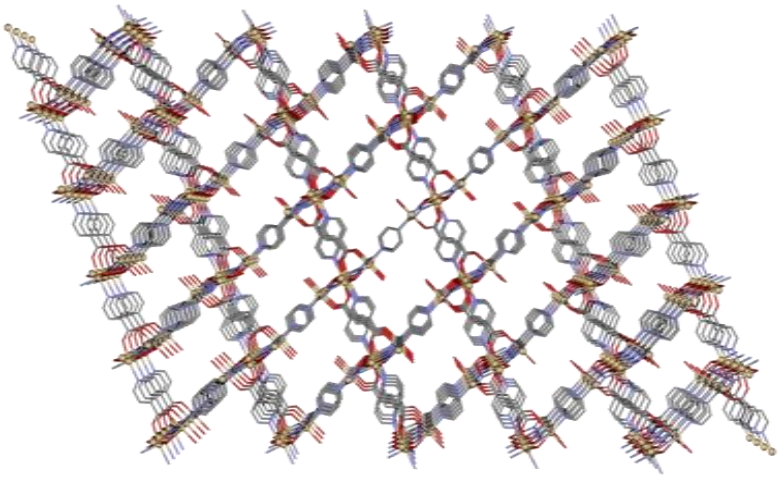

Figure 3. *View down to the b axis in the three-dimensional network in* ***2****.*

In this structure, Cd1 exhibits a distorted octahedral CdN_3O_3 geometry with three nitrogen atoms belonging to three different tetrazolate groups, one hydroxy anion that make triple-bridge between one Cd1 and two Cd2 atoms, one terminal coordination OH^- anion and one oxygen atom pertaining to carboxylate group of 4-carboxypiridine ligand. Cd2 exhibits a distorted octahedral CdN_3O_3 geometry with three nitrogen atoms belonging to three different tetrazolate groups, two triple-bridge hydroxy anions and one oxygen atom pertaining to the carboxylate group of 4-carboxypiridine ligand (Figure 4). In this compound each tetrazolate moiety also coordinates in a tetra-dentate fashion to cadmium atoms (Scheme 1, *b* coordination). To the best of our knowledge, this is the second example reported in the literature in which all the N donors atoms of ptz^- ligand take part in the coordination of diverse ptz-based metal complexes.[14]

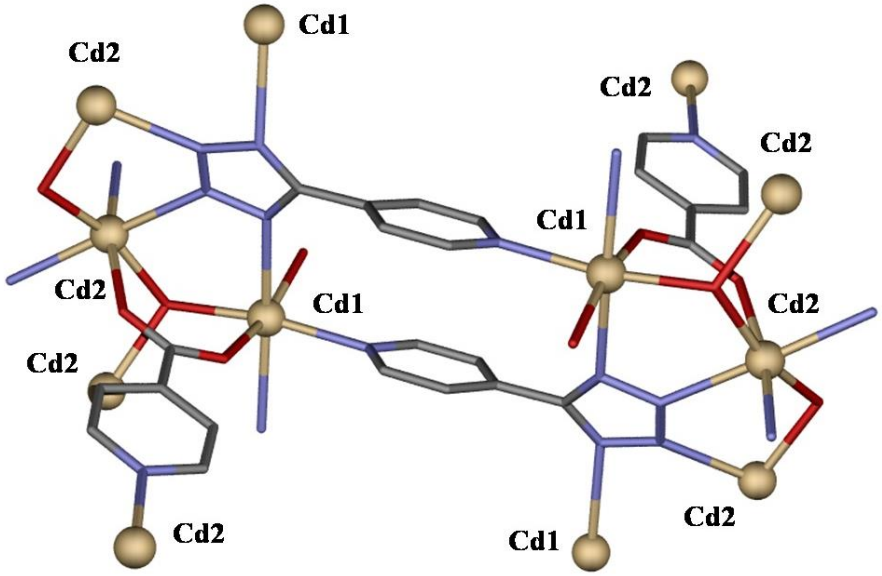

Figure 4. *A view of the metal environment and coordination mode of the ligands for* ***2****.*

The structure of **3** consists of a three-dimensional MOF with channels occupied by disordered solvent water molecules that propagate along the *a* crystallographic axis (Figure 5). The crystalline structure can be described as sheets formed by chains bridged by ptz^- ligands and generated by cadmium atom units by tetrazolates and carboxylates groups. These sheets are bridged by three different terephthalic ligands (Scheme 1, *f, g* and *h* modes) generating a three-dimensional coordination polymer with channels along *a* direction.

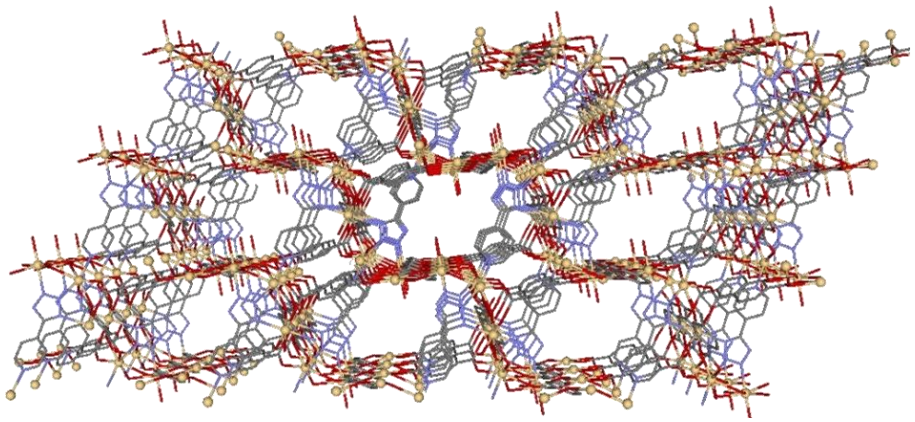

Figure 5. *View of the channels pertaining to 3D network of* ***3*** *in the a direction.*

In this polymer, there are three crystallographically independent Cd^{2+} centers. Cd1 atom adopts an octahedral coordination geometry with a CdN_2O_4 environment in which nitrogen atoms (N1A) pertaining to tetrazolates groups are in *trans* positions imposed by symmetry. The other four positions are occupied by oxygen atoms (O1B and O1D) of carboxylate groups pertaining to four different terephthalic ligands. The Cd2 atom has a pentagonal bipyramidal CdN_2O_5 geometry in which nitrogen atoms (N2A and N9A) of the tetrazolate and pyridine groups, respectively, are in *trans* position (Figure 6).

In the equatorial plane the five positions are occupied by five oxygen atoms pertaining to carboxylate groups of different terephthalic ligands (O1D, O2D, O2B, O2C and O11B). Cd3 atom has a pentagonal bipyramidal $CdNO_6$ geometry. In this case, in the apical positions Cd3 has a nitrogen atom (N3A) of the tetrazolate group and one coordination water molecule. In the equatorial plane the five positions are occupied by five oxygen atoms (O1C, O1C, O2C, O11B and O12B) pertaining to carboxylate groups of different terephthalic ligands.

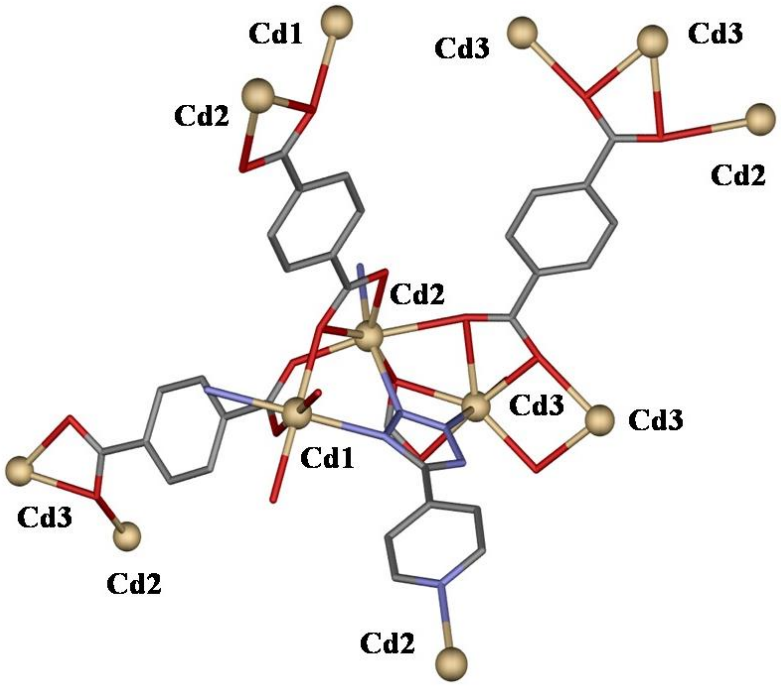

Figure 6. *A view of the metal environment and coordination mode of the ligands for* ***3****.*

Table 1. Crystallographic Data and Structural Refinement Details for **1-3**

compound	**1**	**2**	**3**
chemical formula	$C_{10}H_9N_5O_7Cd_2$	$C_{12}H_{14}N_6O_6Cd_2$	$C_{96}H_{80}N_{24}O_{48}Cd_{16}$
CCDC	930225	930226	930227
M/gmol^{-1}	536.02	563.09	4136.24
T (K)	293	293	293
λ/Å	0.71073	0.71073	0.71073
cryst syst	monoclinic	monoclinic	triclinic
space group	*P21/c*	*C2/c*	*P-1*
a/ Å	13.1992(4)	27.9637(16)	10.102(4)
b/ Å	8.1755(3)	7.2809(4)	10.769(5)
c/ Å	17.2036(5)	19.2168(11)	16.709(7)
α/deg	90	90	108.150(5)
β/deg	129.854(2)	111.8870(10)	106.995(5)
γ/deg	90	90	110.535(4)
V/ Å^3	1425.15(8)	3630.5(4)	1443.5(10)
Z	4	8	1
ρ(g cm-3)	2.498	2.060	4.758
μ(mm-1)	3.033	2.384	5.962
Unique reflections	2804	9183	13794
R(*int*)	0.000	0.021	0.089
GOF on F^2	1.019	1.048	0.934
R1 [I > 2σ(*I*)]	0.043	0.026	0.059
wR2 [I > 2σ(*I*)]	0.075	0.074	0.132

[a] $R(F) = \sum||F_o| - |F_c||/\sum|F_o|$, $wR(F^2) = [\sum w(F_o^2 - F_c^2)^2/\sum wF^4]^{1/2}$

Table S1. Selected Distances (Å) for compound **1**, **2** and **3**

1	**2**	**3**
Cd1 O1 2.294(5)	Cd1 O1 2.213(2)	Cd1 O1B 2.222(6)
Cd1 N9A 2.298(5)	Cd1 O2B 2.248(3)	Cd1 O1B 2.222(6)
Cd1 O1B 2.325(5)	Cd1 N9A 2.273(3)	Cd1 O1D 2.255(7)
Cd1 O2W 2.326(5)	Cd1 O2 2.298(4)	Cd1 O1D 2.255(7)
Cd1 N4A 2.367(6)	Cd1 N1A 2.529(3)	Cd1 N1A 2.424(9)
Cd1 N2A 2.372(6)	Cd1 N4A 2.648(3)	Cd1 N1A 2.424(9)
Cd1 Cd2 3.4730(8)	Cd2 O1 2.257(2)	Cd2 O2B 2.254(7)
Cd2 O1 2.229(5)	Cd2 O1 2.257(2)	Cd2 N9A 2.288(8)
Cd2 O3B 2.263(5)	Cd2 O1B 2.324(3)	Cd2 N2A 2.333(8)
Cd2 O1W 2.280(5)	Cd2 N7B 2.327(3)	Cd2 O2D 2.389(6)
Cd2 O1 2.284(5)	Cd2 N3A 2.351(3)	Cd2 O11B 2.409(6)
Cd2 O1B 2.354(5)	Cd2 N2A 2.378(3)	Cd2 O1D 2.454(6)
Cd2 N1A 2.394(6)		Cd2 C3D 2.757(9)
Cd2 Cd2 3.4390(10)		Cd3 O1W 2.231(7)
Cd2 Cd1 3.4730(8)		Cd3 O12B 2.319(7)
		Cd3 O1C 2.319(6)
		Cd3 O1C 2.321(7)
		Cd3 N3A 2.355(8)
		Cd3 O11B 2.384(7)
		Cd3 O2C 2.541(6)
		Cd3 C10B 2.699(10)

Table S2. Selected Bond Angles (Å) for compound **1**, **2** and **3**

1	2	3
O1 Cd1 N9A 86.81(18)	O1 Cd1 O2B 88.47(10)	O1B Cd1 O1B 180.0(4)
O1 Cd1 O1B 75.98(16)	O1 Cd1 N9A 170.11(10)	O1B Cd1 O1D 89.1(2)
N9A Cd1 O1B 161.05(18)	O2B Cd1 N9A 92.50(11)	O1B Cd1 O1D 90.9(2)
O1 Cd1 O2W 120.44(17)	O1 Cd1 O2 89.93(15)	O1B Cd1 O1D 90.9(2)
N9A Cd1 O2W 89.68(18)	O2B Cd1 O2 165.02(18)	O1B Cd1 O1D 89.1(2)
O1B Cd1 O2W 92.21(16)	N9A Cd1 O2 91.63(16)	O1D Cd1 O1D 180.0
O1 Cd1 N4A 159.01(18)	O1 Cd1 N1A 95.42(8)	O1B Cd1 N1A 90.4(2)
N9A Cd1 N4A 102.0(2)	O2B Cd1 N1A 79.29(11)	O1B Cd1 N1A 89.6(2)
O1B Cd1 N4A 96.91(18)	N9A Cd1 N1A 94.43(10)	O1D Cd1 N1A 84.8(2)
O2W Cd1 N4A 79.06(18)	O2 Cd1 N1A 86.04(17)	O1D Cd1 N1A 95.2(2)
O1 Cd1 N2A 79.99(18)	O1 Cd1 N4A 85.23(9)	O1B Cd1 N1A 89.6(2)
N9A Cd1 N2A 99.6(2)	O2B Cd1 N4A 93.66(11)	O1B Cd1 N1A 90.4(2)
O1B Cd1 N2A 85.35(19)	N9A Cd1 N4A 84.88(10)	O1D Cd1 N1A 95.2(2)
O2W Cd1 N2A 158.21(19)	O2 Cd1 N4A 101.05(18)	O1D Cd1 N1A 84.8(2)
N4A Cd1 N2A 79.8(2)	N1A Cd1 N4A 172.89(10)	N1A Cd1 N1A 180.0(4)
O1 Cd1 Cd2 40.55(11)	O1 Cd2 O1 162.71(5)	O2B Cd2 N9A 87.3(3)
N9A Cd1 Cd2 124.46(14)	O1 Cd2 O1B 80.54(10)	O2B Cd2 N2A 102.3(3)
O1B Cd1 Cd2 42.41(12)	O1 Cd2 O1B 83.81(10)	N9A Cd2 N2A 162.0(3)
O2W Cd1 Cd2 126.98(12)	O1 Cd2 N7B 109.73(10)	O2B Cd2 O2D 125.4(2)
N4A Cd1 Cd2 122.77(14)	O1 Cd2 N7B 86.63(10)	N9A Cd2 O2D 88.4(3)
N2A Cd1 Cd2 62.59(15)	O1B Cd2 N7B 168.30(11)	N2A Cd2 O2D 98.0(3)
O1 Cd2 O3B 89.60(17)	O1 Cd2 N3A 81.53(10)	O2B Cd2 O11B 83.0(2)
O1 Cd2 O1W 99.98(17)	O1 Cd2 N3A 91.80(10)	N9A Cd2 O11B 83.0(3)
O3B Cd2 O1W 88.25(18)	O1B Cd2 N3A 92.17(11)	N2A Cd2 O11B 83.1(2)
O1 Cd2 O1 80.72(18)	N7B Cd2 N3A 94.87(12)	O2D Cd2 O11B 150.0(2)
O3B Cd2 O1 103.47(17)	O1 Cd2 N2A 92.70(10)	O2B Cd2 O1D 78.7(2)
O1W Cd2 O1 168.27(17)	O1 Cd2 N2A 92.07(10)	N9A Cd2 O1D 115.0(3)
O1 Cd2 O1B 95.74(16)	O1B Cd2 N2A 80.99(11)	N2A Cd2 O1D 82.1(2)
O3B Cd2 O1B 174.32(17)	N7B Cd2 N2A 92.66(11)	O2D Cd2 O1D 54.7(2)
O1W Cd2 O1B 92.71(17)	N3A Cd2 N2A 171.73(11)	O11B Cd2 O1D 153.4(2)
O1 Cd2 O1B 75.59(16)		O2B Cd2 C3D 102.4(3)
O1 Cd2 N1A 163.40(18)		N9A Cd2 C3D 101.6(3)
O3B Cd2 N1A 89.40(19)		N2A Cd2 C3D 91.3(3)
O1W Cd2 N1A 96.55(19)		O2D Cd2 C3D 26.8(2)
O1 Cd2 N1A 83.41(18)		O11B Cd2 C3D 173.0(3)
O1B Cd2 N1A 84.93(18)		O1D Cd2 C3D 27.9(2)
O1 Cd2 Cd2 40.96(12)		O1W Cd3 O12B 92.3(3)
O3B Cd2 Cd2 98.64(13)		O1W Cd3 O1C 86.0(2)
O1W Cd2 Cd2 139.70(13)		O12B Cd3 O1C 174.8(2)
O1 Cd2 Cd2 39.76(12)		O1W Cd3 O1C 95.6(3)
O1B Cd2 Cd2 84.23(11)		O12B Cd3 O1C 97.5(2)
N1A Cd2 Cd2 123.01(14)		O1C Cd3 O1C 77.8(2)
O1 Cd2 Cd1 105.18(12)		O1W Cd3 N3A 174.7(3)
O3B Cd2 Cd1 134.69(12)		O12B Cd3 N3A 92.7(3)
O1W Cd2 Cd1 129.00(12)		O1C Cd3 N3A 89.2(2)
O1 Cd2 Cd1 40.76(11)		O1C Cd3 N3A 85.6(3)
O1B Cd2 Cd1 41.75(11)		O1W Cd3 O11B 93.8(3)
N1A Cd2 Cd1 64.66(14)		O12B Cd3 O11B 56.0(2)
Cd2 Cd2 Cd1 70.528(19)		O1C Cd3 O11B 129.0(2)
		O1C Cd3 O11B 152.2(2)
		N3A Cd3 O11B 87.5(2)
		O1W Cd3 O2C 99.9(2)
		O12B Cd3 O2C 131.5(2)
		O1C Cd3 O2C 53.7(2)
		O1C Cd3 O2C 127.3(2)
		N3A Cd3 O2C 75.4(2)
		O11B Cd3 O2C 76.4(2)
		O1W Cd3 C10B 93.1(3)
		O12B Cd3 C10B 27.5(3)
		O1C Cd3 C10B 157.4(3)
		O1C Cd3 C10B 124.6(3)
		N3A Cd3 C10B 90.4(3)
		O11B Cd3 C10B 28.5(3)
		O2C Cd3 C10B 104.5(3)

3.2. Luminescence Properties.

Luminescence properties occupy a special ranking due to the potential applications of visible light emitters in a number of technologically advanced fields.[15] Thanks to its extended aromaticity due to the presence of hexa-atomic rings, pyridine derivative ligands are good candidates for enhanced emissive properties. For this reason we decided to carry out a study of the luminescent properties of these coordination compounds. The excitation and emission spectrum of the ligand 4-ptz at room temperature in solid state have previously been studied.[16]

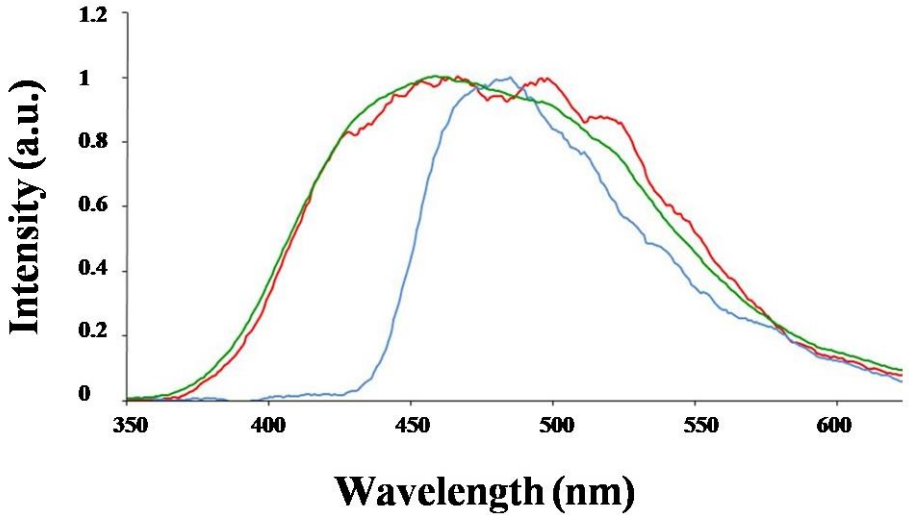

Figure 7. *Emission spectra of **1** (blue), **2** (red) and **3** (green) at room temperature in solid state.*

Using a 330 nm incident radiation (Figure 7), we observed intense emission bands at 485 nm (for **1**), 463 and 497 nm (for **2**) and 459 nm (for **3**). Previous reports about analogous cadmium complexes with azolate ligands showed similar intense bands attributed to ligand-to-ligand electronic transitions.[17] However, they were affected by the coordination of the ligand to the Cd(II) atoms. The decay curves (Figure 8) were fitted to mono exponential function: $I = I_0 + A_1 \exp(-t/\tau)$, where I and I_0 are the luminescent intensities at time t and 0, and τ is defined as the luminescent lifetime. For this function, the

best fit of the experimental luminescence intensities to the above equation led to lifetimes of 0.130, 0.093 and 0.083 ms for **1**, **2** and **3**, respectively.

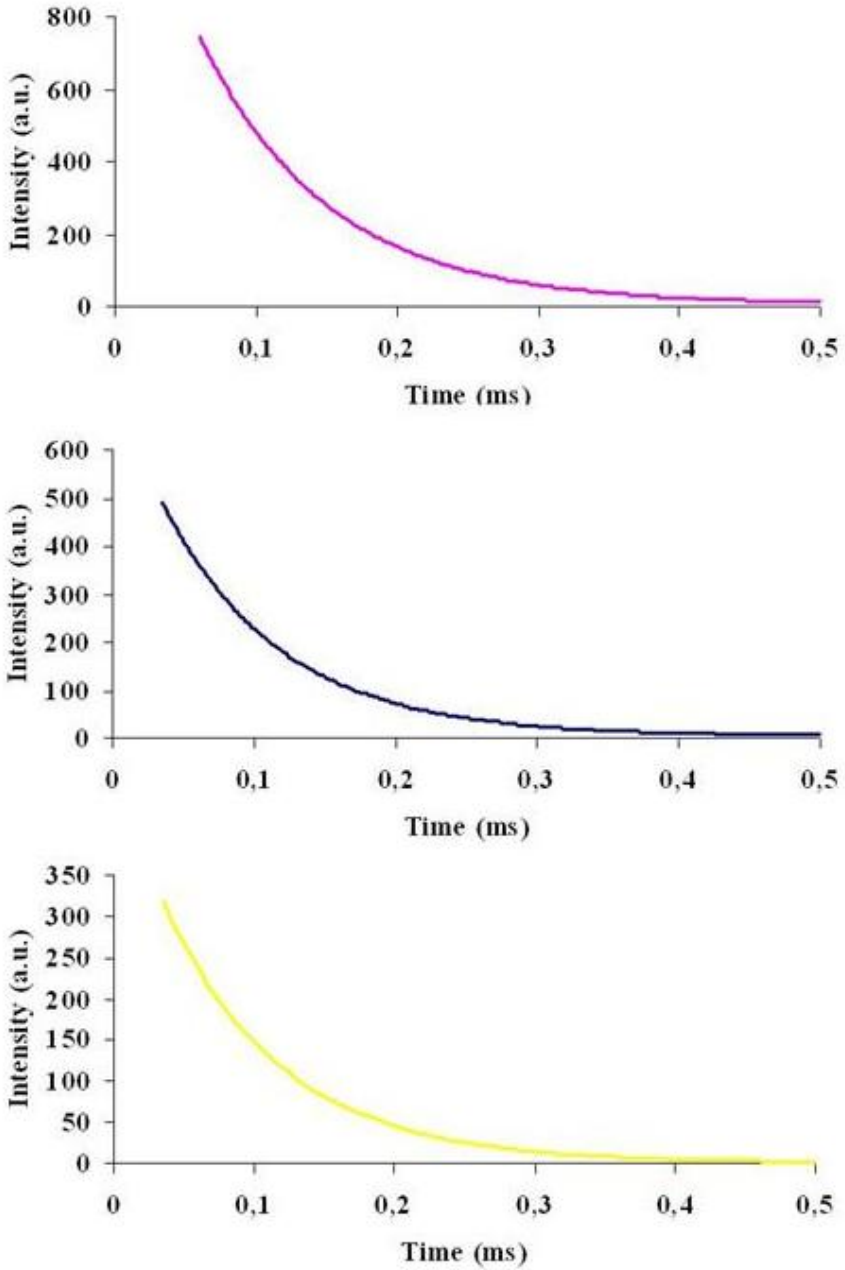

***Figure 8**. Decay time of **1** (pink), **2** (blue) and **3** (yellow) in solid state.*

3.3. Porous Texture.

The porous properties of compounds **1**, **2** and **3** were studied measuring their pore size distribution (PSD) in a Monte Carlo simulation. We have previously used this technique as a fast and simple method to obtain information about the existence of micro- and meso- porosity in crystalline structures, as well as their potential to be adsorbents.[18] PSD analysis represented in Figure 9 shows the existence of well-defined small cavities localised at 5.35, 6.25 and 7.45 Å for **1**, **2** and **3**, respectively. However, the experimental analysis of their adsorption properties using N_2 at 77 K at low pressures revealed that the porous structures collapses during the activation and degasification process at relatively high temperatures (Figure 10). Additionally, the adsorption of H_2 at 77 K and up to 100 bar on **3** revealed to be neglectible.

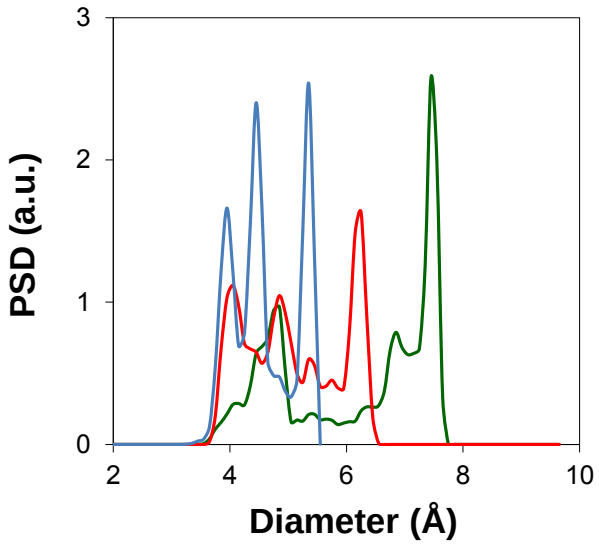

Figure 9. *Pore size distribution of **1** (blue), **2** (red) and **3** (green).*

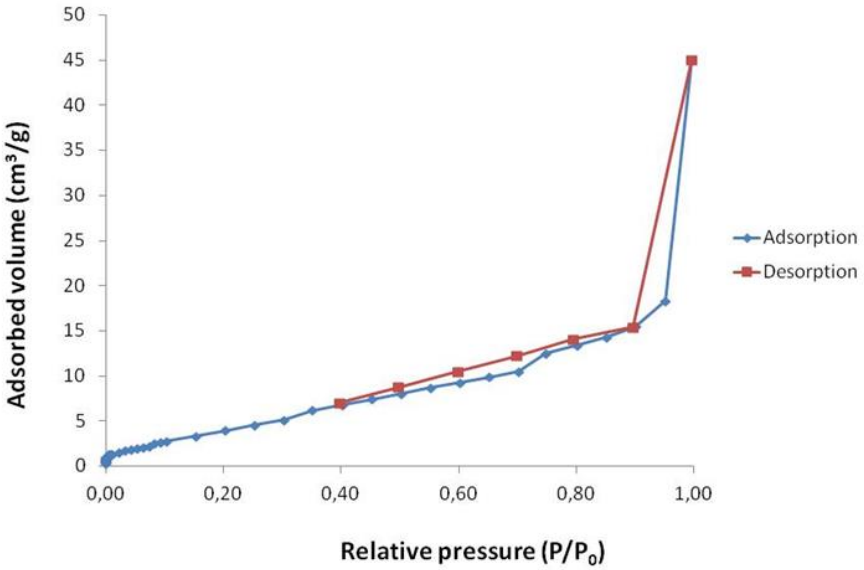

***Figure 10**. Experimental analysis of **3**.*

4. Conclusions

In this work, we have shown that new three dimensional metal- organic frameworks with interesting properties can be synthesized by using classic ligands as 5-(4-pyridyl)tetrazole. The results reported in this paper clearly show that this is a versatile ligand which is able to afford a rich variety of polynuclear complexes with interesting structures. In addition, we have observed that all the studied new 3D-coordination polymers present a high structural diversity in which luminescence and adsorption properties have been studied. These polymers exhibit blue-green long lifetime photoluminescence emission at room temperature in the solid state with long lifetime decays. These results open the door toward the preparation of novel polymers based on this ligand, which could show fascinant physical properties, such as magnetism, luminescence and gases adsorption. Work is already in progress in our laboratory in order to obtain new homo- and heterometallic complexes with similar mixture of ligands containing carboxylate groups.

5. References

[1].- (a) S. Kitagawa, R. Kitaura and S.-I. Noro, *Angew. Chem. In. Ed*., 2004, **43**, 2334; S. Kitagawa, K. Uemura, Chem. Soc. Rev. 2005, **34**, 109; (b) M. Eddaoudi, J. Kim, N. Rosi, D. Vodak, J. Wachter, M. O'Keeffe and O. M. Yaghi, *Science*, 2002, **295**, 469; (c) X. Lin, J. Jia, X. Zhao, K. M. Thomas, A. J. Blake, G. S. Walker, N. R. Champness, P. Hubberstey and M. Schroeder, *Angew. Chem. In. Ed*., 2006, **45**, 7358; (d) F. Nouar, J. F. Eubank, T. Bousquet, L. Wojtas, M. J. Zaworotko and M. Eddaoudi, *J. Am. Chem. Soc.*, 2008, **130**, 1833; (e) S. Horike, S. Shimomura and S. Kitagawa, *Nature Chem.,* 2009, **1**, 695; (f) Z. Wang and S. M. Cohen, *Chem. Soc. Rev.*, 2009, **38**, 1315; (g) H. Furukawa, N. Ko, Y. B. Go, N. Aratani, S. B. Choi, E. Choi, A. O. Yazaydin, R. Q. Snurr, M. O'Keeffe, J. Kim and O. M. Yaghi, *Science*, 2010, **329**, 424; (h) X. Liu, M. Oh and M. S. Lah, *Inorg. Chem.,* 2011, **50**, 5044; (i) M. O'Keeffe and O. M. Yaghi, *Chem. Rev.*, 2012, **112**, 675.

[2].- M. Eddaoudi, J. Kim, N. Rosi, D. Vodak, J. Wachter, M. O'Keefe and O.M. Yaghi, *Science*, 1996, **271**, 49; (b) P. Mahata and S. Natarajan, *Eur. J. Inorg. Chem.*, 2005, 2156; (c) J.-P. Zhang and X.-M. Chen, *J. Am. Chem.l Soc.*, 2008, **130**, 6010; (d) L. J. Murray, M. Dinca and J. R. Long, *Chem. Soc. Rev.*, 2009, **38**, 1294; (e) X. Gu, Z.-H. Lu and Q. Xu, *Chem. Commun.,* 2010, **46**, 7400; (f) T. K. Kim and M. P. Suh, *Chem. Commun.*, 2011, **47**, 4258; (g) T. M. McDonald, W. R. Lee, J. A. Mason, B. M. Wiers, C. S. Hong and J. R. Long, *J. Am. Chem. Soc.*, 2012, **134**, 7056; (h) E.-C. Yang, Z.-Y. Liu, X.-Y. Wu, H. Chang, E.-C. Wang and X.-J. Zhao, *Dalton Trans.*, 2011, **40**, 10082; (i) J. Ferrando-Soria, P. Serra-Crespo, M. de Lange, J. Gascon, F. Kapteijn, M. Julve, J. Cano, F. Lloret, J. Pasan, C. Ruiz-Perez, Y. Journaux and E. Pardo, *J. Am. Chem. Soc.*, 2012, **134**, 15301; (j) D. Sarma, P. Mahata, S. Natarajan, P. Panissod, G. Rogez and M. Drillon, *Inorg. Chem.*, 2012, **51**, 4495; (k) R. M. P. Colodrero, K. E. Papathanasiou, N. Stavgianoudaki, P. Olivera-Pastor, E. R. Losilla, M. A. G. Aranda, L. Leon-Reina, J. Sanz, I. Sobrados, D. Choquesillo-Lazarte, J. M. Garcia-Ruiz, P. Atienzar, F. Rey, K. D. Demadis and A. Cabeza, *Chem. Mater.*, 2012, **24**, 3780.

[3].- Y.-Q. Sun, J. Zhang, Y.-M. Chen, G.-Y. Yang, *Angew. Chem., Int. Ed.*, 2005, **44**, 5814; (b) W.-G. Lu, C.-Y. Su, T.-B. Lu, L. Jiang and J.-M. Chen, *J. Am. Chem. Soc.,* 2006, **128**, 34; (c) A. Y. Robin and K. M. Fromm, *Coord. Chem. Rev.*, 2006, **250**, 2127; (d) O. K. Farha, A. Oezguer Yazaydin, I. Eryazici, C. D. Malliakas, B. G. Hauser, M. G. Kanatzidis, S.-B. T. Nguyen, R. Q. Snurr and J. T. Hupp, *Nature Chem.*, 2010, **2**, 944; (e) P. Maniam and N. Stock, *Inorg. Chem.*, 2011, **50**, 5085; (f) Z.-G. Gu, Y.-T. Liu, X.-J. Hong, Q.-G. Zhan, Z.-P. Zheng, S.-R. Zheng, W.-S. Li, S.-J. Hu and Y.-P. Cai, *Crystal Growth & Design*, 2012, **12**, 2178; (g) L. Qin, J.-S. Hu, M.-D. Zhang, Y.-Z. Li and H.-G. Zheng,

CrystEngComm, 2012, **14**, 8274; (h) Y.-X. Tan, Y.-P. He and J. Zhang, *Cryst. Growth & Des.*, 2012, **12**, 2468.

[4].- (a) Rao, C. N. R.; Natarajan, S. And Vaidhzanathan, R. *Angew. Chem. Int. Ed*., 2004, **43**, 1466; (b) M. Gustafsson, J. Su, H. Yue, Q. Yao and X. Zou, *Cryst. Growth & Des.*, 2012, **12**, 3243; (c) P. Zhang, B. Li, Y. Zhao, X.-G. Meng and T.-L. Zhang, *Chem. Commun.*, 2011, **47**, 7722; (d) H. Sakamoto, R. Matsuda, S. Bureekaew, D. Tanaka and S. Kitagawa, *Chem.-A Eur. J.*, 2009, **15**, 4985; (e) D. Yuan, D. Zhao, D. Sun and H.-C. Zhou, *Angew. Chem., Int. Ed.*, 2010, **49**, 5357; (f) Y. Yan, S. Yang, A. J. Blake, W. Lewis, E. Poirier, S. A. Barnett, N. R. Champness and M. Schroeder, *Chem. Commun.*, 2011, **47**, 9995; (g) D. Kim, X. Song, J. H. Yoon and M. S. Lah, *Cryst. Growth & Des.*, 2012, **12**, 4186.

[5].- (a) Zhang, J. P.; Lin, Y. Y.; Zhang, W. X.; Chen and X. M., *J. Am. Chem. Soc.*, 2005, **127**, 14162; (b) Zheng, S. R.;Yang, Q.Y.;Yang, R.; Pan, M.; Cao, R.and Su, C. Y. *Cryst. Growth & Des.*, 2009, **9**, 2341; (c) C. B. Liu, R. A. S. Ferreira, F. A. Almeida Paz, A. Cadiau, L. D. Carlos, L. S. Fu, J. Rocha and F. N. Shi, *Chem. Commun.*, 2012, **48**, 7964; (d) D. Niu, J. Yang, J. Guo, W.-Q. Kan, S.-Y. Song, P. Du and J.-F. Ma, *Cryst. Growth & Des.*, 2012, **12**, 2397; (e) X.-J. Wang, P.-Z. Li, L. Liu, Q. Zhang, P. Borah, J. D. Wong, X. X. Chan, G. Rakesh, Y. Li and Y. Zhao, *Chem. Commun.*, 2012, **48**, 10286; (f) H. Yang, F. Wang, Y. Kang, T.-H. Li and J. Zhang, *Dalton Trans.*, 2012, **41**, 2873; (g) T.-W. Tseng, T.-T. Luo, S.-Y. Chen, C.-C. Su, K.-M. Chi and K.-L. Lu, *Cryst. Growth & Des.*, 2013, **13**, 510.

[6].- (a) A. Rodríguez-Diéguez and E. Colacio, *Chem. Comm*. 2006, 4140; (b) J. Suárez-Varela, A.J. Mota, H. Aouryaghal, J. Cano, A. Rodríguez-Diéguez, D. Luneau and E. Colacio, *Inorg. Chem*., 2008, **47**, 8143; (c) C. B. Liu, R. A. S. Ferreira, F. A. Almeida Paz, A. Cadiau, L. D. Carlos, L. S. Fu, J. Rocha and F. N. Shi, *Chem. Commun.*, 2012, **48**, 7964; (d) J.-P. Zhang, Y.-Y. Lin, X.-C. Huang and X.-M. Chen, *J. Am. Che. Soc.*, 2005, **127**, 5495.

[7].- A Rodríguez-Diéguez, A. Salinas-Castillo, S. Galli, N. Masciocchi, J. M. Gutiérrez-Zorrilla, P. Vitoria and E. Colacio, *Dalton Trans.,* 2007, 1821.

[8].- J. Kahr, J. P. S. Mowat, A. M. Z. Slawin, R. E. Morris, D. Fairen-Jimenez, P. A. Wright, *Chem. Commun*. 2012, **48**, 6690; (b) B. Wang, A. P. Cote, H. Furukawa, M. O'Keeffe and O. M. Yaghi, *Nature*, 2008, **453**, 207.

[9]. (a) S. L. Zheng, J. H. Yang, X.-L. Yu, X.M. Chen and W. T.Wong, *Inorg. Chem.,* 2004, **43**, 830; (b) S. Skoulika, P. Dallas, M. G. Siskos, Y. Deligiannakis and A. Michaelides,

Chem. Mater., 2003, **15**, 4576; (c) D.-C. Zhong, W.-X. Zhang, F.-L. Cao, L. Jiang and T.-B. Lu, *Chem. Commun.*, 2011, **47**, 1204; (d) L.-H. Cao, H.-Y. Li, S.-Q. Zang, H.-W. Hou and T. C. W. Mak, *Cryst. Growth & Des.*, 2012, **12**, 4299.

[10].- G. M. Sheldrick, *SHELX97, program for crystal structure refinement*, University of Göttingen, Göttingen, Germany, 1997.

[11].- A. L. Spek, *PLATON-94 (V-101094),AMultipurposeCrystallographicTool*, University of Utrecht, The Netherlands, 1994.

[12].- (a) L.D. Gelb and K.E. Gubbins, *Langmuir*, 1999, **15**, 305; (b) T. Düren, F. Millange, G. Férey, K.S. Walton, and R.Q. Snurr, *J. Phys. Chem. C,* 2007, **111**, 5350.

[13].- (a) F. Wang, J. Zhang, S.-M. Chen, Y.-M. Xie, X.-Y. Wu, S.-C. Chen, R.-M. Yu and C.-Z. Lu, *CrystEngComm.,* 2009, **11**, 1526; (b) Y.Chen, Z.-G. Ren, H.-X. Li, X.-Y. Tang, W.-H. Zhang, Y. Zhang and J.-P. Lang, *J. Molecular Structure*, 2008, **875**, 339.

[14].- Zhong-Yi Liu, Xiang-Jun Shi, En-Cui Yang and Xiao-Jun Zhao, *Inorg. Chem. Commun*., 2010, **13**, 1259.

[15].- U. H. F. Bunz, *Chem. Rev.*, 2000, **100**, 1605.

[16] .- J.M. Seco, M. de Araújo Farias, N.M. Bachs, A.B. Caballero, A. Salinas-Castillo and A. Rodríguez-Diéguez*, Inorg. Chim. Acta*, 2010, **363**, 3194.

[17].- X. S. Wang, Y. Z. Tang, X. F. Huang, Z. R. Qu, C. M. Che, P. W. H. Chang and R. G. Xiong, *Inorg. Chem.,* 2005, **44**, 5278.

[18].- (a) D. Fairen-Jimenez, N.A. Seaton, and T. Düren. *Langmuir*, 2010, **26**, 14694; (b) J. Getzschmann, I. Senkovska, D. Wallacher, M. Tovar, D. Fairen-Jimenez, T. Düren, J.M. van Baten, R. Krishna, S. Kaskel, *Microporous and Mesoporous Materials*, 2010, **136**, 50; (c) A. Rossin, D. Fairen-Jimenez, T. Düren, G. Giambastiani, M. Peruzzini and J.G. Vitillo, *Langmuir*, 2011, **27**, 10124; (d) A.J. Calahorro, M.E. Lopez-Viseras, A. Salinas-Castillo, D. Fairen-Jimenez, E. Colacio, J. Cano and A. Rodríguez-Diéguez, *CrystEngComm*, 2012, **14**, 6390.

CAPÍTULO 7.

LUMINESCENCE AND MAGNETIC PROPERTIES OF THREE METAL-ORGANIC FRAMEWORKS BASED ON 5-(1*H*-TETRAZOL-5-YL)ISOPHTHALIC ACID LIGAND

ARTICLE: LUMINESCENCE AND MAGNETIC PROPERTIES OF THREE METAL-ORGANIC FRAMEWORKS BASED ON 5-(1*H*-TETRAZOL-5-YL)ISOPHTHALIC ACID LIGAND.

View Article Online
ARTICLE TYPE www.rsc.org/xxxxxx DOI: 10.1039/C3CE40889H

LUMINESCENCE AND MAGNETIC PROPERTIES OF THREE METAL-ORGANIC FRAMEWORKS BASED ON 5-(1*H*-TETRAZOL-5-YL)ISOPHTHALIC ACID LIGAND

Antonio J. Calahorro,[a] Alfonso Salinas-Castillo,[b] José Manuel Seco,[c] Javier Zuñiga,[d] Enrique Colacio[a] and Antonio Rodríguez-Diéguez.[a,*]

a Departamento de Química Inorgánica, Universidad de Granada, 18071, Granada, Spain. Tel: 0034958240442; E-mail: antonio5@ugr.es
b Departamento de Química Analítica, Universidad de Granada.
c Departamento de Química Aplicada, Facultad de Químicas de San Sebastián, UPV/EHU, Paseo Manuel Lardizábal 3, 20018 San Sebastián.
d Dpto. de Física de la Materia Condensada, Facultad de Ciencia y Tecnología, UPV/EHU, 48080 Bilbao (Spain).

ABSTRACT

Three new metal-organic frameworks based on 5-(1H-tetrazol-5-yl)isophthalic acid complexes $\{[Cd_4(TZI)_2(OH)_2 (H_2O)_4](H_2O)_6\}_n$ (1), $\{[Zn_2(TZI)(OH)(H_2O)_2](H_2O)\}_n$ (2) and $\{[Co_8(TZI)_3(OH)_5((N_3)_2(H_2O)_8](H_2O)_8\}_n$ (3) have been synthesized *in situ* by hydrothermal reactions of 5-cyano-1,3-benzenedicarboxylic acid ligand with cadmium, zinc and cobalt metallic(II) salts in presence of sodium azide in water. Compounds 1 and 2 display intense photoluminescence properties in the solid state at room temperature, while 3 exhibits an antiferromagnetic interaction between cobalt(II) ions with a J value of -

3.8 cm^{-1}. *In situ* hydrothermal syntheses reveal new possibilities to formation on new MOFs to construct new materials with fascinating structures and potential applications.

1. INTRODUCTION

Design of coordination polymers has attracted great attention, not only because of their interesting topological structures, but also for their potential applications in the fields of luminescence, gas adsorption, catalysis, magnetic behaviour and electrical conductivity.[1] In recent years, there has been increasing research interest in the synthesis of extended coordination frameworks by hydrothermal routes.[2] Metal–organic frameworks (MOFs) are an emerging class of crystalline three-dimensional materials. They are mostly constructed from clusters of transition-metal ions held in position in a lattice by ligation to organic molecules.[3]

These systems, are currently attracting increasing attention not only due to their fascinating topologies but also due to their interesting applications in different areas of science. Amongst ligands, multidentate N or O-donor building-blocks have drawn extensive attention in the construction of these systems.[4] So far, considerable efforts have been devoted to the synthesis of unusual coordination polymers based on carboxylate and/or pyridine-based ligands.[5]

On the other hand, 5-substituted 1H-tetrazoles have been shown to be very good polydentate bridging ligands for the formation of multidimensional coordination polymers exhibiting a great structural diversity, which is a consequence of their extensive ability bridging metal ion.[6] Recently, we have designed and prepared novel coordination polymers with different tetrazolate-pyrimidine derivative ligands, with interesting luminescent properties.[7] Moreover, we have demonstrated the use of hydrothemal syntheses to generate *in situ* new ligands.[8]

In this context, and as a part of our continuing studies on nitrogen derivative ligands with carboxylate groups, we present here the synthesis, structural aspects, luminescence properties and magnetic studies of three Metal-Organic-Frameworks, $\{[Cd_4(TZI)_2(OH)_2(H_2O)_4](H_2O)_6\}_n$ **(1),** $\{[Zn_2(TZI)(OH)(H_2O)_2]\ (H_2O)\}_n$ **(2)** and $\{[Co_8(TZI)_3(OH)_5((N_3)_2(H_2O)_8](H_2O)_8\}_n$ **(3)** based on 5-(1*H*-tetrazol-5-yl)isophthalic acid ligand (H_3TZI). We have designed *in situ* by hydrothermal routes this linker because of its similarity to another as the benzene-1,3,5-tricarboxylate (BTC) ligand with which others authors have synthesized a lot of MOFs with interesting physical properties.[9] Moreover, TZI building-block has electron-donating N atoms inducing rich coordination modes and, in particular, is a good candidate for enhanced emissive properties. In our case, compounds **1** and **2** consist in 3D- and 2D-MOFs, respectively, and fluorescence analyses show that they exhibit intense purple photoluminescence in the solid state at room temperature. Otherwise, **3** is a three-dimensional coordination polymer that exhibits an antiferromagnetic interaction between cobalt(II) ions with a J value of -3.8 cm^{-1}.

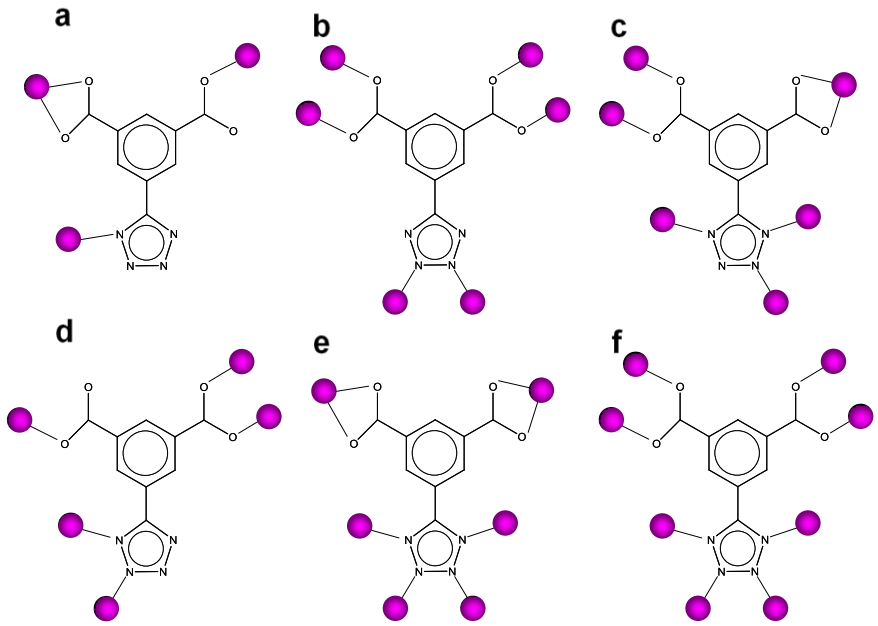

Scheme I. *Coordination modes of* TZI^{-3} *ligand. c, d, e and f modes are novels and present in our compounds while a and b have been reported previously. Compound* ***1*** *and* ***2*** *exhibit c and d mode, respectively, while* ***3*** *shows e and f modes.*

To the best of our knowledge, these are the first examples of crystal structures of MOFs with Cd(II), Zn(II) and Co(II) that contain the TZI^{-3} ligand. There are only two examples of Cu^{II} (3D) and Gd^{III} (2D) coordination compounds in which TZI^{-3} shows *a* and *b* coordination modes (Scheme I).[10] Moreover, this is the first time that TZI^{-3} is synthesized *in situ* by hydrothermal conditions starting with cyanide derivative ligand (Demko–Sharpless reaction[11]) and the first examples of novel coordination modes of this linker (Scheme I, *c*, *d*, *e* and *f*). Describing the structures as SBU, in compounds **1** and **2**, a tetranuclear distorted dicubane $[M_4(OH)_2]$ SBU, where M is Cd and Zn is formed. However, in compound **3**, an octanuclear Co(II) SBU is formed, which according to a literature survey,[12] this octanuclear motif is reported for the first time in cobalt chemistry.

Hydrothermal reactions of the appropriate metal chloride (2 mmol) with 5-(1H-cyano-5-yl)isophthalic acid ligand (1 mmol) and sodium azide (1 mmol) in water (14 ml) at 140 ^{o}C for 12 h followed by cooling down to room temperature over 2 h, yield prismatic yellow, colourless and red crystals of **1** (70% yield based on Cd), **2** (45% yield based on Zn) and **3** (30% yield based on Co), respectively. Crystal structures were determined by single crystal X-ray diffraction methods and found that both compounds exhibit fascinating and different structures.[13] Table S2 and S3 give the main bond lengths and angles of the structures.

2. EXPERIMENTAL

2.1. General.

All analytical reagents were purchased from commercial sources and used without further purification.

2.2. Preparation of MOFs

{[$Cd_4(TZI)_2(OH)_2(H_2O)_4](H_2O)_6$}$_n$ (1): A mixture of $CdCl_2$(366 mg, 2 mmol), 5-(1H-cyano-5-yl)isophthalic acid (191 mg, 1 mmol), sodium azide (65 mg, 1 mmol) and water (14 mL) was sealed in a Teflon-lined acid digestion autoclave and heated at 140°C under autogenous pressure. After 12 h of heating, the reaction vessel was cooled down to room temperature during a period of 2 h. Colourless crystals of 1 were obtained and were washed with H_2O. Yield: 70% based on Cd. Anal. Calcd for (Cd4C18N8O20H28): C 19.05, H 2.49, N 9.90. Experimental : C 19.37, H 2.59, N 9.76. FT-IR (KBr pellet): 3410 (m), 3131 (s), 1618 (m), 1563 (m), 1398 (s), 1384 (s), 757 (w) cm^{-1}

{[$Zn_2(TZI)(OH)(H_2O)_2$] (H_2O)}$_n$ (2): Compound 2 was prepared similar to that of compound 1, but the $ZnCl_2$ (272 mg, 2 mmol) was used instead of $CdCl_2$.Colourless crystals of 2 were obtained and were washed with H_2O. Yield: 45% based on Cd. Anal. Calcd for (Zn2C9N4O8H10): C 25.12, H 2.34, N 13.03. Experimental : C 25.37, H 2.51, N 12.87. FT-IR (KBr pellet): 3388 (s), 1622 (m), 1575 (s), 1450 (m), 1392 (s), 1244 (m), 1105 (w), 759 (m), 729 (m) cm^{-1}

{[$Co_8(TZI)_3(OH)_5((N_3)_2(H_2O)_8](H_2O)_8$}$_n$ (3): Compound 3 was prepared similar to that of compound 1, but the $CoCl_2 \cdot 6H_2O$ (476 mg, 2 mmol) was used instead of $CdCl_2$. Pink crystals of 3 were obtained and were washed with H_2O. Yield: 30% based on Cd. Anal. Calcd for (Co8C27N18O33H46): C 19.98, H 2.86, N 15.54. Experimental : C 20.17, H 3.01, N 15.37. FT-IR (KBr pellet): 3427 (s), 2085 (m), 1623 (m), 1576 (m), 1457 (m), 1373 (s), 763 (w), 724 (m) cm^{-1}

2.3. Physical measurements

Elemental analyses were carried out at the "Centro de Instrumentación Científica" (University of Granada) on a Fisons-Carlo Erba analyser model EA 1108. The IR spectra on powdered samples were recorded with a ThermoNicolet IR200FTIR by using KBr pellets.

2.4. Single-Crystal Structure Determination

Suitable crystals of **1** were mounted on glass fiber and used for data collection. Data were collected with a Bruker AXS APEX CCD area detector equipped with graphite monochromated Mo Kα radiation (λ = 0.71073 Å) by applying the ω-scan method and a StadiVari Stoe. The data were processed with APEX2[14] and corrected for absorption using SADABS.[15] The structure was solved by direct methods using SIR97,[16] revealing positions of all non-hydrogen atoms. These atoms were refined on F^2 by a full matrix least-squares procedure using anisotropic displacement parameters.[17] Aromatic hydrogen atoms were included as fixed contributions riding on attached atoms with isotropic thermal displacement parameters 1.2 times those of the respective atom. The structure has disorder problems with solvent molecules. Attempts to identify the solvent molecules failed in compound **2** and **3**. Instead, a new set of F^2 (*hkl*) values with the contribution from solvent molecules withdrawn was obtained by the SQUEEZE procedure implemented in PLATON-94.[18] Refinement reduced R_1 to 0.042 and 0.083 for **2** and **3**, respectively. Final R(F), wR(F^2) and goodness of fit agreement factors, details on the data collection and analysis can be found in Table S1. Crystallographic data (excluding structure factors) for the reported structure have been deposited with the Cambridge Crystallographic Data Centre as supplementary publication No. CCDC 928815 and 928816 for **2** and **3**, respectively.

2.5. Luminescence measurement

A Varian Cary-Eclipse Fluorescence Spectrofluorimeter solid sample holder accessory was used to obtain the fluorescence spectra. The spectrofluorimeter was equipped with a xenon discharge lamp (peak power equivalent to 75 kW), Czerny-Turner monochromators, R-928 photomultiplier tube which is red sensitive (even 900 nm) with manual or automatic voltage controlled using the Cary Eclipse software

for Windows 95/98/NT system. The photomultiplier detector voltage was 800 V and the instrument excitation and emission slits were set at 10 and 10 nm, respectively.

3. RESULTS AND DISCUSSION

3.1. Structure and crystallographic results

Compound **1** is a three-dimensional coordination polymer in which the asymmetric unit is formed by four different cadmium atoms with very distorted octahedral coordination geometry, two TZI^{-3} ligands with heptadentate coordination mode (Scheme I, *c* mode), two tridentate OH^- anions, four coordination water molecules and six crystallization water molecules. Cd1 and Cd4 exhibit very distorted octahedral CdN_2O_4 geometries with the two nitrogen atoms belonging to two tetrazolate rings in *trans* positions, one OH^- anion and three oxygen atoms pertaining to two carboxylate groups from to two different TZI^{-3} ligands. Cd2 and Cd3 exhibit very distorted octahedral $CdNO_5$ geometries with the one nitrogen atom belonging to tetrazolate group in *trans* positions to one oxygen atom pertaining to carboxylate group, two OH^- anions and two coordination water molecules.

Each triply deprotonated TZI^{-3} ligand connects with six cadmium ions, resulting in the formation of a 3D-MOF (Figure 1), in which each tetrazolate moiety also coordinates in a tridentate fashion to cadmium atoms (Scheme I, *c* mode). The network found in compound **1** is binodal (3,8) with tfz-d; UO3 topology, while compound **2** is a 2D net with kgd topology.

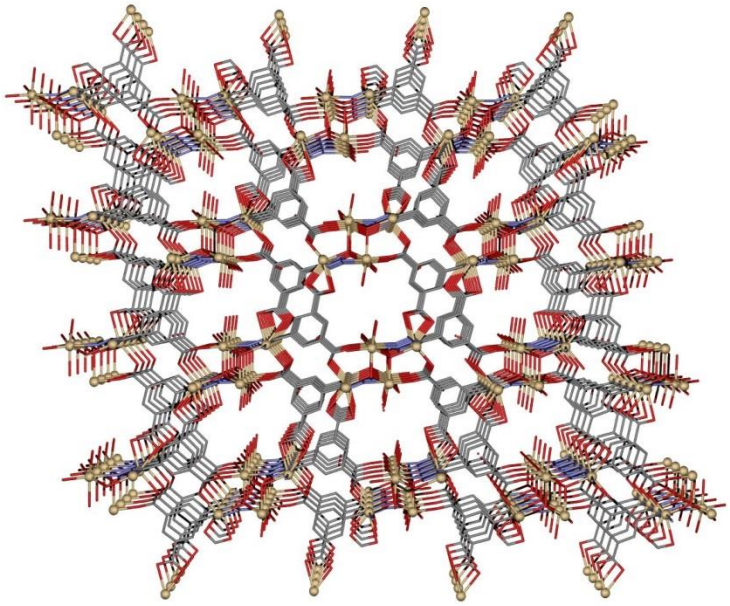

Figure 1. *View down to the a axis in the three-dimensional network in* ***1****.*

Compound **2** crystallises in the triclinic space group *P-1*, the asymmetric unit consisting of two different zinc ions, one TZI^{-3} ligand, one OH^- group, two coordination water molecules and one crystallization water molecule, all in general positions. Zn1 ion exhibits distorted octahedral $ZnNO_5$ geometry with the nitrogen atom belonging to tetrazolate ring in *trans* positions to one oxygen atom pertaining to carboxylate group, two water molecules and two oxygen atoms in *cis* positions pertaining to two different OH^- groups that make triple-bridge between two Zn1 and one Zn2 atoms. Zn2 ion exhibits distorted tetrahedral $ZnNO_3$ geometry with the nitrogen atom belonging to tetrazolate group, two oxygen atoms pertaining to two different carboxylate groups and one OH^- group. Each triply deprotonated TZI^{-3} ligand connects with five zinc ions, resulting in the formation of a 2D-MOF (Figure 2), in which each tetrazolate moiety also coordinates in a bidentate fashion (N1N2) to zinc atoms (Scheme I, *d* mode).

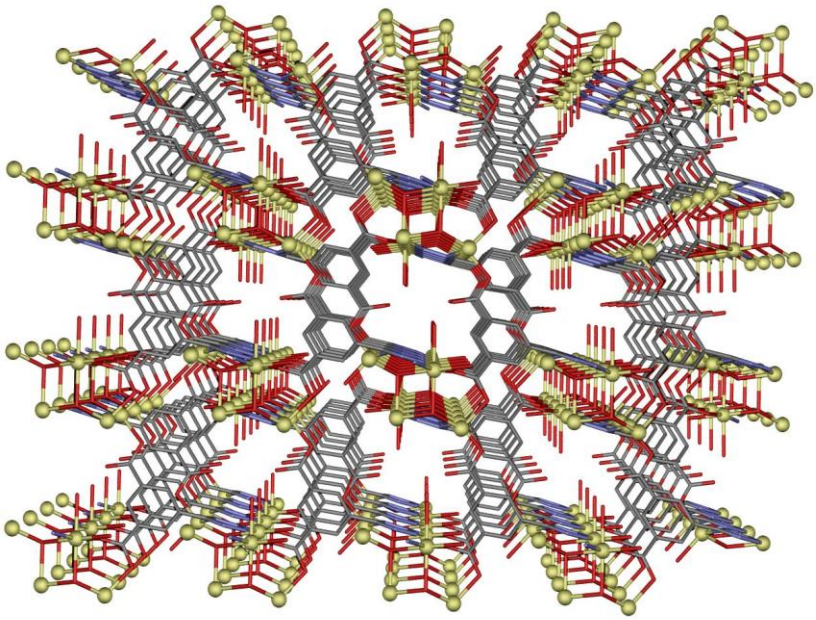

Figure 2. *View down to the a axis in the three-dimensional network in* ***2****.*

The 3D-MOF structure of **3** consists of a three-dimensional MOF with channels occupied by disordered solvent water molecules that propagate along *c* crystallographic axis. The crystalline structure can be described as helical Co(II) chains (Figure 3) along *a* direction connected by octadentate-bridging TZI^{-3} ligands (Scheme 1, *e* and *f* modes).

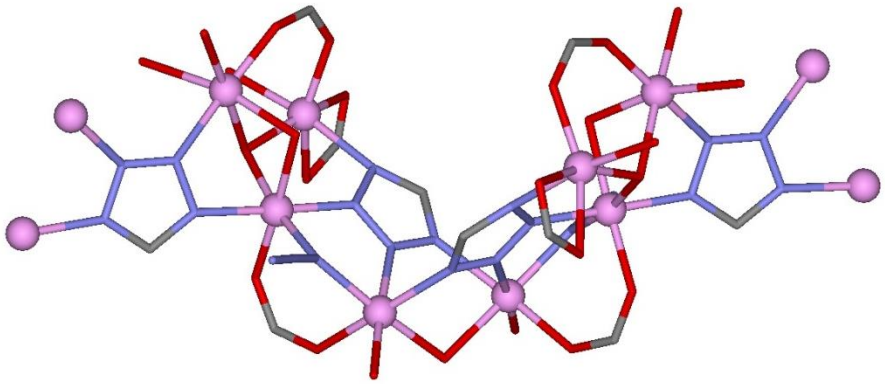

Figure 3. *Helical Co(II) chains in* ***3*** *generated by hydroxyl, carboxylate, azide and tetrazolate-bridged groups.*

Within the cobalt chains can be found hydroxy-bridged Co(II) trimers, dihydroxytetrazolate triply-bridged Co(II) dimers, hydroxy-ditetrazolate triply-bridged Co(II) dimers and azide-tetrazolate-carboxylate triply-bridged Co(II) dimers. Co1 and Co2 exhibit distorted octahedral CdN_3O_3 geometries while Co3 and Co4 exhibit very distorted octahedral $CdNO_5$ polyhedron mainly due, for Co3, to the small bite angle of the carboxylate group pertaining to TZI^{-3} ligand and one triply-hydroxy-bridge between Co3 and Co4. It must be noted that, to the best our knowledge, it´s the first time that azide-tetrazolate-carboxylate triply-bridged Co(II) dimers have been shown. All these bridges afford the helical Co(II) chains that are bridged by triply deprotonated TZI^{-3} ligands generating the 3D network (Figure 4). The topological interpretation of compound **3** according to the literature[19] can be assigned as a complex 3D structure with rod-like shape packed along [100] or as a tetranodal (3,3,3,10) with Point Symbol {4.5.6}2{4^2.5^8.6^19.7^10.8^6}{5^2.6}2

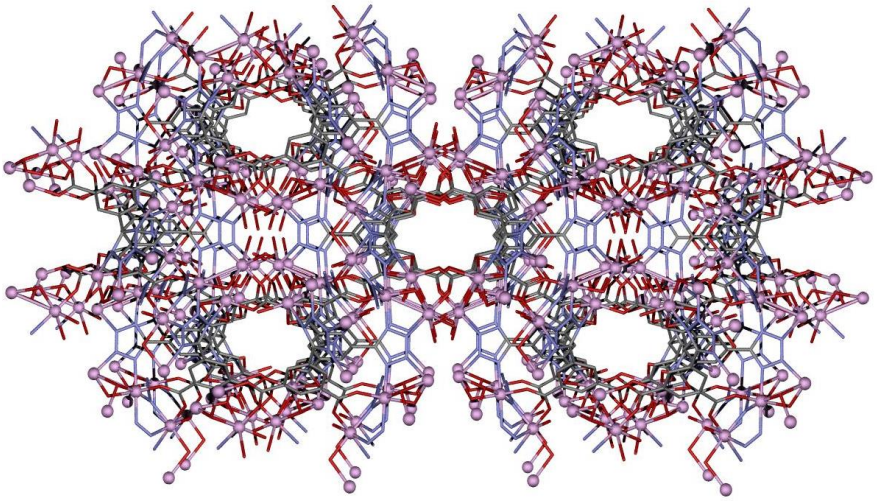

Figure 4. *View down the c axis of the channels in the three-dimensional network of* ***3****. Colour code N = blue, O = red, C = grey and cobalt = dark blue.*

Table S1. Crystallographic Data and Structural Refinement Details for **1-3**

compound	**1**	**2**	**3**
chemical formula	$C_{18}H_{28}N_8O_{20}Cd_4$	$C_9H_{10}N_4O_8Zn_2$	$C_{27}H_{46}N_{18}O_{33}Co_8$
CCDC	ESI	928815	928816
M/gmol^{-1}	1126.08	432.95	1622.26
T (K)	293	293	293
λ/Å	0.71073	0.71073	0.71073
cryst syst	triclinic	triclinic	orthorhombic
space group	*P-1*	*P-1*	*Pbcn*
a/ Å	6.8383(12)	7.711(3)	13.739(2)
b/ Å	10.3778(15)	8.959(3)	24.301(3)
c/ Å	24.2312(14)	9.103(3)	15.179(2)
α/deg	100.651(9)	88.460(5)	90
β/deg	90.439(8)	88.793(4)	90
γ/deg	108.757(6)	74.567(5)	90
V/ Å^3	1596.1(4)	605.9(4)	5067.8(12)
Z	2	2	4
ρ(g cm-3)	2.343	2.373	2.126
μ(mm-1)	2.726	4.016	2.671
Unique reflections	8273	3542	89774
R(*int*)	0.0357	0.020	0.1356
GOF on F^2	1.299	1.033	0.581
R1 [I > 2σ(*I*)]	0.159	0.042	0.083
wR2 [I > 2σ(*I*)]	0.388	0.101	0.206

[a] $R(F) = \sum||F_o| - |F_c||/\sum|F_o|$, $wR(F^2) = [\sum w(F_o^2 - F_c^2)^2/\sum wF^4]^{1/2}$

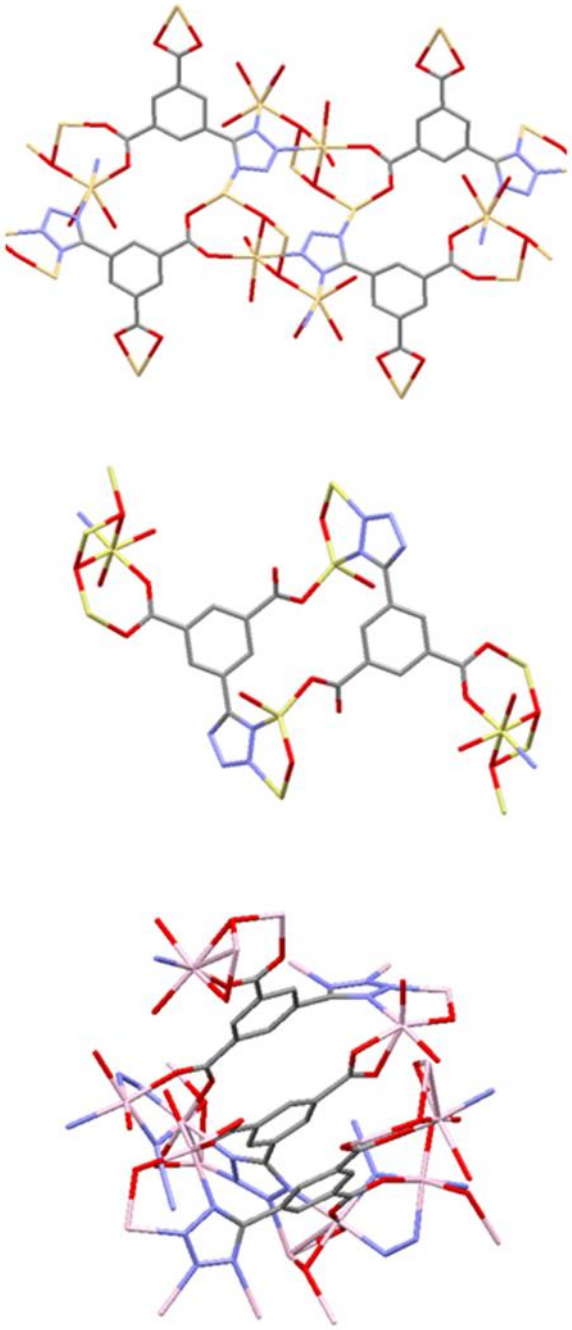

Figure 5. *A view of the metal environment and coordination mode of the ligand for* ***1*** *(up),* ***2****(middle) and* ***3*** *(down).*

Table S2. Selected Distances (Å) for compound **1**, **2** and **3**

1	2	3
Cd1 O1C 2.19(3)	Zn1 O1 2.067(3)	Co1 O2W 2.025(6)
Cd1 O4B 2.23(3)	Zn1 O1A 2.085(3)	Co1 O1 2.066(5)
Cd1 O2B 2.34(3)	Zn1 O1A 2.116(3)	Co1 N3 2.094(7)
Cd1 N4A 2.41(3)	Zn1 N2 2.128(4)	Co1 N7 2.110(7)
Cd1 O1B 2.44(3)	Zn1 O1W 2.132(3)	Co1 O2A 2.153(6)
Cd1 N1A 2.45(3)	Zn1 O2W 2.134(3)	Co1 N4 2.201(7)
Cd1 C8B 2.71(4)	Zn1 Zn1 3.1322(12)	Co2 O2 2.012(6)
Cd2 O3B 2.23(3)	Zn2 O4 1.941(3)	Co2 N2 2.040(6)
Cd2 O1C 2.28(3)	Zn2 O1A 1.955(3)	Co2 N7 2.057(7)
Cd2 O1C 2.29(3)	Zn2 O2 2.017(3)	Co2 O1A 2.058(7)
Cd2 O2W 2.30(5)	Zn2 N1 2.018(4)	Co2 N5 2.092(7)
Cd2 O1W 2.32(2)		Co2 O3A 2.168(7)
Cd2 N3A 2.50(3)		Co3 O4 1.992(6)
Cd2 Cd2 3.359(7)		Co3 O1A 2.093(7)
Cd3 O2C 2.22(3)		Co3 O6 2.160(6)
Cd3 O2C 2.24(3)		Co3 N1 2.174(8)
Cd3 O4W 2.29(4)		Co3 O5 2.176(6)
Cd3 O3W 2.31(3)		Co3 O1W 2.182(8)
Cd3 N2B 2.32(3)		Co3 C15 2.501(9)
Cd3 O1A 2.35(3)		Co4 O3 1.937(8)
Cd3 Cd3 3.354(5)		Co4 O3A 2.087(8)
Cd4 O2C 2.25(3)		Co4 O3W 2.150(18)
Cd4 O2A 2.25(3)		Co4 N6 2.182(8)
Cd4 N4B 2.32(4)		Co4 O1A 2.264(8)
Cd4 N1B 2.34(3)		Co4 O4W 2.34(2)
Cd4 O4A 2.35(3)		

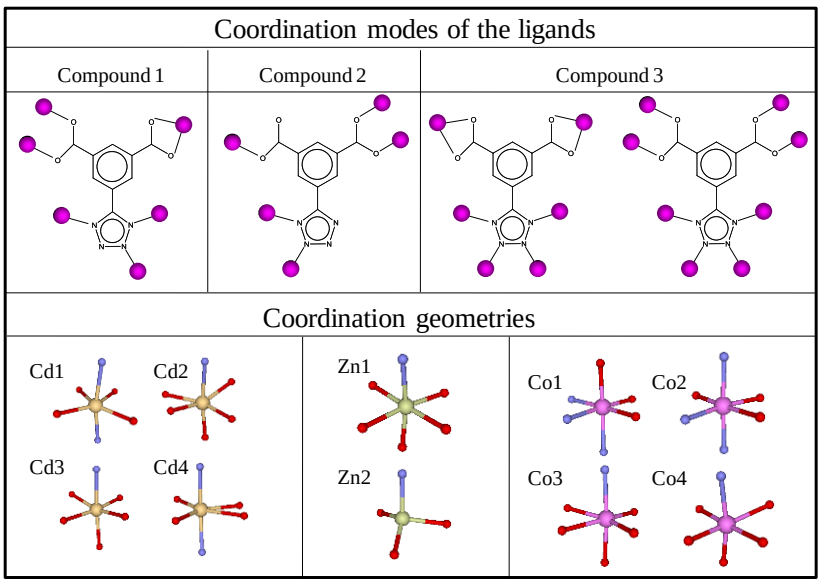

Table S3. Selected Bond Angles (A) for compound **1**, **2** and **3**

1		**2**	**3**	
O1C Cd1 O4B 111.7(10)	O2W Cd2 Cd2 135.4(12)	O1 Zn1 O1A 90.50(12)	O2W Co1 O1 92.9(2)	O4 Co3 N1 97.0(3)
O1C Cd1 O2B 149.4(9)	O1W Cd2 Cd2 118.3(6)	O1 Zn1 O1A 91.63(12)	O2W Co1 N3 176.6(3)	O1A Co3 N1 91.3(3)
O4B Cd1 O2B 98.8(10)	N3A Cd2 Cd2 79.3(7)	O1A Zn1 O1A 83.57(12)	O1 Co1 N3 89.7(3)	O6 Co3 N1 95.6(3)
O1C Cd1 N4A 89.3(11)	O2C Cd3 O2C 82.6(11)	O1 Zn1 N2 171.92(13)	O2W Co1 N7 95.3(3)	O4 Co3 O5 152.5(3)
O4B Cd1 N4A 90.8(11)	O2C Cd3 O4W 162.5(12)	O1A Zn1 N2 97.25(13)	O1 Co1 N7 89.4(3)	O1A Co3 O5 102.0(3)
O2B Cd1 N4A 93.7(10)	O2C Cd3 O4W 99.9(13)	O1A Zn1 N2 91.49(13)	N3 Co1 N7 86.9(3)	O6 Co3 O5 59.9(2)
O1C Cd1 O1B 95.0(9)	O2C Cd3 O3W 89.5(11)	O1 Zn1 O1W 84.63(14)	O2W Co1 O2A 92.6(2)	N1 Co3 O5 80.8(3)
O4B Cd1 O1B 153.3(10)	O2C Cd3 O3W 172.0(11)	O1A Zn1 O1W 173.92(14)	O1 Co1 O2A 88.8(2)	O4 Co3 O1W 91.5(4)
O2B Cd1 O1B 54.6(9)	O4W Cd3 O3W 87.1(13)	O1A Zn1 O1W 92.92(13)	N3 Co1 O2A 85.2(3)	O1A Co3 O1W 85.8(3)
N4A Cd1 O1B 90.1(11)	O2C Cd3 N2B 79.0(10)	N2 Zn1 O1W 87.77(14)	N7 Co1 O2A 171.9(2)	O6 Co3 O1W 84.6(3)
O1C Cd1 N1A 85.0(9)	O2C Cd3 N2B 85.8(11)	O1 Zn1 O2W 89.84(13)	O2W Co1 N4 92.9(2)	N1 Co3 O1W 171.4(4)
O4B Cd1 N1A 100.1(10)	O4W Cd3 N2B 83.9(13)	O1A Zn1 O2W 95.03(12)	O1 Co1 N4 172.9(2)	O5 Co3 O1W 92.0(3)
O2B Cd1 N1A 86.5(9)	O3W Cd3 N2B 91.1(11)	O1A Zn1 O2W 177.97(11)	N3 Co1 N4 84.4(3)	O4 Co3 C15 121.8(3)
N4A Cd1 N1A 168.9(11)	O2C Cd3 O1A 103.6(11)	N2 Zn1 O2W 87.23(14)	N7 Co1 N4 94.1(3)	O1A Co3 C15 132.7(3)
O1B Cd1 N1A 81.0(9)	O2C Cd3 O1A 91.3(11)	O1W Zn1 O2W 88.61(14)	O2A Co1 N4 86.8(2)	O6 Co3 C15 29.0(2)
O1C Cd1 C8B 122.6(10)	O4W Cd3 O1A 93.7(13)	O1 Zn1 Zn1 91.44(9)	O2 Co2 N2 89.9(3)	N1 Co3 C15 86.4(3)
O4B Cd1 C8B 125.5(11)	O3W Cd3 O1A 92.1(12)	O1A Zn1 Zn1 42.16(8)	O2 Co2 N7 95.2(3)	O5 Co3 C15 31.0(2)
O2B Cd1 C8B 26.8(10)	N2B Cd3 O1A 175.9(12)	O1A Zn1 Zn1 41.40(8)	N2 Co2 N7 88.2(3)	O1W Co3 C15 89.7(3)
N4A Cd1 C8B 94.1(11)	O2C Cd3 Cd3 41.5(8)	N2 Zn1 Zn1 95.83(10)	O2 Co2 O1A 93.6(3)	O3 Co4 O3A 90.4(4)
O1B Cd1 C8B 27.9(10)	O2C Cd3 Cd3 41.1(7)	O1W Zn1 Zn1 134.12(10)	N2 Co2 O1A 88.3(3)	O3 Co4 O3W 82.5(5)
N1A Cd1 C8B 81.2(10)	O4W Cd3 Cd3 138.3(11)	O2W Zn1 Zn1 137.17(9)	N7 Co2 O1A 170.6(3)	O3A Co4 O3W 100.1(5)
O3B Cd2 O1C 90.4(10)	O3W Cd3 Cd3 131.0(8)	O4 Zn2 O1A 122.41(13)	O2 Co2 N5 90.1(3)	O3 Co4 N6 170.2(4)
O3B Cd2 O1C 104.6(10)	N2B Cd3 Cd3 79.9(8)	O4 Zn2 O2 99.30(12)	N2 Co2 N5 177.3(3)	O3A Co4 N6 83.4(3)
O1C Cd2 O1C 85.5(9)	O1A Cd3 Cd3 99.9(8)	O1A Zn2 O2 115.31(12)	N7 Co2 N5 94.5(3)	O3W Co4 N6 91.1(5)
O3B Cd2 O2W 95.4(14)	O2C Cd4 O2A 111.1(10)	O4 Zn2 N1 121.15(14)	O1A Co2 N5 89.0(3)	O3 Co4 O1A 98.7(3)
O1C Cd2 O2W 96.1(13)	O2C Cd4 N4B 84.5(12)	O1A Zn2 N1 97.83(14)	O2 Co2 O3A 177.5(3)	O3A Co4 O1A 81.6(3)
O1C Cd2 O2W 159.9(13)	O2A Cd4 N4B 98.8(12)	O2 Zn2 N1 99.40(13)	N2 Co2 O3A 91.8(3)	O3W Co4 O1A 178.0(6)
O3B Cd2 O1W 88.7(9)	O2C Cd4 N1B 86.4(11)		N7 Co2 O3A 86.8(3)	N6 Co4 O1A 87.9(3)
O1C Cd2 O1W 160.5(8)	O2A Cd4 N1B 91.0(11)		O1A Co2 O3A 84.6(3)	O3 Co4 O4W 99.1(6)
O1C Cd2 O1W 75.9(8)	N4B Cd4 N1B 168.5(13)		N5 Co2 O3A 88.1(3)	O3A Co4 O4W 166.4(6)
O2W Cd2 O1W 103.4(13)	O2C Cd4 O4A 148.4(11)		O4 Co3 O1A 105.4(3)	O3W Co4 O4W 90.8(7)
O3B Cd2 N3A 173.7(11)	O2A Cd4 O4A 100.5(11)		O4 Co3 O6 93.3(3)	N6 Co4 O4W 88.4(6)
O1C Cd2 N3A 85.0(10)	N4B Cd4 O4A 90.0(13)		O1A Co3 O6 159.2(3)	O1A Co4 O4W 87.4(6)
O1C Cd2 N3A 79.3(9)	N1B Cd4 O4A 94.2(11)			
O2W Cd2 N3A 80.9(13)	O2C Cd4 O3A 94.5(10)			
O1W Cd2 N3A 97.0(9)	O2A Cd4 O3A 154.3(10)			
O3B Cd2 Cd2 100.2(8)	N4B Cd4 O3A 85.5(12)			
O1C Cd2 Cd2 42.9(6)	N1B Cd4 O3A 88.4(10)			
O1C Cd2 Cd2 42.7(6)	O4A Cd4 O3A 54.0(10)			

3.2. Luminescence Properties

Due to extended aromaticity and the presence of hexa-atomic rings, TZI^{-3} ligand is a good candidate for enhanced emissive properties. Due to this reason we decided to carry out a study of luminescent properties of coordination compounds **1** and **2**. The emission maximum of H_3TZI in solid state has been previously studied by Zhi-Rong *et al*.[20] and has a value of 389 nm, in good agreement with the emissions observed for a series of tetrazolate-carboxylic acid derivative ligands.[21] Using a 330 nm incident radiation, the emission spectrum of the cadmium and zinc MOFs (Figure 6) at room temperature in solid state exhibit intense emission bands centered about 460 and 450 nm, respectively, in concordance with those observed for other MOFs with these types of derivatives ligands.[22] The emission, assigned to intraligand π-π* transitions, is considerably red-shifted with respect to the ligand emission band.

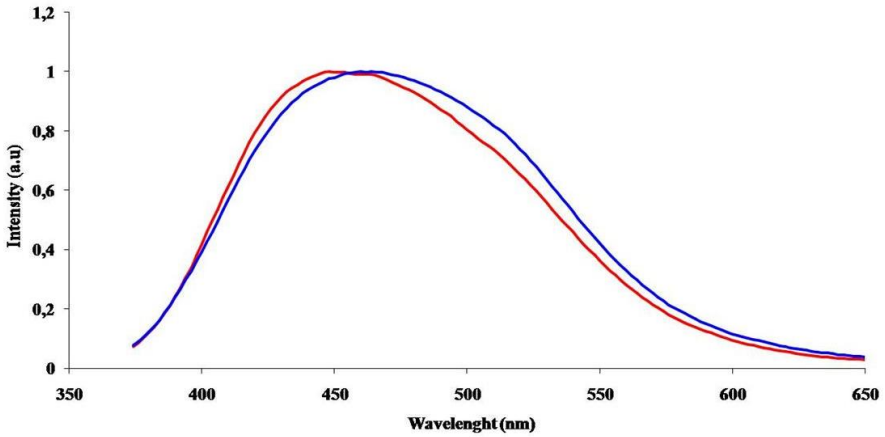

Figure 6. *Emission spectra of **1** (blue line) and **2** (red line) at room temperature in solid state. Horizontal axis: wavelength (nm); vertical axis: intensity (a.u.).*

3.3. Magnetic Properties

The magnetic properties of compound **3** were measured in the 300-2 K and are given in the form χ_M T vs T (χ_M is the magnetic susceptibility per Co_8 unit) in Figure 7.

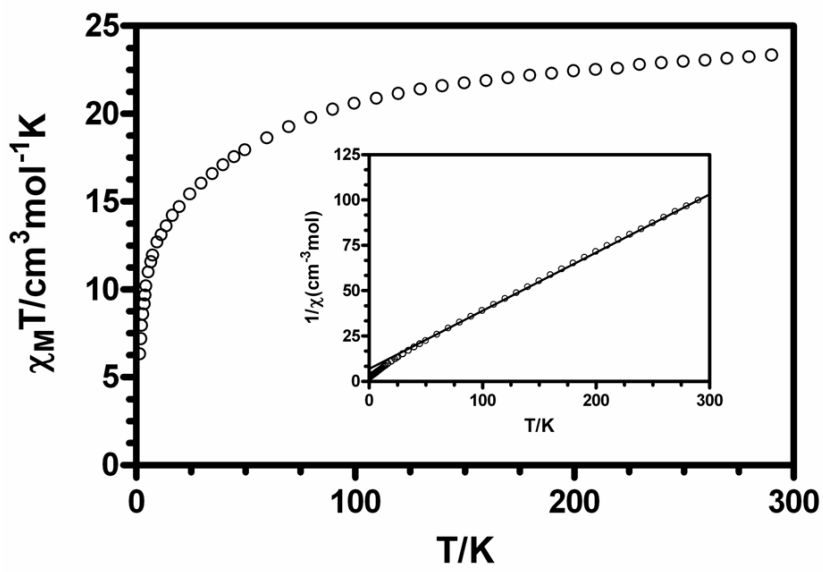

Figure 7*. Temperature dependence of the χ_M T product for **3**. Fit to the Curie-Weiss for data above 50 K (inset).*

The χ_M T product at room temperature (23.44 emuKmol^{-1}) is very high when compared with the expected spin only value for eight cobalt(II) atoms of 15 emuKmol^{-1}, which is a consequence of the first order orbital contribution of the octahedral Co^{2+} with a $^4T_{1g}$ ground term. When the temperature is lowered, the χ_MT steadily decreases to reach a value of 6.29 at 2K. This behavior is due to the anisotropy, promoted by the spin-orbit coupling, of the octahedral Co^{2+} ions and to magnetic exchange between the Co^{2+} ions.

The fact that the value at 2 K is much lower than that expected for eight isolated cobalt(II) ions (~13.6 emuKmol^{-1}) supports the existence of antiferromagnetic exchange interactions between the metal ions. Nevertheless, the

AF interaction must be very weak as the χ_M vs T plot does not show any maximum above 2 K at none of the used magnetic fields (100 and 1000 Oe). Above T = 50 K the magnetic data can be fitted to a Curie–Weiss law with C =3.11 emuKmol^{-1} and Θ = -6.9 K. The negative Weiss parameter can be used to estimate the value of the interaction by using the mean-field expression $\Theta = zJS(S+1)/3k_B$, where z is the number of nearest neighbors, *J* is the magnetic exchange parameter, S is the spin angular momentum, and k_B is the Boltzmann constant. This yields zJ/k_B = 5.5 K (-3.8 cm^{-1}). The *J* value is obviously overestimated as it accounts for the dominant anisotropy of the Co(II) ions and also for the magnetic exchange. The M vs H plot (Figure 8) shows a slow increase of the magnetization without reaching saturation at 5T. The value of the magnetization at 5 T (10.3 μB) is lower than that expected for eight cobalt(II) ions with effective spin S_{eff} = 1/2 (~16.8 μB), thus also confirming the presence of weak antiferromagnetic interaction in this compound.

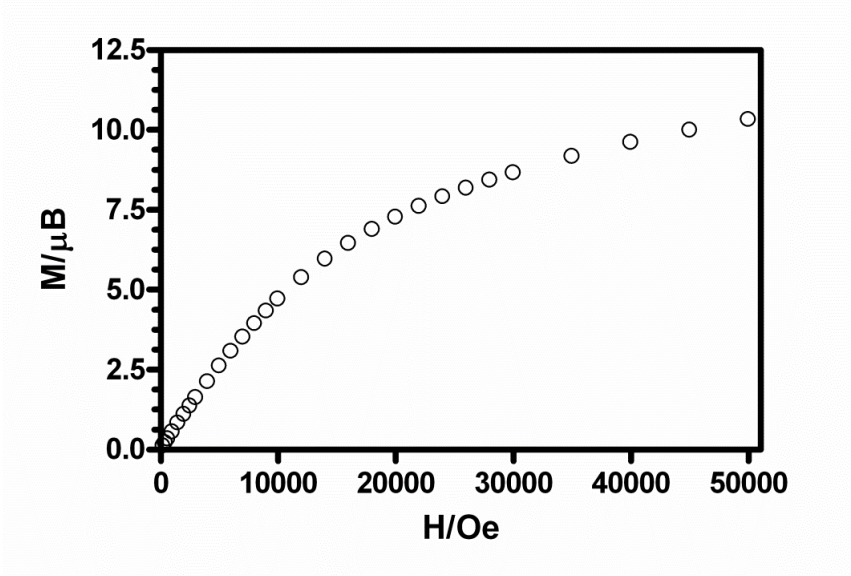

***Figure 8**.- Field dependence of the Magnetization for **3**.*

4. CONCLUSIONS

In this work, we have shown that metal–organic frameworks with luminescent and magnetic properties can be synthesized by using the 5-(1H-tetrazol-5-yl)isophthalic acid igand. Compounds **1** and **2** consist in 3D- and 2D-MOFs, respectively, and fluorescent analyses show that they exhibit intense purple photoluminescence in the solid state at room temperature. **3** is a three-dimensional coordination polymer that exhibits an antiferromagnetic interaction between cobalt(II) ions. Work is in progress in our laboratory in order to obtain new homo- and heterometallic complexes to study their physical properties.

5. REFERENCES

[1].- (a) L. Hou L, D. Li, *Inorg. Chem. Commun*. 2005, **8**, 190; (b) S. L. Qiu, G. S. Zhu, Coord. *Chem. Rev*. 2009, **253**, 2891; (c) J.J. Perry IV, J. A. Perman, M. J. Zaworotko, *Chem. Soc. Rev*. 2009, **38**, 1400; (d) S. Natarajan, P. Mahata, *Chem. Soc. Rev*. 2009, **38**, 2304.

[2].- (a) S. Kitagawa, R. Kitaura and S.-I. Noro, *Angew. Chem., Int. Ed*., 2004, **43**, 2334; (b) S. Kitagawa, K. Uemura, *Chem. Soc. Rev*., 2005, **34**,

109; (c) M. Yoshizawa, T. Kusukawa, M. Kawano, T. Ohhara, I. Tanaka, K. Kurihara, N. Niimura, M. Fujita, *J. Am. Chem. Soc*., 2005, **127**, 2798.

[3].- T.R. Cook, Y.-R. Zheng and P.J. Stang, *Chem. Rev*. 2013, **113**, 734.

[4].- (a) S.M. Humphrey, P.T. Wood, *J. Am. Chem. Soc*., 2004, **126**, 13236; (b) X.-M. Zhang, Y.-Z. Zheng, C.-R. Li, W.-X. Zhang, X.-M. Chen, *Cryst. Growth Des*. 2007, **7**, 980; (c) Y.-Q. Sun, J. Zhang, Y.-M. Chen, G.-Y. Yang, *Angew. Chem., Int. Ed*., 2005, **44**, 5814; (d) W.-G. Lu, C.-Y. Su, T.-B. Lu, L. Jiang, J.-M. Chen, *J. Am. Chem. Soc*., 2006, **128**, 34.

[5]. (a) S. S.-Y. Chui, S. M.-F Lo, J. P. H Charamant, A. G Orpen, I. D Williams, *Science* 1999, **283**, 1148; (b) C. N. R Rao, S Natarajan, R. Vaidhzanathan, *Angew. Chem., Int. Ed*. 2004, **43**, 1466.

[6].- G. Aromi, L.A. Barrios, O. Roubeau, P. Gamez, *Coord. Chem. Rev.,* 2011, **255**, 485.

[7].- A Rodríguez-Diéguez, A. Salinas-Castillo, S. Galli, N. Masciocchi, J. M. Gutiérrez-Zorrilla, P. Vitoria, E. Colacio, *Dalton Trans*. 2007 1821.

[8].- A. Rodríguez-Diéguez, A. Salinas-Castillo, A. Sironi, J.M. Seco and E. Colacio, *CrystEngComm*, 2010, **12**, 1876.

[9].- K. Schlichte, T. Kratzke, S. Kaskel, *Microporous Mesoporous Mater*. 2004*,* **73***,* 81*.*

[10].- F. Nouar, J.F. Eubank, T. Bousquet, L. Wojtas, M.J. Zaworotko, M. Eddaoudi, *J. Am. Chem. Soc*. 2008, **130**, 1833.

[11].- Z.P.Demko and K.B.Sharpless, *J.Org.Chem*., 2001, **66**, 7945.

[12] .- (a) M. Kurmoo, *Chem. Soc. Rev*. 2009, **38**, 1353; (b) M. Murrie, *Chem. Soc. Rev*. 2010, **39**, 1986; (c) G.E. Kostakis, S.P. Perlepes, V.A. Blatov, D.M. Proserpio, A.K. Powell, *Coord. Chem. Rev* 2012, **256**, 1246.

[13].- Crystal Data. **1**: $[C_{18}H_{28}N_8O_{20}Cd_4]$, M = 1126.08, triclinic, space group *P-1*, *a* = 6.38383(12), *b* = 10.3778(15), *c* = 24.2312(12) Å, α = 100.651(9), β = 90.439(8), σ = 108.757(6), *V* = 1596.1(4) Å^3, *Z* = 2. **2**: $[C_9H_{10}N_4O_8Zn_2]$, M = 432.95, triclinic, space group *P-1*, *a* = 7.711(3), *b* = 8.959(3), *c* = 9.103(3) Å, α = 88.460(5), β = 88.793(4), σ = 74.567(5), *V* = 605.9(4) Å^3, *Z* = 2, ρ_{calcd} = 2.373 g cm^{-3}, μ(Mo-Kα) = 4.016 mm^{-1}, *R*1(F_o) = 0.0415, (*wR*2(F_o^2) = 0.1011) with a goodness-of-fit on F^2 1.033. **3**: $[C_{27}H_{46}N_{18}O_{33}Co_8]$, M = 1622.26, orthorhombic, space group *Pbcn*, *a* = 13.739(2), *b* = 24.301(3), *c* = 15.179(2) Å, *V* = 5067.8(12) Å^3, *Z* = 4, ρ_{calcd} = 2.126 g cm^{-3}, μ(Mo-Kα) = 2.671 mm^{-1}, *R*1(F_o) = 0.0827, (*wR*2(F_o^2) = 0.2059) with a goodness-of-fit on F^2 0.581.

[14].- Bruker Apex2, Bruker AXS Inc, Madison, Wisconsin, USA, 2004.

[15].- G. M. Sheldrick, SADABS, Program for Empirical Adsorption Correction, Institute for Inorganic Chemistry, University of Göttingen, Germany, 1996.

[16].- A. Altomare, M. C. Burla, M. Camilla, G. L. Cascarano, C. Giacovazzo, A. Guagliardi, A. G. G. Moliterni, G. Polidori and R. Spagna, J. Appl. Crystallogr., 1999, 32, 115.

[17].-G. M. Sheldrick, SHELX97, Program for Crystal Structure Refinement, University of Göttingen, Göttingen, Germany, 1997.

[18] .- A. L. Spek, PLATON-94 (V-101094),AMultipurposeCrystallographic Tool, University of Utrecht, The Netherlands, 1994.

[19].- M. O´Keefe and O.M. Yaghi, Chem.Rev. 2012, **112**, 675.

[20].- Z.-R. Qu, Z. Xing, B.-Z. Wu, X.-Z. Li and G.-F. Han, *Z. Anorg. Allg. Chem*. 2009, **635**, 39.

[21].- (a) B. Yan, B. Zhou, J. *Photochem, Photobiol. A*, 2005, **171,** 181; (b) L. Zhao, P. Ren, Z. Zhang, M. Fang, W. Shi, P. Cheng*, Sci China Ser B-Chem*, 2009, **52**, 1479.

[22].- J.-Y. Zhang, Y.-Q. Wang, H.-Q. Peng, A.-L. Cheng, E,-Q. Gao, *Struct Chem*., 2008, **19**, 535.

CAPÍTULO 8.

NOVEL METAL-ORGANIC FRAMEWORKS BASED ON 5-BROMONICOTINIC ACID: MULTIFUNCTIONAL MATERIALS WITH H_2 PURIFICATION CAPABILITIES.

ARTICLE: *NOVEL METAL-ORGANIC FRAMEWORKS BASED ON 5-BROMONICOTINIC ACID: MULTIFUNCTIONAL MATERIALS WITH H_2 PURIFICATION CAPABILITIES.*

CrystEngComm

Dynamic Article Links

Cite this: *CrystEngComm*, 2012, **14**, 6390–6393

www.rsc.org/crystengcomm

COMMUNICATION

Novel metal–organic frameworks based on 5-bromonicotinic acid: Multifunctional materials with H_2 purification capabilities†

Antonio J. Calahorro,[a] Marta E. López-Viseras,[a] Alfonso Salinas-Castillo,[b] David Fairen-Jimenez,‡*[c] Enrique Colacio,[a] Joan Cano[d] and Antonio Rodríguez-Diéguez*[a]

Received 6th March 2012, Accepted 18th July 2012
DOI: 10.1039/c2ce25807b

[a]*Departamento de Química Inorgánica, Universidad de Granada, Granada, 18071, Spain. E-mail: antonio5@ugr.es; Tel: 0034958240442*
[b]*Departamento de Química Analítica, Universidad de Granada*
[c]*Institute for Materials and Processes, School of Engineering, The University of Edinburgh, United Kingdom. E-mail: David.Fairen-Jimenez@Northwestern.edu*
[d]*Instituto de Ciencia Molecular (ICMol) and Fundació General de la Universitat de València (FGUV), Catedrático José Beltrán n° 2, Universitat de València, Paterna, València, E-46980, Spain*
‡ Present address: Department of Chemical and Biological Engineering, Northwestern University, Evanston, Illinois, USA

ABSTRACT

Two new metal-organic frameworks based on 5-bromonicotinic acid complexes $[Cd(5\text{-}BrNic)_2]_n$ (**1**) and $[Co(5\text{-}BrNic)_2(H_2O)]_n$ (**2**) have been synthesized by hydrothermal reactions of this ligand with cadmium and cobalt metallic(II) salts in presence of water. Compound **1** displays intense photoluminescence properties in the solid state at room temperature, while **2** exhibits an antiferromagnetic interaction between Co(II) ions with a J value of -4.1 cm^{-1}. Experimental studies,

backed up by Monte Carlo simulations about adsorption, pore size distribution and accessible surface area reveal the capability of 2 for H_2 purification applications.

1. INTRODUCTION

Transition metal–organic frameworks (MOFs), which are diverse in structure and properties, are currently attracting increasing attention not only due to their fascinating topologies but also due to their interesting applications in the areas such as gas adsorption, catalysis, cooperative magnetic behaviour, non-linear optical activity and electrical conductivity.[1]

Compared with conventional microporous inorganic materials such as zeolites, MOFs are more flexible for rational design through selection and tailoring of suitable ligands. Amongst them, multidentate N or O-donor ligands, such as pyridine or carboxylic acids, have drawn extensive attention in the construction of MOFs.[2] Thus, nicotinic acid and isonicotinic acid, as good sources of carboxylate ligand, have been widely applied to construct MOFs.[3]

The addition of electron-donor functionalities such as bromine atoms will extend the aromaticity of the hexa-atomic rings. Thus, nicotinic derivatives ligands are good candidates for enhanced emissive properties. To the best of our knowledge, the existence of luminescent properties on 5-Bromonicotinic ligand (5-BrNic) has been only reported before in a study using lanthanide ions.[4] In terms of adsorption properties, the presence of halogen atoms will increase gas-solid interaction, creating new adsorption sites through the porosity.

From a structural viewpoint, 5-BrNic acid can act as a monodentate, bidentate, bidentate-bridging and tridentate-bridging ligand (Scheme I). In the latter cases, the presence of a bromine atom in meta position with respect to the nitrogen atom and the carboxylate group presumably favours the formation of channels in the three-dimensional structure.

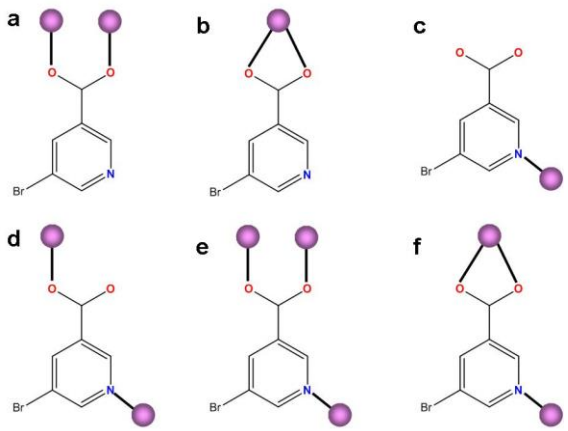

Scheme I. *Some coordination modes of 5-BrNic ligand.*

With the aim of moving forward in this area of research, we report here the hydrothermal synthesis, crystal structures, pore size distribution, geometric surface areas, luminescence and magnetic properties of the complexes $[Cd(5\text{-}BrNic)_2]n$ (1) and $[Co(5\text{-}BrNic)_2(H_2O)]n$ (2) bearing the 5-BrNic ligand.

2. EXPERIMENTAL

2.1. General.

All analytical reagents were purchased from commercial sources and used without further purification.

2.2. Preparation of complexes

$[Cd(5\text{-}BrNic)_2]_n$ (1): A mixture of $CdCl_2$(183 mg, 1 mmol), 5-bromonicotinic acid (*404 mg, 2 mmol*), and water (14 mL) was sealed in a Teflon-lined acid digestion

autoclave and heated at 160°C under autogenous pressure. After 12 h of heating, the reaction vessel was cooled down to room temperature during a period of 2 h. Prismatic colorless crystals of **1** were obtained and were washed with H_2O. Yield: 37% based on Cd. Anal. Calcd for ($CdC_{12}N_2O_4H_6Br$): C 28.02, H 1.18, N 5.45. Experimental: C 28.35, H 1.31, N 5.34. FT-IR (KBr pellet): 3388 (s), 1622 (m), 1575 (s), 1450 (m), 1392 (s), 1244 (m), 1105 (w), 759 (m), 729 (m) cm^{-1}.

$[Co(5\text{-}BrNic)_2(H_2O)]_n$ (2): A mixture of $CoCl_2 \cdot 6H_2O$ (228 mg, 1 mmol), 5-bromonicotinic acid (404 mg, 2 mmol), and water (14 mL) was sealed in a Teflon-lined acid digestion autoclave and heated at 160°C under autogenous pressure. After 12 h of heating, the reaction vessel was cooled down to room temperature during a period of 2 h. Prismatic colorless crystals of **2** were obtained and were washed with H_2O. Yield: 37% based on Cd. Anal. Calcd for ($CoC_{12}N_2O_5H_8Br$): C 28.02, H 1.18, N 5.45. Experimental: C 30.09, H 1.68, N 5.85. FT-IR (KBr pellet): 3354 (s), 1646 (m), 1535 (s), 1427 (m), 1413 (s), 1253 (m), 1116 (w), 737 (m), 716 (m) cm^{-1}.

2.3. Physical measurements

Elemental analyses were carried out at the "Centro de Instrumentación Científica" (University of Granada) on a Fisons-Carlo Erba analyser model EA 1108. The IR spectra on powdered samples were recorded with a ThermoNicolet IR200FTIR by using KBr pellets.

2.4. Luminescence measurement

A Varian Cary-Eclipse Fluorescence Spectrofluorimeter solid sample holder accessory was used to obtain the fluorescence spectra. The spectrofluorimeter was equipped with a xenon discharge lamp (peak power equivalent to 75 kW), Czerny-Turner monochromators, R-928 photomultiplier tube which is red sensitive (even 900 nm) with manual or automatic voltage controlled using the Cary Eclipse software

for Windows 95/98/NT system. The photomultiplier detector voltage was 800 V and the instrument excitation and emission slits were set at 10 and 10 nm, respectively.

2.5. Experimental Isotherms

Excess H_2 adsorption isotherms at 77 K were obtained over the 0-20 bar pressure range by volumetric analysis (PCI instrument from Advanced Materials Corp., Pittsburgh, PA). The non-ideality of hydrogen was taken into account by using the Peng-Robinson equation of state.[1] Prior to the measurements, samples were activated on a high vacuum line (10^{-4} mbar) at 120 C overnight.

2.6. Computational Details

The material was characterized geometrically, starting from the crystallographic coordinates. The geometric pore size distribution was calculated, which is related to the diameter of the largest sphere that can fit into the cavities without overlapping with any of the framework atoms[17] and the accessible surface area[2] using different probe molecules. Additionally, hydrogen adsorption at 77 K on **2** was studied using grand canonical Monte Carlo (GCMC) simulations.[3] In the grand canonical ensemble, the chemical potential, the volume, and the temperature are kept fixed as in adsorption experiments. An atomistic model was used for **2**, with the atoms frozen at the crystallographic positions. In the simulation, hydrogen molecules were randomly moved, rotated, inserted, and deleted, allowing the number of molecules in the framework to fluctuate. The chemical potential was related to the system pressure by the Peng-Robinson equation of state.[4] The standard 12-6 Lennard-Jones (LJ) potential was used to model the interatomic interactions. The parameters for the framework atoms were obtained from the UFF force field,[5] while molecular hydrogen was modeled by two LJ spheres (σH=2.72Å, εH/kB = 10.00 K, dH-H=0.74Å)[6, 7]. The Lorentz_Berthelot mixing rules were employed to calculate the mixed parameters. Interactions beyond 17 Å were neglected for the simulations.

Quantum effects were taken into account using the Feynman-Hibbs effective potential method,[8,] which is sufficiently accurate at 77 K.[6,9,10] A total number of 2×10^7 Monte Carlo steps were performed. The first 50% was used for system equilibration, carefully ensuring that thermodynamic equilibrium was reached, while the remaining steps were used to calculate the ensemble averages.

3. Results and Discussion

3.1. Structure and crystallographic results

Hydrothermal reactions of the appropriate metal chloride (1 mmol) with 5-BrNic (2 mmol) in water (14 ml) at 160 ^{o}C for 12 h followed by cooling down to room temperature over 2 h yield prismatic colourless crystals of 1 (in 70% yield) and pink crystals of 2 (in 45% yield). Crystal structures (see ESI) of 1 and 2 were determined by single crystal X-ray diffraction methods and found that both compounds exhibit different 3D MOF structures. Compound 1 is a three-dimensional coordination polymer in which cadmium atoms present very distorted octahedral coordination geometry and the 5-bromoniconitic ligand possess two different tridentate-bridging coordination modes (Scheme I, e and f modes).

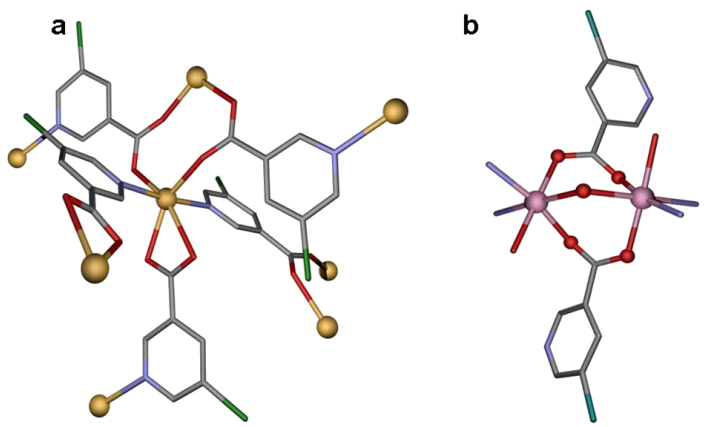

Figure 1. *View of the metal environment and coordination mode of the ligand for 1 (a) and the Co(II) dimer repetition motif for 2 (b). Colour code N = blue, O = red, C = grey, Cd = yellow and Co = pink.*

Compound 1 crystallizes in the monoclinic space group P21/n, the asymmetric unit consisting of two 5-BrNic− ligands and one cadmium ion, all in general positions. Each Cd(II) ion exhibits very distorted octahedral CdN2O4 geometry with the two nitrogen atoms belonging to two pyridine rings and four oxygen atoms pertaining to three different 5-BrNic bridging ligands (Figure 1a). The distortion of the Cd(II) coordination polyhedron is mainly due to the small bite angle of the carboxylate group pertaining to one of the 5-BrNic ligand (O-Cd-O = 54.41^{o}). Each cadmium atom is connected to seven cadmium centres through five 5-BrNic ligands, generating a convoluted three-dimensional structure with Cd···Cd distances through 5-BrNic spacers of 4.507, 7.650, 7.944 and 8.840 Å. The three-dimensional MOF possess small channels that propagate along the c crystallographic axis, in which bromine atoms are oriented to the centre of these channels (Figure 2).

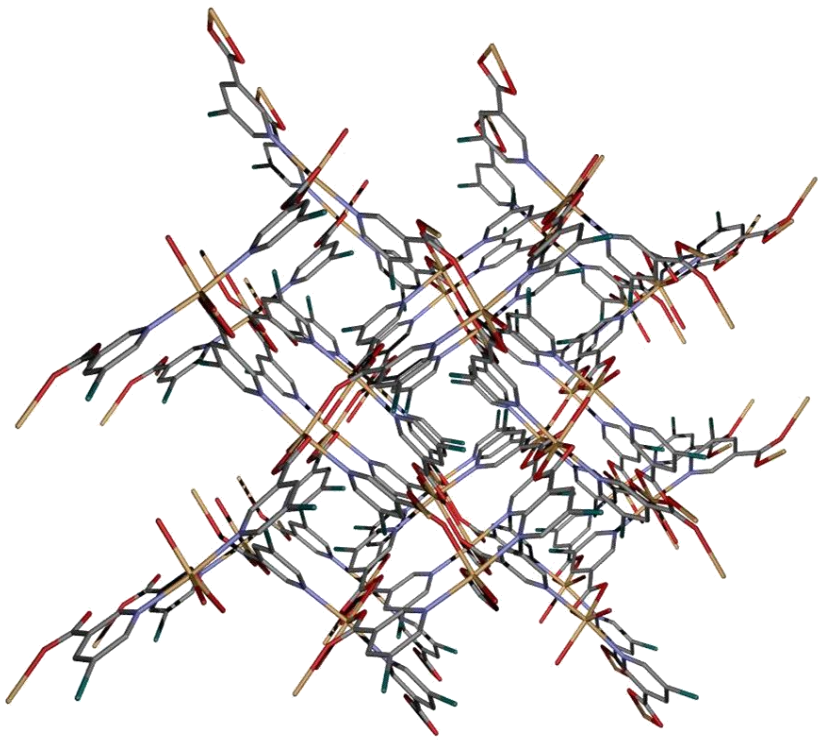

Figure 2. *View down to the c axis in the three-dimensional network in 1.*

The 3D-MOF structure of 2 can be described as aquadicarboxylate triply-bridged Co(II) dimers connected by didentate- and tridentate-bridging 5-bromonicotinate ligands (Scheme I, coordination modes d and e). Within the dinuclear Co_2 units (Figure 1b), each Co(II) ion exhibits a distorted CoN2O4 octahedral geometry, which is made of two pyridine nitrogen atoms and three oxygen atoms from five different 5-BrNic- bridging ligands and the oxygen atom of the bridging water molecule (Figure 1b). Therefore each Co(II) atom is connected to other six cobalt centres affording the 3D network.

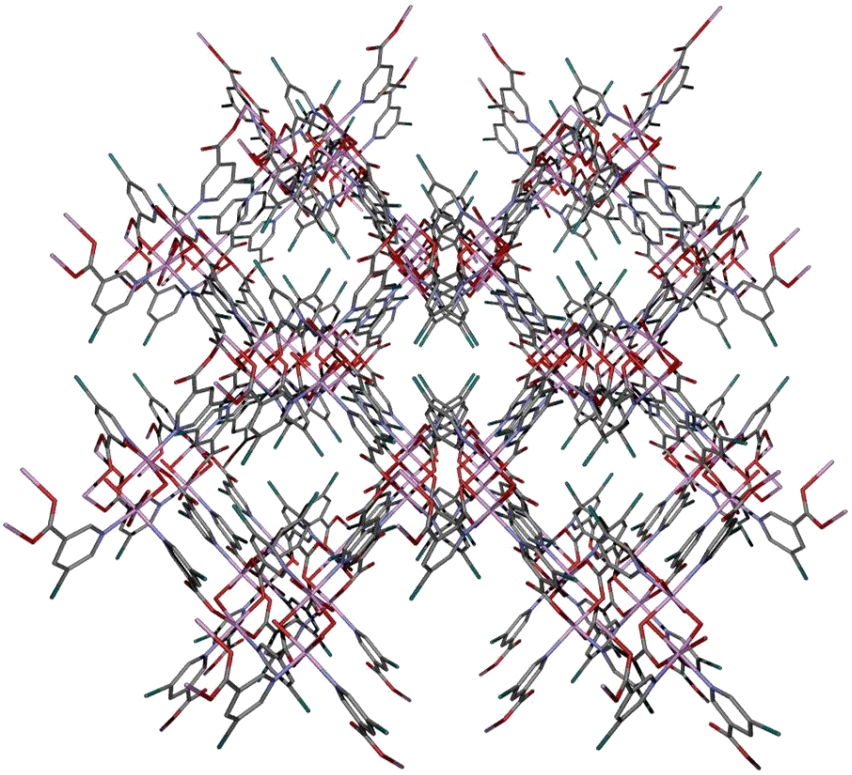

Figure 3. *View down the c axis of the channels in the three-dimensional network of 2.). Colour code N = blue, O = red, C = grey, Cd = yellow and Co = pink.*

Intradinuclear Co···Co distance is 3.512 Å, whereas the Co-Ow-Co bond angle has a value of 112.14°. The three-dimensional MOF possess channels that propagate along the c crystallographic axis in which bromine atoms are oriented to the centre of these channels (Figure 3).

3.2. Luminescence Properties

The emission maximum of 5-BrNic in solid state is 475 nm, in good agreement with the emissions observed for a series of pyridine-carboxylic acid derivative ligands.[5,6] The emission spectrum of 1 (figure 4) at room temperature in solid state exhibit intense emission bands centered about 510 and 518 nm, in concordance with those observed for other MOFs with these types of derivatives ligands.6 The emission, assigned to intraligand π-π* transitions, is considerably red-shifted with respect to the ligand emission band (about 35cm^{-1}).

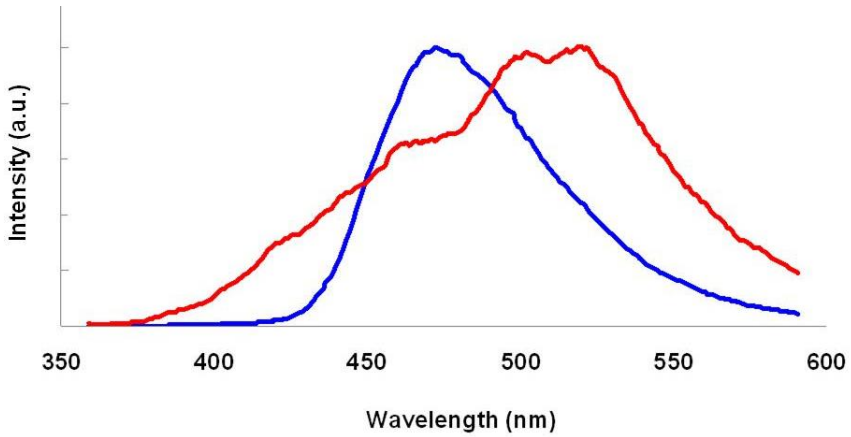

Figure 4. *The emission spectra of* ***1,*** *red line, and 5-BrNic, blue line, in solid state at room temperature.*

3.3. Magnetic Properties

The temperature dependence of χ_M and $\chi_M T$ product (χ_M is the molar susceptibility per Co_2 unit) for 2 at a magnetic field of 0.5 T is given in figure 5. The MT value at room temperature (6.45 cm^3 K mol^{-1}) is significantly higher than that calculated from the spin-only formalism for a dinuclear high-spin Co(II) system (3.75 cm^3 K mol^{-1} for S = 3/2 and g = 2), which indicates that the orbital angular momentum of the Co(II) ions is not quenched and therefore contributes significantly to the magnetic susceptibility. In fact, the spin-orbit coupling causes that the MT product decreases upon lowering the temperature with increasing slope. The lowest possible value expected for $\chi_M T$ at 0 K for two uncoupled octahedral Co(II) ions with only the lowest Kramer doublet populated is usually found in the range 3.0 – 3.4 cm^3 K mol^{-1}. However, the χ_M T value at 2K (0.3 cm^3 K mol^{-1}) is much more smaller than the lower end of the above range, which clearly indicates the presence of an intramolecular antiferromagnetic coupling. This fact is supported by the existence of a maximum in χ_M at 8 K.

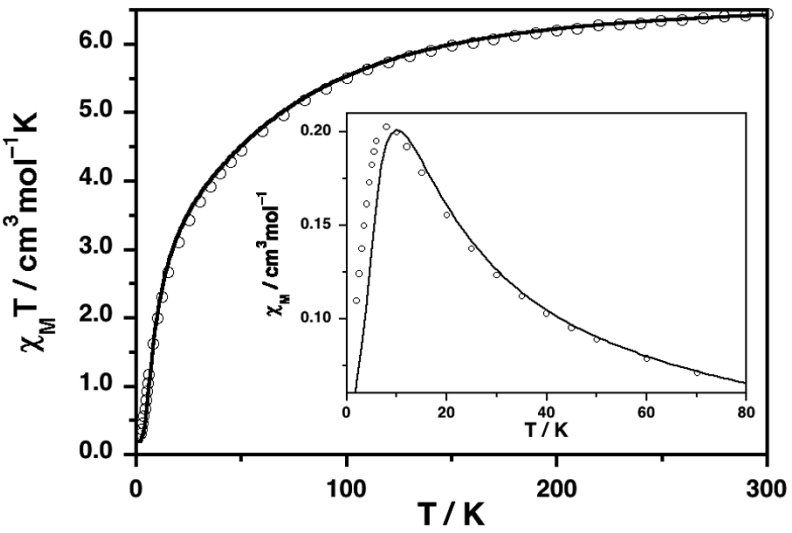

***Figure 5**. Temperature dependence of $\chi_M T$ (Δ) and χ_M (○, inset) for **2**. The solid lines correspond to the best fit.*

In order to determine the intradimer exchange interaction in 2, we have used an empirical approach recently proposed for one of us,[7] where each Co(II) ion in the Kramer's ground doublet state arising form the spin-orbit coupling is considered to have an effective spin Seff = 1/2, which is related with to the real spin (S = 3/2) by a factor of 5/3. The magnetic exchange is assumed to occur between the ground doublets of the Co(II) ions. The contribution of the excited doublets to the magnetic properties of ground doublet state is taken into account in the g factor that is dependent on J, λ, α and Δ ,where J is the isotropic exchange interaction, λ is the spin-orbit coupling, α is the orbital reduction factor defined as α = kA and Δ is the energy gap between the singlet $^4A_2$ and doublet ^4E levels due to the axial distortion. A very good agreement between the simulation and the experimental data above 20 K is reached with the next values: Ak = 1.266, λ = –123.0 cm^{-1}, Δ = –427.3 cm^{-1} and J = –4.1 cm^{-1} with R = 7.4 x 10^{-7}. The large value of Δ is in agreement with the low symmetry of the metal coordination sphere, whereas the values of the λ, α and k lie within the range of those observed in other six-coordinated high-spin Co(II) complexes.9 The maximum in χ_M at 8 K is not perfectly reproduced due to limitations of the model.

3.4. Adsorption Properties

The porous properties of compounds 1 and 2 were first studied by means of their pore size distribution (PSD) and accessible surface area, using different probe molecules ranging from 2.5 to 4.0 Å in a Monte Carlo simulation.[8] PSD analysis shows that whereas 1 is essentially non-porous, 2 presents small cavities localised at 3.75 Å (Figure 6). The small pore size due to the use of small linkers in the synthesis, makes 2 a perfect candidate for molecular sieving and potential H_2 purification, using thin films growth for the synthesis of membranes.[9] Moreover, the analysis of the accessible surface area for different probe molecule diameters (Figure 7) shows an important reduction in the values when the probe size increases (i.e. compare S_{area}= 811m^2/cm^3 (H_2) versus 191 m^2/cm^3 (CH_4)).

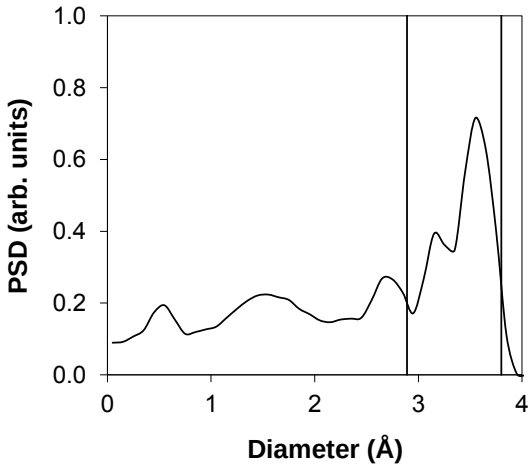

Figure 6. *Pore size distribution of 2. Vertical lines show the kinetic diameter of H_2 (2.89 Å) and CH_4 (3.8 Å). Note that, for every gas molecule, their accessible pore volume will be limited to that larger than the molecule size (i.e. right-side in the PSD).*

The analysis on the molecular sieving capability of 2 was confirmed by means of experimental adsorption of H_2, N_2 and CH_4 on this material. While 2 was not able to adsorb N_2 and CH_4 on the applied experimental conditions (77 K, 1 bar and 298 K up to 20 bar for N_2 and CH_4, respectively), H_2 (77 K) was able to diffuse through the narrow porosity, being able to reach an uptake up to 1.78 mmol/g (Figure 5 and S4). This high H_2/N_2 and H_2/CH_4 selective behaviour has been observed previously in other MOFs.[10] We also used grand canonical Monte Carlo simulations[11] to predict the H_2 adsorption isotherm, which describes correctly the shape of the experimental results (Figure 7) and predicts accurately the maximum on the excess isotherm. The description of the experimental adsorption process is significantly improved after applying a scaling factor (Φ) of 0.91, calculated as the ratio of the experimental and simulated maximum amounts adsorbed, on the simulated curve. The over-prediction in the simulations is generally explained by the existence of structural defects in the experimental sample that limits the micropore volume and the maximum capacity of the real solid. 10b

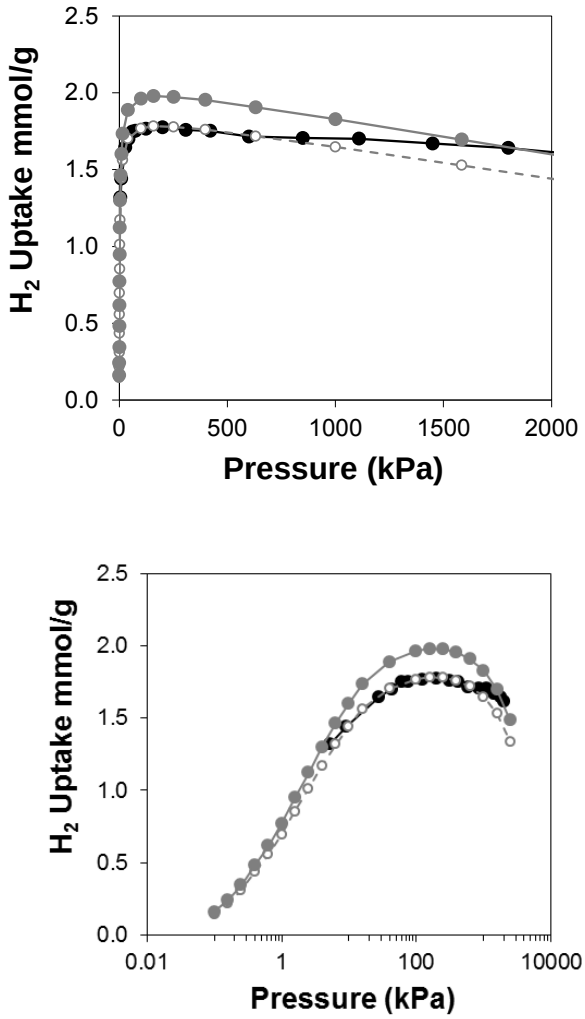

Figure 7. *Experimental, black closed circles, and simulated, grey closed circles, H_2 isotherms at 77 K on 2. Scaled (ϕ = 0.91) simulated isotherms, grey open circles. Note the use of semilog scale.*

4. CONCLUSIONS

In this work, we have shown that novel Metal-Organic Frameworks with luminescent and magnetic properties can be synthesized by using the 5-bromonicotinic ligand. Experimental adsorption and Monte Carlo simulations on

compound 2 reveal its potential properties for H_2 purification. Work is in progress in our laboratory in order to obtain new homo- and heterometallic complexes to study their physical properties.

5. REFERENCES

[1].- *(a)* M. Eddaoudi, J. Kim, N. Rosi, D. Vodak, J. Wachter, M. O'Keefe, O.M. Yaghi, *Science* 1996, **271**, 49; *(b)* L. Xu, G.C. Guo, B. Liu, M.S. Wang, J.S. Huang, *Inorg. Chem. Commun*. 2004, **7**, 1145; *(c)* L. Hou L, D. Li, *Inorg. Chem. Commun*. 2005, **8**, 190; *(d)* P. Mahata, S. Natarajan, Eur. J. Inorg. Chem. 2005, 2156; *(e)* L.S. Long, X.M. Chen, M.L. Tong, Z.G. Sun, Y.P. Ren, R.B. Huang, L.S. Zheng, D*alton Trans*. 2001, 2888.

[2] .- *(a)* W. Chen, H.-M. Yuan, J.-Y. Wang, Z.-Y. Liu, J.-J. Xu, M. Yang, J.-S. Chen, *J. Am. Chem. Soc*. 2003, **125**, 9266; *(b)* S.M. Humphrey, J.S. Chang, S.H. Jhung, J.W. Yoon, P.T. Wood, *Angew. Chem., Int. Ed*. 2007, **46**, 272; *(c)* S.M. Humphrey, P.T. Wood, *J. Am. Chem. Soc*. 2004, **126**, 13236; *(d)* X.-M. Zhang, Y.-Z. Zheng, C.-R. Li, W.-X. Zhang, X.-M. Chen, *Cryst. Growth Des*. 2007, **7**, 980; *(e)* Y.-Q. Sun, J. Zhang, Y.-M. Chen, G.-Y. Yang, *Angew. Chem., Int. Ed*. 2005, **44**, 5814; *(f)* W.-G. Lu, C.-Y. Su, T.-B. Lu, L. Jiang, J.-M. Chen, *J. Am. Chem. Soc*. 2006, **128**, 34.

[3].- *(a)* X.J. Gu, D.F. Xue, *Inorg.Chem*. 2006, **45**, 9257; *(b)* M.B. Zhang, J. Zhang, S.T. Zheng, G.Y. Yang, *Angew.Chem.Int.Ed*. 2005, **44**, 1385; *(c)* J.W. Cheng, J. Zhang, S.T. Zheng, M.B. Zhang, G.Y. Yang, *Angew.Chem.Int.Ed.* 2006, **45**, 73; *(d)* Y.S. Song, B. Yan, Z.X. Chen, *JSolidStateChem*. 2006, **179**, 4037; *(e)* Y.H. Zhao, Z.M. Su, Y. Wang, Y.M. Fu, S.D. Liu, P. Li, *Inorg.Chem.Commun*. 2007, 410.

[4].- Y.-S. Song, B. Yan, Z.-X. Chen, *Journal of Solid State Chemistry* 2004, **177**, 3805.

[5].- B. Yan, B. Zhou, *J. Photochem, Photobiol. A*, 2005, **171,** 181.

[6].- L. Zhao, P. Ren, Z. Zhang, M. Fang, W. Shi, *P. Cheng, Sci China Ser B-Chem*, 2009, **52**, 1479.

[7].- F. Lloret, M. Julve, J. Cano, R. Ruiz-García, E. Pardo, *Inorg. Chim .Acta* 2008, **361**, 3432.

[8].- *(a)* L.D. Gelb; K.E. Gubbins *Langmuir* 1999, **15**, 305; *(b)* T. Düren, F. Millange, G. Férey, K.S. Walton, and R.Q. Snurr *J. Phys. Chem. C* 2007 **111**, 5350.

[9].- Denise Zacher, Osama Shekhah, Christof Wöll and Roland A. Fischer. *Chem. Soc. Rev.*, 2009, **38**, 1418.

[10].- *(a)* B. Chen, S. Ma, F. Zapata, F.R. Fronczek, E.B. Lobkovsky and H.-C. Zhou, *Inorg. Chem*., 2007, **46**, 1233.; *(b)* M. Xue, S. Ma, Z. Jin, R.M. Schaffino, G.S. Zhu, E.B. Lobkovsky, S.L. Qiu, B. Chen B, *Inorg. Chem*., 2008, **47**, 6825.

[11] .- *(a)* Frenkel, D.; Smit, B. Understanding Molecular Simulations: From Algorithms to Applications, 2nd ed.; Academic Press: San Diego, 2002; *(b)* A. Rossin, D. Fairen-Jimenez, T. Düren, G. Giambastiani, M. Peruzzini and J. G. Vitillo, *Langmuir* 2011, **27**, 1012.

CAPÍTULO 9.

First Examples of Metal-Organic-Frameworks with the Novel 3,3'-(1,2,4,5-tetrazine-3,6-diyl)dibenzoic Spacer. Luminescence and Adsorption Properties

ARTICLE: *FIRST EXAMPLES OF METAL-ORGANIC-FRAMEWORKS WITH THE NOVEL 3,3'-(1,2,4,5-TETRAZINE-3,6-DIYL)DIBENZOIC SPACER. LUMINESCENCE AND ADSORPTION PROPERTIES***.**

Inorganic Chemistry

Communication

pubs.acs.org/IC

First Examples of Metal–Organic Frameworks with the Novel 3,3′-(1,2,4,5-Tetrazine-3,6-diyl)dibenzoic Spacer. Luminescence and Adsorption Properties

A. J. Calahorro,[†] Antonio Peñas-Sanjuan,[‡] Manuel Melguizo,[‡] David Fairen-Jimenez,[§] Guillermo Zaragoza,[⊥] Belén Fernández,[∥] Alfonso Salinas-Castillo,[¶] and A. Rodríguez-Diéguez*[,†]

[†]Departamento de Química Inorgánica, Universidad de Granada, Avenida Fuentenueva s/n, 18071 Granada, Spain

[‡]Departamento de Química Inorgánica y Orgánica, Universidad de Jaén, Campus Las Lagunillas, 23071 Jaén, Spain

[§]Department of Chemical & Biological Engineering, Northwestern University, 2145 Sheridan Road, Evanston, Illinois 60208-3120, United States

[⊥]Unidad de Rayos X, RIAIDT Edificio CACTUS, Universidad de Santiago de Compostela, 15782 Santiago de Compostela, Spain

[∥]Instituto de Parasitología y Biomedicina López-Neyra (CSIC), Avenida del Conocimiento s/n, Armilla, Granada

[¶]Departamento de Química Analítica, Universidad de Granada, 18071 Granada, Spain

ABSTRACT

We report the synthesis of a novel ligand, 3,3'-(1,2,4,5-tetrazine-3,6-diyl)dibenzoic acid (1). In this fragment, we have introduced two carboxylate groups with the aim of using this ligand as a linker to construct three-dimensional Metal-Organic-Frameworks (MOF). We have been successful in the formation of zinc (2) and lanthanum (3) MOFs. The Zn compound is a bidimensional structure while lanthanum material is a 3D-MOF with interesting channels. We include the luminescence and adsorption studies on these materials. Moreover, we have evaluated the *in vitro* toxicity of this novel ligand concluding that it can be considered negligible.

1. INTRODUCTION

In the last fifteen years, a great attention has been paid to metal-organic frameworks (MOFs) as a consequence of their functional properties and potential uses in many applications.[1] Recently, the design and study of Zn- and Ln-based MOF has evolved enormously[2] because of their interesting structures and potential applications in areas such as magnetism,[3] luminescence,[4] gas adsorption,[5] sensing, and optical storage.[6] These materials are commonly prepared through a bottom-up approach, using solvothermal methods, connecting transition/lanthanide metal ions with the appropriate bridging ligands. Still, there is a great interest in the design of new bridging ligands that will allow the preparation of novel MOFs.

Here, we have designed a new symmetrically multidentate bridging ligand, 3,3'-(1,2,4,5-tetrazine-3,6-diyl)dibenzoic acid (**1**) (H_2dbtz), which contains two benzoic groups donors, bonding to the metals, and a central tetrazine p-acceptor function. Our idea stems from the use of 3,6-disubstituted-1,2,4,5-tetrazine moieties, who have become popular as efficient electronic spacers in dinuclear and polynuclear systems.[7] This is primarily due to the fact that the tetrazine-based low-lying p* orbital conveys strong p-accepting characteristics, leading to excellent electronic communication between the metal termini.

In this work, we report the structural, luminescence and adsorption properties of the first examples of coordination polymers $[Zn(dbtz)(H_2O)]_n$ (**2**) and $\{[La_2(dbtz)_3(H_2O)_2](H_2O)_6\}_n$ (**3**) with the new multidentate ligand H_2dbtz, shown in scheme I, demonstrating the potential of this new ligand to construct new MOFs with interesting adsorption properties due to the similarity to others linkers, e.g. *NOTT-101* MOF.[8] To the best of our knowledge, these are the first examples of crystal structures of MOFs with ligands that contain the H_2dbtz ligand.

2. EXPERIMENTAL

2.1. General.

All analytical reagents were purchased from commercial sources and used without further purification.

2.2. Preparation of compounds.

Synthesis of 3,3'-(1,2,4,5-tetrazine-3,6-diyl)dibenzoic acid (**1**). Hydrazine hydrate (5.28 ml, 106.57 mmol) was dropwise added to a solution of 3-cyanobenzoic acid (4.00 g, 26.64 mmol) and N-acetyl-L-cysteine (4.39 g, 26.64 mmol) in MeOH (50 ml) at room temperature under Ar atmosphere, and the resulting mixture was stirred at room temperature for 72 h under Ar atmosphere. Then, the yellowish solid in suspension was collected by filtration, washed with methanol (40 ml), resuspended in MeOH (50 ml) and kept under stirring in an open round-bottomed flask at room temperature for 72 h. Finally, the purple solid in suspension was collected by filtration, washed with methanol (40 ml) and dried under vacuum to afford 3,11 g (9.64 mmol, 71 % yield) of the title compound as a spectroscopically pure purple solid. ^{1}H NMR (400 MHz, DMSO-d_6) δ ppm 7.85 (t, J=7.75 Hz, 2 H) 8.27 (d, J=7.86 Hz, 2 H) 8.78 (d, J=8.06 Hz, 2 H) 9.09 (s, 2 H) 13.30 (br. s., 2 H); ^{13}C NMR (101 MHz, DMSO-d_6) δ ppm 128.27, 130.04, 131.61, 132.03, 132.26, 133.10, 163.00, 166.58; HRMS (EI): m/z calcd. for $C_{16}H_{10}N_4O_4$: 322.0702; found: 322.0700.

Preparation of [Zn(dbtz)(H_2O)] (2). A mixture of H_2dbtz (32.2 mg, 0.1 mmol), $Zn(NO_3)_2{\cdot}6H_2O$ (29.75 mg, 0.1 mmol) and a water:acetonitrile (1:1) mixture (10 mL) was placed in a Teflon reactor (23 mL) and heated at 140 °C for 3 d. After the mixture had been cooled to room temperature at a rate of 15 °C·h^{-1}, pink crystals of **2** were obtained with a yield of 81% (based on Zn). C16H10N4O5Zn (Mr = 403.66): calcd. C 47.61, H 2.50, N 13.88; found C 47.23, H 2.32, N 14.11. IR: = 1607 (m), 1591 (m), 1548 (s), 1531 (s), 1459 (s), 1425 (s), 1384 (s), 773(m) cm-1.

Preparation of [La_2(dbtz)$_3$(H_2O)$_8$] (3). A mixture of H_2dbtz (48.3 mg, 0.15 mmol), $LaCl_3{\cdot}7H_2O$ (37.1 mg, 0.1 mmol), and water (10 mL) was placed in a Teflon

reactor (23 mL) and heated at 140 °C for 3 d. After the mixture had been cooled to room temperature at a rate of 15 °C·h^{-1}, pink crystals of **3** were obtained with a yield of 78% (based on La). C48H40N12O20La2 (Mr = 1382.71): calcd. C 41.69, H 2.92, N 12.16; found C 41.92, H 2.81, N 11.98. IR: = 3419 (m), 1607 (m), 1541 (m), 1407 (m), 1384 (s), 776 (m), 736(m) cm-1.

2.3. Physical measurements

Elemental analyses were carried out at the "Centro de Instrumentación Científica" (University of Granada) on a Fisons-Carlo Erba analyser model EA 1108. The IR spectra on powdered samples were recorded with a ThermoNicolet IR200FTIR by using KBr pellets.

2.4. Single-Crystal Structure Determination.

Suitable crystal of compounds were mounted on glass fiber and used for data collection. Data were collected with Bruker X8 Proteum diffractometers at 296(2) K. From the 782 measured reflections, 782 were independent and used to refine 46 parameters with zero restraints. Bruker X8 Kappa ApexII diffractometer (2.8 < 2Θ < 26.3º). Final *R* [I < 2Θ(I)], *R*1 = 0.0350, *wR*2 = 0.0758, final *R* (all data), *R*1 = 0.0599, *wR*2 = 0.0805. Max./min. residual electron density 0.883/-0.843 e $Å^{-3}$. The data were processed with APEX2[9] and corrected for absorption using SADABS.[10] The structures were solved by direct methods using SIR97,[11] revealing positions of all non-hydrogen atoms. These atoms were refined on F^2 by a full matrix least-squares procedure using anisotropic displacement parameters.[12]

2.5. Luminescence measurement

A Varian Cary-Eclipse Fluorescence Spectrofluorimeter solid sample holder accessory was used to obtain the fluorescence spectra. The spectrofluorimeter was

equipped with a xenon discharge lamp (peak power equivalent to 75 kW), Czerny-Turner monochromators, R-928 photomultiplier tube which is red sensitive (even 900 nm) with manual or automatic voltage controlled using the Cary Eclipse software for Windows 95/98/NT system. The photomultiplier detector voltage was 800 V and the instrument excitation and emission slits were set at 10 and 10 nm, respectively.

2.6. Computational Details

The geometric pore size distribution was calculated using the method of Gelb and Gubbins, where the largest sphere that can fit in a random point within a structure without overlapping the van der Waals surface of the framework is recorded for a large number of random points (Figure S6). Additionally, hydrogen adsorption at 77 K on **3** was studied using grand canonical Monte Carlo (GCMC) simulations (Figure 6), performed with our in-house multi-purpose code RASPA. In the grand canonical ensemble, the chemical potential, the volume, and the temperature are kept fixed as in adsorption experiments. An atomistic model was used for **3**, with the atoms frozen at the crystallographic positions. In the simulation, hydrogen molecules were randomly moved, rotated, inserted, and deleted, allowing the number of molecules in the framework to fluctuate. The chemical potential was related to the system pressure by the Peng-Robinson equation of state. The standard 12-6 Lennard-Jones (LJ) potential was used to model the interatomic interactions. The parameters for the framework atoms were obtained from the UFF force field, while molecular hydrogen was modeled by two LJ spheres (σH=2.72Å, εH/kB = 10.00 K, dH-H=0.74Å)[6, 7]. The Lorentz_Berthelot mixing rules were employed to calculate the mixed parameters. Interactions beyond 17 Å were neglected for the simulations. Quantum effects were taken into account using the Feynman-Hibbs effective potential method,′ which is sufficiently accurate at 77 K. A total number of 2×10^7 Monte Carlo steps were performed. The first 50% was used for system equilibration, carefully ensuring that thermodynamic equilibrium was reached, while the remaining steps were used to calculate the ensemble averages.

3. Results and Discussion

3.1. Synthesis and structure of 3,3'-(1,2,4,5-tetrazine-3,6-diyl)dibenzoic acid.

The synthesis of 3,3'-(1,2,4,5-tetrazine-3,6-diyl)dibenzoic acid was performed following a variant of the classical Pinner-type scheme in two steps.[13] Firstly, the reaction between 3-cianobenzoic acid and excess hydrazine catalysed by N-acetylcysteine under inert atmosphere renders the dihydrotetrazine derivative, which was oxidized to give the desired fully aromatic derivative by simple stirring of a methanol suspension of the dihydroderivative in an air atmosphere. Although a similar air oxidation procedure has been reported to aromatise some dihydrotetrazine derivatives,[14] its scope seems to be more general than initially recognized, as proven here.

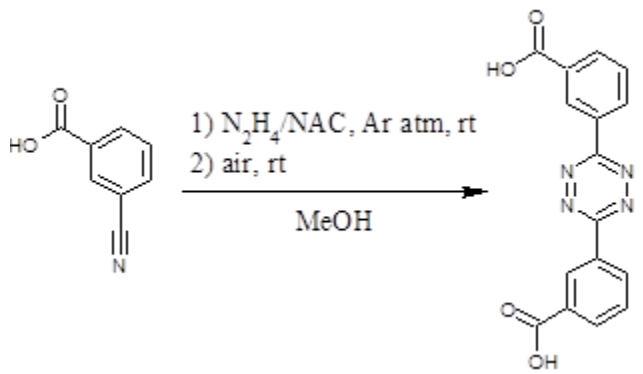

Scheme I. Preparation of 3,3'-(1,2,4,5-tetrazine-3,6-diyl)dibenzoic acid. NAC = N-Acetylcysteine.

3,3'-(1,2,4,5-tetrazine-3,6-diyl)dibenzoic acid (**1**) was characterized by ^{1}H NMR, ^{13}C NMR (figure 2 and 3), EI-HRMS and XR diffraction. Compound **1** crystallizes in the monoclinic space group *P*21/*c*, the asymmetric unit consisting of medium H_2dbtz ligand that grows by symmetry generated an almost linear alignment between the aromatic rings and the terminal carboxylate groups (dihedral angles (6º-3º)) and one crystallization dimethyl-sulfoxide molecule (Figure 1). In the H_2dbtz unit, the bond distances and angles are very similar to those expected in comparison with the

tetrazine and benzene rings.[15] In the structure, there is only one type of hydrogen bond (figure 4), yielding a three-nuclear unit formed by one central H_2dbtz unit and two dimethyl-sulfoxide molecules. In this strong hydrogen bond (O1-H…O3 = 2.565 Å), the oxygen atom pertaining to dimethyl-sulfoxide and one oxygen from carboxylate group are involved. These three-nuclear units are packed thought stacking interactions (3.531(5) Å) among the tetrazine with benzene rings and (3.699(5) Å) benzene-benzene rings of neighbour units (figure 4 and table 1).

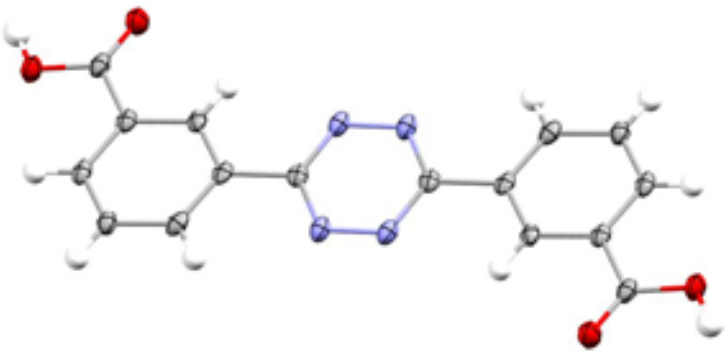

Figure 1. *Crystalline structure of 3,3'-(1,2,4,5-tetrazine-3,6-diyl)dibenzoic acid. Carbon, grey; nitrogen, blue; oxygen, red; sulphur, yellow; hydrogen, white. Dimethyl-sulfoxide molecule has been omitted for clarity. Thermal ellipsoids are drawn at the 50% probability level*.

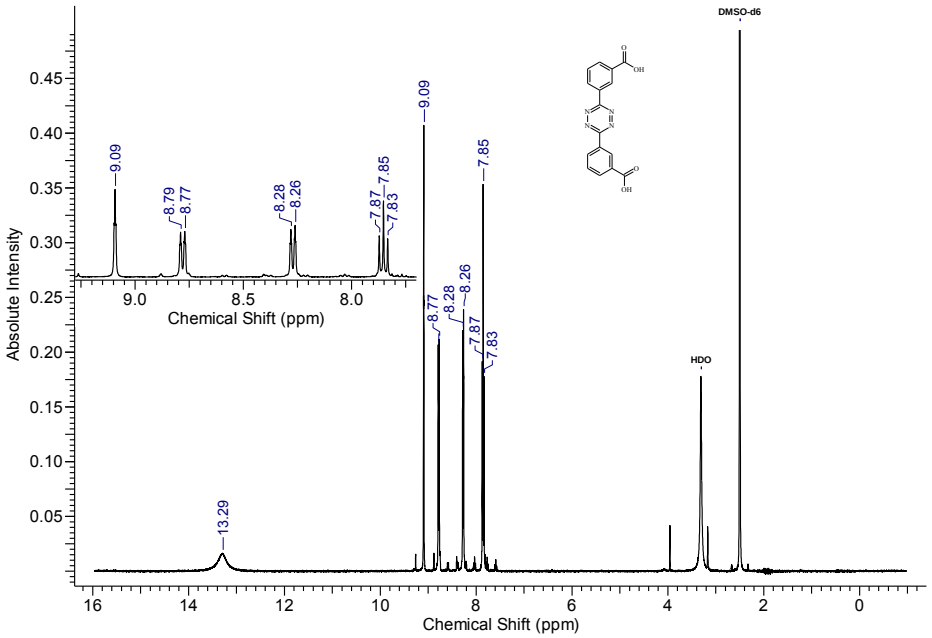

Figure 2. *^{1}H NMR (400 MHz, DMSO-d_6) of 3,3'-(1,2,4,5-tetrazine-3,6-diyl)dibenzoic*

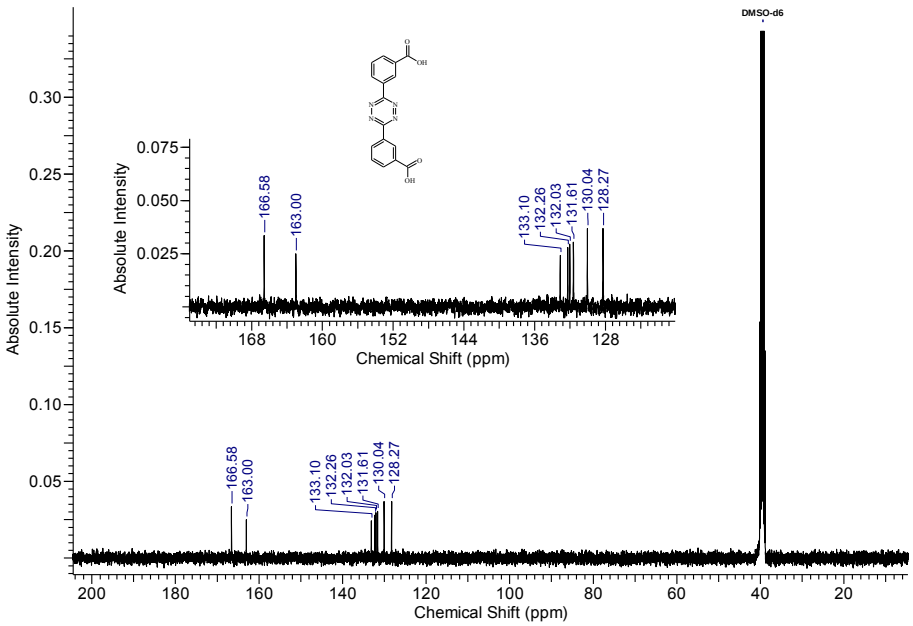

Figure 3. *^{13}C NMR (101 MHz, DMSO-d_6) of 3,3'-(1,2,4,5-tetrazine-3,6-diyl)dibenzoic*

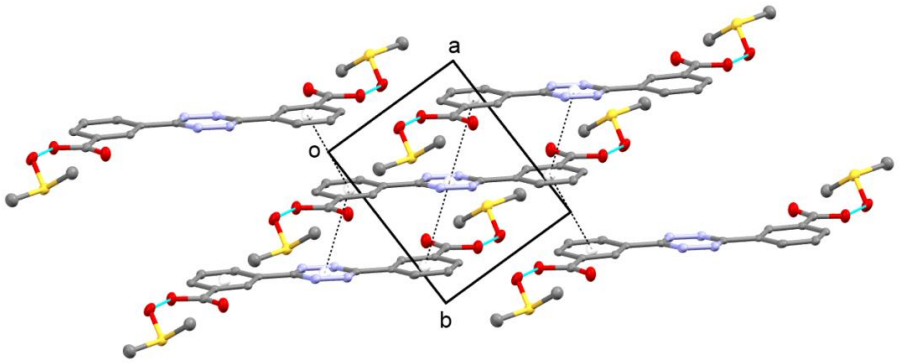

Figure 4. *Hydrogen bonds and π-stacking in 1*

Table 1 *Analysis of Short Ring-Interactions* ***[1]***

Parameter	Cg-Cg	Alpha	Beta	Gamma	Cg1_Perp	Cg2_Perp
Cg(1) → Cg(2)i	3.531(5)	4.6(4)	19.59	23.40	-3.240(3)	3.326(4)
Cg(1) → Cg(2)ii	3.531(5)	4.6(4)	19.59	23.40	-3.240(3)	-3.326(4)
Cg(2) → Cg(1)iii	3.531(5)	4.6(4)	23.40	19.59	-3.240(3)	-3.240(3)
Cg(2) → Cg(1)ii	3.531(5)	4.6(4)	23.40	19.59	-3.240(3)	-3.240(3)
Cg(2) → Cg(2)iv	3.699(5)	0	26.58	26.58	3.308(4)	3.308(4)

Symmetry transformations: (i) -1+X,Y,Z (ii) **-X,1-Y,-Z (iii) 1+X,Y,Z (iv) -X,2-Y,-Z**

[Cg(1) •••C8-N1-(N2*-C8-N1)*-N2]; [Cg(2) = (C2 → C7] Sym Code*(1-x,1-y,-z)

3.2. Structure and crystallographic results of (2) and (3)

Hydrothermal reactions of the appropriate metal salts (1 mmol) with H_2dbtz (1 mmol) in water (10 ml) at 160 °C for 12 h followed by cooling to room temperature

over 3 h yields prismatic pink crystals of **2** (in 57% yield) and **3** (in 75% yield). The crystal structures were determined by single crystal X-ray crystallography.[16]

Compound **2** consists of double-sheets parallel to *ac* plane. These layers can be described as chains generated by the carboxylate groups, pertaining to the ligand along *b* directions that are bridged by the $dbtz^{-2}$ spacer. The metal centers have tetrahedral coordination environtment ZnO4 formed by three oxygen atoms pertaining to three carboxilate groups of three different spacers and one coordinated water molecule.

There are four units of formula [Zn(dbtz)(H_2O)] per cell and, in the crystal structure, each bridging $dbtz^{-2}$ ligand is bound to three metal ions and each metal ion is linked to five other metal ions by three $dbtz^{-2}$ ligands, thus generating stacked-double sheets parallel to the [101] direction.

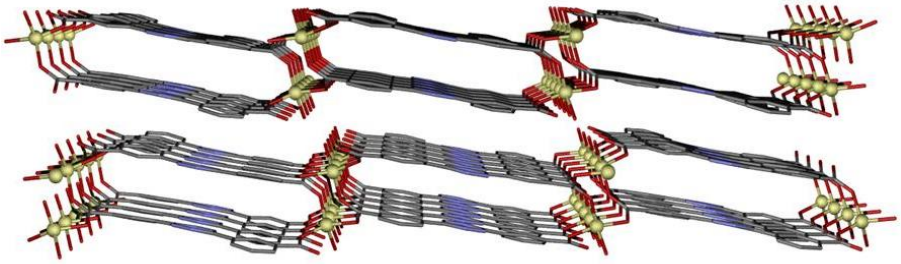

Figure 5. *Representation, down [101], of the two-dimensional* $[Zn(dbtz)(H_2O)]_n$ *layer present in compound* ***2***.

The ligand coordinates to metal center in monodentate and bidentate coordination modes with each one carboxylate group, respectively. The coordinated water molecule generate H bonds with monodentate mode and infinite two-dimensional networks of formula $[Zn(dbtz)(H_2O)]_n$ are thus formed, the values of these H bonds are 2.744(6)and 2.676(6). The association of two such layers by the

bidentate mode thought one of the carboxylate group bridges give rise to double layers $[Zn(dbtz)(H_2O)]_n$. These double layers are separated by stacking interactions (3.719(4) Å) (figure 6, Table 2). Figure 5 shows a perspective view of the double-sheet. Table 3 gives the main bond lengths and angles.

Table 2 *Analysis of Short Ring-Interactions* ***[2]***

Parameter	Cg-Cg	Alpha	Beta	Gamma	Cg1_Perp	Cg2_Perp
Cg(1) →Cg(1)i	4.418(4)	0	47.14	47.14	-3.005(3)	-3.005(3)
Cg(1) →Cg(1)ii	4.795(5)	0	49.46	49.46	-3.116(3)	-3.117(3)
Cg(1) →Cg(1)iii	5.369(5)	0	48.14	48.14	3.583(3)	3.583(3)
Cg(1) →Cg(1)iv	5.683(5)	0	52.35	52.35	3.472(3)	3.472(3)
Cg(1) →Cg(2)i	5.220(5)	9.9(3)	53.01	49.41	-3.397(3)	-3.141(3)
Cg(1) →Cg(2)iii	3.719(4)	9.9(3)	22.02	30.53	3.203(3)	3.448(3)
Cg(1) → Cg(3)ii	4.768(4)	4.1(3)	46.35	46.65	-3.273(3)	-3.291(3)
Cg(2) →Cg(2)iii	5.759(5)	0	54.75	54.75	3.323(3)	3.324(3)
Cg(2) →Cg(3)i	4.596(5)	13.4(3)	33.93	47.16	-3.125(3)	-3.814(3)
Cg(2) →Cg(3)ii	5.035(5)	13.4(3)	56.65	43.34	-3.663(3)	-2.768(3)
Cg(2) →Cg(3)iii	5.153(5)	13.4(3)	57.27	46.58	3.542(3)	2.786(3)
Cg(2) →Cg(3)iv	5.548(5)	13.4(3)	46.34	57.22	3.004(3)	3.831(3)

Symmetry transformations: (i) 1-X,1-Y,-Z (ii) **1-X,2-Y,-Z (iii) 2-X,1-Y,-Z (iv) 2-X,2-Y,-Z**

[Cg(1) = N1-N2-C9-N3-N4-C8]; [Cg(2) = (C2 → C7)]; [Cg(3) = (C10 → C15)]

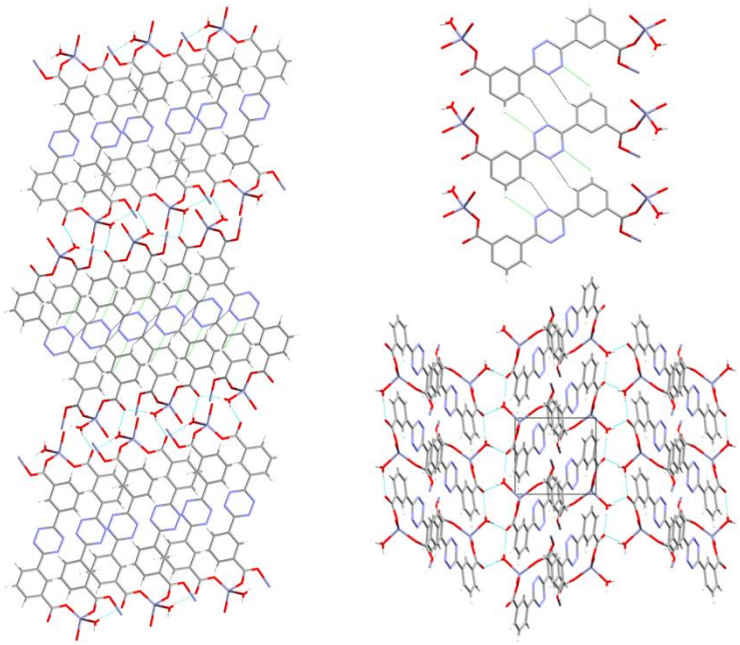

Figure 6. *Hydrogen bonds in 2.*

The crystal structure of **3** consists of a three-dimensional MOF with channels occupied by disordered solvent water molecules that propagate along the *a* crystallographic axis. Each La^{III} ion exhibits a LaO8 coordination environment, which is made of seven oxygen atoms belonging to carboxylate groups of two-deprotonated $dbtz^{-2}$ bridging ligands and one coordination water molecule. The La–O_{water} bond distance is 2.82(3) Å whereas the La–O_{carb} distances are in the range 2.394(19)-2.564(12) Å.

In the structure, La ions are connected by carboxylate groups pertaining to $dbtz^{-2}$ ligands generating double chains along *a* axis direction (figure 7, right). Some oxygen from the carboxylate groups unit two or three lanthanum centers. The dihedral angles between the mean planes of the benzene and tetrazine rings are in the range 7.28-22.67º. These double chains are bridged with others six double chains by $dbtz^{-2}$ ligands (figure 7, left).

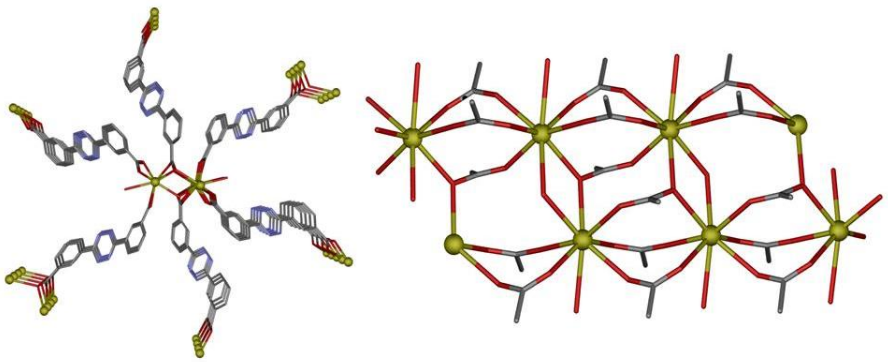

Figure 7. *Each double chain generated by carboxylate groups is bridged to others six throught* $dbtz^{-2}$ *spacers (left). Double chain generated by carboxylate-bridges (right).*

Each lanthanum ion is linked to seventeen other metal ions by seven $dbtz^{-2}$ ligands, generating a three-dimensional structure (figure 8). On considering the $dbtz^{-2}$ ligands as spacer, and the La atoms as nodes, the resulting network generates channels along the *a* axis direction (figure 9). These channels have a diameter of 5.02 Å. The shortest and longest La···La distances through $dbtz^{-2}$ spacers are 4.308 and 18.653 Å, respectively.

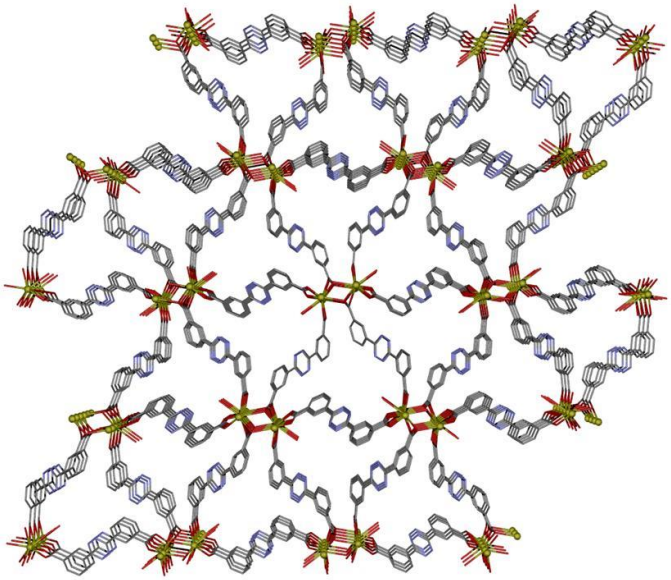

***Figure 8**. Perspective view along a direction of **3** with the channels in which are located the water molecules. Crystallization water molecules and hydrogen atoms have been omited for clarity*.

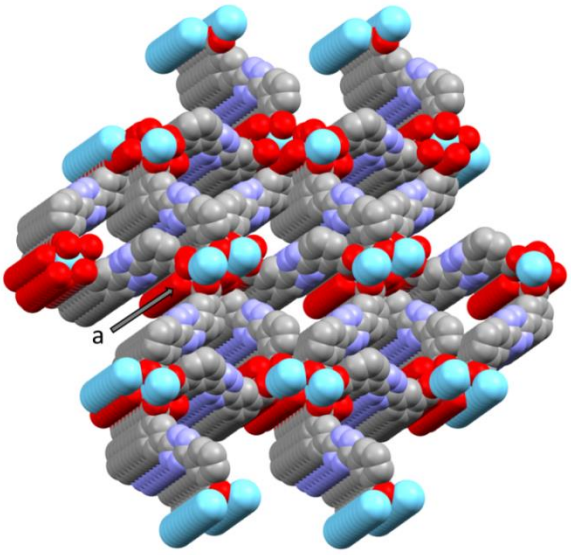

***Figure 9.** Perspective view of the channels in the three-dimensional network in **3**.*

3.3. Luminescence Properties

Thanks to its extended aromaticity and to the presence of polyheterosubstituded hexa-atomic rings, H_2dbtz is a good candidate for enhanced emissive properties, tunable, in principle, by coordination to different metals or environments. The emission spectra of compounds **1–3** in solid state at room temperature are shown in Figure 10. The emission spectrum of **1** and **2** at room temperature in solid state exhibited broad intense emission bands centred about 454 and 461 nm, respectively, upon excitation at 310 nm.

For **3**, using a 310 nm incident radiation, intense emission bands at 453 and 470 nm and a stronger one at 498 nm were observed. The emissions in complexes **2** and **3** are assigned to intraligand p–p* transitions, although a considerable red-shift is observed with respect to the ligand emission band. Moreover, the emission is more intense than that of the free ligand, which may be explained in term of the rigidity. The rigidity of the coordinated ligand reduces the loss of energy, thereby increasing the emission efficiency.[17]

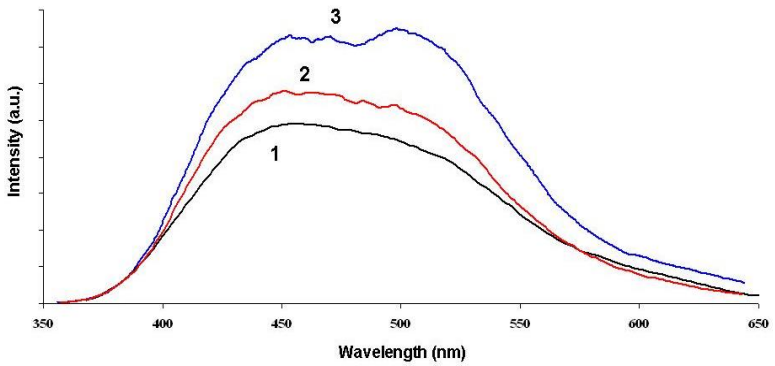

Figure 10. *The emission spectra of* ***1, 2*** *and* ***3*** *in solid state at room temperature*.

3.4. Adsorption Properties

We first studied the porous properties of **3** by means of their pore size distribution (PSD) in a Monte Carlo calculation.[18] PSD analysis shows that it presents narrow cavities localized at 4 Å (Fig. 11). We extended our study running molecular simulations to predict the adsorption uptake of N_2 and H_2 on **3** at 77 K. Due to the presence of very narrow porosity, N_2 molecules cannot adsorb in the porosity. On the other hand, the adsorption isotherm of H_2 (Figure 12) predicts an excess capacity at 77 K and 100 bar of 9.97 mg/g (12.9 mg/cm^3, using a crystal density of 1.29 g/cm^3). We[19] and others[20] have reported recently high H_2 selective behavior on MOFs for stream purification applications. We studied experimentally the porous structure of **3** after solvent removal, during the adsorption of H_2 at 77 K and up to 100 bar. However, the experimental adsorption isotherm revealed that the porous structure collapsed during the activation using conventional methods (heating at 393 K and high vacuum, 10^{-4} bar).

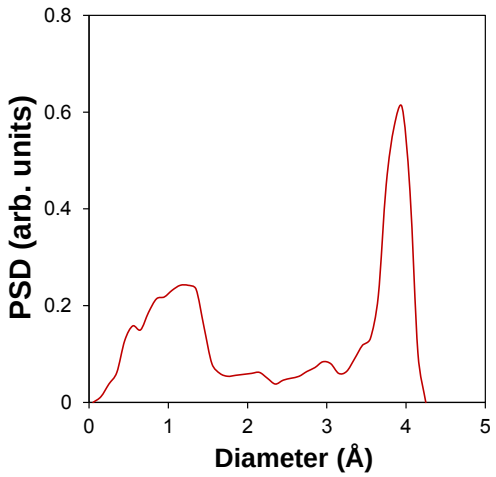

Figure 11. *Geometrical pore size distribution of* ***3****.*

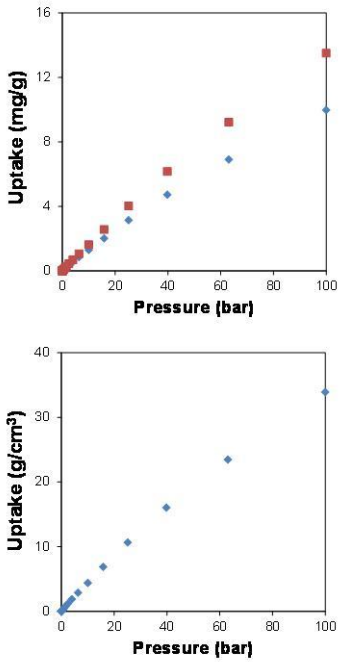

Figure 12. *Absolute, red squares, and excess, blue diamonds, simulated H_2 isotherms at 77 K on* ***3****. Note the use of gravimetric (up) and volumetric (down) uptakes*.

3.5. Biological Properties

We evaluated *in vitro* cytotoxicity of cells exposed to compound **1** at different concentrations and a wide range of incubation times (Figure 13). The results obtained shows that for long incubation times and at the highest concentrations analyzed apparent mild signs of toxicity appeared that can be considered negligible with cell viability greater than 90-80%.

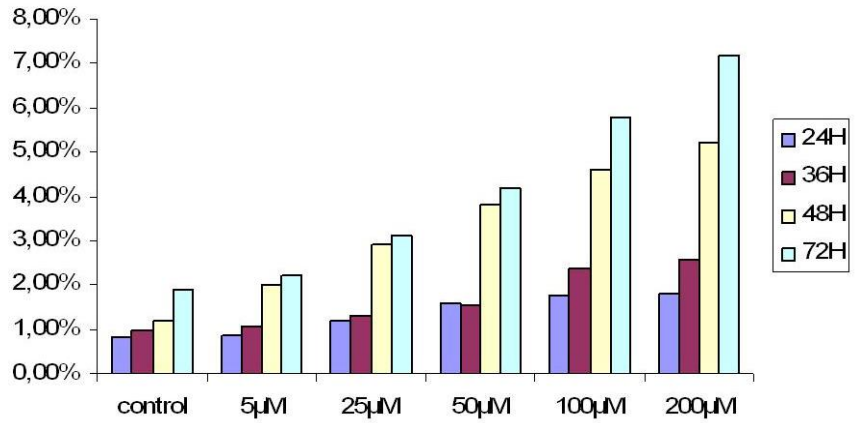

***Figure 13**. Concentration-time toxicity dependence of HEK293 cells exposed to compound **1**. Quantification from three different experiments (mean+s.e.m. (n = 3); * P >0.05.*

Cytotoxicity was analyzed by Hoechst staining as previously described.11 HEK 293 cells were cultured on poly-lysine-coated glass coverslips and were fixed with 4% paraformaldehyde solution (in PBS), followed by three washes in TBS-Tween 0,1%, and incubated with 4, 6-Diamidino-2-phenylindole (DAPI), a specific dye for binding DNA. The blue fluorescence was observed by fluorescence microscopy at 350 nm (UV filter) (Zeiss Axio Imager A1). Normal cells displayed a round nucleus, whilst apoptotic cells were scored as displaying condensed or fragmented nuclei. Minimally 150 nuclei were scored for each condition

4. CONCLUSIONS

These results show that new and interesting materials or MOFs with biomedical applications can be assembled from metal ions and the new H_2dbtz ligand. Work along this line using other paramagnetic/lanthanides metals and XR measures with pressure are in progress in our lab. We are also working in the use of

supercritical activation process to allow the removal of solvent molecules from the porosity, keeping unaffected the porous texture of the as-prepared material.

5. REFERENCES

([1]) (a) Sudik, A.C.; Cote, A.P.; Wong-Foy, A.G.; O'Keeffe, M.; Yaghi, O.M. *Angew. Chem., Int. Ed.* **2006**, *45*, 2528-2533. (b) Kondo, A.; Noguchi, H.; Kajiro, H.; Carlucci, L.; Mercandelli, P.; Proserpio, D.M.; Tanaka, H.; Kaneko, K.; Kanoh, H. *J. Phys. Chem. B,* **2006**, *110*, 25565-25567. (c) Rowsell, J.L.C.; Yaghi, O.M. *J. Am. Chem. Soc.* **2006**, *128*, 1304. (d) Jhung, S.H.; Lee, J.-H.; Cheetham, A.K.; Ferey, G.; Chang, J.S. *J. Catal.* **2006**, *239***,** 97-104. (e) Hong, M. *Cryst. Growth Des.* **2007**, *7***,** 10. (f) Vertova, A.; Cucchi, I.; Fermo, P.; Porta, F.; Proserpio, D.M.; Rondinini, S. *Electrochim. Acta* **2007**, *52*, 2603-2611. (g) Janiak, C. *Dalton Trans.* **2003**, *14,* 2781. (h) Braga, D.; Polito, M.; D'Addario, D.; Grepioni, F. *Cryst. Growth Des.* **2004**, *4,* 1109-1112. (i) Hyde, S.T.; Delgado-Friedrichs, O.; Ramsden, S.J.; Robins, V. *Solid State,* **2006**, 740-752. (j) Yang, S.; Sun, J.; Ramirez-Cuesta, A.J.; Callear, S.K.; David, W.I.F.; Anderson, D.P.; Newby, R,; Blake, A.J.; Parker, J.E.; Tang, C.C.; Schröder, M.*; Nature Chemistry***, 2012**, *4*, 887-894. (k) Long, J. R.; Yaghi, O. M.; *Chem. Soc. Rev*., **2009**, *38*, 1201–1507.

([2]) (a) Almeida Paz, F.A.; Klinowski, J. *Chem. Commun*., **2003**, 1484-1485. (b) Sun, D.; Cao, R.; Liang, Y.; Shi, Q.; Hong, M.J.; *Chem. Soc. Dalton Trans.*, **2002**, 1847-1851. (c) Long, D.-L.; Blake, A.J.; Champness, N.R.; Wilson, C.; Schröder, M. *Angew. Chem. Int. Ed*., **2001**, *40*, 2444-2447. (d) Westin, L.G.; Kritikos, M.; Caneschi, A. *Chem. Commun*., **2003**, 1012-1013. (e) Ma, B.-Q.; Zhang, D.-S.; Gao, S.; Jin, T.-Z.; Yan, C.-H.; Xu, G.-X. *Angew. Chem. Int. Ed.*, **2000**, *39*, 3644-3646.

([3]) (a) Morrish, A.H. *The Physical Principles of Magnetism*; Wiley: New York, **1965**. (b) Chen, Z.; Zhao, B.; Zhang, Y.; Shi, W.; Cheng, P. *Cryst. Growth Des*., **2008**, *8,* 229-233.

([4]) (a) De Lill, D.T.; De Bettencourt-Dias, A.; Cahill, C.L. *Inorg. Chem*., **2007**, *46,* 3960-3965. (b) Lunstroot, K.; Driesen, K.; Nockemann, P.; Gorller-Walrand, C.; Binnemans, K.; Bellayer, S.; Le Bideau, J.; Vioux, A. *Chem. Mater*., **2006**, *18,* 5711-5715. (c) Shunmugam, R.; Tew, G.N. *J. Am. Chem. Soc*., **2005**, *127*, 13567-13572. (d) Rosi, N.L.; Kim, J.; Eddaoudi, M.; Chen, B.L.; O'Keeffe, M.; Yaghi, O.M.; *J. Am. Chem. Soc*., **2005**, *127*, 1504-1518.

([5]) (a) Pan, L.; Adams, K.M.; Hernandez, H.E.; Wang, X.; Zheng, C.; Hattori, Y.; Kaneko, K. *J. Am. Chem. Soc*., **2003**, *125*, 3062-3067. (b) Dawson, R.; Adams, D. J.; Cooper, A. I.; *Chem. Sci*. **2011**, *2*, 1173–1177.

([6]) (a) Kuriki, K.; Koike, Y.; Okamoto, Y. *Chem. Rev*., **2002**, *102,* 2347-2356. (b) Cahill, C.L.; De Lill, D.T.; Frisch, M. *Cryst. Eng. Comm.*, **2007**, *9,* 15-26. (c) Bünzli, J.C.G.; Piguet, C. *Chem. Soc. Rev*., **2005**, *34*, 1048-1077. (d) Robin, A.Y.; Fromm, K.M. *Coord. Chem. Rev.*, **2006**, *250,* 2127-2157. (e) Faulkner, S.; Matthews, J.L. *Comprehensive Coordination Chemistry II*; Elsevier: Oxford, U.K., **2004**, *9*, 913-944. (f) Gheorghe, R.; Cucos, P.; Andruh, M.; Costes, J.P.; Donnadieu, B.; Shova, S. *Chem. Eur. J*., **2005**, *12,* 187-203.

([7]) Kaim, W. Coord. Chem. Rev. **2002**, *230,* 127-139.

([8]) Lin, X.; Telepeni, I.; Blake, A.J.; Dailly, A.; Brown, C.M.; Simmons, J.M.; Zoppi, M.; Walker, G.S.; Thomas, K.M.; Mays, T.J.; Hubberstey, P.; Champness, N.R.and Schröder, M., J. *Am. Chem. Soc*, **2009**, *1331*, 2159-2171.

[[9]] Bruker Apex2, Bruker AXS Inc, Madison, Wisconsin, USA, 2004.

[[10]] Sheldrick, G.M., SADABS, Program for empirical adsorption correction, Institute for Inorganic Chemistry, University of Göttingen, Germany, 1996.

[11] A.. Altomare, M. C. Burla, M. Camilla, G.L. Cascarano, C. Giacovazzo, A. Guagliardi, A. G. G. Moliterni, G. Polidori, R. Spagna. J. Appl. Crystallogr. 32 (1999) 115.

[12] Sheldrick, G. M., SHELX 97, Program for crystal structure refinement, University of Göttingen, Göttingen, Germany, 1997.

(**13**) Pinner, A.; Liebig, J. Ann. *Chem.* **1897**, *297,* 221-271.

(**14**) Cutivet, A.; Leroy, E.; Pasquinet, E.; Poullain, D. *Tetrahedron Lett.*, **2008**, *49*, 2748-2751.

(**15**) Kaszynski, P.; Young, V.G. *J. Am. Chem. Soc.* **2000**, *122,* 2087-2090.

(**16**) Crystal Data. **1**: [C20H22N4O6S2], *M* = 478.56, triclinic, space group *P-1*, *a* = 6.3054(6), *b* = 8.0715(9), *c* = 11.4005(13) Å, α = 73.397(7), β = 82.195(7), σ = 85.851(7), *V* = 550.53(10) Å3, *Z* = 1, *ρ*calcd = 1.443 g cm-3, *μ*(Mo-*K*α) = 0.287 mm-1, *R*1(*Fo*) = 0.0598, (*wR*2(*Fo2*) = 0.1468) with a goodness-of-fit on *F2* 1.015. **2**: [C16H10N4O5Zn], *M* = 403.67, monoclinic, space group *P21/n*, *a* = 7.247(4), *b* = 6.814(4), *c* = 29.631(17) Å, β = 90.015(9), *V* = 1463.3(15) Å3, *Z* = 4, *ρ*calcd = 1.832 g cm-3, *μ*(Mo-*K*α) = 1.72 mm-1, *R*1(*Fo*) = 0.0495, (*wR*2(Fo^2) = 0.1113) with a goodness-of-fit on *F2* 1.02. **3**: [C24H12N6O10La], *M* = 683.31, monoclinic, space group *P21/c*, *a* = 5.1474(10), *b* = 18.232(4), *c* = 26.783(5) Å, β = 90.08(3), *V* = 2513.5(9) Å3, *Z* = 4, *ρ*calcd = 1.806 g cm-3, *μ*(Mo-*K*α) = 1.771 mm-1, *R*1(*Fo*) = 0.0727, (*wR*2(Fo^2) = 0.1677) with a goodness-of-fit on *F2* 1.034. Data were collected by *ω and ψ scans* on a Bruker APEXII diffractometer with graphite-monochromated MoK radiation (= 0.71073 Å). The structures were solved by direct methods and refined on F2 by the SHELX-97 program.

(**17**) (a) Aldridge, S.; Downs, A.J.; *The Group 13 Metals Aluminium, Gallium, Indium and Thallium,* , Ed.: John Wiley & Sons , 2011. (b) Rodríguez-Diéguez, A.; Salinas-Castillo, A.; Sironi, A.; Seco, J.M. and Colacio, E. *CrystEngComm*, **2010**, *12*, 1876–

1879. (c) Tan, B.; Xie, Z.-L.; Feng, M.-L.; Hu, B.; Wu, Z.-F. and Huang, X.-Y. *Dalton Trans.*, **2012**, *41*, 10576-10584.

([18]) (a) Gelb, L.D.; Gubbins, K.E. *Langmuir* **1999**, *15*, 305; (b) Düren, T.; Millange, F.; Férey,G.; Walton, K.S.; Snurr, R.Q. *J. Phys. Chem. C* **2007**, *111*, 5350-5357.

([19]) Calahorro, A.J.; López-Viseras, M.E.; Salinas-Castillo, A.; Fairen-Jimenez, D.; Colacio, E.; Cano, J.; Rodríguez-Diéguez, A. *Cryst.Eng.Comm*, **2012**, *14*, 6390-6393.

([20]) (a) Chen, B.; Ma, S.; Zapata, F.; Fronczek, F.R.; Lobkovsky, E.B.; Zhou, H.C. *Inorg. Chem*, **2007**, *46*, 1233-1236; (b) Xue, M.; Ma, S.; Jin, Z.; Schaffino, R.M.; Zhu, G.S.; Lobkovsky, E.B.; Qiu, S.L.; Chen, B.L. *Inorg. Chem*, **2008**, *47*, 6825-6828.

CAPÍTULO 10.

MODULAR STRUCTURE OF A MICROPOROUS MOF BASED ON CU_2 PADDLE-WHEELS WITH HIGH CO_2 SELECTIVITY

ARTICLE: *MODULAR STRUCTURE OF A MICROPOROUS MOF BASED ON Cu_2 PADDLE-WHEELS WITH HIGH CO_2 SELECTIVITY*

ABSTRACT

The synthesis of a new MOF with Cu_2 paddle-wheels connected to glutarate and 1,3-bis(4-pyridyl)propane) linkers has been explored. Experimental gas adsorption measurements reveal that the MOF is essentially non-porous to methane whereas it presents a Type III isotherm upon CO_2 adsorption, leading to high capacity and outstanding CO_2 selectivity.

1. INTRODUCTION

The use of porous adsorbents (*e.g.* zeolites and activated carbons) in industrial separation and purification processes plays an important role in the global economy.[1] Extensive research has been performed to develop selective adsorbents for applications such as the purification of hydrogen and natural gas, mainly composed of methane, as well as carbon capture.[2] These efforts towards the development of these selective materials have turned in the last years to metal-organic frameworks (MOFs) due to their structural diversity and functional properties.[3] MOFs are obtained by the self-assembly of metal clusters and organic linkers, resulting in tailored nanoporous host materials. The high internal surface areas and large pore volumes make MOFs promising candidates for gas adsorption and separation applications.

Many adsorption isotherms of small gas molecules on MOFs at room temperature show the most common Type I (*i.e.* Langmuir) shape. However, some MOFs exhibit unusual adsorption behaviours, such as the existence of steps during the adsorption process. The existence of steps could be explained either by the sequential filling of the different cavities or adsorption sites of the structure,[4]

especially at low temperature, or by the existence of flexible structures in the phenomena described as gate opening, breathing or swing effect (*e.g.* MIL-53 and ZIF-8).[5] In the latter flexible cases, the increase in pressure provokes structural changes that induce a modification in the pore shape and volume. On the other hand, unusual Type V (*i.e.* sigmoid) isotherms have been observed in the absence of structural changes during the adsorption of CO_2 and CH_4, as a result of relatively weak gas-MOF versus gas-gas interactions.[6]

The existence of isotherms with unusual shapes on MOFs, such as Type V, offers outstanding possibilities in the design of materials for gas storage and gas separation applications. When a gas is adsorbed, the adsorbent is regenerated by reducing the pressure. A good adsorbent for a "pressure-swing" process needs to have a high selectivity but also a high deliverable capacity, *i.e.* the difference between the amount adsorbed at the maximum adsorption pressure and the amount adsorbed at the regeneration pressure. An isotherm that is convex to the pressure axis but has a high capacity, such as Type III, has this feature. In order to obtain a material with high selectivity, we have recently explored the gas purification capabilities of a MOF constituted of 5-bromonicotinic acid linked to cobalt metal corners, demonstrating that it is possible to synthetize high selective materials by using classical ligands.[7] However, the narrow porosity of this MOF, which allows for molecular sieving of H_2/CH_4 mixtures, also implies low pore volumes and therefore low adsorption capacities. The design of a porous material with high pore volumes and molecular sieving behaviour with high selectivities remains an open issue.

In this work, we have designed the synthesis of a new MOF (**1**) with Cu_2 paddle-wheels connected to glutarate (glu) and 1,3-bis(4-pyridyl)propane (bpp) ligands. We believe that the conformational freedom of the glutarate ligand could promote the self-assembly of MOFs with novel topologies. Herein, we describe the synthesis,[8] crystal structure,[9] TG, high pressure X-ray experiments up to 4.5 GPa, gas adsorption properties and grand canonical Monte Carlo simulations of the MOF $[Cu_2(glu)_2(\mu\text{-bpp})]\cdot 2H_2O$ (**1**). This compound presents unexpected adsorption behaviour with Type I and Type III isotherms, for H_2 and CO_2, respectively, high CO_2/CH_4 selectivity and a high adsorption capacity.

2. EXPERIMENTAL

2.1. General.

All analytical reagents were purchased from commercial sources and used without further purification.

2.2. Preparation of $[Cu_2(glu)_2(\mu\text{-bpp})]\cdot 2H_2O$ (1).

The reaction in water solvent of the copper sulfate (0.25mmol, 0.0628 g), glutaric acid (0.25 mmol, 0.033 g), urea (0.872 mmol, 0.054 g) and 4,4'-trimethylene-dipyridine (0.25 mmol, 0.046 g) led to a blue solution, which kept at room temperature for one week gave rise to green crystals of complex **1**, which were filtered off and air-dried. Yield: 60%. Anal. Calc. for $C_{23}H_{26}Cu_2N_2O_8$: C, 47.18; H, 4.48; N, 4.78. Experimental: C, 47.05; H, 4.61; N, 4.83**.** FT-IR (KBr pellet): 3431 (brs), 2939 (m), 1611 (s), 1416 (s), 1313 (m), 1058 (w), 1019 (w), 817 (m), 643 (m) cm^{-1}.

2.3. Physical measurements

Elemental analyses were carried out at the "Centro de Instrumentación Científica" (University of Granada) on a Fisons-Carlo Erba analyser model EA 1108. The IR spectra on powdered samples were recorded with a ThermoNicolet IR200FTIR by using KBr pellets.

Microanalysis of C, H and N were performed in a Fisons Instruments EA-1008 analyser. The thermal behaviour of **1** was studied under an air flow in Shimadzu TGA-50 and Shimadzu DSC- 50 equipment, at heating rates of 20 °C min-1 and 10 °C min-1, respectively. IR spectra were recorded on a ThermoNicolet IR 200 spectrometer using KBr pellets. All this equipment is sited at the Centre of Scientific Instrumentation of the University of Granada.

2.4. Single-Crystal Structure Determination.

Suitable crystals of 1 were mounted on a glass fibre and used for data collection on a Bruker AXS APEX CCD area detector equipped with graphite monochromated Mo Kα radiation (λ = 0.71073 Å) by applying the ω-scan method. Lorentz-polarization and empirical absorption corrections were applied. The structure was solved by direct methods and refined with full-matrix least-squares calculations on F^2 using the program SHELXS97.[10] Anisotropic temperature factors were assigned to all atoms except for hydrogen atoms, which are riding their parent atoms with an isotropic temperature factor arbitrarily chosen as 1.2 times that of the respective parent. Attempts to identify the solvent molecules failed in compound 1. Instead, a new set of F^2 (hkl) values with the contribution from solvent molecules withdrawn was obtained by the SQUEEZE procedure implemented in PLATON-94.[11] Several crystals of 1 were measured and the structure was solved form the best data we were able to collect. Final R(F), wR(F^2) and goodness of fit agreement factors, details on the data collection and analysis can be found in crystal data. Selected bond lengths and angles are given in Tables 1

2.5. Gas Adsorption Isotherms.

Volumetric N_2 gas adsorption isotherms were undertaken using a Micromeritics Instrument Corporation (Norcross, Georgia, USA) ASAP 2020 system. Approximately 300-500 mg of the corresponding solid product was transferred to a preweighed sample tube and evacuated under dynamic vacuum at 150 °C on the gas adsorption apparatus until the outgas rate was <5 μmHg. The sample tube was reweighed to obtain a consistent mass for the degassed modified product. High-pressure adsorption isotherms of H_2 at 77 K and CH_4 and CO_2 at 273 K were determined using a bench-scale volumetric adsorption instrument equipped with two Baratron absolute pressure transducers (MKS type 627B). Their pressure range span from 0 to 1.33 bar and from 0 to 33.33 bar, respectively. The reading accuracy was 0.05% of the usable measurement range. Prior to all the measurements, samples were degassed at 425 K for 12 h. All gases used were of 99.999% purity.

Helium was used for the dead volume determination.

2.6. Gas Adsorption Simulations and Computational Structural Characterization

The adsorption of CO_2 was investigated using grand canonical Monte Carlo (GCMC) simulations, performed with the in-house multi-purpose code RASPA.[12] We used a rigid atomistic model for **1**, in which the framework atoms were kept fixed at their crystallographic positions. Solid-fluid and fluid-fluid interactions were calculated using a Lennard-Jones (LJ) + Coulomb potential. LJ parameters for the framework atoms were taken from the Universal Force Field (UFF),[13] the CO_2, LJ parameters from the TraPPE force field.[14] Lorentz-Berthelot mixing rules were used for all cross terms, and LJ interactions beyond 12 Å were neglected. Coulombic interactions were modelled by placing partial charges on the framework atoms. The partial charges were calculated using an extended charge equilibration method,[15] and the long-range electrostatic interactions were calculated using the Ewald summation method. $6{\cdot}10^4$ Monte Carlo equilibration cycles were performed plus $4{\cdot}10^4$ production cycles to calculate the ensemble averages. In one cycle, an average of *N* moves were performed, where *N* is the number of molecules in the system (which fluctuates in GCMC). Monte Carlo moves used with equal probability were translation, rotation, insertion, deletion, and random reinsertion of an existing molecule at a new position. To calculate the gas-phase fugacity, we used the Peng-Robinson (PR) equation of state (EOS)[16].

Table 2. *Lennard-Jones parameters for framework atoms and the gas molecules.*

	σ [Å]	**ε/k [K]**	**q [e]**
C	3.431	52.838	
N	3.261	34.722	
O	3.119	30.192	
H	2.571	22.142	
Cu	3.114	62.397	
C_CO_2	2.800	27.000	+0.70
O_CO_2	3.050	79.000	-0.35

The pore volume, used to compute excess adsorption from the simulated absolute adsorption, was obtained using a Widom particle insertion method, by probing the structure with a helium molecule at room temperature, recording a large number of random points not overlapping the van der Waals volume of the framework.[17] The pore size distributions was calculated using the method of Gelb and Gubbins,[18] where the largest sphere that can fit in a random point within a structure without overlapping the van der Waals surface of the framework is recorded for a large number of random points.

2.7. High Pressure X-Ray Diffraction

High pressure single crystal study was undertaken using a custom made Diamond Anvil Cell equipped with 0.5 mm culets and a ~40° opening. A small crystal of the sample was loaded in the pre-pressed and drilled steel gasket along with a methanol-ethanol mixture (4:1) and a small ruby sphere for pressure calibration. Data were collected using a single phi scan in the Extreme conditions beamline at Diamond Light Source, using a focused beam of 40 keV as defined by a 20 μm pinhole. Short acquisitions were performed to avoid large radiation damage, anyway visible at the end of the experiment in the form of a brown spot in the center of the crystal. Data were collected using an Agilent Atlas CCD calibrated with a NIST ruby

sphere and integrated using the Crysalis package and its high pressure dedicated abilities[19]. Diamond overlapping peaks were masked out of the integration. Despite attempts no lower or higher symmetry were identified for the given datasets up to 4.5 GPa. The known structure was used for refinement with SHELXL97.[i] Due to the small amount of data and their low intrinsic quality aromatic rings were constrained using the AFIX66 routine and other C-C and C-O distances restrained to 1.54 and 1.25 Å respectively. The squeeze routine was applied to correct the intensities from the disorder solvent.

3. RESULTS AND DISCUSSION

3.1. Structure and crystallographic results

Figure 1 shows the single-crystal XRD structure of **1**, solved in the space group *C2/c*. Table S1 lists selected bond distances and angles. The copper metal centre of the paddle-wheel adopts a slightly distorted square pyramidal coordination geometry with the bond angles only deviating slightly from 90º and 180º. The Cu(II) atom is bonded to four oxygen atoms of the bridging carboxylate groups pertaining to four different glutarate ligands (Cu–O = 1.907(6)–2.004(6) Å) in the basal plane. The Cu(II) atom is also bonded to one bpp ligand (Cu–N = 2.162(6) Å) in the axial position to complete the distorted square-pyramidal coordination geometry. In the structure, Cu_2 units are bridged by glutarate dianions to form a distorted 2D square grid, with Cu_2 units linked along the [011] and [01-1] directions. These 2D square grids are further pillared by bpp ligands extending from the axial sites of the Cu_2 paddle wheels along the [102] direction to form the MOF.

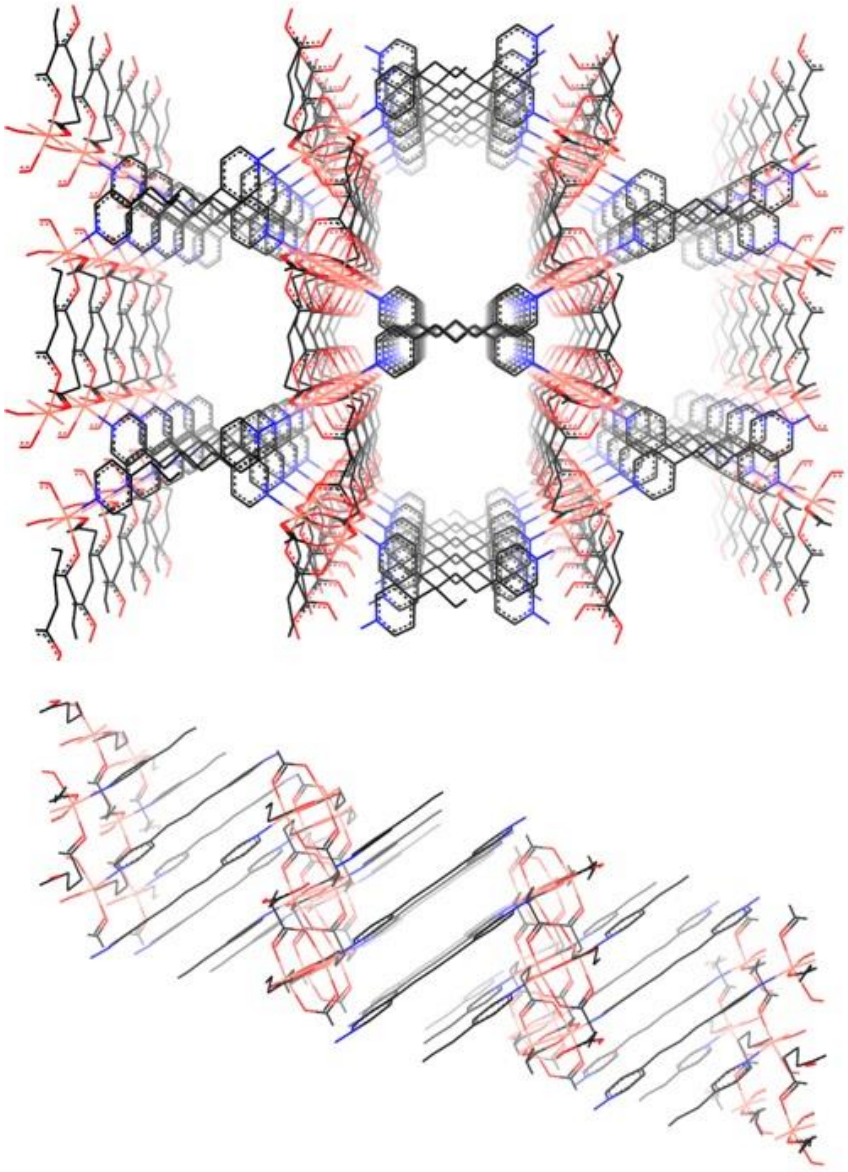

Figure 1. *(top) Perspective view through the c axis of the channels in the three-dimensional network of* ***1*** *and, (bottom) through the b axis of the bpp pillars linking different sheets. Color code N = blue, O = red, C = black and Cu = orange. Hydrogen atoms have been omitted for clarity.*

Table 1. *Selected Distances (Å) and Bond Angles (°) for compound 1*

N1A C2A 1.331(7)	C2A N1A C6A 116.4(4)	O8B C7B C6B 118.1(4)
N1A C6A 1.340(6)	C2A N1A Cu1 120.8(3)	C3B O1B Cu1 124.9(3)
N1A Cu1 2.161(4)	C6A N1A Cu1 121.8(3)	C3B O2B Cu1 123.3(3)
C2A C3A 1.374(8)	N1A C2A C3A 123.8(5)	C7B O8B Cu1 120.8(3)
C3A C4A 1.383(8)	C2A C3A C4A 120.3(5)	C7B O9B Cu1 126.0(3)
C4A C5A 1.395(7)	C3A C4A C5A 116.2(5)	O8B Cu1 O1B 91.09(17)
C4A C7A 1.512(7)	C3A C4A C7A 124.7(5)	O8B Cu1 O2B 87.62(16)
C5A C6A 1.382(7)	C5A C4A C7A 119.0(5)	O1B Cu1 O2B 168.17(14)
C7A C8A 1.519(6)	C6A C5A C4A 119.8(5)	O8B Cu1 O9B 167.41(14)
C8A C7A 1.519(6)	N1A C6A C5A 123.3(5)	O1B Cu1 O9B 89.27(16)
C3B O1B 1.257(6)	C4A C7A C8A 115.7(5)	O2B Cu1 O9B 89.46(15)
C3B O2B 1.269(6)	C7A C8A C7A 109.9(6)	O8B Cu1 N1A 102.41(15)
C3B C4B 1.482(7)	O1B C3B O2B 123.6(4)	O1B Cu1 N1A 96.39(14)
C4B C5B 1.515(7)	O1B C3B C4B 119.6(4)	O2B Cu1 N1A 95.38(14)
C5B C6B 1.534(6)	O2B C3B C4B 116.8(5)	O9B Cu1 N1A 90.05(15)
C6B C7B 1.506(6)	C3B C4B C5B 116.3(4)	O8B Cu1 Cu1 86.27(11)
C7B O9B 1.240(6)	C4B C5B C6B 111.9(4)	O1B Cu1 Cu1 83.64(10)
C7B O8B 1.246(6)	C7B C6B C5B 112.9(4)	O2B Cu1 Cu1 84.54(10)
C7B C6B 1.506(6)	O9B C7B O8B 125.0(5)	O9B Cu1 Cu1 81.26(11)
O1B Cu1 1.976(3)	O9B C7B C6B 117.0(4)	N1A Cu1 Cu1 171.31(11)
O2B C3B 1.269(6)		
O2B Cu1 1.981(3)		
O8B Cu1 1.970(4)		
O9B C7B 1.240(6)		
O9B Cu1 1.985(4)		
Cu1 Cu1 2.6332(12)		

With a similar approach, Hwang *et al.* have recently published a MOF with the same metal ions and ligands but different solvent $[\{Cu_2(glu)_2(\mu\text{-bpp})\}\cdot(C_3H_6O)]_n$ (**2**).[20] In contrast to **1**, this structure presents a very different arrangement of the bpp ligands based in the tilt of the pyridyl fragments respect to the propane chain that interconnects them (Figure 2 and Figure 3). The dihedral angles between the pyridyl rings and the propane chain are 5.99° and 82.83º for **1** and **2**, respectively. The co-planarity showed in **1** causes the stacking of the bpp ligands in an "accordion" fashion along the *c* axis (Figure 1, bottom), an aspect that does not take place in **2**. We believe that this characteristic is fundamental for the behaviour of **1** in terms of gas adsorption.

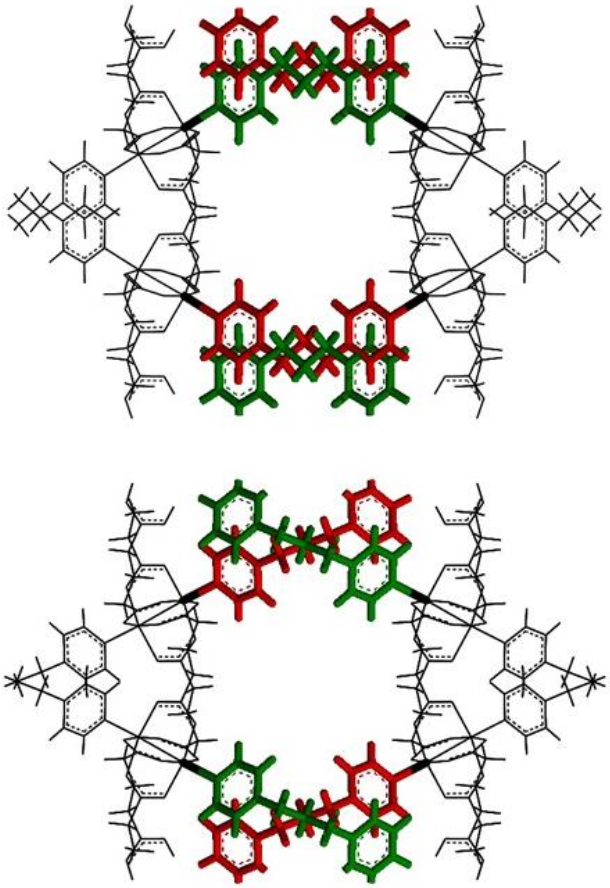

***Figure 2**. Differences between **1** (top) and **2** (bottom). Note the distinctive tilt in the pyridyl ligands respect to the propane chains that connect them. The different molecular fragments have been indicated in red and green for clarity.*

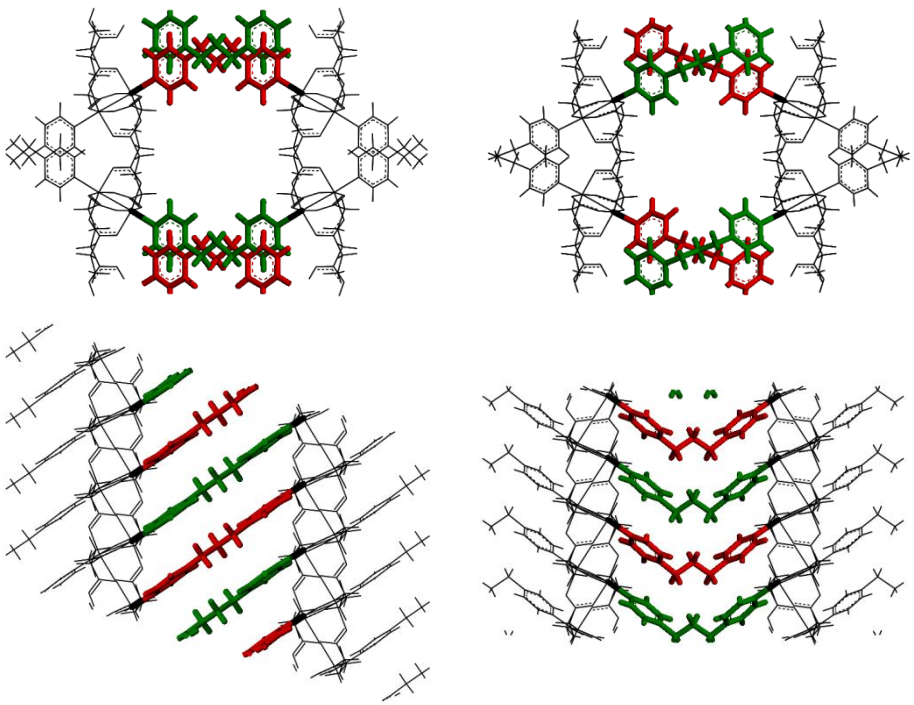

Figure 3. *Comparison between the MOF structures (left)* ***1*** *and (right)* ***2***[21]*, along the (top) c and (bottom) b axis. The different molecular fragments have been indicated in red and green for clarity. Note the different arrangement of the bpp ligands based in the tilt of the pyridyl fragments respect to the propane chain that interconnects them.*

3.2. Adsorption Properties

We first analysed the porosity of **1** geometrically. Figure 4 shows the comparison of the pore size distribution (PSD) of **1** and **2**. Both structures present an open-porosity centred at *ca.* 6 Å, broad enough to be, in principle, accessible for gas adsorption. However, when running the experimental gas adsorption isotherms on **1**, we found that it was essentially non-porous to N_2 at 1 bar and 77 K. On the other hand, Figure 5 shows how CO_2 and H_2 can access into the porosity when increasing the pressure up to 30 bar at 273 K and 77 K, respectively, whereas CH_4 (273 K) access remains impeded. More interesting is the shape of the isotherms: while the H_2 isotherm can be classified as a Type I, the CO_2 isotherm presents a Type III shape,

and almost no adsorption up to 10 bar. In the studied conditions, **1** showed a maximum uptake of 2.24, 15.75 and 0.25 wt. % for H_2, CO_2 and CH_4, respectively. High H_2 and CH_4 selectivity in MOFs has been reported previously.[22]

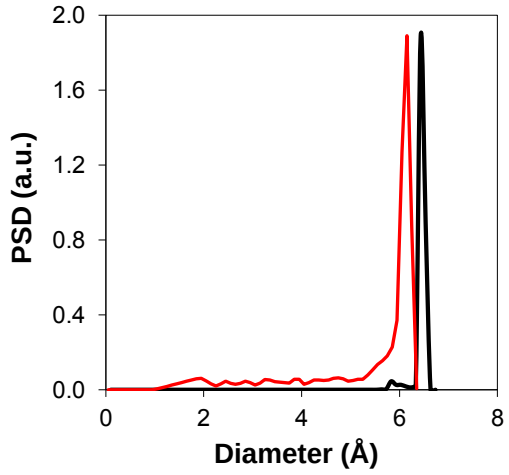

Figure 4. *Pore size distribution (PSD) of* ***1****, red line, and* ***2****, black line.*

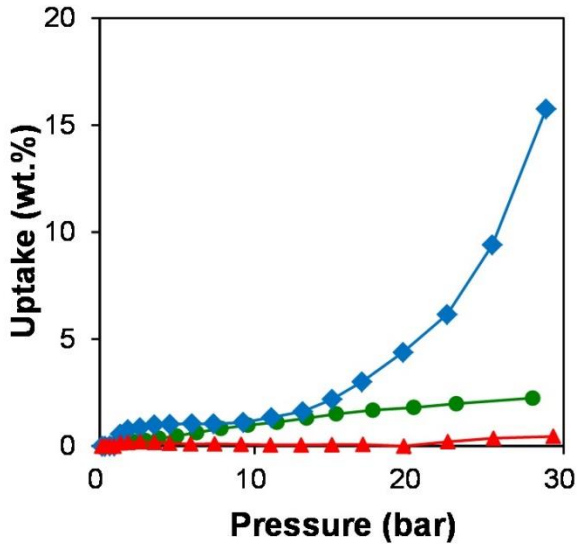

Figure 5. *Adsorption isotherms on* ***1*** *obtained at 77 K (H_2, green circles) and 273 K (CO_2, blue diamonds; CH_4, red triangles).*

However, and to the best of our knowledge, this is the first time that a microporous material, including not only MOFs but also zeolites and activated carbons, shows this behaviour. The existence of Type III isotherms generally implies a low interaction between the adsorbate (*i.e.* the gas molecules) and the adsorbent (*i.e.* the MOF).[23,6a] This could suggest that the interaction between **1** and CO_2 (Type III) is much lower compared to that of the H_2 (Type I). This idea is counterintuitive since the CO_2 molecules generally present higher interaction with an adsorbent due to the higher molecular weight and the presence of a strong quadrupole moment.

A second possibility to this behaviour would be the existence of a molecular sieve effect, where the differences between the size of the H_2, CO_2 and CH_4 molecules play an important role in the diffusion of the gases through the porosity. In this case, a small molecule such as H_2 may diffuse through a narrow porosity, whereas CH_4 and CO_2 are hindered. Only high pressures allow enough potential energy to either overdue the kinetic barrier in the diffusion, or to provoke a gate opening or breathing effect and therefore a structural change. This explanation is, however, not compatible with the relatively broad 6 Å porosity found in this material. Moreover, the use of gran canonical Monte Carlo (GCMC) simulations for CO_2 adsorption on a crystallographic rigid model, shown in Figure 6, confirms the goodness of the experimental maximum capacity value, but not the shape of the isotherm. Since GCMC simulations are in thermodynamic equilibrium, the existence of experimental kinetic barriers due to the presence of narrow porosity will not be detected using this technique. In a similar way, Feldblyum *et al.* were able to explain the disconnection between porous performance, as predicted by crystallography, and porous texture measured by gas adsorption.[24] Using positron annihilation lifetime spectroscopy, they explained these differences due to the presence of densified layers at the surface of the material, preventing the entry of small molecular species into the bulk porosity.

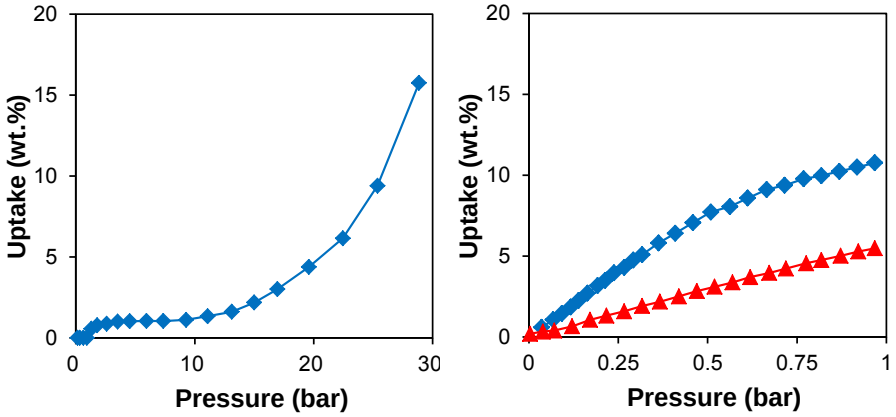

Figure 6. *Comparison between the experimental CO_2 adsorption isotherms on (left)* ***1****, and (right)* ***2****. Blue diamonds, 273 K; red triangles, 298 K. The adsorption isotherm for* ***1*** *at 273 K presents a Type III shape and no adsorption at 1 bar, whereas* ***2*** *presents a Type I shape.*

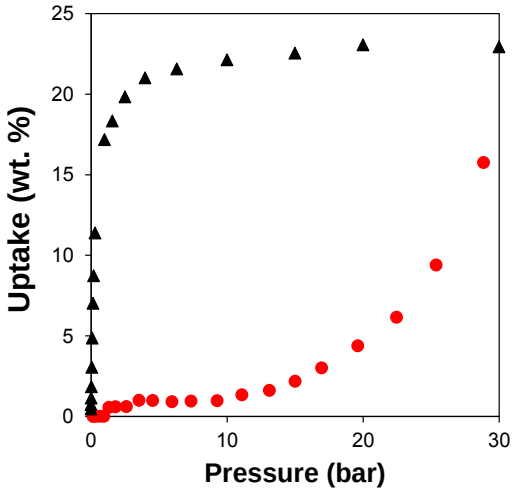

Figure 7. *CO_2 experimental, black triangles, and simulated, red circles, adsorption isotherms on* ***1*** *273 K. The simulated isotherm is able to provide a good estimation of the CO_2 capacity of the material. However, the simulated data overpredicts the experimental amount adsorbed at lower pressures.*

To analyse why MOFs **1** and **2** present a different behaviour regarding CO_2 adsorption, we studied the most flexible modes of the framework using a high pressure X-Ray diffraction study up to 4.5 GPa. Despite the possible conformational rearrangements, the bpp ligand in **1** remains stiff and largely unchanged throughout compression, while the glutarate-Cu moiety experiences a small but progressive distortion. The rearrangement of the distorted glutarate-Cu plane allows the bpp pillars to bend rigidly with respect to it, closing the 'accordion' and bringing different planes significantly closer, by shifting them laterally with respect to each other. As symmetry implies this is completely mirrored by a change in the beta angle. While this complex mechanism seems to be largely due to the flexibility of the Cu-glutarate paddle-wheel, in **2** the difference in the bpp conformation inhibits the distorted 2D layers from shifting with respect to each other and no flexibility can therefore be observed.

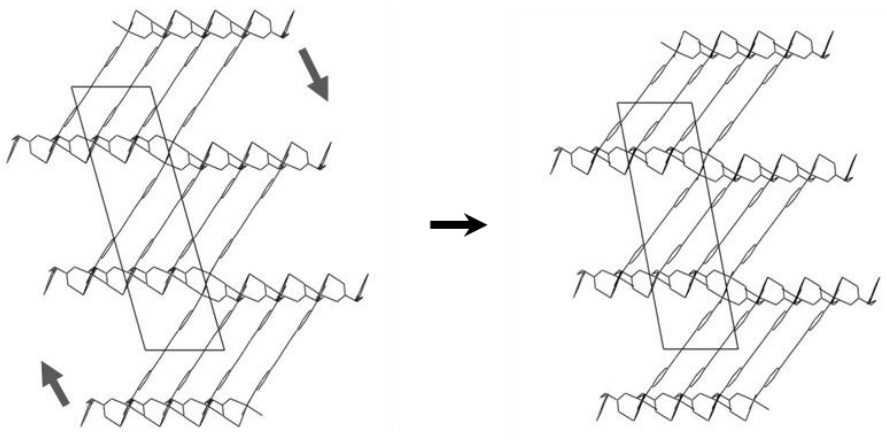

Figure 7. *The ambient pressure structure of **1** (left) with arrows indicating the deformation modes. On the right, the resulting structure at 4.5 GPa.*

Further experimental work using *in situ* XRD to confirm the existence or not of structural changes during gas adsorption or the existence of densified surface layers or structural defects preventing the access to the porosity is in progress, with the aim of studying the mechanism of action of this metal-organic framework.

5. REFERENCES

[1].- (a) B. Chen, S. Ma, F. Zapata, F.R. Fronczek, E.B. Lobkovsky and H.-C. Zhou, *Inorg.Chem*., 2007, **46**, 1233; (b) H.B.T. Jeazet, C. Staudt and C. Janiak, *Chem.Commun*, 2012, **48**, 2140; (c) H.Z.Chen and T.-S. Chung, *Int.J.HydrogenEnerg*, 2012, **37**, 6001.

[2].- J. Shang, G. Li, R. Singh, Q. Gu, K.M. Nairn, T.J. Bastow, N. Medhekar, C.M. Doherty, A.J. Hill, J.Z. Liu and P.A. Webley, *J.Am.Chem.Soc,* 2012, **134**, 19246.

[3].- H.-C. Zhou, J.R. Long and O.M. Yaghi, *Chem. Rev*. 2012, **112**, 673.

[4].- J. Getzschmann, I. Senkovska, D. Wallacher, M. Tovar, D. Fairen-Jimenez, T. Düren, J.M. van Baten, R. Krishna and S. Kaskel, *Micropor.Mesopor.Mat*, 2010, **136**, 50.

[5].- (a) K. Uemura, R. Matsuda and S. Kitagawa, *J. Solid State Chem*. 2005, **178**, 2420; (b) N.A. Ramsahye, G. Maurin, S. Bourrelly, P.L. Llewellyn, T. Loiseau, C. Serre and G. Ferey, *Chem.Commun*. 2007, 3261; (c) D. Fairen-Jimenez, S.A. Moggach, M.T. Wharmby, P.A. Wright, S. Parsons and T.J. Düren, *J.Am.Chem.Soc*. 2011, **133**, 8900.

[6].- (a) D. Fairen-Jimenez, N.A. Seaton and T. Düren, *Langmuir,* 2010, **26**, 14694; (b) A.R. Millward and O.M. Yaghi,. *J. Am. Chem. Soc*. 2005, **127**, 17998.

[7].- A.J. Calahorro, M.E. López-Viseras, A. Salinas-Castillo, D. Fairen-Jimenez, E. Colacio, J. Cano and A. Rodríguez-Diéguez*, Cryst.Eng.Comm*, 2012, **14**, 6390.

[8].- Synthesis of $[Cu_2(glu)_2(\mu\text{-bpp})]\cdot 2H_2O$ (**1**). The reaction in water solvent of the copper sulfate (0.25mmol, 0.0628 g), glutaric acid (0.25 mmol, 0.033 g), urea (0.872 mmol, 0.054 g) and 1,3-bis(4-pyridyl)propane (0.25 mmol, 0.046 g) led to a blue solution, which kept at room temperature for one week gave rise to green crystals of complex **1**, which were filtered off and air-dried. Yield: 60%. Anal. Calc. for $C_{23}H_{26}Cu_2N_2O_8$: C, 47.18; H, 4.48; N, 4.78. Experimental: C, 47.05; H, 4.61; N, 4.83. FT-IR (KBr pellet): 3431 (brs), 2939 (m), 1611 (s), 1416 (s), 1313 (m), 1058 (w), 1019 (w), 817 (m), 643 (m) cm^{-1}.

[9].- Crystal data: $C_{23}H_{26}Cu_2N_2O_8$, *fw* = 585.54 g mol^{-1}; monoclinic, *C2/c*, *a* = 28.265(5), *b* = 13.127(5), *c* = 8.729(5), *β* = 106.779(5), *V* = 3101(2) $Å^3$; *Z* = 4; T = 293 K; ρ_{calc} = 1.254 g cm^{-3}; *F*(000) = 1200; μ(Mo-Kα) = 1.411 cm^{-1}. Data collected on a Bruker Axs APEX automated diffractometer at RT, $R1(F_o)$ = 0.0326 ($wR2(F_o^2)$ = 0.0752) for 17018 unique reflections (R_{int} = 0.0865) with a goodness-of-fit on F^2 1.048. For both structures, data were collected by ωθv/2h scans ($2\theta_{max}$ = 56º) on a Bruker SMART

CCD diffractometer with graphite-monochromated MoKα radiation (λ = 0.71073). The structures were solved by direct methods and refined on F2 by the SHELX-97 program.11 CCDC xxxxxx. See http://dx.doi.org/10.1039/xxxxxxx for crystallographic data in CIF or other electronic format.

[10].- G. M. Sheldrick, *SHELX97*, University of Göttingen, Göttingen, Germany, 1997.

[11].- A. L. Spek, *PLATON-94 (V-101094), A multipurpose Crystallographic Tool*, University of Utrecht, The Netherlands, 1994.

[12].- (a) Dubbeldam, D.; Calero, S.; Ellis, D. E.; Snurr, R. Q. RASPA 1.0; Northwestern University: Evanston, IL, 2008; (b) D. Frenkel and B. Smit, *Understanding Molecular Simulations: From Algorithms to Applications*, 2nd ed., Academic Press, San Diego, 2002.

[13].- A. K. Rappé, C. J. Casewit, K. S. Colwell, W. A. G. III and W. M. Skiff, *J. Am. Chem. Soc.*, 1992, *114*, 10024-10035

[14].- M. G. Martin and J. I. Siepmann, *J. Phys. Chem. B*, 1998, 102, 2569

[15].- C.E. Wilmer, K.C. Kim and R.Q. Snurr. *J. Phys. Chem. Lett.*, 2012, 3, pp 2506–2511.

[16].- Reid, R. C.; Prausnitz, J. M.; Poling, B. E. The Properties of Gases and Liquids, 4th ed.; McGraw-Hill: New York, 1987.

[17].- (a) A. Leach, *Molecular modelling : principles and applications*, Pearson Prentice Hall, 2001.; (b) A. L. Myers and P. A. Monson, *Langmuir*, 2002, *18*, 10261.

[18].- L. D. Gelb and K. E. Gubbins, *Langmuir*, 1998, *15*, 305-308.

[19].- Oxford Diffraction (2006). Oxford Diffraction Ltd., Abingdon, England.

[20].- I.H. Hwang, J.M. Bae, W.-S. Kim, Y.D. Jo, C. Kim, Y. Kim, S.-J. Kim and S. Huh, *Dalton Trans.*, 2012, **41**, 12759.

[21].- I.H. Hwang, J.M. Bae, W.-S. Kim, Y.D. Jo, C. Kim, Y. Kim, S.-J. Kim and S. Huh, *Dalton Trans.*, 2012, *41*, 12759.

[22].- (a) B. Chen, S. Ma, F. Zapata, F. R. Fronczek, E. B. Lobkovsky and H.-C. Zhou, *Inorg. Chem.*, 2007, **46**, 1233; (b) M. Xue, S. Ma, Z. Jin, R.M. Schaffino, G. S. Zhu, E.B. Lobkovsky, S.L. Qiu andB. L. Chen, *Inorg. Chem.*, 2008, **47**, 6825.

[23].- J. Rouquerol, F. Rouquerol, K.S.W. Sing, *Adsorption by Powders and Porous Solids*, Academic Press: San Diego, CA, 1999.

[24].- J. I. Feldblyum, M. Liu, D. W. Gidley and A.J. Matzger. *J. Am. Chem. Soc*. 2011, **133**, 18257.

CONCLUSIONES GENERALES

CONCLUSIONES

Esta Tesis Doctoral se marcó como objetivo general diseñar, sintetizar y estudiar las propiedades de nuevos Polímeros de Coordinación Multidimensionales (o también llamados Metal-Organic Frameworks). En este trabajo de investigación se ha presentado un total de 17 compuestos con estructuras cristalinas fascinantes y propiedades muy interesantes en los campos de magnetismo, adsorción y luminiscencia. Para sintetizar estos sistemas se ha empleado fundamentalmente reactores solvotermales y, por otro lado, métodos convencionales de síntesis. Básicamente, estos materiales están formados por iones metálicos de transición y ligandos orgánicos empleando entre éstos, fundamentalmente, ligandos nitrogenados con grupos carboxilato.

Las conclusiones generales a las que se han llegado son las que a continuación se detallan:

1. Los métodos solvotermales siguen siendo una herramienta excelente para el diseño de nuevas redes multidimensionales con diferentes propiedades, ya que empleando esta técnica se han conseguido sintetizar 16 compuestos de los 17 presentados en esta Tesis Doctoral.

2. Utilizando el ligando 2-aminopirimidina se ha obtenido un polímero bidimensional de cadmio de fórmula $[CdCl_2(PymNH_2)]$ que presenta luminiscencia en estado sólido, siendo éste uno de los pocos compuestos existentes con este ligando que muestra fosforescencia con dos tiempos de vida media, τ_1 = 0.12 ms y τ_2 = 2.89 ms.

3. El uso de métodos solvotermales puede generar estructuras fascinants y novedosas diferentes a las sintetizadas hasta el momento por rutas convencionales. Por ejemplo, partiendo de una sal de lantano junto con el ligando 2-cianopirimidina se logró la oxidación y descomposición del mismo para obtener el ligando aniónico oxalato, generando *in situ* en el seno de la reacción hidrotermal el compuesto de lantano $[La_2(ox)_3(H_2ox)(H_2O)_2](H_2O)_8$, el cual es una red tridimensional con interesantes canales en las tres direcciones del espacio, aunque no presenta capacidad experimental de adsorción. Sin embargo, sí que presenta luminiscencia en estado sólido a temperatura ambiente, siendo uno de los pocos compuestos con este ligando que posee propiedades luminiscentes.

4. La síntesis *in situ* de ligandos de tipo tetrazol mediante la cicloadición [2+3] de grupos carbonitrilo utilizando métodos solvotermales es una excelente herramienta para la construcción de nuevos materiales poliméricos multidimensionales debido a que, en esta Tesis Doctoral, se han conseguido sintetizar un total de 7 compuestos de los 17 presentados mediante esta ruta sintética.

5. Se ha logrado sintetizar *in situ* en el seno de una reacción hidrotermal un nuevo ligando, 4'-tetrazolato-4-bifenil carboxilato, al llevar a cabo la síntesis del derivado cianurado (ácido 4'-ciano-4-bifenil carboxílico) con cloruro de cadmio y azida sódica, generando un nuevo compuesto de coordinación de fórmula $[Cd(TBPC)(H_2O)]_n$. Se han aislado cristales de este material y se ha determinado su estructura cristalina resultando ser un MOF tridimensional de cadmio muy empaquetado debido a fuertes interacciones de *stacking* entre los anillos aromáticos del ligando sintetizado, motivo por el que este material no posee canales relativamente grandes y, por lo tanto, no presenta porosidad aunque sí muestra luminiscencia en estado sólido debido la aromaticidad extendida del linker en cuestión.

6. Se han obtenido dos novedosos MOFs tridimensionales de zinc de fórmula $Zn(1,3\text{-tzbaa})]_n$ y $[Zn(1,4\text{-tzbaa})]_n$ utilizando para ello dos derivados cianurados y recurriendo a la reacción de Demko mencionada con anterioridad, el ácido 3-cianofenil acético y ácido 4-cianofenil acético, sintetizados ambos *in situ* en el seno de la reacción. Estos compuestos de zinc muestran interesantes propiedades luminiscentes debido, a la conjugación del grupo tetrazolato con el grupo fenilo, con unos valores de máximos de emisión de 449 y 479 nm, respectivamente, tras ser excitados con una longitud de onda de 350 nm.

7. Basándose en el ligando 4-piridintetrazolato (4-ptz) se han conseguido sintetizar y caracterizar tres nuevos materiales tridimensionales de cadmio, de fórmula $[Cd_2(ptz)(squarate)(OH)(H_2O)_2]_n$, $\{[Cd_2(ptz)(4\text{-carboxypyridine})(OH)_2]\cdot(H_2O)_2\}_n$ y $\{[Cd_5(ptz)_2(terephtalate)_4(H_2O)_2](H_2O)_2\cdot(CH_3OH)_4\}_n$. Estos materiales muestran propiedades luminiscentes y tras realizar estudios teóricos de adsorción se corroboró que no son materiales porosos.

8. En condiciones hidrotermales, se han obtenido tres estructuras tridimensionales cristalinas de fórmula $\{[Cd_4(TZI)_2(OH)_2\ (H_2O)_4](H_2O)_6\}_n$, $\{[Zn_2(TZI)(OH)(H_2O)_2](H_2O)\}_n$ y $\{[Co_8(TZI)_3(OH)_5((N_3)_2(H_2O)_8](H_2O)_8\}_n$, en los

que el ligando TZI (ácido 5-(1H-tetrazol-5-il)isoftálico) muestra su potencial como *building block* con una gran capacidad de coordinación a diferentes centros metálicos, coordinando desde tres hasta ocho átomos metálicos a través de los dos grupos carboxilato y el anillo de tetrazolatoexistentes en este linker. Se han estudiados las propiedades físicas de estos materiales obtenidos corroborando que los compuestos de cadmio y zinc presentan luminiscencia en estado sólido a temperatura ambiente debido a interacciones de tipo π-π* entre los anillos aromáticos. Además, para el compuesto de cobalto se estudiaron experimentalmente sus propiedades magnéticas observando un comportamiento global antiferromagnético con un valor de J=-3.8 cm^{-1}. En este caso, no se pudieron realizar cálculos teóricos para determinar el valor de la constante de acoplamiento y poder corroborar los datos experimentales obtenidos debido a la gran anisotropía de los iones de cobalto(II) octaédricos.

9. A partir del ligando ácido 5-bromonicotínico, y empleando métodos solvotermales, se han obtenido dos nuevas estructuras tridimensionales cristalinas de fórmula $[Cd(5\text{-}BrNic)_2]_n$ y $[Co(5\text{-}BrNic)_2(H_2O)]_n$, en las que dicho ligando se coordina a los diferentes centros metálicos empleando cuatro nuevos modos de coordinación a través del grupo carboxilato y del átomo de nitrógeno del anillo piridínico. Además, estos compuestos muestran luminiscencia en estado sólido asignadas a transiciones π-π* existentes entre los anillos aromáticos.

10. Para el compuesto $[Co(5\text{-}BrNic)_2(H_2O)]_n$ se realizaron medidas de susceptibilidad magnética que mostraron un ordenamiento antiferromagnético débil con un valor de constante de acoplamiento de -4.1 cm^{-1}. Para ese compuesto, además, se realizaron simulaciones moleculares de tipo Monte Carlo en las que se determinó su distribución de tamaño de poro (3.75 Å), así como las correspondientes isotermas de adsorción en las que se comprobó que este MOF es capaz de adsorber H_2 de forma selectiva frente a CO_2, hecho que se corroboró con las medidas experimentales en las que se obtenía una capacidad de adsorción de 1.78 mmol/g. Por lo tanto, este novedoso MOF de cobalto puede ser empleado como un potencial purificador de H_2.

11. Se ha conseguido sintetizar un nuevo ligando orgánico con un esqueleto dibenceno-tetrazínico, (ácido 3,3'-(1,2,4,5-tetrazina-3,6-diil)dibenzoico), caracterizado mediante ^{1}H-RMN, ^{13}C-RMN, Análisis Elemental, Espectroscopía de Infrarrojo y Difracción de Rayos-X de monocristal. A este

nuevo ligando se le realizaron pruebas biológicas para comprobar su citotoxicidad mediante la exposición a células HEK293 a distintas concentraciones y periodos de incubacióncon la intención de comprobar su posible uso en la construcción de materiales que se puedan utilizar para la liberación controlada de fármacos con aplicaciones biomédicas.

12. Asimismo, con este ligando se han conseguido obtener los primeros polímeros de coordinación, $[Zn(dbtz)(H_2O)]_n$, y $\{[La_2(dbtz)_3(H_2O)_2](H_2O)_6\}_n$, que consisten en estructuras bi- y tridimensionales, respectivamente, que poseen interesantes propiedades luminiscentes debido a la aromaticidad extendida que presenta el ligando tetrazínico, con unos máximos de emisión de 461 y 498 nm, respectivamente, tras ser excitados a 350 nm.

13. Empleando rutas sintéticas convencionales, se ha conseguido sintetizar un nuevo e interesante material que consiste en un MOF tridimensional de cobre con forma de panal de abeja de fórmula $[Cu_2(glu)_2(\mu\text{-bpp})]\cdot 2H_2O$ formado por dímeros de cobre se enlazados a través de los ligandos ácido glutárico y 1,3-bis(4-piridil)propano. Este MOF presenta una única y relevante diferencia estructural respecto a otro muy similar y recientemente publicado de fórmula $[\{Cu_2(glu)_2(\mu\text{-bpp})\}\cdot(C_3H_6O)]_n$. Esta diferencia radica en el diferente empaquetamiento del ligando piridínico debido al distinto ángulo diedro existente entre los anillos de piridina en ambos compuestos. Mientras que en material sintetizado en esta Tesis el ángulo tiene un valor de 5.99°, para el otro compuesto es de 82.83°. Esta diferencia es la causante de un empaquetamiento con forma de acordeón en la red cristalina, modificando notablemente las propiedades de adsorción. El nuevo material sintetizado en esta Tesis Doctoral presenta una adsorción selectiva de CO_2 frente a H_2 y CH_4, con unas capacidades de adsorción de 15.75, 2.24 y 0.25 wt.%, respectivamente. Además, cabe resaltar que la isoterma de adsorción de CO_2 es de tipo III, siendo éste el primer ejemplo de material microporoso que muestra este tipo de isoterma propia de materiales mesoporosos, por lo que la novedad de este material queda más que irrefutablemente justificada.


UNIVERSITATIS·GRANATENSIS
CAROLVS·RO·IMP·SEMPER·AVG·HISPANN·REX·FUNDATOR

ANEXOS

Polyhedron 30 (2011) 1295–1298

Contents lists available at ScienceDirect

Polyhedron

journal homepage: www.elsevier.com/locate/poly

A new 2D cadmium chloride network with 2-aminopyrimidine displaying long lifetime photoluminescence emission

Alfonso Salinas-Castillo [a], A.J. Calahorro [b], Duane Choquesillo-Lazarte [c], José M. Seco [d], Antonio Rodríguez-Diéguez [b,*]

[a] Instituto de Biología Molecular y Celular, Universidad Miguel Hernández, 03202 Elche, Alicante, Spain
[b] Departamento de Química Inorgánica, Universidad de Granada, 18071 Granada, Spain
[c] Laboratorio de Estudios Cristalográficos, IACT-CSIC, E-18100 Granada, Spain
[d] Departamento de Química Aplicada, Facultad de Química de San Sebastián, Universidad del País Vasco, Paseo Manuel Lardizábal, 20008 San Sebastián, Spain

ARTICLE INFO

Article history:
Received 25 July 2010
Accepted 9 February 2011
Available online 19 February 2011

Keywords:
Hydrothermal
Polymer
Phosphorescence

ABSTRACT

The hydrothermal reaction of $CdCl_2$ with 2-aminopyrimidine in water yields a 2D metal–organic coordination framework $[CdCl_2(PymNH_2)]$ (**1**) ($PymNH_2$ = 2-aminopyrimidine). This compound consists of $Cd_2(\mu\text{-}Cl)_2$ corner-sharing chains bridged by $PymNH_2$ through the endocyclic ring nitrogen atoms. Interestingly, this polymer exhibits long lifetime photoluminescence emission at room temperature in the solid state with long lifetimes decay.

1. Introduction

In recent years, there has been increasing research interest in the design and synthesis of extended coordination frameworks as potential zeolitic, magnetic, conducting, nonlinear optical materials, etc. [1]. Although most of these systems have been synthesized by controlled mixing of suitable soluble molecular components, solvothermal conditions have provided increasing success in alternative pathways to the preparation of single-crystalline supramolecular solids, including metal–organic coordination networks and hydrogen-bonded systems. 2-Substituted-pyrimidine ligands have been shown to be excellent and versatile building blocks, with charge and multi-connectivity abilities, to produce under conventional and hydrothermal conditions multidimensional coordination polymers with interesting properties [2]. Moreover, many six- or seven-coordinated and some five- or eight-coordinated Cd(II) coordination polymers [3] have recently received attention because of their excellent photoluminescence properties, well beyond the interest raised by their new structural features. Although some studies on the luminescent properties of 2-aminopyrimidine have been reported so far [4], however, no examples of Cd(II) coordination polymers containing this ligand and exhibiting luminescence properties exist. Recently, we have designed and prepared novel coordination polymers with different pyrimidine derivative ligands, with interesting luminescent properties [5]. In this context, and as a part of our continuing studies in this field, we present here the synthesis, structural aspects and luminescence properties of $[CdCl_2(PymNH_2)]$.

2. Experimental

2.1. General

All analytical reagents were purchased from commercial sources and used without further purification.

2.2. Preparation of $[CdCl_2(PymNH_2)]$

A mixture of $CdCl_2{\cdot}2.5H_2O$ (0.080 g, 0.350 mmol), $PymNH_2$ (0.097 g, 0.350 mmol) and distilled water (10 mL) was sealed in a Teflon-lined acid digestion autoclave and heated at 160 °C under autogenous pressure. After 12 h of heating, the reaction vessel was slowly cooled down to room temperature during a period of about 4 h. Colourless crystals of the compound under study were obtained. Yield: 64 %, based on Cd. *Anal.* Calc. for $C_4H_5CdCl_2N_3$: C, 17.26; H, 1.81; N, 15.09. Found: C, 17.35; H, 1.91; N, 15.24%.

2.3. Physical measurements

Elemental analyses were carried out at the "Centro de Instrumentación Científica" (University of Granada) on a Fisons-Carlo Erba analyser model EA 1108. The IR spectra on powdered samples

* Corresponding author. Tel.: +34 958243236.
E-mail address: antonio5@ugr.es (A. Rodríguez-Diéguez).

0277-5387/$ - see front matter Crown Copyright © 2011 Published by Elsevier Ltd. All rights reserved.
doi:10.1016/j.poly.2011.02.019

were recorded with a ThermoNicolet IR200FT-IR by using KBr pellets.

2.4. Single-crystal structure determination

Suitable crystal of $[CdCl_2(PymNH_2]$ was mounted on glass fiber and used for data collection. Data were collected with Bruker X8 Proteum diffractometers at 296(2) K. From the 782 measured reflections, 782 were independent and used to refine 46 parameters with zero restraints. Bruker X8 Kappa ApexII diffractometer ($2.8 < 2\theta < 26.3°$). Final R [$I < 2\sigma(I)$], $R_1 = 0.0350$, $wR_2 = 0.0758$, final R (all data), $R_1 = 0.0599$, $wR_2 = 0.0805$. Maximum/minimum residual electron density 0.883/−0.843 e Å^{-3}. The data were processed with APEX2 [6] and corrected for absorption using SADABS [7]. The structures were solved by direct methods using SIR97 [8], revealing positions of all non-hydrogen atoms. These atoms were refined on F^2 by a full matrix least-squares procedure using anisotropic displacement parameters [9].

2.5. Luminescence measurement

A Varian Cary-Eclipse Fluorescence Spectrofluorimeter solid sample holder accessory was used to obtain the fluorescence spectra. The spectrofluorimeter was equipped with a xenon discharge lamp (peak power equivalent to 75 kW), Czerny-Turner monochromators, R-928 photomultiplier tube which is red sensitive (even 900 nm) with manual or automatic voltage controlled using the Cary Eclipse software for Windows 95/98/NT system. The photomultiplier detector voltage was 800 V and the instrument excitation and emission slits were set at 10 and 10 nm, respectively.

3. Results and discussion

Colourless crystals of the compound under study were obtained by hydrothermal reaction of $CdCl_2$ and 2-aminopyrimidine in 1:1 M ratio. This compound crystallizes in the monoclinic space group $P2_1/m$. The coordination environment around the metal atom is shown in Fig. 1. The cadmium(II) ion, which lies on an inversion centre, exhibits a compressed octahedral geometry with a N_2Cl_4 donor set. In this description, four symmetry-related μ_2-chlorine bridging atoms are located in equatorial positions [Cd1–Cl1 2.611(2) Å], whereas two symmetry-related nitrogen atoms belonging to two μ_2-$PymNH_2$ bridging ligands occupy the axial positions [Cd1–N3 2.417(4) Å] (Table 1).

Owing to the inversion centre located on each cadmium(II) ion, the μ_2-$PymNH_2$ ligands are coordinated in *trans* positions resulting in a linear chain $[Cd(PymNH_2)]_n^{n+}$ with the aromatic ring displaying a zigzag distribution along the *b*-axis. Similar *trans*-axial

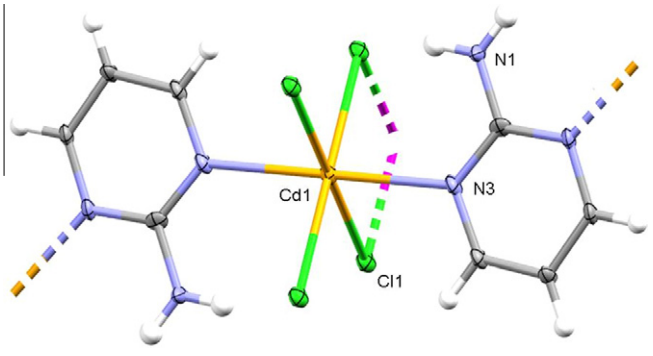

Fig. 1. Coordination environment of cadmium(II) in compound **1**. Symmetry codes: (i) *x*, *y*, *z*; (ii) −*x*, −*y*, 1 − *z*; (iii) 1 + *x*, *y*, *z*; (vi) 1 − *x*, −*y*, 1 − *z*; (v) *x*, 1/2 − *y*, *z*. Thermal ellipsoids are drawn at the 50% probability level.

Table 1
Crystallographic data and structural refinement details.

Compound	$[CdCl_2(PymNH_2)]$
CCDC	717413
Chemical formula	$C_4H_5CdCl_2N_3$
M (g mol^{-1})	278.41
T (K)	296(2)
λ (Å)	1.54178
Crystal system	monoclinic
Space group	$P2_1/m$
a (Å)	3.7645(14)
b (Å)	13.636(9)
c (Å)	7.266(5)
α (°)	90
β (°)	96.66(3)
γ (°)	90
V (Å^3)	370.5(4)
Z	2
ρ (g cm^{-3})	2.496
μ (mm^{-1})	3.58
Unique reflections	782
R_{int}	0.069
Goodness-of-fit (GOF) on F^2	0.987
R_1 [$I > 2\sigma(I)$][a]	0.035
wR_2 [$I > 2\sigma(I)$][a]	0.076

[a] $R(F) = \Sigma||F_o| - |F_c||/\Sigma|F_o|$, $wR(F^2) = [\Sigma w(F_o^2 - F_c^2)^2/\Sigma wF^4]^{1/2}$.

arrangements have been reported in *trans*-$[MX_4(PymNH_3)_2]$ (M = Co, Ni; X = Cl, Br) [10] and *trans*-$[MX_4(PymNH_3)_2]$ (M = Cu, X = Br) [11]. Chloride anions act as bridges between neighbouring metal centres [Cd–Cl–Cd 91.47(6)°, Cd···Cd separation of 3.764 Å] connecting neighbouring 2-amino-pyrimidine-cadmium chains, which result in a 2D undulating layered network parallel to the *ab* plane (Fig. 2). A cobalt(II) complex with similar crystal structure have been reported previously by Pike et al. (*Cmcm* space group; $a = 3.6139(2)$, $b = 14.3170(7)$, $c = 12.9986(7)$; bond distances, Co–Cl = 2.4668(6) Å and Co–N = 2.228(3) Å) [12]. Multi π,π-stacking interactions between pyrimidine rings of $PymNH_2$ ligands (centroid–centroid distance 3.764 Å) and N–H···Cl hydrogen bonding (3.277 Å, 255.0°) reinforce the 2D layer.

4. Luminescence properties

Among the most studied properties of materials containing aromatic molecules, in molecular crystals, organic polymers, coordination compounds or even donor–acceptor pairs, luminescence occupies a special ranking, due to the potential applications of visible light emitters [13] in a number of technologically advanced fields. Thanks to its extended aromaticity and to the presence of hexa-atomic rings, 2-aminopyrimidine is a good candidate for enhanced emissive properties. The excitation and emission spectrum of $[CdCl_2(PymNH_2)]$ in the solid state at room temperature is shown in Fig. 3.

Using a 340 nm incident radiation, intense emission band at 510 was observed. Previous reports, about analogous cadmium complexes with azolate ligands, show similar intense bands, which were attributed to ligand-to-ligand electronic transitions [14].

These analogous compounds are multidimensional cadmium complexes with other N-heterocyclic ligand. For 2D $[Cd(pmtz)_2]$ when excited at 340 nm present one very intense (and broad) emission band at 416 nm [5]. For 2,6-bis[(4-methylphenylimino)ethyl]pyridine $CdCl_2$ CH_3CN and 2,6-bis[1-(2,6-diethylphenylimino)ethyl]pyridine $CdCl_2$ $0.5CH_3CN$, using a 330 nm incident radiations, intense emission bands at 495 and 489 nm were observed [14b]. These values are similar to those found in our compound. We have assigned this band to an intraligand transition, which is affected by the coordination of the ligand to the Cd(II)

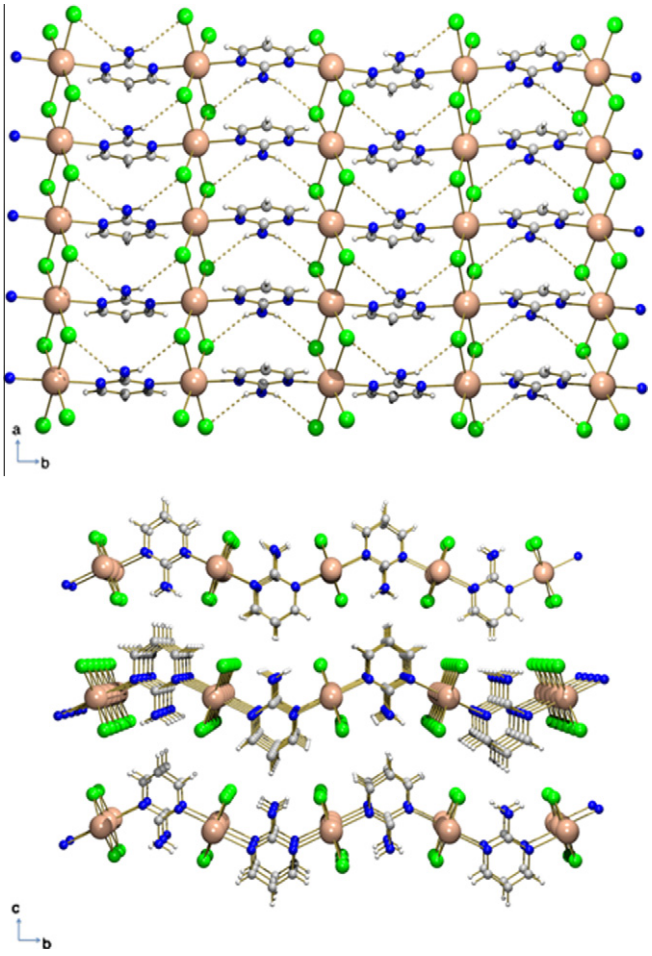

Fig. 2. View of the 2D layer structure of **1** in the *ab* plane (top). View down of the *a*-axis showing undulated layers stacked along *c*-axis (bottom).

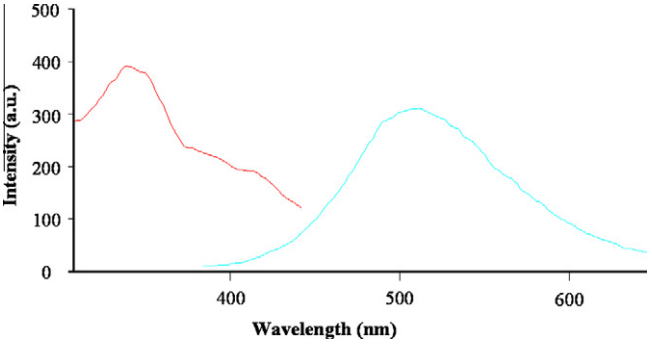

Fig. 3. Excitation (red) and emission (blue) spectra of compound [$CdCl_2(PymNH_2)$] at room temperature in the solid state. Horizontal axis: wavelength (nm); vertical axis: intensity (a.u.). (For interpretation of the references to colour in this figure legend, the reader is referred to the web version of this article.)

atom. The luminescence decay curve of the compound was obtained at room temperature. We try to fit the data to a mono exponential function but these data were impossible to fitted, for this reason the decay curve was fitted to double exponential function: $I = I_0 + A_1 \exp(-t/\tau_1) + A_2 \exp(-t/\tau_2)$, where I and I_0 are the luminescent intensities at time t and 0, τ_1 and τ_2 are defined as the luminescent lifetimes. For this function, the best fit of the experimental luminescence intensities to the above equation led to the lifetimes of 0.12 ms and 2.89 ms for τ_1 and τ_2 respectively, thus indicating phosphorescence. Photoluminescence in the ultraviolet–visible comprises two similar phenomena: fluorescence and phosphorescence. The large separation between excitation and emission luminescence (typically phosphorescence occurs at longer wavelength than fluorescence) together with such long lifetimes (the average lifetime of the electron in the excited state in fluorescent is only 10^{-5}–10^{-8} s and the average lifetime for phosphorescence ranges from 10^{-4} to 10^{4} s) might indicate phosphorescence rather than fluorescence in [$CdCl_2(PymNH_2)$]. Nevertheless, because we have no other experimental results supporting phosphorescence in this compound and because the phosphorescence emission is sometimes accompanied with fluorescence emission, we prefer to describe the observed photoluminescence as long lifetime photoluminescence emission. Few coordination polymers shown decay with two values of τ, however, some mono-dimensional examples have been reported [15]. Recently, one two-dimensional compound that shows phosphorescence properties with two values of τ (177 and 464.1 μs) has been reported by Zhao et al. [16].

To the best of our knowledge, there is no previously reported coordination polymers synthesized with 2-aminopyrimidine that show phosphorescent properties.

5. Conclusions

In this work we have shown that new polymers with interesting properties can be synthesized by using old ligands such as $PymNH_2$ (2-aminopyrimidine). We present a 2D metal–organic coordination framework [$CdCl_2(PymNH_2)$] which is made of $Cd_2(\mu\text{-}Cl)_2$ corner-sharing chains bridged by $PymNH_2$ through the endocyclic ring nitrogen atoms. It is of interest that this compound exhibits long lifetime photoluminescence emission at room temperature in the solid state and it represents one of the few examples of polymeric compounds with two lifetime decay values. This result opens the door toward the preparation of new coordination polymers with interesting luminescent properties synthesized with 2-aminopyrimidine and other related ligands. Work along this line is in progress in our laboratory.

Acknowledgments

This work was supported by the Junta de Andalucía (FQM-4228), the University of Granada (post-doctoral contract to A. Rodríguez-Diéguez), A.J. Calahorro thanks Predoctoral Fellowship from the Junta de Andalucía, D. Choquesillo-Lazarte thanks CSIC-EU for an I3P postdoctoral research contract. The project "Factoría de Cristalización, CONSOLIDER INGENIO-2010" provided X-ray structural facilities for this work.

References

[1] (a) B. Moulton, M.J. Zaworotko, Chem. Rev. 101 (2001) 1629;
(b) A. Oxtoby, N.R. Champness, Coord. Chem. Rev. 246 (2003) 145;
(c) C. Janiak, Dalton Trans. (2003) 2781;
(d) S. Kitagawa, R. Kitaura, S.-I. Noro, Angew. Chem., Int. Ed. 43 (2004) 2334;
(e) M. Eddaoudi, D.B. Moler, H.-L. Li, B. Chen, T.M. Reineke, M. O'Keeffe, O.M. Yaghi, Acc. Chem. Res. 34 (2001) 319;
(f) S. Kitagawa, K. Uemura, Chem. Soc. Rev. 34 (2005) 109;
(g) G. Férey, C. Mellot-Draznieks, C. Serre, F. Millange, Acc. Chem. Res. 38 (2005) 217;
(h) S.R. Batten, Curr. Opin. Solid State Mater. Sci. 5 (2001) 107;
(i) O.R. Evans, W. Lin, Acc. Chem. Res. 35 (2002) 511;
(j) Y. García, V. Niel, M.C. Muñoz, J.A. Real, Top. Curr. Chem. 233 (2004) 229;
(k) M. Yoshizawa, T. Kusukawa, M. Kawano, T. Ohhara, I. Tanaka, K. Kurihara, N. Niimura, M. Fujita, J. Am. Chem. Soc. 127 (2005) 2798;
(l) B. Kesanli, W.B. Lin, Coord. Chem. Rev. 246 (2003) 305;
(m) J.S. Miller, M. Drillon, Magnetism: Molecules to Materials, vols. I–V, VCH, Weinheim, 2001–2005.;
(n) E. Coronado, P. Day, Chem. Rev. 104 (2004) 5419.

[2] (a) J.A.R. Navarro, B. Lippert, Coord. Chem. Rev. 185 (1999) 653;
(b) J.A.R. Navarro, E. Barea, M.A. Galindo, J.M. Salas, M.A. Romero, M. Quirós, N. Masciocchi, S. Galli, A. Sironi, B. Lippert, J. Solid State Chem. 178 (2005) 2436;
(c) A. Rodríguez-Diéguez, J. Cano, R. Kivekäs, A. Debdoubi, E. Colacio, Inorg. Chem. 46 (2007) 2503;
(d) A. Rodríguez-Diéguez, H. Aouryaghal, A.J. Mota, E. Colacio, Acta Crystallogr., Sect. E 64 (2008) m618/1;
(e) J. Suárez-Varela, A.J. Mota, H. Aouryaghal, J. Cano, A. Rodríguez-Diéguez, D. Luneau, E. Colacio, Inorg. Chem. 47 (2008) 8143.
[3] (a) J.C. Dai, X.T. Wu, Z.Y. Fu, S.M. Hu, W.X. Du, C.P. Cui, L.M. Wu, H.H. Zhang, R.Q. Sun, Chem. Commun. (2002) 12;
(b) J. Fan, H.F. Zhu, T. Okamura, W.Y. Sun, W.X. Tang, N. Ueyamab, New J. Chem. 27 (2003) 1409;
(c) J. Tao, X. Yin, Z.B. Wei, R.B. Huang, L.S. Zheng, Eur. J. Inorg. Chem. (2004) 125;
(d) X. Shi, G.S. Zhu, Q.R. Fang, G. Wu, G. Tian, R.W. Wang, D.L. Zhang, M. Xue, S.L. Qiu, Eur. J. Inorg. Chem. (2004) 185;
(e) S. Skoulika, P. Dallas, M.G. Siskos, Y. Deligiannakis, A. Michaelides, Chem. Mater. 15 (2003) 4576;
(f) J. Luo, M.C. Hong, R.H. Wang, R. Cao, L. Han, Z.Z. Lin, Eur. J. Inorg. Chem. (2003) 2705;
(g) S.L. Zheng, J.H. Yang, X.-L. Yu, X.M. Chen, W.T. Wong, Inorg. Chem. 43 (2004) 830;
(h) D.D. Wu, T.C.W. Mak, Inorg. Chim. Acta 253 (1996) 15;
(i) Z.F. Chen, R.G. Xiong, B.F. Abrahams, X.Z. You, C.M.J. Che, J. Chem. Soc., Dalton Trans. (2001) 2453.
[4] N. Nishi, M. Kinoshita, Chem. Phys. Lett. 27 (1974) 342.
[5] A. Rodríguez-Diéguez, A. Salinas-Castillo, S. Galli, N. Masciocchi, J.M. Gutiérrez-Zorrilla, P. Vitoria, E. Colacio, Dalton Trans. (2007) 1821.
[6] Bruker APEX2, Bruker AXS Inc., Madison, Wisconsin, USA, 2004.
[7] G.M. Sheldrick, SADABS, Program for Empirical Adsorption Correction, Institute for Inorganic Chemistry, University of Göttingen, Germany, 1996.
[8] A. Altomare, M.C. Burla, M. Camilla, G.L. Cascarano, C. Giacovazzo, A. Guagliardi, A.G.G. Moliterni, G. Polidori, R. Spagna, J. Appl. Crystallogr. 32 (1999) 115.
[9] G.M. Sheldrick, SHELX 97, Program for Crystal Structure Refinement, University of Göttingen, Göttingen, Germany, 1997.
[10] M.E. Masaki, B.J. Prince, M.M. Turnbull, J. Coord. Chem. 55 (2002) 1337.
[11] G. Pon, R.D. Willett, W.T. Robinson, M.M. Turnbull, Inorg. Chim. Acta 255 (1997) 325.
[12] R.D. Pike, M.J. Lim, E.A.L. Willcor, T.A. Tronic, J. Chem. Crystallogr. 36 (2006) 781.
[13] U.H.F. Bunz, Chem. Rev. 100 (2000) 1605.
[14] (a) X.S. Wang, Y.Z. Tang, X.F. Huang, Z.R. Qu, C.M. Che, P.W.H. Chang, R.G. Xiong, Inorg. Chem. 44 (2005) 5278;
(b) R.-Q. Fan, H. Chen, P. Wang, Y.-L. Yang, Y.-B. Yin, W. Hasi, J. Coord. Chem. 9 (2010) 1514.
[15] E.J. Fernández, A. Laguna, J.M. López-de-Luzuriaga, M. Montiel, M.E. Olmos, J. Pérez, Inorg. Chim. Acta 358 (2005) 4293.
[16] L. Zhao, Y. Chen, H. Zhang, C. Li, R. Sun, Q. Yang, J. Mol. Struct. 920 (2009) 441.

CrystEngComm

Cite this: *CrystEngComm*, 2012, **14**, 6390–6393

www.rsc.org/crystengcomm

COMMUNICATION

Novel metal–organic frameworks based on 5-bromonicotinic acid: Multifunctional materials with H_2 purification capabilities†

Antonio J. Calahorro,[a] Marta E. López-Viseras,[a] Alfonso Salinas-Castillo,[b] David Fairen-Jimenez,‡*[c] Enrique Colacio,[a] Joan Cano[d] and Antonio Rodríguez-Diéguez*[a]

Received 6th March 2012, Accepted 18th July 2012
DOI: 10.1039/c2ce25807b

Two new metal–organic frameworks based on 5-bromonicotinic acid complexes $[Cd(5\text{-}BrNic)_2]_n$ (1) and $[Co(5\text{-}BrNic)_2(H_2O)]_n$ (2) have been synthesized by hydrothermal reactions of this ligand with cadmium and cobalt metallic(II) salts in the presence of water. Compound 1 displays intense photoluminescence properties in the solid state at room temperature, while 2 exhibits an antiferromagnetic interaction between Co(II) ions with a *J* value of $-4.1\ cm^{-1}$. Experimental studies, backed up by Monte Carlo simulations about adsorption, pore size distribution and accessible surface area reveal the capability of 2 for H_2 purification applications.

Transition metal–organic frameworks (MOFs), which are diverse in structure and properties, are currently attracting increasing attention not only due to their fascinating topologies but also due to their interesting applications in areas such as gas adsorption, catalysis, cooperative magnetic behaviour, non-linear optical activity and electrical conductivity.[1] Compared with conventional microporous inorganic materials such as zeolites, MOFs are more flexible for rational design through selection and tailoring of suitable ligands. Amongst them, multidentate N or O-donor ligands, such as pyridine or carboxylic acids, have drawn extensive attention in the construction of MOFs.[2] Thus, nicotinic acid and isonicotinic acid, as good sources of carboxylate ligand, have been widely applied to construct MOFs.[3]

The addition of electron-donor functionalities such as bromine atoms will extend the aromaticity of the hexa-atomic rings. Thus, nicotinic derivatives ligands are good candidates for enhanced emissive properties. To the best of our knowledge, the existence of luminescent properties on the 5-bromonicotinic ligand (5-BrNic) has only been reported before in a study using lanthanide ions.[4] In terms of adsorption properties, the presence of halogen atoms will increase gas–solid interaction, creating new adsorption sites through the porosity. From a structural viewpoint, 5-BrNic acid can act as a monodentate, bidentate, bidentate-bridging and tridentate-bridging ligand (Scheme 1). In the latter cases, the presence of a bromine atom in the *meta* position with respect to the nitrogen atom and the carboxylate group presumably favours the formation of channels in the three-dimensional structure. With the aim of moving forward in this area of research, we report here the hydrothermal synthesis, crystal structures, pore size distribution, geometric surface areas, luminescence and magnetic properties of the complexes $[Cd(5\text{-}BrNic)_2]_n$ (**1**) and $[Co(5\text{-}BrNic)_2(H_2O)]_n$ (**2**) bearing the 5-BrNic ligand.

Hydrothermal reactions of the appropriate metal chloride (1 mmol) with 5-BrNic (2 mmol) in water (14 ml) at 160 °C for 12 h followed by cooling down to room temperature over 2 h yield prismatic colourless crystals of **1** (in 70% yield) and pink crystals of **2** (in 45% yield). Crystal structures (see ESI†) of **1** and **2** were determined by single crystal X-ray diffraction methods and found that both compounds exhibit different 3D MOF structures. Compound **1** is a three-dimensional coordination polymer in

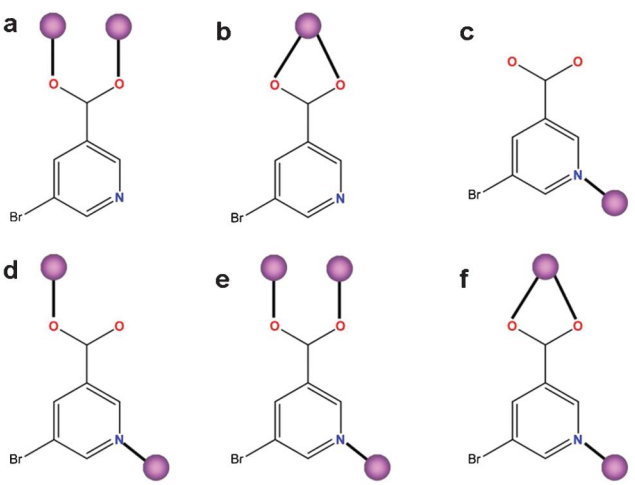

Scheme 1 Some coordination modes of 5-BrNic ligand.

[a]*Departamento de Química Inorgánica, Universidad de Granada, Granada, 18071, Spain. E-mail: antonio5@ugr.es; Tel: 0034958240442*
[b]*Departamento de Química Analítica, Universidad de Granada*
[c]*Institute for Materials and Processes, School of Engineering, The University of Edinburgh, United Kingdom. E-mail: David.Fairen-Jimenez@Northwestern.edu*
[d]*Instituto de Ciencia Molecular (ICMol) and Fundació General de la Universitat de València (FGUV), Catedrático José Beltrán n° 2, Universitat de València, Paterna, València, E-46980, Spain*
‡ Present address: Department of Chemical and Biological Engineering, Northwestern University, Evanston, Illinois, USA
† Electronic supplementary information (ESI) available. CCDC reference numbers 869626 and 869627. For ESI and crystallographic data in CIF or other electronic format see DOI: 10.1039/c2ce25807b

which cadmium atoms present very distorted octahedral coordination geometry and the 5-bromoniconitic ligand possesses two different tridentate-bridging coordination modes (Scheme 1, e and f modes).

Compound **1** crystallises in the monoclinic space group *P*21/*n*, the asymmetric unit consisting of two 5-BrNic$^-$ ligands and one cadmium ion, all in general positions. Each Cd(II) ion exhibits very distorted octahedral CdN_2O_4 geometry with the two nitrogen atoms belonging to two pyridine rings and four oxygen atoms pertaining to three different 5-BrNic bridging ligands (Fig. 1a). The distortion of the Cd(II) coordination polyhedron is mainly due to the small bite angle of the carboxylate group pertaining to one of the 5-BrNic ligands (O–Cd–O = 54.41°). Each cadmium atom is connected to seven cadmium centres through five 5-BrNic ligands, generating a convoluted three-dimensional structure with Cd···Cd distances through 5-BrNic spacers of 4.507, 7.650, 7.944 and 8.840 Å. The three-dimensional MOF possess small channels that propagate along the *c* crystallographic axis, in which bromine atoms are oriented to the centre of these channels (Fig. 2).

The 3D-MOF structure of **2** can be described as aquadicarboxylate triply-bridged Co(II) dimers connected by didentate- and tridentate-bridging 5-bromonicotinate ligands (Scheme 1, coordination modes d and e). Within the dinuclear Co_2 units (Fig. 1b), each Co(II) ion exhibits a distorted CoN_2O_4 octahedral geometry, which is made of two pyridine nitrogen atoms and three oxygen atoms from five different 5-BrNic$^-$ bridging ligands and the oxygen atom of the bridging water molecule (Fig. 1b). Therefore each Co(II) atom is connected to another six cobalt centres affording the 3D network.

Intradinuclear Co···Co distance is 3.512 Å, whereas the Co–O_w–Co bond angle has a value of 112.14°. The three-dimensional MOF possess channels that propagate along the *c* crystallographic axis in which bromine atoms are oriented to the centre of these channels (Fig. 3).

The emission maximum of 5-BrNic in the solid state is 475 nm, in good agreement with the emissions observed for a series of pyridine-carboxylic acid derivative ligands.[5,6] The emission spectrum of **1** (Fig. S1†) at room temperature in the solid state exhibits intense emission bands centered about 510 and 518 nm, in concordance with those observed for other MOFs with these types of derivative ligands.[6] The emission, assigned to intraligand π–π* transitions, is considerably red-shifted with respect to the ligand emission band (about 35 cm^{-1}).

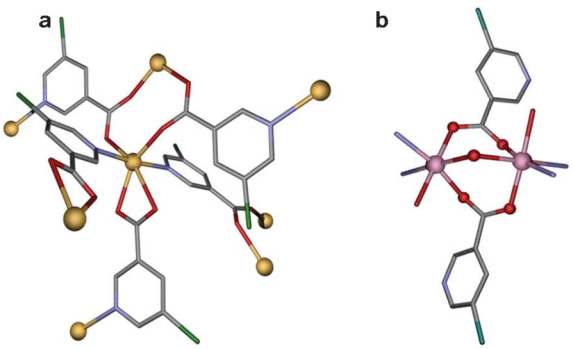

Fig. 1 View of the metal environment and coordination mode of the ligand for **1** (a) and the Co(II) dimer repetition motif for **2** (b). Colour code N = blue, O = red, C = grey, Cd = yellow and Co = pink.

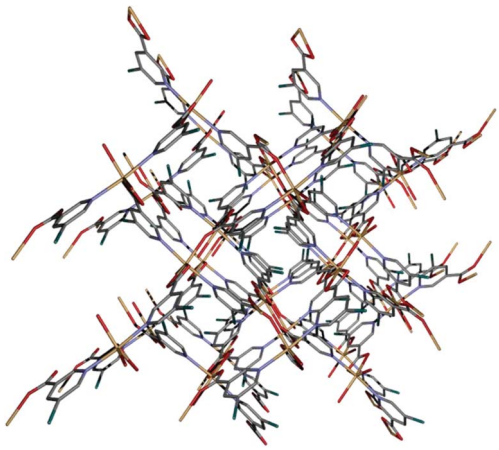

Fig. 2 View down to the *c* axis in the three-dimensional network in **1**.

The temperature dependence of χ_M and $\chi_M T$ product (χ_M is the molar susceptibility per Co_2 unit) for **2** at a magnetic field of 0.5 T is given in Fig. S2.† The $\chi_M T$ value at room temperature (6.45 cm^3 K mol^{-1}) is significantly higher than that calculated from the spin-only formalism for a dinuclear high-spin Co(II) system (3.75 cm^3 K mol^{-1} for $S = 3/2$ and $g = 2$), which indicates that the orbital angular momentum of the Co(II) ions is not quenched and therefore contributes significantly to the magnetic susceptibility. In fact, the spin–orbit coupling causes the $\chi_M T$ product decrease upon lowering the temperature with increasing slope. The lowest possible value expected for $\chi_M T$ at 0 K for two uncoupled octahedral Co(II) ions with only the lowest Kramer doublet populated is usually found in the range 3.0–3.4 cm^3 K mol^{-1}. However, the $\chi_M T$ value at 2 K (0.3 cm^3 K mol^{-1}) is much smaller than the lower end of the above range, which clearly indicates the presence of an intramolecular antiferromagnetic coupling. This fact is supported by the existence of a maximum in χ_M at 8 K.

In order to determine the *intradimer* exchange interaction in **2**, we have used an empirical approach recently proposed for one of us,[7] where each Co(II) ion in the Kramer's ground doublet state arising form the spin–orbit coupling is considered to have an

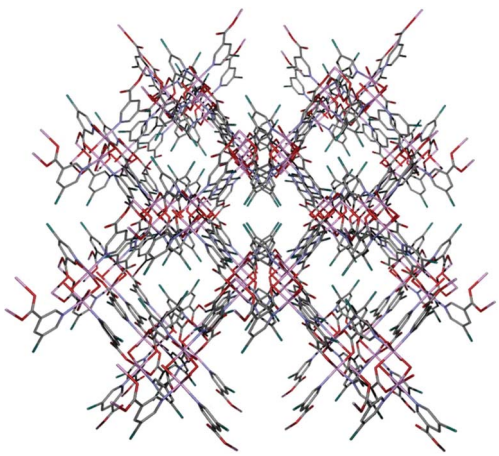

Fig. 3 View down the *c* axis of the channels in the three-dimensional network of **2**.). Colour code N = blue, O = red, C = grey, Cd = yellow and Co = pink.

effective spin $S_{eff} = 1/2$, which is related with to the real spin ($S = 3/2$) by a factor of 5/3. The magnetic exchange is assumed to occur between the ground doublets of the Co(II) ions. The contribution of the excited doublets to the magnetic properties of ground doublet state is taken into account in the g factor that is dependent on J, λ, α and Δ ,where J is the isotropic exchange interaction, λ is the spin–orbit coupling, α is the orbital reduction factor defined as $\alpha = kA$ and Δ is the energy gap between the singlet $^4A_2$ and doublet ^4E levels due to the axial distortion. A very good agreement between the simulation and the experimental data above 20 K is reached with the next values: $Ak = 1.266$, $\lambda = -123.0\ cm^{-1}$, $\Delta = -427.3\ cm^{-1}$ and $J = -4.1\ cm^{-1}$ with $R = 7.4 \times 10^{-7}$. The large value of Δ is in agreement with the low symmetry of the metal coordination sphere, whereas the values of the λ, α and k lie within the range of those observed in other six-coordinated high-spin Co(II) complexes.[9] The maximum in χ_M at 8 K is not perfectly reproduced due to limitations of the model.

The porous properties of compounds **1** and **2** were first studied by means of their pore size distribution (PSD) and accessible surface area, using different probe molecules ranging from 2.5 to 4.0 Å in a Monte Carlo calculation.[8] PSD analysis shows that whereas **1** is essentially non-porous, **2** presents small cavities localised at 3.75 Å (Fig. 4). The small pore size due to the use of small linkers in the synthesis, makes **2** a perfect candidate for molecular sieving and potential H_2 purification, using thin film growth for the synthesis of membranes.[9] Moreover, the analysis of the accessible surface area for different probe molecule diameters (Fig. S3, ESI†) shows an important reduction in the values when the probe size increases (*i.e.* compare $S_{area} = 811\ m^2\ cm^{-3}$ (H_2) *versus* $191\ m^2\ cm^{-3}$ (CH_4)).

The analysis on the molecular sieving capability of **2** was confirmed by means of experimental adsorption of H_2, N_2 and CH_4 on this material. While **2** was not able to adsorb N_2 and CH_4 on the applied experimental conditions (77 K, 1 bar and 298 K up to 20 bar for N_2 and CH_4, respectively), H_2 (77 K) was able to diffuse through the narrow porosity, being able to reach an uptake up to 1.78 mmol g^{-1} (Fig. 5 and S4†). This high H_2/N_2 and H_2/CH_4 selective behaviour has been observed previously in other

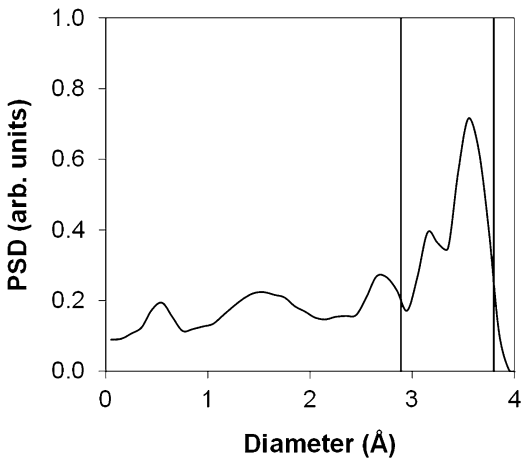

Fig. 4 Pore size distribution of **2**. Vertical lines show the kinetic diameter of H_2 (2.89 Å) and CH_4 (3.8 Å). Note that, for every gas molecule, their accessible pore volume will be limited to that larger than the molecule size (*i.e.* right-side in the PSD).

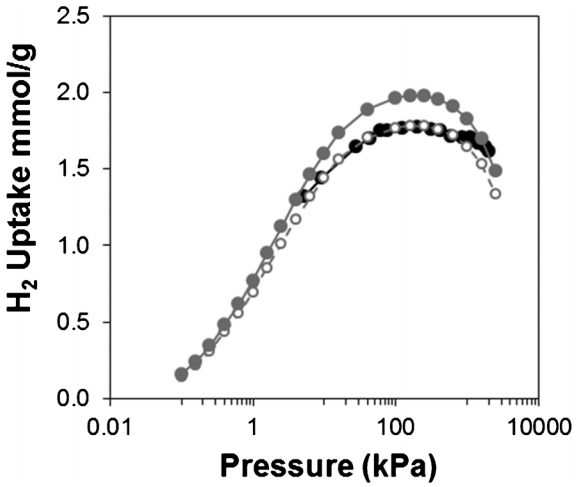

Fig. 5 Experimental, black closed circles, and simulated, grey closed circles, H_2 isotherms at 77 K on **2**. Scaled ($\phi = 0.91$) simulated isotherms, grey open circles. Note the use of the semilog scale.

MOFs.[10] We also used grand canonical Monte Carlo simulations[11] to predict the H_2 adsorption isotherm, which describes correctly the shape of the experimental results (Fig. 5 and S4†) and predicts accurately the maximum on the excess isotherm. The description of the experimental adsorption process is significantly improved after applying a scaling factor (ϕ) of 0.91, calculated as the ratio of the experimental and simulated maximum amounts adsorbed, on the simulated curve. The over-prediction in the simulations is generally explained by the existence of structural defects in the experimental sample that limits the micropore volume and the maximum capacity of the real solid.[11b]

In this work, we have shown that novel metal–organic frameworks with luminescent and magnetic properties can be synthesized by using the 5-bromonicotinic ligand. Experimental adsorption and Monte Carlo simulations on compound **2** reveal its potential properties for H_2 purification. Work is in progress in our laboratory in order to obtain new homo- and heterometallic complexes to study their physical properties.

Acknowledgements

This work was supported by the Junta de Andalucía (FQM-4228) (A.J. Calahorro for a predoctoral grant). D. F-J. thanks the European Commission for a Marie Curie Intra-European fellowship (PIEF-GA-2009-236665).

References

1 (*a*) M. Eddaoudi, J. Kim, N. Rosi, D. Vodak, J. Wachter, M. O'Keefe and O. M. Yaghi, *Science*, 1996, **271**, 49; (*b*) L. Xu, G. C. Guo, B. Liu, M. S. Wang and J. S. Huang, *Inorg. Chem. Commun.*, 2004, **7**, 1145; (*c*) L. Hou and D. Li, *Inorg. Chem. Commun.*, 2005, **8**, 190; (*d*) P. Mahata and S. Natarajan, *Eur. J. Inorg. Chem.*, 2005, 2156; (*e*) L. S. Long, X. M. Chen, M. L. Tong, Z. G. Sun, Y. P. Ren, R. B. Huang and L. S. Zheng, *J. Chem. Soc., Dalton Trans.*, 2001, 2888.

2 (*a*) W. Chen, H.-M. Yuan, J.-Y. Wang, Z.-Y. Liu, J.-J. Xu, M. Yang and J.-S. Chen, *J. Am. Chem. Soc.*, 2003, **125**, 9266; (*b*) S. M. Humphrey, J. S. Chang, S. H. Jhung, J. W. Yoon and P. T. Wood, *Angew. Chem., Int. Ed.*, 2007, **46**, 272; (*c*) S. M. Humphrey and P. T. Wood, *J. Am. Chem. Soc.*, 2004, **126**, 13236; (*d*) X.-M. Zhang, Y.-Z. Zheng, C.-R. Li, W.-X. Zhang and X.-M. Chen, *Cryst. Growth Des.*,

2007, **7**, 980; (*e*) Y.-Q. Sun, J. Zhang, Y.-M. Chen and G.-Y. Yang, *Angew. Chem., Int. Ed.*, 2005, **44**, 5814; (*f*) W.-G. Lu, C.-Y. Su, T.-B. Lu, L. Jiang and J.-M. Chen, *J. Am. Chem. Soc.*, 2006, **128**, 34.

3 (*a*) X. J. Gu and D. F. Xue, *Inorg. Chem.*, 2006, **45**, 9257; (*b*) M. B. Zhang, J. Zhang, S. T. Zheng and G. Y. Yang, *Angew. Chem., Int. Ed.*, 2005, **44**, 1385; (*c*) J. W. Cheng, J. Zhang, S. T. Zheng, M. B. Zhang and G. Y. Yang, *Angew. Chem., Int. Ed.*, 2006, **45**, 73; (*d*) Y. S. Song, B. Yan and Z. X. Chen, *J. Solid State Chem.*, 2006, **179**, 4037; (*e*) Y. H. Zhao, Z. M. Su, Y. Wang, Y. M. Fu, S. D. Liu and P. Li, *Inorg. Chem. Commun.*, 2007, **10**, 410.

4 Y.-S. Song, B. Yan and Z.-X. Chen, *J. Solid State Chem.*, 2004, **177**, 3805.

5 B. Yan and B. Zhou, *J. Photochem. Photobiol., A*, 2005, **171**, 181.

6 L. Zhao, P. Ren, Z. Zhang, M. Fang, W. Shi and P. Cheng, *Sci. China, Ser. B: Chem.*, 2009, **52**, 1479.

7 F. Lloret, M. Julve, J. Cano, R. Ruiz-García and E. Pardo, *Inorg. Chim. Acta*, 2008, **361**, 3432.

8 (*a*) L. D. Gelb and K. E. Gubbins, *Langmuir*, 1999, **15**, 305; (*b*) T. Düren, F. Millange, G. Férey, K. S. Walton and R. Q. Snurr, *J. Phys. Chem. C*, 2007, **111**, 15350.

9 D. Zacher, O. Shekhah, C. Wöll and R. A. Fischer, *Chem. Soc. Rev.*, 2009, **38**, 1418.

10 (*a*) B. Chen, S. Ma, F. Zapata, F. R. Fronczek, E. B. Lobkovsky and H.-C. Zhou, *Inorg. Chem.*, 2007, **46**, 1233; (*b*) M. Xue, S. Ma, Z. Jin, R. M. Schaffino, G. S. Zhu, E. B. Lobkovsky, S. L. Qiu and B. L. Chen, *Inorg. Chem.*, 2008, **47**, 6825.

11 (*a*) D. Frenkel, B. Smit, *Understanding Molecular Simulations: From Algorithms to Applications*, 2nd ed.; Academic Press: San Diego2002; (*b*) A. Rossin, D. Fairen-Jimenez, T. Düren, G. Giambastiani, M. Peruzzini and J. G. Vitillo, *Langmuir*, 2011, **27**, 10124.

Inorganic Chemistry

Communication

pubs.acs.org/IC

First Examples of Metal–Organic Frameworks with the Novel 3,3′-(1,2,4,5-Tetrazine-3,6-diyl)dibenzoic Spacer. Luminescence and Adsorption Properties

A. J. Calahorro,[†] Antonio Peñas-Sanjuan,[‡] Manuel Melguizo,[‡] David Fairen-Jimenez,[§] Guillermo Zaragoza,[⊥] Belén Fernández,[∥] Alfonso Salinas-Castillo,[¶] and A. Rodríguez-Diéguez*[,†]

[†]Departamento de Química Inorgánica, Universidad de Granada, Avenida Fuentenueva s/n, 18071 Granada, Spain

[‡]Departamento de Química Inorgánica y Orgánica, Universidad de Jaén, Campus Las Lagunillas, 23071 Jaén, Spain

[§]Department of Chemical & Biological Engineering, Northwestern University, 2145 Sheridan Road, Evanston, Illinois 60208-3120, United States

[⊥]Unidad de Rayos X, RIAIDT Edificio CACTUS, Universidad de Santiago de Compostela, 15782 Santiago de Compostela, Spain

[∥]Instituto de Parasitología y Biomedicina López-Neyra (CSIC), Avenida del Conocimiento s/n, Armilla, Granada

[¶]Departamento de Química Analítica, Universidad de Granada, 18071 Granada, Spain

Supporting Information

ABSTRACT: We report the synthesis of a novel ligand, 3,3′-(1,2,4,5-tetrazine-3,6-diyl)dibenzoic acid (**1**). In this fragment, we have introduced two carboxylate groups with the aim of using this ligand as a linker to construct three-dimensional metal–organic frameworks (MOFs). We have been successful in the formation of zinc (**2**) and lanthanum (**3**) MOFs. The zinc compound is a two-dimensional structure, while the lanthanum material is a three-dimensional MOF with interesting channels. We include the luminescence and adsorption studies of these materials. Moreover, we have evaluated the in vitro toxicity of this novel ligand, concluding that it can be considered negligible.

In the last 15 years, great attention has been paid to metal–organic frameworks (MOFs) as a consequence of their functional properties and potential uses in many applications.[1] Recently, the design and study of zinc- and lanthanum-based MOF has evolved enormously[2] because of their interesting structures and potential applications in areas such as magnetism,[3] luminescence,[4] gas adsorption,[5] sensing, and optical storage.[6] These materials are commonly prepared through a bottom-up approach, using solvothermal methods, connecting transition/lanthanide metal ions with the appropriate bridging ligands. Still, there is great interest in the design of new bridging ligands that will allow the preparation of novel MOFs. Here, we have designed a new symmetrically multidentate bridging ligand, 3,3′-(1,2,4,5-tetrazine-3,6-diyl)dibenzoic acid (**1**; H_2dbtz), which contains two benzoic group donors, bonding to the metals, and a central tetrazine p-acceptor function. Our idea stems from the use of 3,6-disubstituted 1,2,4,5-tetrazine moieties, which have become popular as efficient electronic spacers in dinuclear and polynuclear systems.[7] This is primarily due to the fact that the tetrazine-based low-lying p* orbital conveys strong p-accepting characteristics, leading to excellent electronic communication between the metal termini. In this work, we report the structural, luminescence, and adsorption properties of the first examples of coordination polymers $[Zn(dbtz)(H_2O)]_n$ (**2**) and $\{[La_2(dbtz)_3(H_2O)_2](H_2O)_6\}_n$ (**3**) with the new multidentate ligand H_2dbtz, shown in Scheme S1, demonstrating the potential of this new ligand to construct new MOFs with interesting adsorption properties because of their similarity to other linkers, e.g., NOTT-101 MOF.[8] To the best of our knowledge, these are the first examples of crystal structures of MOFs with ligands that contain the H_2dbtz ligand.

The synthesis (see SI file) of **1** was performed following a variation of the classical Pinner-type scheme in two steps.[9] First, the reaction between 3-cianobenzoic acid and excess hydrazine catalyzed by *N*-acetylcysteine under an inert atmosphere renders the dihydrotetrazine derivative, which was oxidized to give the desired fully aromatic derivative by simple stirring of a methanol suspension of the dihydro derivative in an air atmosphere. Although a similar air oxidation procedure has been reported to aromatize some dihydrotetrazine derivatives,[10] its scope seems to be more general than initially recognized, as proven here.

1 was characterized by ^{1}H and ^{13}C NMR spectrometry [Supporting Information (SI), Figures S1 and S2], electron-impact high-resolution mass spectrometry (HRMS), and X-ray diffraction.[12] Compound **1** crystallizes in the monoclinic space group $P2_1/c$; the asymmetric unit consisting of a medium H_2dbtz ligand that grows by symmetry generated an almost linear alignment between the aromatic rings and terminal carboxylate groups (dihedral angles 3–6°) and one crystallization dimethyl sulfoxide (DMSO) molecule (Figure 1). In the H_2dbtz unit, the bond distances and angles are very similar to those expected in comparison with the tetrazine and benzene rings.[11] In the structure, there is only one type of hydrogen bond (SI, Figure S3), yielding a trinuclear unit formed by one central H_2dbtz unit and two DMSO molecules. In this strong hydrogen bond (O1–H···O3 = 2.565 Å), the oxygen atom pertaining to DMSO and one oxygen atom from the carboxylate group are involved. These

Received: October 20, 2012
Published: January 3, 2013

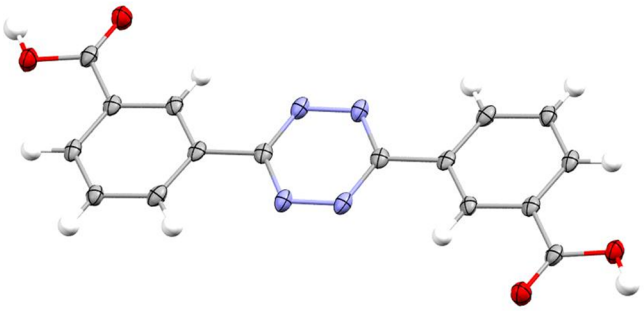

Figure 1. Crystalline structure of **1**. Color code: carbon, gray; nitrogen, blue; oxygen, red; sulfur, yellow; hydrogen, white. The DMSO molecule has been omitted for clarity. Thermal ellipsoids are drawn at the 50% probability level.

trinuclear units are packed through stacking interactions among the tetrazine with benzene rings [3.531(5) Å] and benzene−benzene rings of neighboring units [3.699(5) Å] (SI, Figure S3 and Table S1).

Hydrothermal reactions (see SI file) of the appropriate metal salts (1 mmol) with H_2dbtz (1 mmol) in water (10 mL) at 160 °C for 12 h followed by cooling to room temperature over 3 h yield prismatic pink crystals of **2** (in 57% yield) and **3** (in 75% yield). The crystal structures were determined by single-crystal X-ray crystallography.[12]

Compound **2** consists of double sheets parallel to the *ac* plane. These layers can be described as chains generated by the carboxylate groups, pertaining to the ligand along the *b* directions that are bridged by the $dbtz^{2-}$ spacer. The metal centers have tetrahedral coordination environment ZnO_4 formed by three oxygen atoms, pertaining to three carboxylate groups of three different spacers and one coordinated water molecule.

There are four units of formula $[Zn(dbtz)(H_2O)]$ per cell, and in the crystal structure, each bridging $dbtz^{2-}$ ligand is bound to three metal ions and each metal ion is linked to five other metal ions by three $dbtz^{2-}$ ligands, thus generating stacked double sheets parallel to the [101] direction. The ligand coordinates to the metal center in monodentate and bidentate coordination modes with each carboxylate group, respectively. The coordinated water molecule generates hydrogen bonds with monodentate mode, and infinite two-dimensional networks of the formula $[Zn(dbtz)(H_2O)]_n$ are thus formed; the values of these hydrogen bonds are 2.744(6) and 2.676(6) Å. The association of two such layers by the bidentate mode through one of the carboxylate group bridges gives rise to double layers $[Zn(dbtz)(H_2O)]_n$. These double layers are separated by stacking interactions [3.719(4) Å] (SI, Figure S4 and Table S2). Figure 2 shows a perspective view of the double sheet. The SI, Table S3, gives the main bond lengths and angles.

The crystal structure of **3** consists of a three-dimensional MOF with channels occupied by disordered solvent water molecules

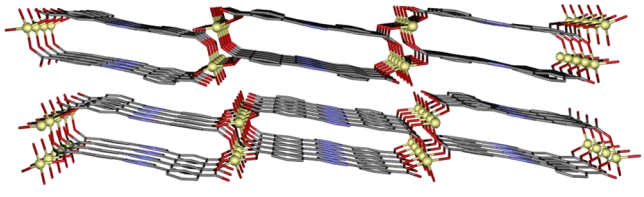

Figure 2. Representation, down [101], of the two-dimensional $[Zn(dbtz)(H_2O)]_n$ layer present in compound **2**.

that propagate along the *a* crystallographic axis. Each La^{III} ion exhibits a LaO_8 coordination environment, which is made of seven oxygen atoms belonging to carboxylate groups of two deprotonated $dbtz^{2-}$ bridging ligands and one coordination water molecule. The $La-O_{water}$ bond distance is 2.82(3) Å, whereas the $La-O_{carb}$ distances are in the range of 2.394(19)−2.564(12) Å. In the structure, lanthanum ions are connected by carboxylate groups pertaining to $dbtz^{2-}$ ligands, generating double chains along the *a*-axis direction. Some oxygen atoms from the carboxylate groups unite two or three lanthanum centers. The dihedral angles between the mean planes of the benzene and tetrazine rings are in the range 7.28−22.67°. These double chains are bridged with six other double chains by $dbtz^{2-}$ ligands.

Each lanthanum ion is linked to 17 other metal ions by 7 $dbtz^{2-}$ ligands, generating a three-dimensional structure (Figure 3). Considering the $dbtz^{2-}$ ligands as spacers and the lanthanum

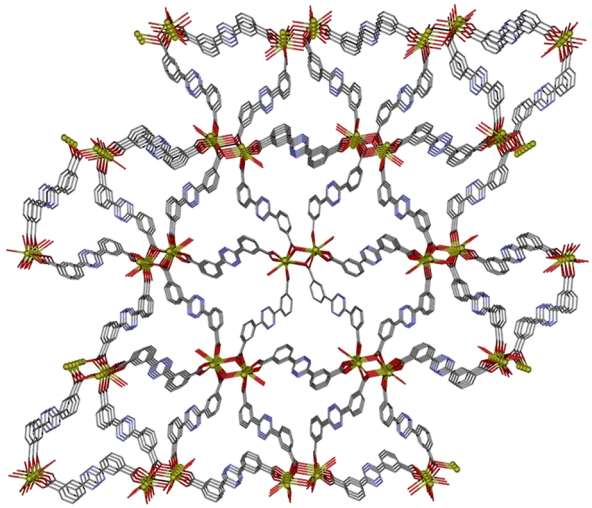

Figure 3. Perspective view along the *a* direction of **3** with the channels in which are located the water molecules. Crystallization water molecules and hydrogen atoms have been omited for clarity.

atoms as nodes, the resulting network generates channels along the *a*-axis direction (SI, Figure S5). These channels have a diameter of 5.02 Å. The shortest and longest La···La distances through $dbtz^{2-}$ spacers are 4.308 and 18.653 Å, respectively.

Thanks to its extended aromaticity and to the presence of polyheterosubstituted hexaatomic rings, H_2dbtz is a good candidate for enhanced emissive properties, tunable, in principle, by coordination to different metals or environments. The emission spectra of compounds **1**−**3** in the solid state at room temperature are shown in (SI, Figure S8). The emission spectra of **1** and **2** at room temperature in the solid state exhibit broad intense emission bands centered at about 454 and 461 nm, respectively, upon excitation at 310 nm. For **3**, using 310 nm incident radiation, intense emission bands at 453 and 470 nm and a stronger one at 498 nm were observed. The emissions in complexes **2** and **3** are assigned to intraligand p−p* transitions, although a considerable red shift is observed with respect to the ligand emission band. Moreover, the emission is more intense than that of the free ligand, which may be explained in terms of the rigidity. The rigidity of the coordinated ligand reduces the loss of energy, thereby increasing the emission efficiency.[13]

We first studied the porous properties of **3** by means of their pore-size distribution (PSD) in a Monte Carlo calculation.[14]

dx.doi.org/10.1021/ic302318j | *Inorg. Chem.* 2013, 52, 546−548

PSD analysis shows that it presents narrow cavities localized at 4 Å (SI, Figure S6). We extended our study by running molecular simulations to predict the adsorption uptake of N_2 and H_2 on **3** at 77 K. Because of the presence of a very narrow porosity, N_2 molecules cannot adsorb in the porosity. On the other hand, the adsorption isotherm of H_2 (SI, Figure S9) predicts an excess capacity at 77 K and 100 bar of 9.97 mg·g^{-1} (12.9 mg·cm^{-3}, using a crystal density of 1.29 g·cm^{-3}). We[15] and others[16] have reported recently high H_2-selective behavior on MOFs for stream purification applications. We studied experimentally the porous structure of **3** after solvent removal, during the adsorption of H_2 at 77 K and up to 100 bar. However, the experimental adsorption isotherm revealed that the porous structure collapsed during activation using conventional methods (heating at 393 K and high vacuum and 10^{-4} bar).

We evaluated the in vitro cytotoxicity of cells exposed to compound **1** at different concentrations and a wide range of incubation times (SI, Figure S7). The results obtained show that for long incubation times and at the highest concentrations analyzed apparent mild signs of toxicity appeared that can be considered negligible with cell viability greater than 80−90%.

These results show that new and interesting materials or MOFs with biomedical applications can be assembled from metal ions and the new H_2dbtz ligand. Work along this line using other paramagnetic/lanthanide metals and X-ray measurements with pressure are in progress in our laboratory. We are also working on the use of a supercritical activation process to allow the removal of solvent molecules from the porosity, keeping the porous texture of the as-prepared material unaffected.

■ ASSOCIATED CONTENT

Ⓢ Supporting Information

X-ray crystallographic data in CIF format, ^{1}H and ^{13}C NMR, crystal structure pictures, computational details, cytotoxicity, preparation of **2** and **3**, luminescence and adsorption graphics, and additional references. This material is available free of charge via the Internet at http://pubs.acs.org. CCDC reference numbers are 902753−902755. The atomic coordinates for these structures have also been deposited with the Cambridge Crystallographic Data Centre. The coordinates can be obtained, upon request, from the Director, Cambridge Crystallographic Data Centre, 12 Union Road, Cambridge CB2 1EZ, U.K.

■ AUTHOR INFORMATION

Corresponding Author

*E-mail: antonio5@ugr.es.

Notes

The authors declare no competing financial interest.

■ ACKNOWLEDGMENTS

This work was supported by the Junta de Andalucía (Predoctoral Grant FQM-4228 to A.J.C.), the University of Granada, and the Department of Energy's Office of Energy Efficiency and Renewable Energy, Fuel Cell Technologies Program under Grant DE-FC36-08GO18137. B.F. thanks to the MEC for the postdoctoral contract "Juan de la Cierva".

■ REFERENCES

(1) (a) Kondo, A.; Noguchi, H.; Kajiro, H.; Carlucci, L.; Mercandelli, P.; Proserpio, D. M.; Tanaka, H.; Kaneko, K.; Kanoh, H. *J. Phys. Chem. B* **2006**, *110*, 25565−25567. (b) Rowsell, J. L. C.; Yaghi, O. M. *J. Am. Chem. Soc.* **2006**, *128*, 1304. (c) Hong, M. *Cryst. Growth Des.* **2007**, *7*, 10. (d) Vertova, A.; Cucchi, I.; Fermo, P.; Porta, F.; Proserpio, D. M.; Rondinini, S. *Electrochim. Acta* **2007**, *52*, 2603−2611. (e) Janiak, C. *Dalton Trans.* **2003**, *14*, 2781. (f) Yang, S.; Sun, J.; Ramirez-Cuesta, A. J.; Callear, S. K.; David, W. I. F.; Anderson, D. P.; Newby, R.; Blake, A. J.; Parker, J. E.; Tang, C. C.; Schröder, M. *Nat. Chem.* **2012**, *4*, 887−894. (g) Long, J. R.; Yaghi, O. M. *Chem. Soc. Rev.* **2009**, *38*, 1201−1507.

(2) (a) Almeida Paz, F. A.; Klinowski, J. *Chem. Commun.* **2003**, 1484−1485. (b) Long, D.-L.; Blake, A. J.; Champness, N. R.; Wilson, C.; Schröder, M. *Angew. Chem., Int. Ed.* **2001**, *40*, 2444−2447. (c) Ma, B.-Q.; Zhang, D.-S.; Gao, S.; Jin, T.-Z.; Yan, C.-H.; Xu, G.-X. *Angew. Chem., Int. Ed.* **2000**, *39*, 3644−3646.

(3) (a) Morrish, A. H. *The Physical Principles of Magnetism*; Wiley: New York, 1965. (b) Chen, Z.; Zhao, B.; Zhang, Y.; Shi, W.; Cheng, P. *Cryst. Growth Des.* **2008**, *8*, 229−233.

(4) (a) Shunmugam, R.; Tew, G. N. *J. Am. Chem. Soc.* **2005**, *127*, 13567−13572. (b) Rosi, N. L.; Kim, J.; Eddaoudi, M.; Chen, B. L.; O'Keeffe, M.; Yaghi, O. M. *J. Am. Chem. Soc.* **2005**, *127*, 1504−1518.

(5) (a) Pan, L.; Adams, K. M.; Hernandez, H. E.; Wang, X.; Zheng, C.; Hattori, Y.; Kaneko, K. *J. Am. Chem. Soc.* **2003**, *125*, 3062−3067. (b) Dawson, R.; Adams, D. J.; Cooper, A. I. *Chem. Sci.* **2011**, *2*, 1173−1177.

(6) (a) Kuriki, K.; Koike, Y.; Okamoto, Y. *Chem. Rev.* **2002**, *102*, 2347−2356. (b) Bünzli, J. C. G.; Piguet, C. *Chem. Soc. Rev.* **2005**, *34*, 1048−1077. (c) Robin, A. Y.; Fromm, K. M. *Coord. Chem. Rev.* **2006**, *250*, 2127−2157.

(7) Kaim, W. *Coord. Chem. Rev.* **2002**, *230*, 127−139.

(8) Lin, X.; Telepeni, I.; Blake, A. J.; Dailly, A.; Brown, C. M.; Simmons, J. M.; Zoppi, M.; Walker, G. S.; Thomas, K. M.; Mays, T. J.; Hubberstey, P.; Champness, N. R.; Schröder, M. *J. Am. Chem. Soc.* **2009**, *1331*, 2159−2171.

(9) Pinner, A.; Liebig, J. *Ann. Chem.* **1897**, *297*, 221−271.

(10) Cutivet, A.; Leroy, E.; Pasquinet, E.; Poullain, D. *Tetrahedron Lett.* **2008**, *49*, 2748−2751.

(11) Kaszynski, P.; Young, V. G. *J. Am. Chem. Soc.* **2000**, *122*, 2087−2090.

(12) Crystal data for **1** ($C_{20}H_{22}N_4O_6S_3$), M = 478.56, triclinic, space group $P\bar{1}$, a = 6.3054(6) Å, b = 8.0715(9) Å, c = 11.4005(13) Å, α = 73.397(7)°, β = 82.195(7)°, γ = 85.851(7)°, V = 550.53(10) Å^3, Z = 1, ρ_{calcd} = 1.443 g·cm^{-3}, μ(Mo Kα) = 0.287 mm^{-1}, R1(F_o) = 0.0598, and wR2(F_o^2) = 0.1468 with a GOF on F^2 = 1.015. Crystal data for **2** ($C_{16}H_{10}N_4O_5Zn$): M = 403.67, monoclinic, space group $P2_1/n$, a = 7.247(4) Å, b = 6.814(4) Å, c = 29.631(17) Å, β = 90.015(9)°, V = 1463.3(15) Å^3, Z = 4, ρ_{calcd} = 1.832 g·cm^{-3}, μ(Mo Kα) = 1.72 mm^{-1}, R1(F_o) = 0.0495, and wR2(F_o^2) = 0.1113 with a GOF on F^2 = 1.02. Crystal data for **3** ($C_{24}H_{12}N_6O_{10}La$): M = 683.31, monoclinic, space group $P2_1/c$, a = 5.1474(10) Å, b = 18.232(4) Å, c = 26.783(5) Å, β = 90.08(3)°, V = 2513.5(9) Å^3, Z = 4, ρ_{calcd} = 1.806 g·cm^{-3}, μ(Mo Kα) = 1.771 mm^{-1}, R1(F_o) = 0.0727, and wR2(F_o^2) = 0.1677 with a GOF on F^2 = 1.034. Data were collected by ω and ψ scans on a Bruker APEXII diffractometer with graphite-monochromated Mo Kα radiation (λ = 0.71073 Å). The structures were solved by direct methods and refined on F^2 by the *SHELX-97* program.

(13) (a) Aldridge, S.; Downs, A. J. *The Group 13 Metals Aluminium, Gallium, Indium and Thallium*; John Wiley & Sons: New York, 2011. (b) Rodríguez-Diéguez, A.; Salinas-Castillo, A.; Sironi, A.; Seco, J. M.; Colacio, E. *CrystEngComm* **2010**, *12*, 1876−1879. (c) Tan, B.; Xie, Z.-L.; Feng, M.-L.; Hu, B.; Wu, Z.-F.; Huang, X.-Y. *Dalton Trans.* **2012**, *41*, 10576−10584.

(14) (a) Gelb, L. D.; Gubbins, K. E. *Langmuir* **1999**, *15*, 305. (b) Düren, T.; Millange, F.; Férey, G.; Walton, K. S.; Snurr, R. Q. *J. Phys. Chem. C* **2007**, *111*, 5350−5357.

(15) Calahorro, A. J.; López-Viseras, M. E.; Salinas-Castillo, A.; Fairen-Jimenez, D.; Colacio, E.; Cano, J.; Rodríguez-Diéguez, A. *CrystEngComm* **2012**, *14*, 6390−6393.

(16) (a) Chen, B.; Ma, S.; Zapata, F.; Fronczek, F. R.; Lobkovsky, E. B.; Zhou, H. C. *Inorg. Chem.* **2007**, *46*, 1233−1236. (b) Xue, M.; Ma, S.; Jin, Z.; Schaffino, R. M.; Zhu, G. S.; Lobkovsky, E. B.; Qiu, S. L.; Chen, B. L. *Inorg. Chem.* **2008**, *47*, 6825−6828.

Polyhedron 52 (2013) 315–320

Contents lists available at SciVerse ScienceDirect

Polyhedron

journal homepage: www.elsevier.com/locate/poly

Novel 3D lanthanum oxalate metal-organic-framework: Synthetic, structural, luminescence and adsorption properties

Antonio J. Calahorro [a], David Fairen-Jiménez [b], Anfonso Salinas-Castillo [c], Marta E. López-Viseras [a], Antonio Rodríguez-Diéguez [a,*]

[a] Departamento de Química Inorgánica, Universidad de Granada, 18071 Granada, Spain
[b] Institute for Materials and Processes, School of Engineering, The University of Edinburgh, United Kingdom
[c] Departamento de Química Analítica, Universidad de Granada, 18071 Granada, Spain

ARTICLE INFO

Article history:
Available online 23 September 2012

Keywords:
Hydrothermal
MOF
Luminescence properties
Adsorption

ABSTRACT

The hydrothermal reaction of $La(NO_3)_3$ with 2-pyrimidinecarbonitrile in water yields a 3D metal-organic coordination framework $[La_2(ox)_3(H_2ox)(H_2O)_2](H_2O)_8$ (**1**) (ox = oxalate). This compound has channels with hosted water molecules inside and shows an intense photoluminescence emission at room temperature in the solid state. Due to the great channels that this compound possesses we have analyzed the experimental and simulated adsorption properties. This is one of the few examples of three-dimensional lanthanum polymers based only on oxalate ligand.

1. Introduction

In recent years, a great deal of attention has been paid to metal-organic frameworks (MOFs) due to their intrinsic properties [1]. Although most of these systems have been synthesized by controlled mixing of suitable soluble molecular components, solvothermal conditions have provided increasing success in alternative pathways to the preparation of single-crystalline supramolecular solids, including metal-organic coordination networks and hydrogen-bonded systems. Among others, the design and study of Ln-based MOF has evolved enormously [2] because of their interesting structures and potential applications in fields such as magnetism [3], luminescence [4], gas adsorption [5], sensing and optical storage [6]. Three-dimensional coordination compounds have been commonly prepared through a bottom-up approach, connecting lanthanide ions with the appropriate bridging ligands. In this way, there is still a great interest in the search for bridging ligands, which can produce new materials with intriguing structures and physical properties. Oxalate anion ($C_2O_4^{2-}$, ox) has been extensively used as bridging ligand to construct a great variety of multidimensional polynuclear complexes that exhibit interesting structures and physical properties (magnetic, magneto-optical, magnetic conductor, superconductor, etc.) [7]. Although numerous examples of 2D and 3D oxalate-bridged metal complexes exist, only a few of them are three-dimensional lanthanum systems based only on oxalate [8]. On the other hand, we have recently demonstrated the use of hydrothermal syntheses to generate *in situ* new ligands [9]. A similar process has been shown to occur for pyrimidine-2-carboxamide-oxime [10], 5-pyrimidyltetrazole [11], pyrimidine-4,6-dicarboxylate ligand [12] and pyridine-2-carboxylic acid [13] species, which react with metal ions under hydrothermal conditions to afford oxalate-bridged polymeric complexes. In this context, drastic hydrothermal conditions have been employed to obtain novel metal-organic frameworks containing oxalate bridges generated *in situ* from the decomposition and oxidation of 2-pyrimidinecarbonitrile with the aim of studying the physical properties of the isolated species (Scheme 1).

As a contribution to this field, we report herein on the synthetic, structural, luminescence and adsorption properties of this novel 3D-polymer of formula: $[La_2(ox)_3(H_2ox)(H_2O)_2](H_2O)_8$. The compound shows intense photoluminescence at room temperature in solid state. Experimental adsorption studies, backed up by grand canonical Monte Carlo simulations, have been realized to study its porous properties.

2. Experimental and simulation procedures

2.1. General

All analytical reagents were purchased from commercial sources and used without further purification.

2.2. Preparation of $[La_2(ox)_3(H_2ox)(H_2O)_2](H_2O)_8$

A mixture of $La(NO_3)_3{\cdot}x$H2O (0.097 g, 0.300 mmol), 2-pyrimidinecarbonitrile (0.054 g, 0.450 mmol) and distilled water

* Corresponding author. Tel.: +34 958243236.
E-mail address: antonio5@ugr.es (A. Rodríguez-Diéguez).

0277-5387/$ - see front matter © 2012 Elsevier Ltd. All rights reserved.
http://dx.doi.org/10.1016/j.poly.2012.09.018

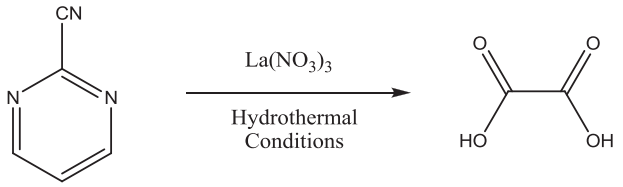

Scheme 1. "*In situ*" formation of oxalate ligand in compound **1** by hydrothermal routes.

Table 1
Crystallographic data and structural refinement details.

Compound	**1**
Chemical formula	$C_8H_{22}La_2O_{26}$
CCDC	884936
M (g mol^{-1})	812.08
T (K)	293
λ (Å)	0.71073
Crystal system	triclinic
Space group	$P\bar{1}$
Unit cell dimensions	
a (Å)	10.016(2)
b (Å)	11.380(3)
c (Å)	12.821(3)
α (°)	80.39(3)
β (°)	80.65(3)
γ (°)	66.34(3)
V (Å^3)	1312.3(5)
Z	2
ρ (g cm^{-3})	2.055
μ (mm^{-1})	3.315
Unique reflections	6323
R_{int}	0.085
Goodness-of-fit (GOF) on F^2	0.830
R_1[a] [$I > 2\sigma(I)$]	0.046
wR_2[a] [$I > 2\sigma(I)$]	0.096

[a] $R(F) = \sum||F_o| - |F_c||/\sum|F_o|$, $wR(F^2) = [\sum w(F_o^2 - F_c^2)^2/\sum wF^4]^{1/2}$.

(10 mL) was sealed in a Teflon-lined acid digestion autoclave and heated at 160 °C under autogenous pressure. After 24 h of heating, the reaction vessel was slowly cooled down to room temperature during a period of about 4 h. Colorless powder and yellow crystals of the compound under study were obtained. Yield: 64%, based on La. *Anal.* Calc. for $C_8H_{22}O_{26}La_2$: C, 11.83; H, 2.73. Found: C, 12.05; H, 2.81. IR data (KBr pellet τ/cm^{-1}): 442(m), 660(w), 826(m), 1404(s), 1580(m), 1633(s), 3064(w), 3213(s).

2.3. Elemental analysis

Elemental analysis was carried out on a Fisons-Carlo Erba analyser model EA 1108. The IR spectra on powdered samples were recorded with a ThermoNicolet IR200FTIR by using KBr pellets.

Table 2
Bond distances for La1 and La2 (Å).

La1 O2A	2.436(12)
La1 O2B	2.472(9)
La1 O1C	2.484(10)
La1 O1E	2.495(11)
La1 O2E	2.500(11)
La1 O1W	2.515(11)
La1 O3B	2.521(12)
La1 O4C	2.536(11)
La1 O3A	2.553(11)
La2 O2D	2.454(12)
La2 O4A	2.483(11)
La2 O2C	2.488(11)
La2 O3C	2.504(10)
La2 O1A	2.511(12)
La2 O4B	2.537(11)
La2 O1D	2.545(11)
La2 O1B	2.546(12)
La2 O2W	2.578(10)

2.4. Single-crystal structure determination

Suitable crystal of $[La_2(ox)_3(H_2ox)(H_2O)_2](H_2O)_8$ (**1**) was mounted on glass fiber and used for data collection. Data was collected using a Bruker AXS APEX CCD area detector equipped with graphite monochromated Mo Kα radiation (λ = 0.71073 Å) by applying the ω-scan method. The data was processed with APEX2 [14] and corrected for absorption using SADABS [15]. The structure was solved by direct methods using SIR97 [16], revealing positions of all non-hydrogen atoms. These atoms were refined on F^2 by a full matrix least-squares procedure using anisotropic displacement parameters (excluding C1B, C2B and O2B atoms) [17]. Hydrogen atoms pertaining to protonated oxalate (B) were located. Hydrogen atoms bonded to water molecules could not be reliably positioned. Attempts to identify the solvent molecules (water) failed. Instead, a new set of F^2 (hkl) values with the contribution from solvent molecules was obtained by the SQUEEZE procedure implemented in PLATON-94 [18]. Refinement reduced R_1 to 0.046. It should be noted that all crystals undergo a very fast degradation when they are removed from the mother liquor which has a high impact on the quality of the data. Several crystals of compound were measured and the structures were solved from the best data we were able to collect. Final $R(F)$, $wR(F^2)$ and goodness of fit agreement factors, details on the data collection and analysis can be found in Table 1.

2.5. Luminescence measurements

A Varian Cary-Eclipse Fluorescence Spectrofluorimeter solid sample holder accessory was used to obtain the fluorescence spectrum. The spectrofluorimeter was equipped with a xenon discharge

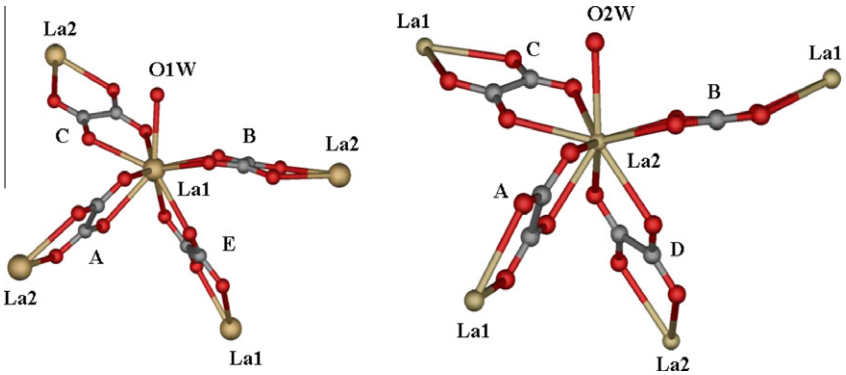

Fig. 1. Coordination environments of different lanthanum(III) ions in compound **1**. Metal centers are connected by different oxalate ligands (A, B, C, D and E).

Table 3
Bond angles for La1 and La2 (°).

O2A La1 O2B 74.2(4)	O2D La2 O4AC 135.7(4)
O2A La1 O1C 141.1(4)	O2D La2 O2C 93 6(4)
O2B La1 O1C 126.3(3)	O4A La2 O2C 77.6(4)
O2A La1 O1E 82.8(4)	O2D La2 O3C 70.0(4)
O2B La1 O1E 62.8(3)	O4A La2 O3C 136.5(3)
O1C La1 O1E 134.8(4)	O2C La2 O3C 64.6(4)
O2A La1 O2E 132.4(4)	O2D La2 O1A 71.7(4)
O2B La1 O2E 115.6(3)	O4A La2 O1A 64.4(4)
O1C La1 O2E 73.2(4)	O2C La2 O1A 70.7(4)
O1E La1 O2E 65.3(4)	O3C La2 O1A 117.5(4)
O2A La1 O1W 82.0(4)	O2D La2 O4B 126.8(4)
O2B La1 O1W 71.7(3)	O4A La2 O4B 72.5(4)
O1C La1 O1W 76.0(4)	O2C La2 O4B 139.7(4)
O1E La1 O1W 134.4(4)	O3C La2 O4B 125.2(4)
O2E La1 O1W 145.5(4)	O1A La2 O4B 117.2(4)
O2A La1 O3B 136.7(4)	O2D La2 O1D 64.6(4)
O2B La1 O3B 62.6(4)	O4A La2 O1D 94.0(4)
O1C La1 O3B 72.8(3)	O2C La2 O1D 138.9(4)
O1E La1 O3B 77.7(4)	O3C La2 O1D 128.5(4)
O2E La1 O3B 71.6(4)	O1A La2 O1D 69.5(4)
O1W La1 O3B 84.7(4)	O4B La2 O1D 70.5(4)
O2A La1 O4C 79.5(4)	O2D La2 O1B 75.7(4)
O2B La1 O4C 138.0(3)	O4A La2 O1B 1369(4)
O1C La1 O4C 63.6(4)	O2C La2 O1B 138.4(4)
O1E La1 O4C 144.7(4)	O3C La2 O1B 74.0(4)
O2E La1 O4C 106.3(4)	O1A La2 O1B 137.6(4)
O1W La1 O4C 72.7(4)	O4B La2 O1B 64.4(4)
O3B La1 O4C 134.4(4)	O1D La2 O1B 72.4(4)
O2A La1 O3A 64.7(4)	O2D La2 O2W 141.9(4)
O2B La1 O3A 123.1(3)	O4A La2 O2W 78.6(4)
O1C La1 O3A 110.3(4)	O2C La2 O2W 76.4(4)
O1E La1 O3A 74.2(4)	O3C La2 O2W 72.5(4)
O2E La1 O3A 72.9(4)	O1A La2 O2W 134.4(4)
O1W La1 O3A 133.9(4)	O4B La2 O2W 71.7(4)
O3B La1 O3A 141.4(4)	O1D La2 O2W 142.0(4)
O4C La1 O3A 70.6(4)	O1B La2 O2W 87.7(4)

lamp (peak power equivalent to 75 kW), Czerny–Turner monochromators, R-928 photomultiplier tube which is red sensitive (even 900 nm) with manual or automatic voltage controlled using the Cary Eclipse software for Windows 95/98/NT system. The photomultiplier detector voltage was 800 V and the instrument excitation and emission slits were set at 10 and 10 nm, respectively.

2.6. Gas adsorption procedures

N2 adsorption isotherm was recorded at 77 K using a Micromeritics ASAP 2020 instrument. Prior to the measurements, the sample was degassed at 383 K using a heating rate of 5 K min^{-1} for 18 h.

The adsorption of N_2 was also investigated using grand canonical Monte Carlo (GCMC) simulations [19]. We used an atomistic model for structure **1**, in which the framework atoms were kept fixed at the crystallographic positions. We used the standard Lennard–Jones (LJ) 12-6 potential to model the interatomic interactions between the framework and N_2. Apart from the LJ, we included electrostatic interactions between N_2 molecules. The parameters for the framework atoms were obtained from the UFF force field [20]. N_2 was modeled using the TraPPE potential with charges placed on each atom and at the center of mass [21]. The Lorentz–Berthelot mixing rules were employed to calculate fluid/solid parameters. Interactions beyond 18 Å were neglected. 10^7 Monte Carlo steps were performed, the first 40% of which were used for equilibration, and the remaining steps were used to calculate the ensemble averages. To calculate the gas-phase fugacity we used the Peng–Robinson equation of state [22].

3. Results and discussion

3.1. Structure and crystallographic results

Yellow crystals of compound **1** were obtained by hydrothermal reaction of $La(NO_3)_3$ with 2-pyrimidinecarbonitrile in 2:3 molar ratio. This compound crystallizes in the triclinic space group $P\bar{1}$. The crystal structure was determined by single-crystal X-ray crystallography (Table 1) and consists of a three-dimensional metal-organic framework with channels that propagate along the *a*, *b* and *c* crystallographic axes and hosted water molecules inside the channels. This complex is built up from the connection of lanthanum atoms with bischelating oxalate ligands (Fig. 1).

This oxalate anion can be obtained by conventional routes but, in this case, it has been synthesized from 2-pyrimidinecarbonitrile [9c]. The asymmetric unit has two different La^{3+} ions, three oxalate ligands, two half oxalates, two coordination water molecules, and

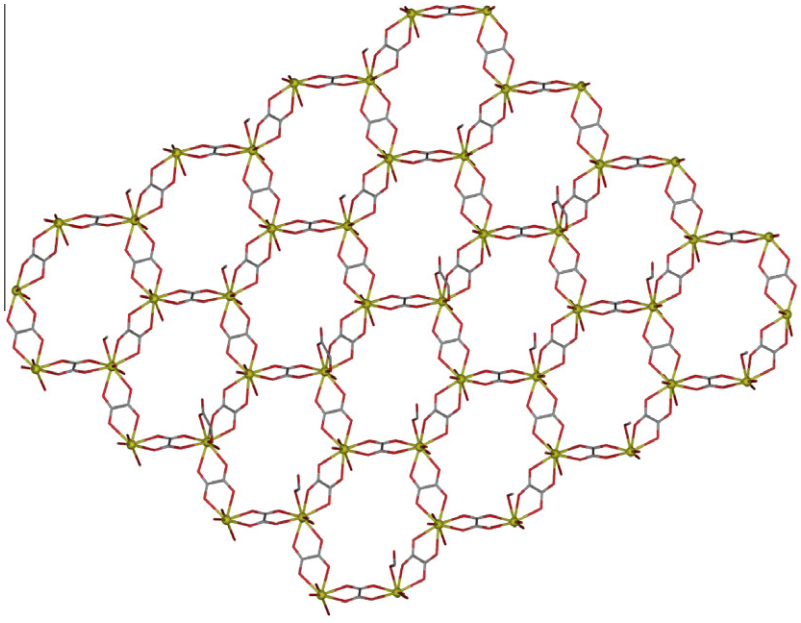

Fig. 2. View down the *c* axis of a layer of **1** and 6 metalmembered rings insides of two-dimensional sheets.

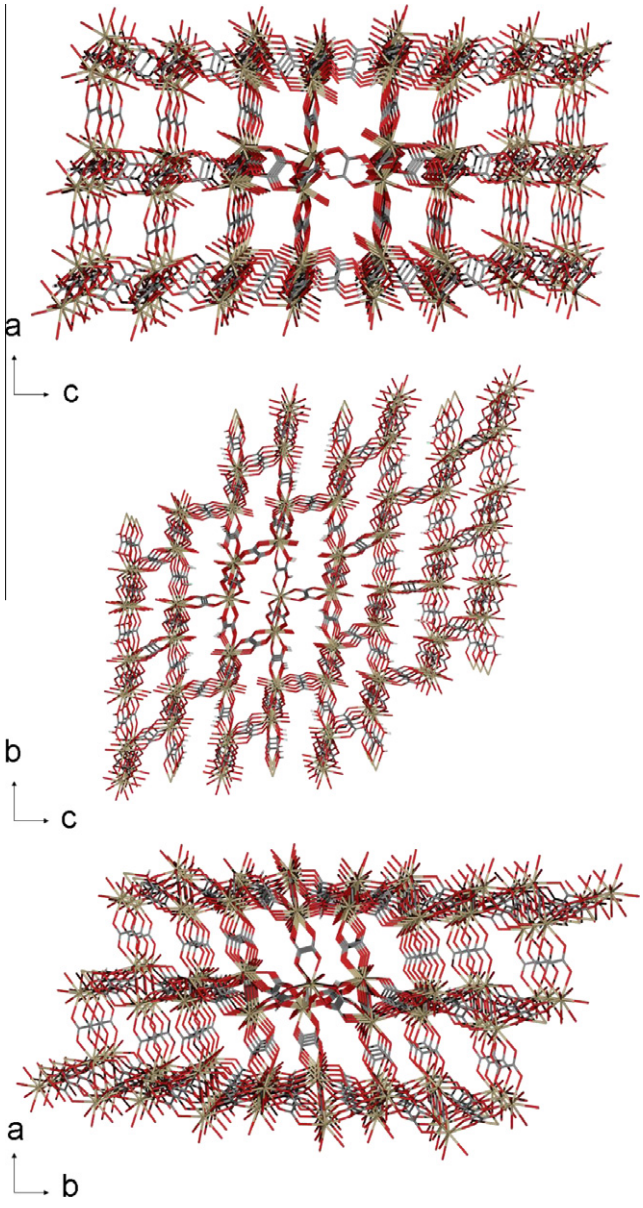

Fig. 3. View of the channels pertaining to 3D network of **1** in the *ac* (top), *bc* (middle) and *ab* (bottom) planes.

eight crystallization water molecules. The La^{3+} ions exhibit an unsymmetrical LaO9 coordination environment which is made of eight oxygen atoms from four oxalate ligands and one oxygen atom pertaining to one coordination water molecule. The coordination environments around the metal atoms are shown in Fig. 1. The La–O_{ox} bond distances are in the range 2.436(12)–2.553(11) Å and 2.454(12)–2.546(12) Å for La1 and La2, respectively. The La–O_{water} distances are 2.515(11) and 2.578(10) for La1 and La2, respectively. Bond distances and bond angles in the coordination sphere of La1 and La2 are listed in Tables 2 and 3, respectively.

The LaO9 coordination sphere is unsymmetrical and can be considered as intermediate between several nine-vertex polyhedra [23]. The coordination polyhedron of the lanthanum atom is a distorted mono-capped square antiprism, with O3A and O2W, the longer distances from the lanthanum, occupying the cap position with 2.553(11) and 2.578(10) Å, respectively. It should be noted that similar LaO9 coordination environments have been previously reported for the compound $[La(H_2O)(C_2O_4)_2]\cdot(CN_3H_6)$ [24]. The structure can be described of honey-comb layers bridged by oxalate ligands, parallel to the *ab* plane, constructed from alternately fused 6 metalmembered rings, in which metal centers are bridged by oxalate groups in a bisdidentate mode (Fig. 2). In these 2D layers, each lanthanum ion is coordinated to others three lanthanum ions by three oxalate-bridged ligands. In turn, these 2D layers are bridged by other oxalate in the *c* axis direction generating a three-dimensional polymer.

This compound has channels with hosted water molecules. These disorder water molecules generate a complicated hydrogen bond network in the channels (ESI, Fig. S2). There is a great structural disorder in the compound with these crystallization water molecules. Fig. 3 shows the channels generated in the *a*, *b* and *c* crystallographic axes, accounting for the 44% of the cell volume.

3.2. Luminescence properties

The emission spectrum of the compound **1** (Fig. 4) at room temperature in solid state displays strong blue fluorescent emission band at 450 nm under excitation at 330 nm [25,26]. The ox ligand exhibited no emission spectra when excited at 330 nm, which probably indicates that it is neither metal-to-ligand charge transfer nor ligand-to-metal charge transfer. As is well-known, the characteristic luminescence of La^{3+} should not lie at 450 nm [25]. So the observed emission at 450 nm may be connected with the oxide-to-La(III) absorption band (charge-transfer spin transition) [27]. The

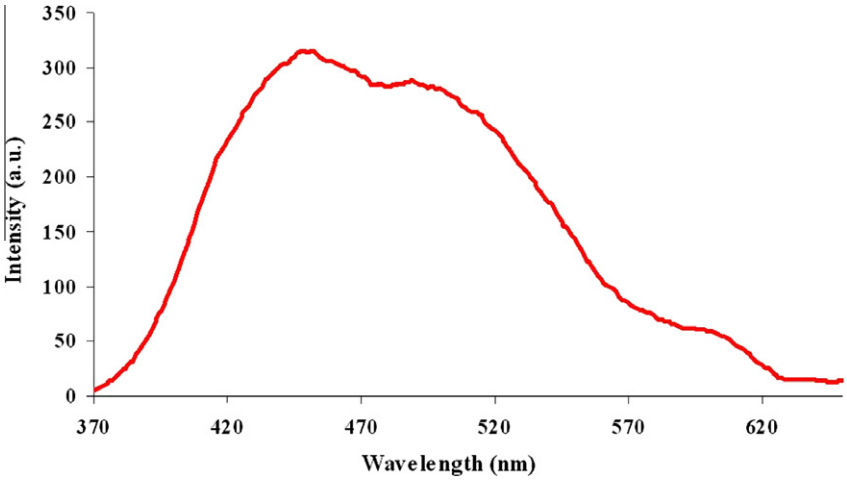

Fig. 4. Emission spectrum of compound $[La_2(ox)_3(H_2ox)(H_2O)_2](H_2O)_8$ at room temperature in the solid state. Horizontal axis: wavelength (nm); vertical axis: intensity (a.u.), λ_{ex} = 330 nm.

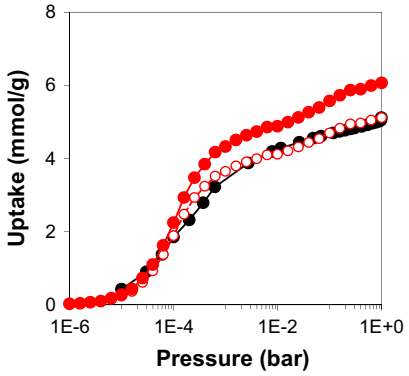

Fig. 5. Experimental, black closed circles, and simulated, red closed circles, N_2 isotherms at 77 K on **1**. Scaled ($\Phi = 0.85$) simulated isotherms, red open circles. Note the semilog scale in the representation. (Color online.)

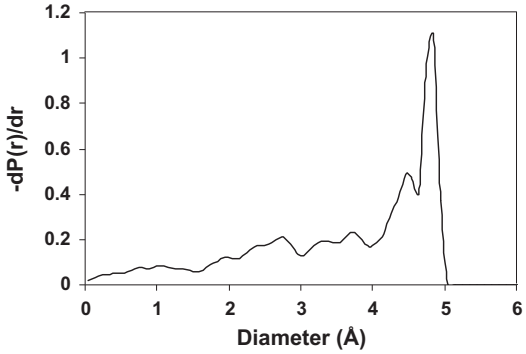

Fig. 6. Geometric pore size distribution of **1**.

high-dimensional condensed polymeric structure leads to significant enhancement of fluorescence intensity [28].

3.3. Adsorption properties

The porosity of structure **1** after solvent removal by heating under vacuum was determined by N_2 adsorption at 77 K (Fig. 5 and S1). Structure **1** presents a porous structure with a maximum uptake of 5.11 mmol/g. Grand canonical Monte Carlo (GCMC) simulation [18] of N_2 adsorption isotherm correctly describes the shape of the isotherm but slightly overpredicts the experimental capacity. The description of the experimental adsorption process is improved after applying a scaling factor (Φ) of 0.84, calculated as the ratio of the experimental and simulated maximum amounts adsorbed, on the simulated curve. The over-prediction in the simulations, performed on a perfect structure devoid of any porous defect, is generally explained by the existence of structural defects in the experimental sample that limits the micropore volume and the maximum capacity of the real solid [29]. Calculated BET surface areas on the experimental and simulated N_2 isotherms, using the consistency criteria suggested in the literature, correspond to 420 and 492 m^2/g, respectively.

Besides the N_2 adsorption isotherms, the geometric pore size distribution was calculated using a Monte Carlo technique which determines the diameter of the largest sphere that can fit into the cavities without overlapping with any of the framework atoms [30]. Fig. 6 shows that the maximum is localized around 4.8 Å of diameter.

4. Conclusions

We have succeeded in obtaining, via an hydrothermal method, a 3D channelled lanthanum MOF containing oxalate bridging ligand, the latter being generated *in situ* in the course of the hydrothermal reaction. This oxalate anion can be used by conventional routes but, in this case, it has been synthesized from 2-pyrimidinecarbonitrile. This MOF exhibits an intense blue photoluminescence emission at room temperature in the solid state and it represents one of the few examples of three-dimensional polymeric compounds based only on oxalate ligand. Calculated BET surface areas on the experimental and simulated N_2 isotherms, correspond to 420 and 492 m^2/g, respectively.

Acknowledgments

This work was supported by the Junta de Andalucía (FQM-4228) (A.J. Calahorro for a predoctoral grant). D.F.-J. thanks the European Commission for a Marie Curie Intra-European fellowship (PIEF-GA-2009-236665).

Appendix A. Supplementary data

CCDC 884936 contains the supplementary crystallographic data for (**1**). These data can be obtained free of charge via http://www.ccdc.cam.ac.uk/conts/retrieving.html, or from the Cambridge Crystallographic Data Centre, 12 Union Road, Cambridge CB2 1EZ, UK; fax: (+44) 1223-336-033; or e-mail: deposit@ccdc.cam.ac.uk. Supplementary data associated with this article can be found, in the online version, at http://dx.doi.org/10.1016/j.poly.2012.09.018.

References

[1] (a) A.C. Sudik, A.P. Cote, A.G. Wong-Foy, M. O'Keeffe, O.M. Yaghi, Angew. Chem. Int. Ed. 45 (2006) 2528;
(b) A. Kondo, H. Noguchi, H. Kajiro, L. Carlucci, P. Mercandelli, D.M. Proserpio, H. Tanaka, K. Kaneko, H. Kanoh, J. Phys. Chem. B 110 (2006) 25565;
(c) J.L.C. Rowsell, O.M. Yaghi, J. Am. Chem. Soc. 128 (2006) 1304;
(d) S.H. Jhung, J.-H. Lee, A.K. Cheetham, G. Ferey, J.S. Chang, J. Catal. 239 (2006) 97;
(e) M. Hong, Cryst. Growth Des. 7 (2007) 10;
(f) A. Vertova, I. Cucchi, P. Fermo, F. Porta, D.M. Proserpio, S. Rondinini, Electrochim. Acta 52 (2007) 2603;
(g) C. Janiak, Dalton Trans. 14 (2003) 2781;
(h) D. Braga, M. Polito, D. D'Addario, F. Grepioni, Cryst. Growth Des. 4 (2004) 1109;
(i) S.T. Hyde, O. Delgado-Friedrichs, S.J. Ramsden, V. Robins, Solid State Sci. (2006) 740.
[2] (a) F.A. Almeida Paz, J. Klinowski, Chem. Commun. (2003) 1484;
(b) D. Sun, R. Cao, Y. Liang, Q. Shi, M.J. Hong, Chem. Soc. Dalton Trans. (2002) 1847;
(c) D.-L. Long, A.J. Blake, N.R. Champness, C. Wilson, M. Schröder, Angew. Chem. Int. Ed. 40 (2001) 2444;
(d) L.G. Westin, M. Kritikos, A. Caneschi, Chem. Commun. (2003) 1012;
(e) C.-D. Wu, C.-Z. Lu, H.-H. Zhuang, J.-S. Hang, J. Am. Chem. Soc. 124 (2002) 3836;
(f) B.-Q. Ma, D.-S. Zhang, S. Gao, T.-Z. Jin, C.-H. Yan, G.-X. Xu, Angew. Chem. Int. Ed. 39 (2000) 3644.
[3] (a) A.H. Morrish, The Physical Principles of Magnetism, Wiley, New York, 1965;
(b) Z. Chen, B. Zhao, Y. Zhang, W. Shi, P. Cheng, Cryst. Growth Des. 8 (2008) 229.
[4] (a) D.T. de Lill, A. de Bettencourt-Dias, C.L. Cahill, Inorg. Chem. 46 (2007) 3960;
(b) K. Lunstroot, K. Driesen, P. Nockemann, C. Gorller-Walrand, K. Binnemans, S. Bellayer, J. Le Bideau, A. Vioux, Chem. Mater. 18 (2006) 5711;
(c) R. Shunmugam, G.N. Tew, J. Am. Chem. Soc. 127 (2005) 13567;
(d) N.L. Rosi, J. Kim, M. Eddaoudi, B.L. Chen, M. O'Keeffe, O.M. Yaghi, J. Am. Chem. Soc. 127 (2005) 1504;
(e) W.S. Liu, T.Q. Jiao, Y.Z. Li, Q.Z. Liu, M.Y. Tan, H. Wang, L.F. Wang, J. Am. Chem. Soc. 126 (2004) 2280.
[5] L. Pan, K.M. Adams, H.E. Hernandez, X. Wang, C. Zheng, Y. Hattori, K. Kaneko, J. Am. Chem. Soc. 125 (2003) 3062.
[6] (a) K. Kuriki, Y. Koike, Y. Okamoto, Chem. Rev. 102 (2002) 2347;
(b) C.L. Cahill, D.T. de Lill, M. Frisch, Cryst. Eng. Comm. 9 (2007) 15;
(c) O. Guillou, C. Daiguebonne, Handbook on the Physics and Chemistry of Rare Earths, vol. 34, Elsevier, Amsterdam, The Netherlands, 2005. pp. 5;

(d) R.J. Hill, D.L. Long, P. Hubberstey, M. Schroder, N.R.J. Champness, Solid State Chem. 178 (2005) 2414;
(e) J.C.G. Bünzli, C. Piguet, Chem. Soc. Rev. 34 (2005) 1048;
(f) A.Y. Robin, K.M. Fromm, Coord. Chem. Rev. 250 (2006) 2127;
(g) S. Faulkner, J.L. Matthews, Comprehensive Coordination Chemistry II, vol. 9, Elsevier, Oxford, UK, 2004. pp. 913;
(h) C. Piguet, J.-C.G. Bünzli, Chem. Soc. Rev. 28 (1999) 347;
(i) R. Gheorghe, P. Cucos, M. Andruh, J.P. Costes, B. Donnadieu, S. Shova, Chem. Eur. J. 12 (2005) 187.

[7] (a) S. Decurtins, R. Pellaux, A. Hauser, M.E. Von Arx, in: O. Kahn (Ed.), Magnetism: A Supramolecular Function, Kluwer, Dordrecht, 1996, p. 487;
(b) M. Pilkington, S. Decurtins, in: J.A. MacCleverty, T.J. Meyer (Eds.), Comprehensive Coordination Chemistry II, From Biology to Nanaotechnology, vol. 7, Elsevier, Amsterdam, 2004. pp. 177;
(c) M. Pilkington, S. Decurtins, Perspect. Supramol. Chem. 7 (2003) 275;
(d) R. Clément, S. Decurtins, M. Gruselle, C. Train, Monatsh. Chem. 134 (2003) 117. and references therein;
(e) H. Tamaki, Z.J. Zhong, N. Matsumoto, S. Kida, M. Koikawa, N. Achiwa, I. Hashimoto, H. Okawa, J. Am. Chem. Soc. 114 (1992) 6974;
(f) P.J. Day, J. Chem. Soc., Dalton Trans. (1997) 701;
(g) E. Coronado, J.R. Galán-Mascarós, C. Martí-Gastaldo, Inorg. Chem. 45 (2006) 1882;
(h) E. Coronado, J.R. Galán-Mascarós, C.J. Gómez-García, V. Laukhin, Nature 408 (2000) 447;
(i) D. Armentano, G.D. Munno, T.F. Mastroprieto, M. Julve, F. Lloret, J. Am. Chem. Soc. 127 (2005) 10778;
(j) E. Cariati, R. Macchi, D. Roberto, R. Ugo, S. Galli, N. Casati, P. Macchi, A. Sironi, L. Bogani, A. Caneschi, D. Gatteschi, J. Am. Chem. Soc. 129 (2007) 9410.

[8] S.-H. Huang, G.-D. Zhou, T.C.W. Mak, J. Crystallogr. Spectrosc. Res. 21 (1991) 127.

[9] (a) A. Rodríguez-Diéguez, J. Cano, R. Kivekäs, A. Debdoubi, E. Colacio, Inorg. Chem. 46 (2007) 2503;
(b) A. Rodríguez-Diéguez, A. Salinas-Castillo, A. Sironi, J.M. Seco, E. Colacio, CrystEngComm 12 (2010) 1876;
(c) A. Rodríguez-Diéguez, J. Seco, E. Colacio, Eur. J. Inorg. Chem. (2012) 203.

[10] A. Rodriguez-Dieguez, R. Kivekäs, H. Sakiyama, A. Debdoubi, E. Colacio, Dalton Trans. (2007) 2145.

[11] A. Rodríguez-Diéguez, E. Colacio, Chem. Commun. (2006) 4140.

[12] J. Cepeda, R. Balda, G. Beobide, O. Castillo, J. Fernández, A. Luque, S. Pérez-Yáñez, P. Román, D. Vallejo-Sánchez, Inorg. Chem. 50 (2001) 8437.

[13] J.Y. Lu, J. Macías, J. Lu, J.E. Cmaidalka, Cryst. Growth Des. 2 (2002) 485.

[14] Bruker Apex2, Bruker AXS Inc., Madison, Wisconsin, USA, 2004.

[15] G.M. Sheldrick, SADABS, Program for Empirical Adsorption Correction, Institute for Inorganic Chemistry, University of Göttingen, Germany, 1996.

[16] A. Altomare, M.C. Burla, M. Camilla, G.L. Cascarano, C. Giacovazzo, A. Guagliardi, A.G.G. Moliterni, G. Polidori, R. Spagna, J. Appl. Crystallogr. 32 (1999) 115.

[17] G.M. Sheldrick, SHELX97, Program for Crystal Structure Refinement, University of Göttingen, Göttingen, Germany, 1997.

[18] A.L. Spek, PLATON-94 (V-101094), A Multipurpose Crystallographic Tool, University of Utrecht, The Netherlands, 1994.

[19] D. Frenkel, B. Smit, Understanding Molecular Simulations: From Algorithms to Applications, second ed., Academic Press, San Diego, 2002.

[20] A.K. Rappé, C.J. Casewit, K.S. Colwell, W.A. Goddard, W.M. Skiff, J. Am. Chem. Soc. 114 (1992) 10024.

[21] J.J. Potoff, J.I. Siepmann, AIChE J. 47 (2001) 1676.

[22] R.C. Reid, J.M. Pausnitz, B.E. Poling, The Properties of Gases and Liquids, fourth ed., McGraw-Hill, Companies, New York, 1987.

[23] A. Ruiz-Martínez, D. Casanova, S. Álvarez, Chem. Eur. J. 14 (2008) 1291.

[24] Fabrice Fourcade-Cavillou, Jean-Christian Trombe, Solid State Sci. 4 (2002) 1199.

[25] P. Mahata, S. Natarajan, Inorg. Chem. 46 (2007) 1250.

[26] S.M. Ying, J.G. Mao, Cryst. Growth Des. 6 (2006) 964.

[27] Li. Zhang, W. Gu, B. Li, X. Liu, D.Z. Liao, Inorg. Chem. 46 (2007) 622.

[28] (a) D. Rendell, Fluorescence and Phosphorescence, Wiley, New York, 1987;
(b) C.M. Che, C.W. Wan, K.Y. Ho, Z.Y. Zhou, New J. Chem. 25 (2001) 63;
(c) L.-Z. Zhang, Y. Xiong, P. Cheng, G.-Q. Tang, L.-J. Wang, D.-Z. Liao, J. Mater. Chem. 11 (2001) 2903;
(d) Z.-P. Deng, S. Gao, L.-H. Huo, Appl. Organomet. Chem. 21 (2007) 978;
(e) Z.-P. Deng, S. Gao, Z.-B. Zhu, L.-H. Huo, Z. Anorg. Allg. Chem. 634 (2008) 593.

[29] A. Rossin, D. Fairen-Jimenez, T. Düren, G. Giambastiani, M. Peruzzini, J.G. Vitillo, Langmuir 27 (2011) 10124.

[30] L.D. Gelb, K.E. Gubbins, Langmuir 15 (1998) 305.

View Article Online
ARTICLE TYPE www.rsc.org/xxxxxx DOI: 10.1039/C3CE40869X

LUMINESCENCE AND MAGNETIC PROPERTIES OF THREE METAL-ORGANIC FRAMEWORKS BASED ON 5-(1*H*-TETRAZOL-5-YL)ISOPHTHALIC ACID LIGAND

Antonio J. Calahorro,[a] Alfonso Salinas-Castillo,[b] José Manuel Seco,[c] Javier Zuñiga,[d] Enrique Colacio[a] and Antonio Rodríguez-Diéguez.[a,*]

Received (in XXX, XXX) Xth XXXXXXXXX 200X, Accepted Xth XXXXXXXXX 200X
First published on the web Xth XXXXXXXXX 200X
DOI: 10.1039/b000000x

Three new metal-organic frameworks based on 5-(1H-tetrazol-5-yl)isophthalic acid complexes $\{[Cd_4(TZI)_2(OH)_2(H_2O)_4](H_2O)_6\}_n$ (1), $\{[Zn_2(TZI)(OH)(H_2O)_2](H_2O)\}_n$ (2) and $\{[Co_8(TZI)_3(OH)_5((N_3)_2(H_2O)_8](H_2O)_8\}_n$ (3) have been synthesized *in situ* by hydrothermal reactions of 5-cyano-1,3-benzenedicarboxylic acid ligand with cadmium, zinc and cobalt metallic(II) salts in presence of sodium azide in water. Compounds 1 and 2 display intense photoluminescence properties in the solid state at room temperature, while 3 exhibits an antiferromagnetic interaction between cobalt(II) ions with a J value of -3.8 cm^{-1}. *In situ* hydrothermal syntheses reveal new possibilities to formation on new MOFs to construct new materials with fascinating structures and potential applications.

Design of coordination polymers has attracted great attention, not only because of their interesting topological structures, but also for their potential applications in the fields of luminescence, gas adsorption, catalysis, magnetic behaviour and electrical conductivity.[1] In recent years, there has been increasing research interest in the synthesis of extended coordination frameworks by hydrothermal routes.[2] Metal–organic frameworks (MOFs) are an emerging class of crystalline three-dimensional materials. They are mostly constructed from clusters of transition-metal ions held in position in a lattice by ligation to organic molecules.[3] These systems, are currently attracting increasing attention not only due to their fascinating topologies but also due to their interesting applications in different areas of science. Amongst ligands, multidentate N or O-donor building-blocks have drawn extensive attention in the construction of these systems.[4] So far, considerable efforts have been devoted to the synthesis of unusual coordination polymers based on carboxylate and/or pyridine-based ligands.[5] On the other hand, 5-substituted 1H-tetrazoles have been shown to be very good polydentate bridging ligands for the formation of multidimensional coordination polymers exhibiting a great structural diversity, which is a consequence of their extensive ability bridging metal ion.[6] Recently, we have designed and prepared novel coordination polymers with different tetrazolate-pyrimidine derivative ligands, with interesting luminescent properties.[7] Moreover, we have demonstrated the use of hydrothemal syntheses to generate *in situ* new ligands.[8]

In this context, and as a part of our continuing studies on nitrogen derivative ligands with carboxylate groups, we present here the synthesis, structural aspects, luminescence properties and magnetic studies of three Metal-Organic-Frameworks, $\{[Cd_4(TZI)_2(OH)_2(H_2O)_4](H_2O)_6\}_n$ **(1),** $\{[Zn_2(TZI)(OH)(H_2O)_2](H_2O)\}_n$ **(2)** and $\{[Co_8(TZI)_3(OH)_5((N_3)_2(H_2O)_8](H_2O)_8\}_n$ **(3)** based on 5-(1*H*-tetrazol-5-yl)isophthalic acid ligand (H_3TZI). We have designed *in situ* by hydrothermal routes this linker because of its similarity to another as the benzene-1,3,5-tricarboxylate (BTC) ligand with which others authors have synthesized a lot of MOFs with interesting physical properties.[9] Moreover, TZI building-block has electron-donating N atoms inducing rich coordination modes and, in particular, is a good candidate for enhanced emissive properties. In our case, compounds **1** and **2** consist in 3D- and 2D-MOFs, respectively, and fluorescence analyses show that they exhibit intense purple photoluminescence in the solid state at room temperature. Otherwise, **3** is a three-dimensional coordination polymer that exhibits an antiferromagnetic interaction between cobalt(II) ions with a J value of -3.8 cm^{-1}.

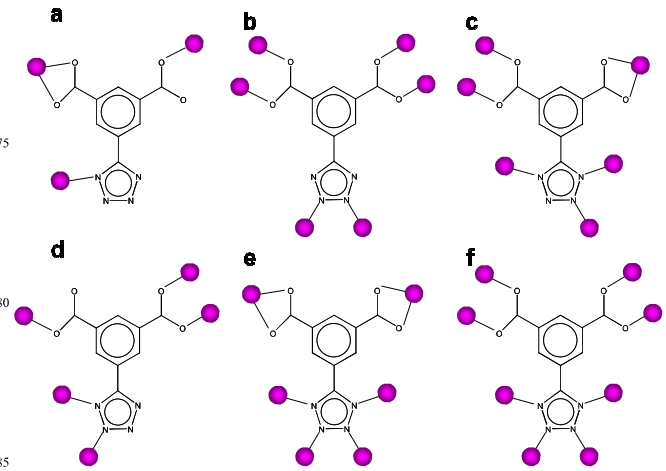

Scheme I. Coordination modes of TZI^{-3} ligand. *c*, *d*, *e* and *f* modes are novels and present in our compounds while *a* and *b* have been reported previously. Compound **1** and **2** exhibit *c* and *d* mode, respectively, while **3** shows *e* and *f* modes.

To the best of our knowledge, these are the first examples of crystal structures of MOFs with Cd(II), Zn(II) and Co(II) that contain the TZI^{-3} ligand. There are only two examples of Cu^{II}

View Article Online
DOI: 10.1039/C3CE40869H

(3D) and Gd^{III} (2D) coordination compounds in which TZI^{-3} shows *a* and *b* coordination modes (Scheme I).[10] Moreover, this is the first time that TZI^{-3} is synthesized *in situ* by hydrothermal conditions starting with cyanide derivative ligand (Demko–Sharpless reaction[11]) and the first examples of novel coordination modes of this linker (Scheme I, *c*, *d*, *e* and *f*). Describing the structures as SBU, in compounds **1** and **2**, a tetranuclear distorted dicubane $[M_4(OH)_2]$ SBU, where M is Cd and Zn is formed. However, in compound **3**, an octanuclear Co(II) SBU is formed, which according to a literature survey,[12] this octanuclear motif is reported for the first time in cobalt chemistry.

Hydrothermal reactions of the appropriate metal chloride (2 mmol) with 5-(1H-cyano-5-yl)isophthalic acid ligand (1 mmol) and sodium azide (1 mmol) in water (14 ml) at 140 ºC for 12 h followed by cooling down to room temperature over 2 h, yield prismatic yellow, colourless and red crystals of **1** (70% yield based on Cd), **2** (45% yield based on Zn) and **3** (30% yield based on Co), respectively. Crystal structures (see ESI, Table S1 and Figure S1) were determined by single crystal X-ray diffraction methods and found that both compounds exhibit fascinating and different structures.[13] Table S2 and S3 give the main bond lengths and angles of the structures.

Compound **1** is a three-dimensional coordination polymer in which the asymmetric unit is formed by four different cadmium atoms with very distorted octahedral coordination geometry, two TZI^{-3} ligands with heptadentate coordination mode (Scheme I, *c* mode), two tridentate OH^- anions, four coordination water molecules and six crystallization water molecules. Cd1 and Cd4 exhibit very distorted octahedral CdN_2O_4 geometries with the two nitrogen atoms belonging to two tetrazolate rings in *trans* positions, one OH^- anion and three oxygen atoms pertaining to two carboxylate groups from to two different TZI^{-3} ligands. Cd2 and Cd3 exhibit very distorted octahedral $CdNO_5$ geometries with the one nitrogen atom belonging to tetrazolate group in *trans* positions to one oxygen atom pertaining to carboxylate group, two OH^- anions and two coordination water molecules. Each triply deprotonated TZI^{-3} ligand connects with six cadmium ions, resulting in the formation of a 3D-MOF (Figure 1), in which each tetrazolate moiety also coordinates in a tridentate fashion to cadmium atoms (Scheme I, *c* mode). The network found in compound **1** is binodal (3,8) with tfz-d; UO3 topology, while compound **2** is a 2D net with kgd topology.

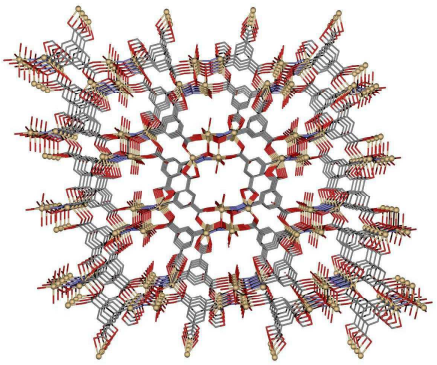

Figure 1. View down to the *a* axis in the three-dimensional network in **1**.

Compound **2** crystallises in the triclinic space group *P-1*, the asymmetric unit consisting of two different zinc ions, one TZI^{-3} ligand, one OH^- group, two coordination water molecules and one crystallization water molecule, all in general positions. Zn1 ion exhibits distorted octahedral $ZnNO_5$ geometry with the nitrogen atom belonging to tetrazolate ring in *trans* positions to one oxygen atom pertaining to carboxylate group, two water molecules and two oxygen atoms in *cis* positions pertaining to two different OH^- groups that make triple-bridge between two Zn1 and one Zn2 atoms. Zn2 ion exhibits distorted tetrahedral $ZnNO_3$ geometry with the nitrogen atom belonging to tetrazolate group, two oxygen atoms pertaining to two different carboxylate groups and one OH^- group. Each triply deprotonated TZI^{-3} ligand connects with five zinc ions, resulting in the formation of a 2D-MOF (Figure 2), in which each tetrazolate moiety also coordinates in a bidentate fashion (N1N2) to zinc atoms (Scheme I, *d* mode).

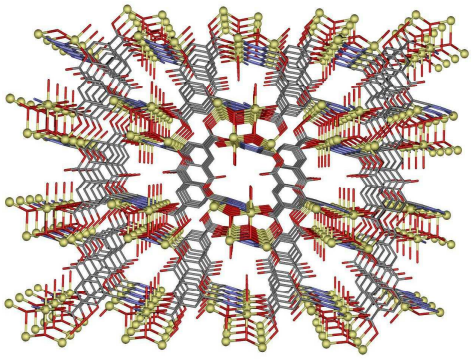

Figure 2. View down to the *a* axis in the three-dimensional network in **2**.

The 3D-MOF structure of **3** consists of a three-dimensional MOF with channels occupied by disordered solvent water molecules that propagate along *c* crystallographic axis. The crystalline structure can be described as helical Co(II) chains (Figure S2) along *a* direction connected by octadentate-bridging TZI^{-3} ligands (Scheme 1, *e* and *f* modes).

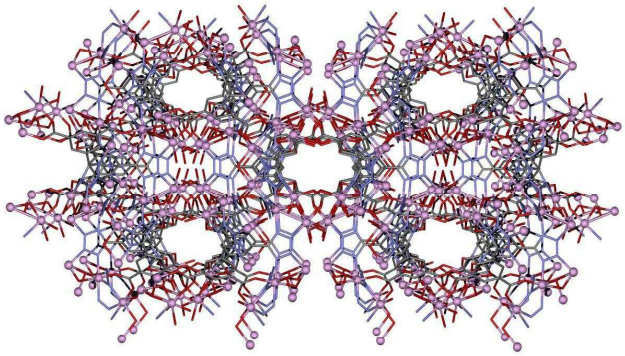

Figure 3. View down the *c* axis of the channels in the three-dimensional network of **3**. Colour code N = blue, O = red, C = grey and cobalt = dark blue.

Within the cobalt chains can be found hydroxy-bridged Co(II) trimers, dihydroxytetrazolate triply-bridged Co(II) dimers, hydroxy-ditetrazolate triply-bridged Co(II) dimers and azide-

View Article Online
DOI: 10.1039/C3CE40869H

tetrazolate-carboxylate triply-bridged Co(II) dimers. Co1 and Co2 exhibit distorted octahedral CdN_3O_3 geometries while Co3 and Co4 exhibit very distorted octahedral $CdNO_5$ polyhedron mainly due, for Co3, to the small bite angle of the carboxylate group pertaining to TZI^{-3} ligand and one triply-hydroxy-bridge between Co3 and Co4. It must be noted that, to the best our knowledge, it´s the first time that azide-tetrazolate-carboxylate triply-bridged Co(II) dimers have been shown. All these bridges afford the helical Co(II) chains that are bridged by triply deprotonated TZI^{-3} ligands generating the 3D network (Figure 3). The topological interpretation of compound **3** according to the literature[14] can be assigned as a complex 3D structure with rod-like shape packed along [100] or as a tetranodal (3,3,3,10) with Point Symbol {4.5.6}2{4^2.5^8.6^19.7^10.8^6}{5^2.6}2

Due to extended aromaticity and the presence of hexa-atomic rings, TZI^{-3} ligand is a good candidate for enhanced emissive properties. Due to this reason we decided to carry out a study of luminescent properties of coordination compounds **1** and **2**. The emission maximum of H_3TZI in solid state has been previously studied by Zhi-Rong *et al*.[15] and has a value of 389 nm, in good agreement with the emissions observed for a series of tetrazolate-carboxylic acid derivative ligands.[16] Using a 330 nm incident radiation, the emission spectrum of the cadmium and zinc MOFs (Figure S3) at room temperature in solid state exhibit intense emission bands centered about 460 and 450 nm, respectively, in concordance with those observed for other MOFs with these types of derivatives ligands.[17] The emission, assigned to intraligand π-π* transitions, is considerably red-shifted with respect to the ligand emission band.

The magnetic properties of compound **3** were measured in the 300-2 K and are given in the form $\chi_M T$ vs T (χ_M is the magnetic susceptibility per Co_8 unit) in Figure 4.

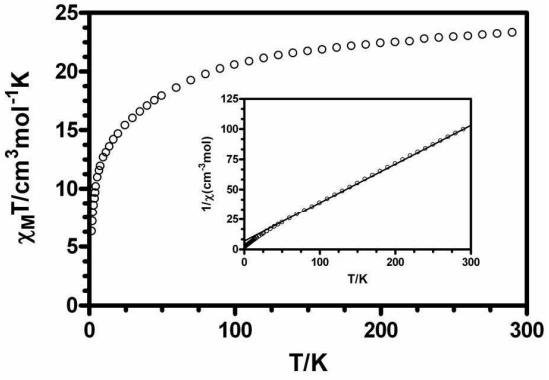

Figure 4.- Temperature dependence of the $\chi_M T$ product for **3**. Fit to the Curie-Weiss for data above 50 K (inset).

The $\chi_M T$ product at room temperature (23.44 emuKmol^{-1}) is very high when compared with the expected spin only value for eight cobalt(II) atoms of 15 emuKmol^{-1}, which is a consequence of the first order orbital contribution of the octahedral Co^{2+} with a $^4T_{1g}$ ground term. When the temperature is lowered, the $\chi_M T$ steadily decreases to reach a value of 6.29 at 2K. This behavior is due to the anisotropy, promoted by the spin-orbit coupling, of the octahedral Co^{2+} ions and to magnetic exchange between the Co^{2+} ions. The fact that the value at 2 K is much lower than that expected for eight isolated cobalt(II) ions (~13.6 emuKmol^{-1}) supports the existence of antiferromagnetic exchange interactions between the metal ions. Nevertheless, the AF interaction must be very weak as the χ_M vs T plot does not show any maximum above 2 K at none of the used magnetic fields (100 and 1000 Oe). Above T = 50 K the magnetic data can be fitted to a Curie–Weiss law with C =3.11 emuKmol^{-1} and θ = -6.9 K. The negative Weiss parameter can be used to estimate the value of the interaction by using the mean-field expression $\theta = zJS(S+1)/3k_B$, where z is the number of nearest neighbors, *J* is the magnetic exchange parameter, S is the spin angular momentum, and k_B is the Boltzmann constant. This yields zJ/ k_B = 5.5 K (-3.8 cm^{-1}). The *J* value is obviously overestimated as it accounts for the dominant anisotropy of the Co(II) ions and also for the magnetic exchange. The M vs H plot (Figure S4) shows a slow increase of the magnetization without reaching saturation at 5T. The value of the magnetization at 5 T (10.3 μB) is lower than that expected for eight cobalt(II) ions with effective spin S_{eff} = 1/2 (~16.8 μB), thus also confirming the presence of weak antiferromagnetic interaction in this compound.

In this work, we have shown that metal–organic frameworks with luminescent and magnetic properties can be synthesized by using the 5-(1H-tetrazol-5-yl)isophthalic acid igand. Compounds **1** and **2** consist in 3D- and 2D-MOFs, respectively, and fluorescent analyses show that they exhibit intense purple photoluminescence in the solid state at room temperature. **3** is a three-dimensional coordination polymer that exhibits an antiferromagnetic interaction between cobalt(II) ions. Work is in progress in our laboratory in order to obtain new homo- and heterometallic complexes to study their physical properties.

This work was supported by the MEC of Spain (Project CTQ2011-24478 and MINECO MAT2012-34740) and the Junta de Andalucía (FQM-4228) (A.J. Calahorro for a predoctoral grant).

a Departamento de Química Inorgánica, Universidad de Granada, 18071, Granada, Spain. Tel: 0034958240442; E-mail: antonio5@ugr.es
b Departamento de Química Analítica, Universidad de Granada.
c Departamento de Química Aplicada, Facultad de Químicas de San Sebastián, UPV/EHU, Paseo Manuel Lardizábal 3, 20018 San Sebastián.
d Dpto. de Física de la Materia Condensada, Facultad de Ciencia y Tecnología, UPV/EHU, 48080 Bilbao (Spain).

† CCDC reference numbers 928815 and 928816 for **2** and **3**, respectively. For crystallographic data in CIF format see DOI.

1.- (a) L. Hou L, D. Li, *Inorg. Chem. Commun*. 2005, **8**, 190; (b) S. L. Qiu, G. S. Zhu, Coord. *Chem. Rev*. 2009, **253**, 2891; (c) J.J. Perry IV, J. A. Perman, M. J. Zaworotko, *Chem. Soc. Rev*. 2009, **38**, 1400; (d) S. Natarajan, P. Mahata, *Chem. Soc. Rev*. 2009, **38**, 2304.
2.- (a) S. Kitagawa, R. Kitaura and S.-I. Noro, *Angew. Chem., Int. Ed*., 2004, **43**, 2334; (b) S. Kitagawa, K. Uemura, *Chem. Soc. Rev*., 2005, **34**, 109; (c) M. Yoshizawa, T. Kusukawa, M. Kawano, T. Ohhara, I. Tanaka, K. Kurihara, N. Niimura, M. Fujita, *J. Am. Chem. Soc*., 2005, **127**, 2798.
3.- T.R. Cook, Y.-R. Zheng and P.J. Stang, *Chem. Rev*. 2013, **113**, 734.
4.- (a) S.M. Humphrey, P.T. Wood, *J. Am. Chem. Soc*., 2004, **126**, 13236; (b) X.-M. Zhang, Y.-Z. Zheng, C.-R. Li, W.-X. Zhang, X.-M. Chen, *Cryst. Growth Des*. 2007, **7**, 980; (c) Y.-Q. Sun, J. Zhang, Y.-M. Chen, G.-Y. Yang, *Angew. Chem., Int. Ed*., 2005, **44**, 5814; (d) W.-G. Lu, C.-Y. Su, T.-B. Lu, L. Jiang, J.-M. Chen, *J. Am. Chem. Soc*., 2006, **128**, 34.
5. (a) S. S.-Y. Chui, S. M.-F Lo, J. P. H Charamant, A. G Orpen, I. D Williams, *Science* 1999, **283**, 1148; (b) C. N. R Rao, S Natarajan, R. Vaidhzanathan, *Angew. Chem., Int. Ed*. 2004, **43**, 1466.

View Article Online
DOI: 10.1039/C3CE40869H

6.- G. Aromi, L.A. Barrios, O. Roubeau, P. Gamez, *Coord. Chem. Rev.,* 2011, **255**, 485.
7.- A Rodríguez-Diéguez, A. Salinas-Castillo, S. Galli, N. Masciocchi, J. M. Gutiérrez-Zorrilla, P. Vitoria, E. Colacio, *Dalton Trans*. 2007 1821.
8.- A. Rodríguez-Diéguez, A. Salinas-Castillo, A. Sironi, J.M. Seco and E. Colacio, *CrystEngComm*, 2010, **12**, 1876.
9.- K. Schlichte, T. Kratzke, S. Kaskel, *Microporous Mesoporous Mater*. 2004, **73**, 81.
10.- F. Nouar, J.F. Eubank, T. Bousquet, L. Wojtas, M.J. Zaworotko, M. Eddaoudi, *J. Am. Chem. Soc*. 2008, **130**, 1833.
11.- Z.P.Demko and K.B.Sharpless, *J.Org.Chem*., 2001, **66**, 7945.
12 .- (a) M. Kurmoo, *Chem. Soc. Rev*. 2009, **38**, 1353; (b) M. Murrie, *Chem. Soc. Rev*. 2010, **39**, 1986; (c) G.E. Kostakis, S.P. Perlepes, V.A. Blatov, D.M. Proserpio, A.K. Powell, *Coord. Chem. Rev* 2012, **256**, 1246.
13.- Crystal Data. **1**: $[C_{18}H_{28}N_8O_{20}Cd_4]$, M = 1126.08, triclinic, space group *P-1*, a = 6.38383(12), b = 10.3778(15), c = 24.2312(12) Å, α = 100.651(9), β = 90.439(8), σ = 108.757(6), V = 1596.1(4) Å^3, Z = 2. **2**: $[C_9H_{10}N_4O_8Zn_2]$, M = 432.95, triclinic, space group *P-1*, a = 7.711(3), b = 8.959(3), c = 9.103(3) Å, α = 88.460(5), β = 88.793(4), σ = 74.567(5), V = 605.9(4) Å^3, Z = 2, ρ_{calcd} = 2.373 g cm^{-3}, μ(Mo-Kα) = 4.016 mm^{-1}, $R1(F_o)$ = 0.0415, ($wR2(F_o^2)$ = 0.1011) with a goodness-of-fit on F^2 1.033. **3**: $[C_{27}H_{46}N_{18}O_{33}Co_8]$, M = 1622.26, orthorhombic, space group *Pbcn*, a = 13.739(2), b = 24.301(3), c = 15.179(2) Å, V = 5067.8(12) Å^3, Z = 4, ρ_{calcd} = 2.126 g cm^{-3}, μ(Mo-Kα) = 2.671 mm^{-1}, $R1(F_o)$ = 0.0827, ($wR2(F_o^2)$ = 0.2059) with a goodness-of-fit on F^2 0.581. *More information, see ESI.*
14.- M. O´Keefe and O.M. Yaghi, Chem.Rev. 2012, **112**, 675.
15.- Z.-R. Qu, Z. Xing, B.-Z. Wu, X.-Z. Li and G.-F. Han, *Z. Anorg. Allg. Chem*. 2009, **635**, 39.
16.- (a) B. Yan, B. Zhou, J. *Photochem, Photobiol. A*, 2005, **171,** 181; (b) L. Zhao, P. Ren, Z. Zhang, M. Fang, W. Shi, P. Cheng, *Sci China Ser B-Chem*, 2009, **52**, 1479.
17.- J.-Y. Zhang, Y.-Q. Wang, H.-Q. Peng, A.-L. Cheng, E,-Q. Gao, *Struct Chem*., 2008, **19**, 535.

Chemical Communications

Dynamic Article Links ►

Cite this: DOI: 10.1039/c0xx00000x

www.rsc.org/xxxxxx

COMMUNICATION TYPE

Modular Structure of a Microporous MOF based on Cu_2 paddle-wheels with high CO_2 Selectivity

José M. Seco,[a] David Fairen-Jimenez,[b,*] Antonio J. Calahorro,[c] Laura Méndez-Liñán,[c] Manuel Pérez-Mendoza,[c] Nicola Casati,[d] Enrique Colacio[c] and Antonio Rodríguez-Diéguez[c,*]

Received (in XXX, XXX) Xth XXXXXXXXX 20XX, Accepted Xth XXXXXXXXX 20XX
DOI: 10.1039/b000000x

The synthesis of a new MOF with Cu_2 paddle-wheels connected to glutarate and 1,3-bis(4-pyridyl)propane) linkers has been explored. Experimental gas adsorption measurements reveal that the MOF is essentially non-porous to methane whereas it presents a Type III isotherm upon CO_2 adsorption, leading to high capacity and outstanding CO_2 selectivity.

The use of porous adsorbents (*e.g.* zeolites and activated carbons) in industrial separation and purification processes plays an important role in the global economy.[1] Extensive research has been performed to develop selective adsorbents for applications such as the purification of hydrogen and natural gas, mainly composed of methane, as well as carbon capture.[2] These efforts towards the development of these selective materials have turned in the last years to metal-organic frameworks (MOFs) due to their structural diversity and functional properties.[3] MOFs are obtained by the self-assembly of metal clusters and organic linkers, resulting in tailored nanoporous host materials. The high internal surface areas and large pore volumes make MOFs promising candidates for gas adsorption and separation applications.

Many adsorption isotherms of small gas molecules on MOFs at room temperature show the most common Type I (*i.e.* Langmuir) shape. However, some MOFs exhibit unusual adsorption behaviours, such as the existence of steps during the adsorption process. The existence of steps could be explained either by the sequential filling of the different cavities or adsorption sites of the structure,[4] especially at low temperature, or by the existence of flexible structures in the phenomena described as gate opening, breathing or swing effect (*e.g.* MIL-53 and ZIF-8).[5] In the latter flexible cases, the increase in pressure provokes structural changes that induce a modification in the pore shape and volume. On the other hand, unusual Type V (*i.e.* sigmoid) isotherms have been observed in the absence of structural changes during the adsorption of CO_2 and CH_4, as a result of relatively weak gas-MOF versus gas-gas interactions.[6]

The existence of isotherms with unusual shapes on MOFs, such as Type V, offers outstanding possibilities in the design of materials for gas storage and gas separation applications. When a gas is adsorbed, the adsorbent is regenerated by reducing the pressure. A good adsorbent for a "pressure-swing" process needs to have a high selectivity but also a high deliverable capacity, *i.e.* the difference between the amount adsorbed at the maximum adsorption pressure and the amount adsorbed at the regeneration pressure. As shown in Figure S2 at the Electronic Supplementary Information (ESI), an isotherm that is convex to the pressure axis but has a high capacity, such as Type III, has this feature. In order to obtain a material with high selectivity, we have recently explored the gas purification capabilities of a MOF constituted of 5-bromonicotinic acid linked to cobalt metal corners, demonstrating that it is possible to synthetize high selective materials by using classical ligands.[7] However, the narrow porosity of this MOF, which allows for molecular sieving of H_2/CH_4 mixtures, also implies low pore volumes and therefore low adsorption capacities. The design of a porous material with high pore volumes and molecular sieving behaviour with high selectivities remains an open issue.

In this work, we have designed the synthesis of a new MOF (**1**) with Cu_2 paddle-wheels connected to glutarate (glu) and 1,3-bis(4-pyridyl)propane (bpp) ligands. We believe that the conformational freedom of the glutarate ligand could promote the self-assembly of MOFs with novel topologies. Herein, we describe the synthesis,[8] crystal structure,[9] TG, high pressure X-ray experiments up to 4.5 GPa, gas adsorption properties and grand canonical Monte Carlo simulations of the MOF $[Cu_2(glu)_2(\mu\text{-bpp})]\cdot 2H_2O$ (**1**). This compound presents unexpected adsorption behaviour with Type I and Type III isotherms, for H_2 and CO_2, respectively, high CO_2/CH_4 selectivity and a high adsorption capacity.

Figure 1 shows the single-crystal XRD structure of **1**, solved in the space group *C2/c*. Table S1 lists selected bond distances and angles. The copper metal centre of the paddle-wheel adopts a slightly distorted square pyramidal coordination geometry with the bond angles only deviating slightly from 90º and 180º. The Cu(II) atom is bonded to four oxygen atoms of the bridging carboxylate groups pertaining to four different glutarate ligands (Cu–O = 1.907(6)–2.004(6) Å) in the basal plane. The Cu(II) atom is also bonded to one bpp ligand (Cu–N = 2.162(6) Å) in the axial position to complete the distorted square-pyramidal coordination geometry. In the structure, Cu_2 units are bridged by glutarate dianions to form a distorted 2D square grid, with Cu_2 units linked along the [011] and [01-1] directions. These 2D square grids are further pillared by bpp ligands extending from the axial sites of the Cu_2 paddle wheels along the [102] direction to form the MOF.

With a similar approach, Hwang *et al.* have recently published

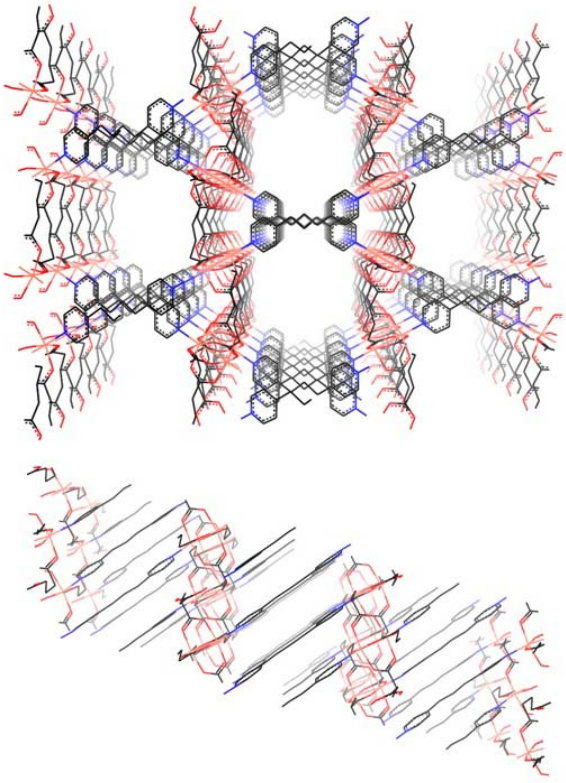

Figure 1. (*top*) Perspective view through the *c* axis of the channels in the three-dimensional network of **1** and, (*bottom*) through the *b* axis of the bpp pillars linking different sheets. Color code N = blue, O = red, C = black and Cu = orange. Hydrogen atoms have been omitted for clarity.

A MOF with the same metal ions and ligands but different solvent $[\{Cu_2(glu)_2(\mu\text{-bpp})\}\cdot(C_3H_6O)]_n$ (**2**).[10] In contrast to **1**, this structure presents a very different arrangement of the bpp ligands based in the tilt of the pyridyl fragments respect to the propane chain that interconnects them (Figure 2 and Figure S3). The dihedral angles between the pyridyl rings and the propane chain are 5.99º and 82.83º for **1** and **2**, respectively. The co-planarity showed in **1** causes the stacking of the bpp ligands in an "accordion" fashion along the *c* axis (Figure 1, bottom), an aspect that does not take place in **2**. We believe that this characteristic is fundamental for the behaviour of **1** in terms of gas adsorption.

We first analysed the porosity of **1** geometrically. Figure S4 shows the comparison of the pore size distribution (PSD) of **1** and **2**. Both structures present an open-porosity centred at *ca.* 6 Å, broad enough to be, in principle, accessible for gas adsorption. Indeed, Figure S5 shows the expected Type I isotherms found on **2** for both H_2 and CO_2. However, when running the experimental gas adsorption isotherms on **1**, we found that it was essentially non-porous to N_2 at 1 bar and 77 K. On the other hand, Figure 3 show how CO_2 and H_2 can access into the porosity when increasing the pressure up to 30 bar at 273 K and 77 K, respectively, whereas CH_4 (273 K) access remains impeded. More interesting is the shape of the isotherms: while the H_2 isotherm can be classified as a Type I, the CO_2 isotherm presents a Type III shape, and almost no adsorption up to 10 bar. In the studied conditions, **1** showed a maximum uptake of 2.24, 15.75 and 0.25 wt. % for H_2, CO_2 and CH_4, respectively. High H_2 and CH_4 selectivity in MOFs has been reported previously.[11]

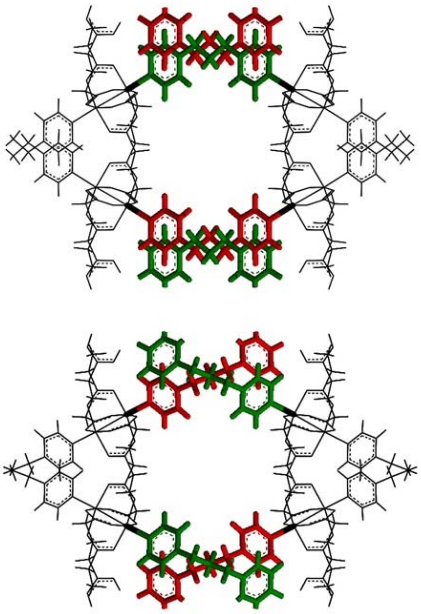

Figure 2. Differences between **1** (*top*) and **2** (*bottom*). Note the distinctive tilt in the pyridyl ligands respect to the propane chains that connect them. The different molecular fragments have been indicated in red and green for clarity.

However, and to the best of our knowledge, this is the first time that a microporous material, including not only MOFs but also zeolites and activated carbons, shows this behaviour. The existence of Type III isotherms generally implies a low interaction between the adsorbate (*i.e.* the gas molecules) and the adsorbent (*i.e.* the MOF).[12,6a] This could suggest that the interaction between **1** and CO_2 (Type III) is much lower compared to that of the H_2 (Type I). This idea is counterintuitive since the CO_2 molecules generally present higher interaction with an adsorbent due to the higher molecular weight and the presence of a strong quadrupole moment.

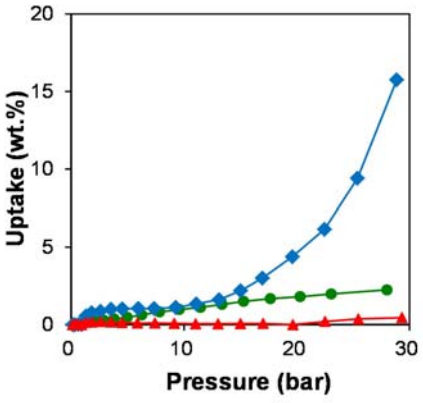

Figure 3. Adsorption isotherms on **1** obtained at 77 K (H_2, green circles) and 273 K (CO_2, blue diamonds; CH_4, red triangles).

A second possibility to this behaviour would be the existence of a molecular sieve effect, where the differences between the size of the H_2, CO_2 and CH_4 molecules play an important role in the diffusion of the gases through the porosity. In this case, a small molecule such as H_2 may diffuse through a narrow

porosity, whereas CH_4 and CO_2 are hindered. Only high pressures allow enough potential energy to either overdue the kinetic barrier in the diffusion, or to provoke a gate opening or breathing effect and therefore a structural change. This explanation is, however, not compatible with the relatively broad 6 Å porosity found in this material. Moreover, the use of gran canonical Monte Carlo (GCMC) simulations for CO_2 adsorption on a crystallographic rigid model, shown in Figure S5, confirms the goodness of the experimental maximum capacity value, but not the shape of the isotherm. Since GCMC simulations are in thermodynamic equilibrium, the existence of experimental kinetic barriers due to the presence of narrow porosity will not be detected using this technique. In a similar way, Feldblyum *et al.* were able to explain the disconnection between porous performance, as predicted by crystallography, and porous texture measured by gas adsorption.[13] Using positron annihilation lifetime spectroscopy, they explained these differences due to the presence of densified layers at the surface of the material, preventing the entry of small molecular species into the bulk porosity.

To analyse why MOFs **1** and **2** present a different behaviour regarding CO_2 adsorption, we studied the most flexible modes of the framework using a high pressure X-Ray diffraction study up to 4.5 GPa. Despite the possible conformational rearrangements, the bpp ligand in **1** remains stiff and largely unchanged throughout compression, while the glutarate-Cu moiety experiences a small but progressive distortion. The rearrangement of the distorted glutarate-Cu plane allows the bpp pillars to bend rigidly with respect to it, closing the 'accordion' and bringing different planes significantly closer, by shifting them laterally with respect to each other. As symmetry implies this is completely mirrored by a change in the beta angle. While this complex mechanism seems to be largely due to the flexibility of the Cu-glutarate paddle-wheel, in **2** the difference in the bpp conformation inhibits the distorted 2D layers from shifting with respect to each other and no flexibility can therefore be observed.

Further experimental work using *in situ* XRD to confirm the existence or not of structural changes during gas adsorption or the existence of densified surface layers or structural defects preventing the access to the porosity is in progress, with the aim of studying the mechanism of action of this metal-organic framework.

This work was supported by the Junta de Andalucía (FQM-4228) (A.J. Calahorro for a predoctoral grant) and the MEC of Spain (Project CTQ2011-24478). D. F-J. thanks the Royal Society for a University Research Fellowship.

Notes and references

[a]*Departamento de Química Aplicada, Facultad de Ciencias Químicas de San Sebastián, Universidad del País Vasco, Spain.*
[b]*Dept. of Chemical Engineering & Biotechnology, University of Cambridge, Pembroke Street, Cambridge CB2 3RA, United Kingdom. Email: df334@cam.ac.uk; website: http://people.ds.cam.ac.uk/df334*
[c]*Departamento de Química Inorgánica, Universidad de Granada, Avda Fuentenueva s/n, 18071, Granada, Spain. Email: antonio5@ugr.es*
[d]*Paul Scherrer Institute, WLGA/229, Villigen PSI, 5232, Switzerland.*

†Electronic Supplementary Information (ESI) available: [Synthesis of coordination compound **1**, X-ray collecting data and IR spectrum, bond distances and angles tables, pore size distribution, experimental gas adsorption, molecular simulations details and high-pressure X-ray diffraction]. See DOI: 10.1039/b000000x/. CCDC 941413-941417 contain the supplementary crystallographic data for this paper. These data can be obtained free of charge from The Cambridge Crystallographic Data Centre via www.ccdc.cam.ac.uk/data_request/cif.

1.- (a) B. Chen, S. Ma, F. Zapata, F.R. Fronczek, E.B. Lobkovsky and H.-C. Zhou, *Inorg.Chem*., 2007, **46**, 1233; (b) H.B.T. Jeazet, C. Staudt and C. Janiak, *Chem.Commun*, 2012, **48**, 2140; (c) H.Z.Chen and T.-S. Chung, *Int.J.HydrogenEnerg*, 2012, **37**, 6001.

2.- J. Shang, G. Li, R. Singh, Q. Gu, K.M. Nairn, T.J. Bastow, N. Medhekar, C.M. Doherty, A.J. Hill, J.Z. Liu and P.A. Webley, *J.Am.Chem.Soc,* 2012, **134**, 19246.

3.- H.-C. Zhou, J.R. Long and O.M. Yaghi, *Chem. Rev*. 2012, **112**, 673.

4.- J. Getzschmann, I. Senkovska, D. Wallacher, M. Tovar, D. Fairen-Jimenez, T. Düren, J.M. van Baten, R. Krishna and S. Kaskel, *Micropor.Mesopor.Mat*, 2010, **136**, 50.

5.- (a) K. Uemura, R. Matsuda and S. Kitagawa, *J. Solid State Chem*. 2005, **178**, 2420; (b) N.A. Ramsahye, G. Maurin, S. Bourrelly, P.L. Llewellyn, T. Loiseau, C. Serre and G. Ferey, *Chem.Commun*. 2007, 3261; (c) D. Fairen-Jimenez, S.A. Moggach, M.T. Wharmby, P.A. Wright, S. Parsons and T.J. Düren, *J.Am.Chem.Soc*. 2011, **133**, 8900.

6.- (a) D. Fairen-Jimenez, N.A. Seaton and T. Düren, *Langmuir,* 2010, **26**, 14694; (b) A.R. Millward and O.M. Yaghi,. *J. Am. Chem. Soc*. 2005, **127**, 17998.

7.- A.J. Calahorro, M.E. López-Viseras, A. Salinas-Castillo, D. Fairen-Jimenez, E. Colacio, J. Cano and A. Rodríguez-Diéguez*, Cryst.Eng.Comm*, 2012, **14**, 6390.

8.- Synthesis of $[Cu_2(glu)_2(\mu\text{-bpp})]\cdot 2H_2O$ (**1**). The reaction in water solvent of the copper sulfate (0.25mmol, 0.0628 g), glutaric acid (0.25 mmol, 0.033 g), urea (0.872 mmol, 0.054 g) and 1,3-bis(4-pyridyl)propane (0.25 mmol, 0.046 g) led to a blue solution, which kept at room temperature for one week gave rise to green crystals of complex **1**, which were filtered off and air-dried. Yield: 60%. Anal. Calc. for $C_{23}H_{26}Cu_2N_2O_8$: C, 47.18; H, 4.48; N, 4.78. Experimental: C, 47.05; H, 4.61; N, 4.83. FT-IR (KBr pellet): 3431 (brs), 2939 (m), 1611 (s), 1416 (s), 1313 (m), 1058 (w), 1019 (w), 817 (m), 643 (m) cm^{-1}.

9.- Crystal data: $C_{23}H_{26}Cu_2N_2O_8$, *fw* = 585.54 g mol^{-1}; monoclinic, *C2/c*, *a* = 28.265(5), *b* = 13.127(5), *c* = 8.729(5), β = 106.779(5), *V* = 3101(2) $Å^3$; *Z* = 4; T = 293 K; ρ_{calc} = 1.254 g cm^{-3}; *F*(000) = 1200; μ(Mo-Kα) = 1.411 cm^{-1}. Data collected on a Bruker Axs APEX automated diffractometer at RT, $R1(F_o)$ = 0.0326 ($wR2(F_o^2)$ = 0.0752) for 17018 unique reflections (R_{int} = 0.0865) with a goodness-of-fit on F^2 1.048. For both structures, data were collected by ωθv/2h scans ($2\theta_{max}$ = 56º) on a Bruker SMART CCD diffractometer with graphite-monochromated MoKα radiation (λ = 0.71073). The structures were solved by direct methods and refined on F2 by the SHELX-97 program.11 CCDC xxxxxx. See http://dx.doi.org/10.1039/xxxxxxx for crystallographic data in CIF or other electronic format.

10.- I.H. Hwang, J.M. Bae, W.-S. Kim, Y.D. Jo, C. Kim, Y. Kim, S.-J. Kim and S. Huh, *Dalton Trans.*, 2012, **41**, 12759.

11.- (a) B. Chen, S. Ma, F. Zapata, F. R. Fronczek, E. B. Lobkovsky and H.-C. Zhou, *Inorg. Chem.*, 2007, **46**, 1233; (b) M. Xue, S. Ma, Z. Jin, R.M. Schaffino, G. S. Zhu, E.B. Lobkovsky, S.L. Qiu andB. L. Chen, *Inorg. Chem.*, 2008, **47**, 6825.

12.- J. Rouquerol, F. Rouquerol, K.S.W. Sing, *Adsorption by Powders and Porous Solids*, Academic Press: San Diego, CA, 1999.

13.- J. I. Feldblyum, M. Liu, D. W. Gidley and A.J. Matzger. *J. Am. Chem. Soc*. 2011, **133**, 18257.

EurJIC European Journal of Inorganic Chemistry
ChemPubSoc Europe
FULL PAPER

DOI: 10.1002/ejic.201((will be filled in by the editorial staff))

BLUE-GREEN LONG LIFETIME PHOTOLUMINESCENCE EMISSION OF 3D CADMIUM METAL-ORGANIC FRAMEWORKS BASED ON THE 5-(4-PYRIDYL)TETRAZOLE LIGAND

Antonio J. Calahorro,[a] Alfonso Salinas-Castillo,[b] David Fairen-Jimenez,[c] Jose M. Seco,[d] Claudio Mendicute-Fierro,[d] Santiago Gómez-Ruiz,[e] Marta E. López-Viseras[a] and Antonio Rodríguez-Diéguez.[a,*]

Keywords: : Hydrothermal / Cadmium / MOF / Luminescence /

Three new metal-organic frameworks based on 5-(4-pyridyl)tetrazole have been synthesized by hydrothermal routes mixing this linker with cadmium(II) chloride in the presence of secondary ligands such as squaric acid, 4-carboxypyridine and terephtalic acid in water. Hydrothermal syntheses reveal new possibilities to rational formation on MOFs by mixtures of different linkers using the appropriate stoichiometry. These polymers exhibit blue-green long lifetime photoluminescence emission at room temperature in the solid state with long lifetime decays. Theoretical studies about pore size distribution and experimental gas adsorption studies have also been included.

[a] Departamento de Química Inorgánica, Universidad de Granada, 18071, Granada, Spain. Tel: 0034958240442; E-mail: antonio5@ugr.es
[b] Departamento de Química Analítica, Universidad de Granada18071, Granada, Spain.
[c] Dept. of Chemical Engineering & Biotechnology, University of Cambridge, United Kingdom.
[e] Departamento de Química Aplicada, Facultad de Ciencias Químicas de San Sebastián, UPV/EHU, 20018 San Sebastián (Spain).
[e] Departamento de Química Inorgánica y Analítica, Universidad Rey Juan Carlos, Móstoles, Madrid (Spain).

Introduction

In recent years, there has been an increasing research interest in the design and synthesis of extended coordination frameworks as multi-functional materials.[1] Metal−organic frameworks (MOFs), are attracting increasing attention not only due to their fascinating topologies but also because of their interesting applications in areas such as gas adsorption, catalysis, magnetic behaviour, non-linear optical activity and electrical conductivity.[2] The major task for the synthesis of these MOFs is to choose appropriate metal-connecting nodes and bridging ligands to get the desired porous properties. Amongst the most interesting ligands, multidentate N and O-donor bridging ligands have drawn extensive attention in the construction of these novel systems.[3] So far, considerable efforts have been devoted to the synthesis of unusual coordination polymers based on carboxylate and pyridine-based ligands,[4] while there are also many examples of synthetic materials derived from polydentate aromatic nitrogen heterocyclic ligands, such as pyrazoles, imidazoles, triazoles and tetrazoles.[5] In recent years, solvothermal conditions have provided increasing success in alternative pathways to the preparation of single-crystalline supramolecular solids, including metal–organic coordination networks and hydrogen-bonded systems. Nitrogen-based ligands have been shown to be excellent and versatile building blocks, with charge and multi-connectivity ability, to produce multidimensional coordination polymers under conventional and hydrothermal conditions.[6] Recently, we have designed and prepared novel MOFs with different pyrimidine derivate ligands showing interesting luminescent properties[7] as well as zeolitic imidazolate frameworks (ZIFs) with high pore volumes and extra-framework containing zinc imidazolate units on the internal surface.[8] On the other hand, many six- or seven-coordinated and some five- or eight-coordinated Cd(II) coordination polymers have recently received attention because of their excellent photoluminescence properties,[9] well beyond the interest raised by their new structural features. Moreover, the Cd(II) ion has a d^{10} configuration and the required softness that permits a wide variety of geometries and coordination numbers and that may allow the construction of non interpenetrating high-dimensional structures with good thermal stability.

In this context, and as a part of our ongoing studies on nitrogen ligands, we present here the synthesis, structural aspects, adsorption, theoretical studies and luminescence properties of three novel metal-organic frameworks based on 5-(4-pyridyl)tetrazole (Hptz), $[Cd_2(ptz)(squarate)(OH)(H_2O)_2]_n$ **(1),** $\{[Cd_2(ptz)(4\text{-carboxypyridine})(OH)_2]\cdot(H_2O)_2\}_n$ **(2)** and $\{[Cd_5(ptz)_2(terephtalate)_4(H_2O)_2]\cdot(H_2O)_2\cdot(CH_3OH)_4\}_n$ **(3)**.

We have designed these 3D-MOFs by using of secondary ligands with carboxylate groups such as, squarate and terephthalic acid, and 4-carboxypyridine generated *"in situ"* using 4-cyanopyridine by hydrothermal routes.

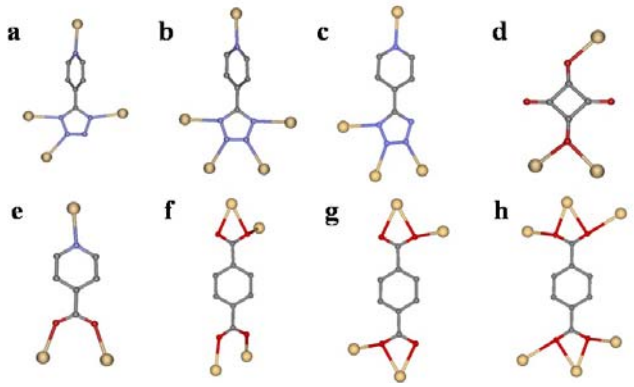

Scheme 1. Observed coordination modes for the ligands pertaining to compounds **1** (a, b), **2** (c, d) and **3** (e, f, g, h). Colour code N = blue, O = red, C = grey and Cd = tan.

We have chosen these tetrazolate/carboxylate derivative ligands because these building-blocks have aromatic rings and electron-donating N atoms inducing rich coordination modes and, in particular, are good candidates for enhanced emissive properties.

Results and Discussion

Hydrothermal reactions of cadmium chloride (2 mmol) with Naptz (1 mmol) and a secondary ligand (1 mmol) in water (14 ml) at 140 ºC for 12 h followed by cooling down to room temperature over 2 h, yield prismatic colourless crystals of **1** (40% yield) and **3** (50% yield), respectively. Compound **2** was obtained *in situ* by hydrothermal reaction of cadmium chloride (2 mmol) with 4-cyanopyridine (2 mmol) and sodium azide (1 mmol) in water (14 ml) at 140 ºC for 12 h. Colourless crystals of **2** (35% yield) were obtained. Crystal structures were determined by single crystal X-ray diffraction methods and found that both compounds exhibit fascinating and different 3D-MOF structures. Selected bond lengths and angles of the studied structures are given in Tables S1 and S2.

Description of the structures.

The crystal structure of **1** consists of a three-dimensional coordination polymer in which the asymmetric unit includes two crystallographically independent Cd^{2+} centers, one squarate anion (Scheme 1, *d* coordination), one ptz^- ligand, one OH-bridge anion and two coordination water molecules (Figure 1). Each cadmium atom adopts a very distorted octahedral coordination geometry.

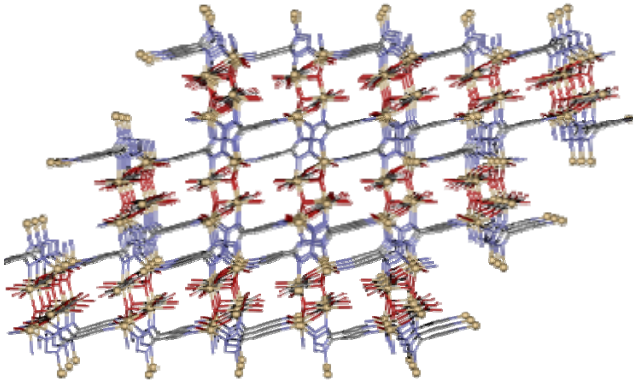

Figure 1. View of the 3D network of **1** in the *ac* plane.

The Cd1 atom has a CdN_3O_3 environment in *fac* disposition which is coordinated with one oxygen atom pertaining to one squarate dianion, three nitrogen atoms from three different tetrazolate groups (N2A, N4A and N9A), one oxygen atom (O1) from a OH^- anion and one water molecule. The Cd2 atom has a $CdNO_5$ environment and is coordinated to one N atom (N1A) of a tetrazolate group, two O atoms from two different squarate ligands in *trans* positions, two O1 atoms from two OH^- anions in *cis* positions and one water molecule (Figure 2). Although the ptz^- ligand has five N donors, only three N donors from the tetrazole ring and one N donor from the pyridyl ring bind to four Cd^{2+} centers (Scheme 1, *a* coordination). This coordination mode of the ligand has been shown only in compounds such as $[Cu_2(ptz)CN]_n$ and $\{Ag[\mu_4\text{-}(ptz)]\}_n$.[10]

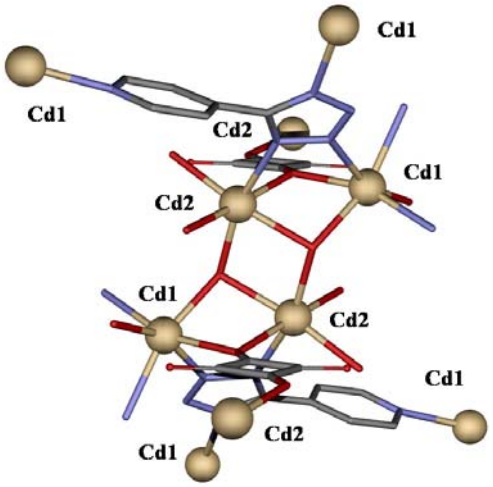

Figure 2. A view of the metal environment and coordination mode of the ligands for **1**.

Compound **2** is a three-dimensional coordination polymer (Figure 3) in which the asymmetric unit is formed by two different cadmium atoms with distorted octahedral fashion, one ptz^- ligand with a pentadentate-bridging coordination mode (Scheme 1, *b* coordination), one monodeprotonated tridentate-bridging 2-carboxypyridine (Scheme 1, *e*), one bridging-OH^- anion and one coordinated OH^- anion.

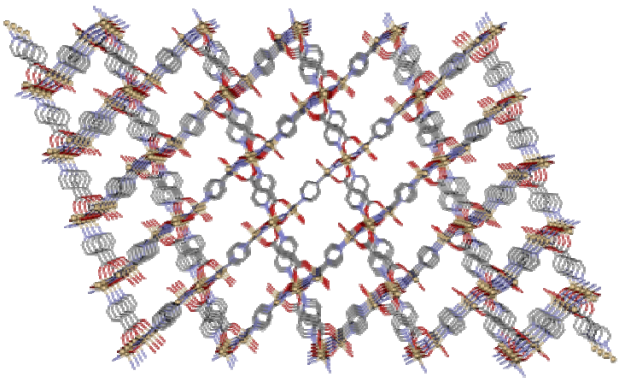

Figure 3. View down to the *b* axis in the three-dimensional network in **2**.

In this structure, Cd1 exhibits a distorted octahedral CdN_3O_3 geometry with three nitrogen atoms belonging to three different

tetrazolate groups, one hydroxy anion that make triple-bridge between one Cd1 and two Cd2 atoms, one terminal coordination OH^- anion and one oxygen atom pertaining to carboxylate group of 4-carboxypiridine ligand. Cd2 exhibits a distorted octahedral CdN_3O_3 geometry with three nitrogen atoms belonging to three different tetrazolate groups, two triple-bridge hydroxy anions and one oxygen atom pertaining to the carboxylate group of 4-carboxypiridine ligand (Figure 4). In this compound each tetrazolate moiety also coordinates in a tetra-dentate fashion to cadmium atoms (Scheme 1, *b* coordination). To the best of our knowledge, this is the second example reported in the literature in which all the N donors atoms of ptz^- ligand take part in the coordination of diverse ptz-based metal complexes.[11]

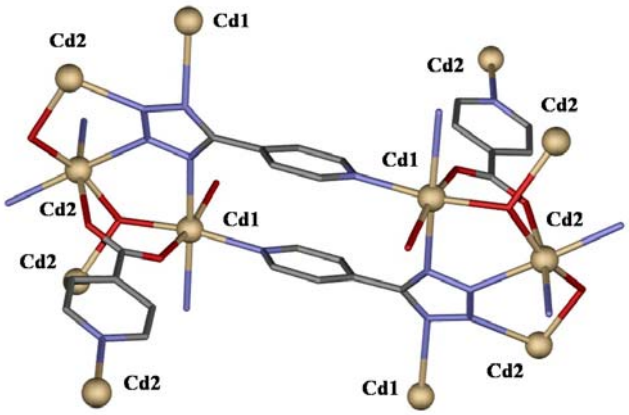

Figure 4. A view of the metal environment and coordination mode of the ligands for **2**.

The structure of **3** consists of a three-dimensional MOF with channels occupied by disordered solvent water molecules that propagate along the *a* crystallographic axis (Figure 5). The crystalline structure can be described as sheets formed by chains bridged by ptz^- ligands and generated by cadmium atom units by tetrazolates and carboxylates groups. These sheets are bridged by three different terephthalic ligands (Scheme 1, *f, g* and *h* modes) generating a three-dimensional coordination polymer with channels along *a* direction.

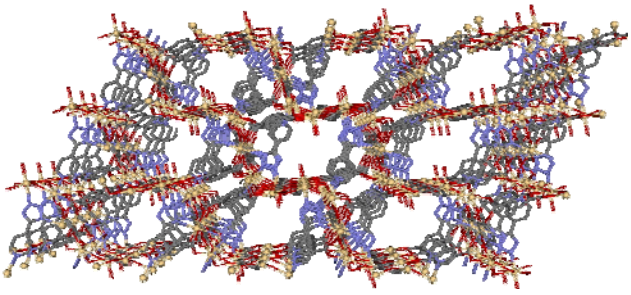

Figure 5. View of the channels pertaining to 3D network of **3** in the *a* direction.

In this polymer, there are three crystallographically independent Cd^{2+} centers. Cd1 atom adopts an octahedral coordination geometry with a CdN_2O_4 environment in which nitrogen atoms (N1A) pertaining to tetrazolates groups are in *trans* positions imposed by symmetry. The other four positions are occupied by oxygen atoms (O1B and O1D) of carboxylate groups pertaining to four different terephthalic ligands. The Cd2 atom has a pentagonal bipyramidal CdN_2O_5 geometry in which nitrogen atoms (N2A and N9A) of the tetrazolate and pyridine groups, respectively, are in *trans* position (Figure 6). In the equatorial plane the five positions are occupied by five oxygen atoms pertaining to carboxylate groups of different terephthalic ligands (O1D, O2D, O2B, O2C and O11B). Cd3 atom has a pentagonal bipyramidal $CdNO_6$ geometry. In this case, in the apical positions Cd3 has a nitrogen atom (N3A) of the tetrazolate group and one coordination water molecule. In the equatorial plane the five positions are occupied by five oxygen atoms (O1C, O1C, O2C, O11B and O12B) pertaining to carboxylate groups of different terephthalic ligands.

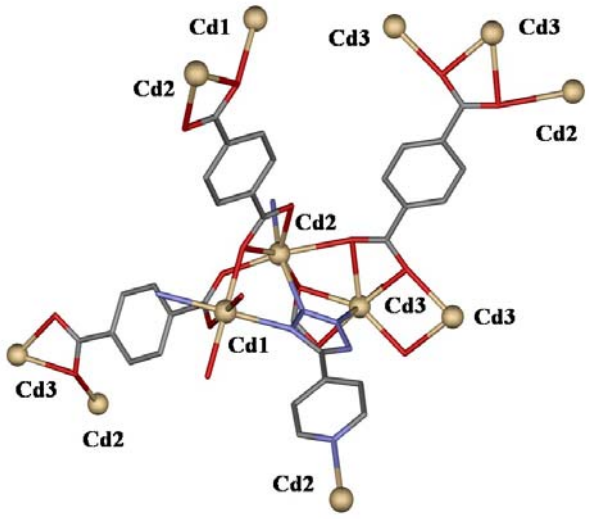

Figure 6. A view of the metal environment and coordination mode of the ligands for **3**.

Luminescence Properties.

Luminescence properties occupy a special ranking due to the potential applications of visible light emitters in a number of technologically advanced fields.[12] Thanks to its extended aromaticity due to the presence of hexa-atomic rings, pyridine derivative ligands are good candidates for enhanced emissive properties. For this reason we decided to carry out a study of the luminescent properties of these coordination compounds. The excitation and emission spectrum of the ligand 4-ptz at room temperature in solid state have previously been studied.[13]

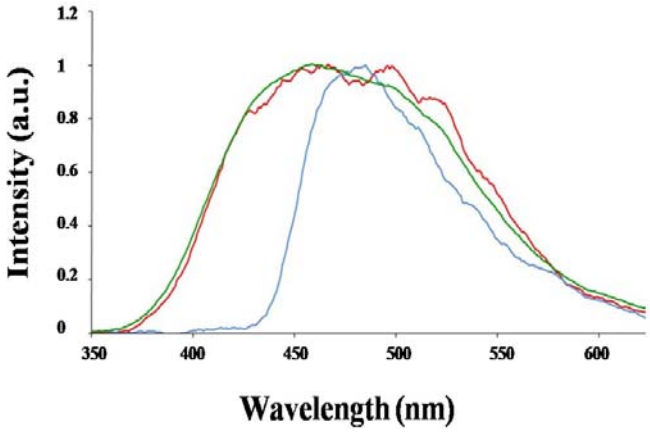

Figure 7. Emission spectra of **1** (blue), **2** (red) and **3** (green) at room temperature in solid state.

Using a 330 nm incident radiation (Figure 7), we observed intense emission bands at 485 nm (for **1**), 463 and 497 nm (for **2**) and 459 nm (for **3**). Previous reports about analogous cadmium complexes with azolate ligands showed similar intense bands attributed to ligand-to-ligand electronic transitions.[14] However, they were affected by the coordination of the ligand to the Cd(II) atoms. The decay curves (Figure S1) were fitted to mono exponential function: $I = I_0 + A_1 \exp(-t/\tau)$, where I and I_0 are the luminescent intensities at time t and 0, and $\tau$is defined as the luminescent lifetime. For this function, the best fit of the experimental luminescence intensities to the above equation led to lifetimes of 0.130, 0.093 and 0.083 ms for **1**, **2** and **3**, respectively.

Porous Texture.

The porous properties of compounds **1**, **2** and **3** were studied measuring their pore size distribution (PSD) in a Monte Carlo simulation. We have previously used this technique as a fast and simple method to obtain information about the existence of micro- and meso- porosity in crystalline structures, as well as their potential to be adsorbents.[15] PSD analysis represented in Figure 8 shows the existence of well-defined small cavities localised at 5.35, 6.25 and 7.45 Å for **1**, **2** and **3**, respectively. However, the experimental analysis of their adsorption properties using N_2 at 77 K at low pressures revealed that the porous structures collapses during the activation and degasification process at relatively high temperatures (Figure S2). Additionally, the adsorption of H_2 at 77 K and up to 100 bar on **3** revealed to be neglectible.

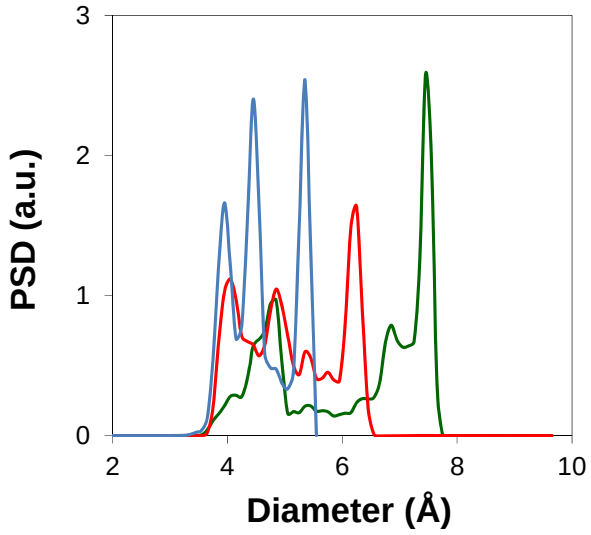

Figure 8. Pore size distribution of **1** (blue), **2** (red) and **3** (green).

Conclusions

In this work, we have shown that new three dimensional metal-organic frameworks with interesting properties can be synthesized by using classic ligands as 5-(4-pyridyl)tetrazole. The results reported in this paper clearly show that this is a versatile ligand which is able to afford a rich variety of polynuclear complexes with interesting structures. In addition, we have observed that all the studied new 3D-coordination polymers present a high structural diversity in which luminescence and adsorption properties have been studied. These polymers exhibit blue-green long lifetime photoluminescence emission at room temperature in the solid state with long lifetime decays. These results open the door toward the preparation of novel polymers based on this ligand, which could show fascinant physical properties, such as magnetism, luminescence and gases adsorption. Work is already in progress in our laboratory in order to obtain new homo- and heterometallic complexes with similar mixture of ligands containing carboxylate groups.

Experimental Section

General Procedures: Unless otherwise stated, all reactions were conducted by hydrothermal conditions, with the reagents purchased commercially and used without further purification.

Preparation of complexes.

$[Cd_2(ptz)(squarate)(OH)(H_2O)_2]_n$ (1): A mixture of $CdCl_2$ (366 mg, 2 mmol), 5-(4-pyridyl)tetrazole sodium salt (Naptz) (169 mg, 1 mmol), squaric acid (114 mg, 1 mmol) and water (14 mL) was sealed in a Teflon-lined acid digestion autoclave and heated at 140 °C under autogenous pressure. After 12 h of heating, the reaction vessel was cooled down to room temperature during a period of 2 h. Prismatic colorless crystals of **1** were obtained and were washed with H_2O. Yield: 41% based on Cd. Anal. Calcd for ($Cd_2C_{16}N_{10}O_7H_9$): C 28.20, H 1.33, N 20.57. Experimental: C 28.37, H 1.39, N 20.51. FT-IR (KBr pellet): 3425 (s), 1718 (w), 1605 (m), 1509 (s), 1466 (s), 771 (m), 735 (m) cm^{-1}.

$\{[Cd_2(ptz)(4\text{-carboxypyridine})(OH)_2]\cdot(H_2O)_2\}_n$ (2): A mixture of $CdCl_2$(366 mg, 2 mmol), 4-cyanopyridine (208 mg, 2 mmol), sodium azide (65 mg, 1 mmol) and water (14 mL) was sealed in a Teflon-lined acid digestion autoclave and heated at 140°C under autogenous pressure. After 12 h of heating, the reaction vessel was cooled down to room temperature during a period of 2 h. Prismatic colorless crystals of **2** were obtained and were washed with H_2O. Yield: 37% based on Cd. Anal. Calcd for ($Cd_2C_{12}N_6O_6H_{14}$): C 25.45, H 2.49, N 14.85. Experimental: C 25.35, H 2.41, N 14.97. FT-IR (KBr pellet): 3388 (s), 1622 (m), 1575 (s), 1450 (m), 1392 (s), 1244 (m), 1105 (w), 759 (m), 729 (m) cm^{-1}.

$\{[Cd_5(ptz)_2(terephtalate)_4(H_2O)_2](H_2O)_2\cdot(CH_3OH)_4\}_n$ (3): Compound 3 was prepared similar to that of compound **1**, but the terephthalic acid (166 mg, 1 mmol) was used instead of squaric acid. Prismatic colourless crystals of **3** were obtained and were washed with H_2O. Yield: 53% based on Cd. Anal. Calcd for ($Cd_5C_{48}N_{10}O_{23}H_{46}$): C 33.89, H 2.73, N 8.24. Experimental: C 33.99, H 2.76, N 8.21. FT-IR (KBr pellet): 3416 (m), 3128 (s), 1626 (m), 1544 (s), 1400 (s), 1219 (w), 1020 (m), 747 (m), 714 (m) cm^{-1}.

Physical measurements.

Elemental analyses were carried out at the "Centro de Instrumentación Científica" (University of Granada) on a Fisons-Carlo Erba analyser model EA 1108. IR spectra on powdered samples were recorded with a ThermoNicolet IR200FTIR using KBr pellets.

Single-Crystal Structure Determination.

Suitable crystals of **1-3** were mounted on a glass fibre and used for data collection on a Bruker AXS APEX CCD area detector equipped with graphite monochromated Mo Kα radiation (λ = 0.71073 Å) by applying the ω-scan method. Lorentz-polarization and empirical absorption corrections were applied. The structures were solved by direct methods and refined with full-matrix least-squares calculations on F^2 using the program SHELXS97.[16] Anisotropic temperature factors were assigned to all atoms except for hydrogen atoms, which are riding their parent atoms with an isotropic temperature factor arbitrarily chosen as 1.2 times that of the respective parent. Attempts to identify the solvent molecules (water and methanol) failed in compounds **2** and **3**. Instead, a new set of F^2 (hkl) values with the contribution from solvent molecules withdrawn was obtained by the SQUEEZE procedure implemented in PLATON-94.[17] Refinement reduced R_1 to 0.026 and 0.059 for **2** and **3**, respectively. Several crystals of **2** and **3** were measured and the structure was solved from the best data we were able to collect. Final R(F), wR(F^2) and goodness of fit agreement factors, details on the data collection and analysis can be found in Table 1. Selected bond lengths and angles are given in Tables S1 and S2 (ESI). CCDC reference numbers for the structures of **1-3** were 930225-930227. Copies of the data can be obtained free of charge upon application to CCDC, 12 Union Road, Cambridge CB2 1EZ, U.K. (fax, (+44)1223 336-033; e-mail, deposit@ ccdc.cam.ac.uk).

Table 1. Crystallographic Data and Structural Refinement Details for **1-3**

compound	1	2	3
chemical formula	$C_{10}H_9N_5O_7Cd_2$	$C_{12}H_{14}N_6O_6Cd_2$	$C_{96}H_{80}N_{24}O_{48}Cd_{16}$
CCDC	930225	930226	930227
M/gmol^{-1}	536.02	563.09	4136.24
T (K)	293	293	293
λ/Å	0.71073	0.71073	0.71073
cryst syst	monoclinic	monoclinic	triclinic
space group	*P21/c*	*C2/c*	*P-1*
a/ Å	13.1992(4)	27.9637(16)	10.102(4)
b/ Å	8.1755(3)	7.2809(4)	10.769(5)
c/ Å	17.2036(5)	19.2168(11)	16.709(7)
α/deg	90	90	108.150(5)
β/deg	129.854(2)	111.8870(10)	106.995(5)
γ/deg	90	90	110.535(4)
V/ Å^3	1425.15(8)	3630.5(4)	1443.5(10)
Z	4	8	1
ρ(g cm-3)	2.498	2.060	4.758
μ(mm-1)	3.033	2.384	5.962
Unique reflections	2804	9183	13794
R(*int*)	0.000	0.021	0.089
GOF on F^2	1.019	1.048	0.934
R1 [I > 2*σ*(*I*)]	0.043	0.026	0.059
wR2 [I > 2*σ*(*I*)]	0.075	0.074	0.132

[a] $R(F) = \sum||F_o| - |F_c||/\sum|F_o|$, $wR(F^2) = [\sum w(F_o^2 - F_c^2)^2/\sum wF^4]^{1/2}$

Luminescence measurements.

A Varian Cary-Eclipse Fluorescence Spectrofluorimeter was used to record the fluorescence spectra. The spectrofluorimeter was equipped with a xenon discharge lamp (peak power equivalent to 75 kW), Czerny-Turner monochromators, R-928 photomultiplier tube which is red sensitive (even 900 nm) with manual or automatic voltage controlled using the Cary Eclipse software for Windows 95/98/NT system. The photomultiplier detector voltage was 700 V and the instrument excitation and emission slits were set at 5 and 5 nm, respectively.

Computational Details.

The material was characterized geometrically, starting from the crystallographic coordinates. The pore size distributions were calculated using the method of Gelb and Gubbins, where the largest sphere that can fit in a random point within a structure without overlapping the van der Waals surface of the framework is recorded for a large number of random points.[18]

Supporting Information (see footnote on the first page of this article): Crystal Data, Luminescence Properties, N_2-Adsorption-Desorption Isotherm.

Acknowledgments

This work was supported by the MEC of Spain (Project CTQ2011-24478), the Junta de Andalucía (FQM-4228) (A.J. Calahorro for a predoctoral grant) and the Royal Society (UK) with a University Research Fellowship (D. F.-J.)..

[1] (a) S. Kitagawa, R. Kitaura, S. I. Noro, *Angew. Chem. In. Ed.* **2004**, *43*, 2334; S. Kitagawa, K. Uemura, *Chem. Soc. Rev.* **2005**, *34*, 109-119; (b) M. Eddaoudi, J. Kim, N. Rosi, D. Vodak, J. Wachter, M. O'Keeffe, O. M. Yaghi, *Science* **2002**, *295*, 469-472; (c) X. Lin, J. Jia, X. Zhao, K. M. Thomas, A. J. Blake, G. S. Walker, N. R. Champness, P. Hubberstey, M. Schroeder, *Angew. Chem. In. Ed.* **2006**, *45*, 7358-7364; (d) F. Nouar, J. F. Eubank, T. Bousquet, L. Wojtas, M. J. Zaworotko, M. Eddaoudi, *J. Am. Chem. Soc.* **2008**, *130*, 1833-1835; (e) S. Horike, S. Shimomura, S. Kitagawa, *Nature Chem.* **2009**, *1*, 695-704; (f) Z. Wang, S. M. Cohen, *Chem. Soc. Rev.* **2009**, *38*, 1315-1329; (g) H. Furukawa, N. Ko, Y. B. Go, N. Aratani, S. B. Choi, E. Choi, A. O. Yazaydin, R. Q. Snurr, M. O'Keeffe, J. Kim, O. M. Yaghi, *Science* **2010**, *329*, 424-428; (h) X. Liu, M. Oh, M. S. Lah, *Inorg. Chem.* **2011**, *50*, 5044-5053; (i) M. O'Keeffe, O. M. Yaghi, *Chem. Rev*. **2012**, *112*, 675-702.

[2] (a) P. Mahata, S. Natarajan, Eur. J. Inorg. Chem. **2005**, 2156-2163; (b) J. P. Zhang, X. M. Chen, *J. Am. Chem. Soc.* **2008**, *130*, 6010-6017; (c) L. J. Murray, M. Dinca, J. R. Long, *Chem. Soc. Rev.* **2009**, *38*, 1294-1314; (d) X. Gu, Z. H. Lu, Q. Xu, *Chem. Commun*. **2010**, *46*, 7400-7402; (e) T. K. Kim, M. P. Suh, Chem. Commun. **2011**, *47*, 4258-4260; (f) T. M. McDonald, W. R. Lee, J. A. Mason, B. M. Wiers, C. S. Hong, J. R. Long, *J. Am. Chem. Soc.* **2012**, *134*, 7056-7065; (g) E. C. Yang, Z. Y. Liu, X. Y. Wu, H. Chang, E. C. Wang, X. J. Zhao, *Dalton Trans.* **2011**, *40*, 10082-10089; (h) J. Ferrando-Soria, P. Serra-Crespo, M. de Lange, J. Gascon, F. Kapteijn, M. Julve, J. Cano, F. Lloret, J. Pasan, C. Ruiz-Perez, Y. Journaux, E. Pardo, *J. Am. Chem. Soc.* **2012**, *134*, 15301-15304; (i) D. Sarma, P. Mahata, S. Natarajan, P. Panissod, G. Rogez, M. Drillon, *Inorg. Chem.* **2012**, *51*, 4495-4501; (j) R. M. P. Colodrero, K. E. Papathanasiou, N. Stavgianoudaki, P. Olivera-Pastor, E. R. Losilla, M. A. G. Aranda, L. Leon-Reina, J. Sanz, I. Sobrados, D. Choquesillo-Lazarte, J. M. Garcia-Ruiz, P. Atienzar, F. Rey, K. D. Demadis, A. Cabeza, *Chem. Mater.* **2012**, *24*, 3780-3792.

[3] (a) Y. Q. Sun, J. Zhang, Y. M. Chen, G. Y. Yang, *Angew. Chem. Int. Ed.* **2005**, *44*, 5814-5817; (b) W. G. Lu, C. Y. Su, T. B. Lu, L. Jiang, J. M. Chen, *J. Am. Chem. Soc.* **2006**, *128*, 34-35; (c) A. Y. Robin, K. M. Fromm, *Coord. Chem. Rev.* **2006**, *250*, 2127-2157; (d) O. K. Farha, A. Oezguer Yazaydin, I. Eryazici, C. D. Malliakas, B. G. Hauser, M. G. Kanatzidis, S. B. T. Nguyen, R. Q. Snurr, J. T. Hupp, *Nature Chem.* **2010**, *2*, 944-948; (e) P. Maniam, N. Stock, *Inorg. Chem.* **2011**, *50*, 5085-5097; (f) Z. G. Gu, Y. T. Liu, X. J. Hong, Q. G. Zhan, Z. P. Zheng, S. R. Zheng, W. S. Li, S. J. Hu, Y. P. Cai, *Crystal Growth Des.*

2012, *12*, 2178-2186; (g) L. Qin, J. S. Hu, M. D. Zhang, Y. Z. Li, H. G. Zheng, *CrystEngComm.* **2012**, *14*, 8274-8279; (h) Y. X. Tan, Y. P. He, J. Zhang, *Cryst. Growth Des.* **2012**, *12*, 2468-2471.

[4] (a) C. N. R. Rao, S. Natarajan, Vaidhyanathan, R. *Angew. Chem. Int. Ed.* **2004**, *43*, 1466-1496; (b) M. Gustafsson, J. Su, H. Yue, Q. Yao, X. Zou, *Cryst. Growth Des.* **2012**, *12*, 3243-3249; (c) P. Zhang, B. Li, Y. Zhao, X. G. Meng, T. L. Zhang, *Chem. Commun.* **2011**, *47*, 7722-7724; (d) H. Sakamoto, R. Matsuda, S. Bureekaew, D. Tanaka, S. Kitagawa, *Chem. A Eur. J.* **2009**, *15*, 4985-4989; (e) D. Yuan, D. Zhao, D. Sun, H. C. Zhou, *Angew. Chem. Int. Ed.* **2010**, *49*, 5357-5361; (f) Y. Yan, S. Yang, A. J. Blake, W. Lewis, E. Poirier, S. A. Barnett, N. R. Champness, M. Schroeder, *Chem. Commun*. **2011**, *47*, 9995-9997; (g) D. Kim, X. Song, J. H. Yoon, M. S. Lah, *Cryst. Growth Des.* **2012**, *12*, 4186-4193.

[5] (a) J. P. Zhang, Y. Y. Lin, W. X. Zhang, X. M. Chen, *J. Am. Chem. Soc.* **2005**, *127*, 14162-14163; (b) S. R. Zheng, Q.Y. Yang, R. Yang, M. Pan, R.Cao, C. Y. Su, *Cryst. Growth Des.* **2009**, *9*, 2341-2353; (c) C. B. Liu, R. A. S. Ferreira, F. A. Almeida Paz, A. Cadiau, L. D. Carlos, L. S. Fu, J. Rocha, F. N. Shi, *Chem. Commun.* **2012**, *48*, 7964-7966; (d) D. Niu, J. Yang, J. Guo, W. Q. Kan, S. Y. Song, P. Du, J. F. Ma, *Cryst. Growth Des.* **2012**, *12*, 2397-2410; (e) X. J. Wang, P. Z. Li, L. Liu, Q. Zhang, P. Borah, J. D. Wong, X. X. Chan, G. Rakesh, Y. Li, Y. Zhao, *Chem. Commun.* **2012**, *48*, 10286-10288; (f) H. Yang, F. Wang, Y. Kang, T. H. Li, J. Zhang, *Dalton Trans.* **2012**, *41*, 2873-2876; (g) T. W. Tseng, T. T. Luo, S. Y. Chen, C. C. Su, K. M. Chi, K. L. Lu, *Cryst. Growth Des.* **2013**, *13*, 510-517.

[6] (a) A. Rodríguez-Diéguez, E. Colacio, *Chem. Comm.* **2006**, 4140-4142; (b) J. Suárez-Varela, A. J. Mota, H. Aouryaghal, J. Cano, A. Rodríguez-Diéguez, D. Luneau, E. Colacio, *Inorg. Chem.* **2008**, *47*, 8143-8158; (c) C. B. Liu, R. A. S. Ferreira, F. A. Almeida Paz, A. Cadiau, L. D. Carlos, L. S. Fu, J. Rocha, F. N. Shi, Chem. Commun. **2012**, *48*, 7964-7966; (d) J. P. Zhang, Y. Y. Lin, X. C. Huang, X. M. Chen, *J. Am. Chem. Soc.* **2005**, *127*, 5495-5506.

[7] A. Rodríguez-Diéguez, A. Salinas-Castillo, S. Galli, N. Masciocchi, J. M. Gutiérrez-Zorrilla, P. Vitoria, E. Colacio, *Dalton Trans.* **2007**, 1821-1828.

[8] J. Kahr, J. P. S. Mowat, A. M. Z. Slawin, R. E. Morris, D. Fairen-Jimenez, P. A. Wright, *Chem. Commun.* **2012**, *48*, 6690-6692; (b) B. Wang, A. P. Cote, H. Furukawa, M. O'Keeffe, O. M. Yaghi, *Nature* **2008**, *453*, 207-211.

[9] (a) S. L. Zheng, J. H. Yang, X. L. Yu, X. M. Chen, W. T.Wong, *Inorg. Chem.* **2004**, *43*, 830-838; (b) S. Skoulika, P. Dallas, M. G. Siskos, Y. Deligiannakis, A. Michaelides, *Chem. Mater.* **2003**, *15*, 4576-4582; (c) D. C. Zhong, W. X. Zhang, F. L. Cao, L. Jiang, T. B. Lu, *Chem. Commun.* **2011**, *47*, 1204-1206; (d) L. H. Cao, H. Y. Li, S. Q. Zang, H. W. Hou, T. C. W. Mak, *Cryst. Growth Des.* **2012**, *12*, 4299-4301.

[10] G. M. Sheldrick, SHELX97, program for crystal structure refinement, University of Göttingen, Göttingen, Germany, 1997.

[11] A. L. Spek, PLATON-94 (V-101094), A Multipurpose Crystallographic Tool, University of Utrecht, The Netherlands, 1994.

[12] (a) L.D. Gelb, K.E. Gubbins, *Langmuir* **1999**, *15*, 305-308; (b) T. Düren, F. Millange, G. Férey, K.S. Walton, R. Q. Snurr, *J. Phys. Chem. C.* **2007**, *111*, 15350-15356.

[13] (a) F. Wang, J. Zhang, S. M. Chen, Y. M. Xie, X. Y. Wu, S. C. Chen, R. M. Yu, C. Z. Lu, *CrystEngComm.* **2009**, *11*, 1526-1528; (b) Y. Chen, Z. G. Ren, H. X. Li, X. Y. Tang, W. H. Zhang, Y. Zhang, J. P. Lang, *J. Mol. Struct.* **2008**, *875*, 339-345.

[14] Y. L. Zhong, X. J. Shi, E. C. Yang, X. J. Zhao, *Inorg. Chem. Commun*. **2010**, *13*, 1259-1262.

[15] U. H. F. Bunz, *Chem. Rev*. **2000**, *100*, 1605-1644.

[16] J. M. Seco, M. de Araújo Farias, N. M. Bachs, A. B. Caballero, A. Salinas-Castillo, A. Rodríguez-Diéguez, *Inorg. Chim. Acta* ***2010***, *363*, 3194-3199.

[17] X. S. Wang, Y. Z. Tang, X. F. Huang, Z. R. Qu, C. M. Che, P. W. H. Chang, R. G. Xiong, *Inorg. Chem.* **2005**, *44*, 5278-5285.

[18] (a) D. Fairen-Jimenez, N.A. Seaton, T. Düren. Langmuir **2010**, *26*, 14694-14699; (b) J. Getzschmann, I. Senkovska, D. Wallacher, M. Tovar, D. Fairen-Jimenez, T. Düren, J. M. van Baten, R. Krishna, S. Kaskel, *Microporous and Mesoporous Materials* **2010**, *136*, 50-58; (c) A. Rossin, D. Fairen-Jimenez, T. Düren, G. Giambastiani, M. Peruzzini, J. G. Vitillo, *Langmuir* **2011**, *27*, 10124-10131; (d) A. J. Calahorro, M. E. Lopez-Viseras, A. Salinas-Castillo, D. Fairen-Jimenez, E. Colacio, J. Cano, A. Rodríguez-Diéguez, *CrystEngComm*. **2012**, *14*, 6390-6393.

Entry for the Table of Contents (Please choose one layout)

Layout 1:

Key Topic

Three new metal-organic frameworks based on 5-(4-pyridyl)tetrazole have been synthesized by hydrothermal routes mixing this linker with cadmium(II) chloride in the presence of secondary ligands such as squaric acid, 4-carboxypyridine and terephtalic acid in water. Hydrothermal syntheses reveal new possibilities to rational formation on MOFs by mixtures of different linkers using the appropriate stoichiometry. These polymers exhibit blue-green long lifetime photoluminescence emission at room temperature in the solid state with long lifetime decays.

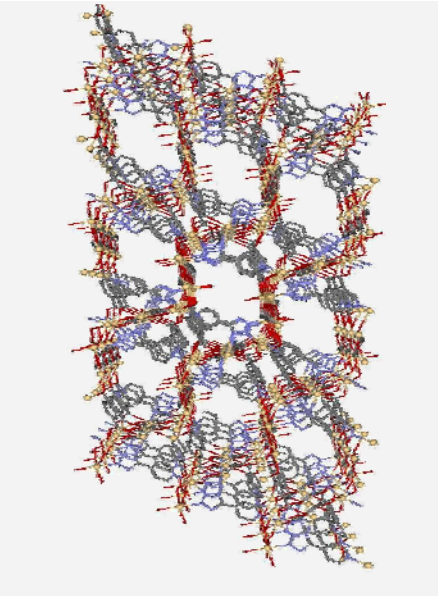

Antonio J. Calahorro, Alfonso Salinas-Castillo, David Fairen-Jimenez, Jose M. Seco, Claudio Mendicute-Fierro, Santiago Gómez-Ruiz, Marta E. López-Viseras and Antonio Rodríguez-Diéguez*

Blue-green long lifetime photoluminescence emission of 3D cadmium metal-organic frameworks Based on the 5-(4-pyridyl)tetrazole Ligand

Keywords: Hydrothermal / Cadmium / MOF / Luminescence /

Supporting Information

BLUE-GREEN LONG LIFETIME PHOTOLUMINESCENCE EMISSION OF 3D CADMIUM METAL-ORGANIC FRAMEWORKS BASED ON THE 5-(4-PYRIDYL)TETRAZOLE LIGAND

Antonio J. Calahorro,[a] Alfonso Salinas-Castillo,[b] David Fairen-Jimenez,[c] Jose M. Seco,[d] Claudio Mendicute-Fierro,[d] Santiago Gómez-Ruiz,[e] Marta E. López-Viseras,[a] and Antonio Rodríguez-Diéguez.[a,*]

Index

1. Crystal Data.

Table S1. Selected Distances (Å) for compound **1**, **2** and **3**

1	2	3
Cd1 O1 2.294(5)	Cd1 O1 2.213(2)	Cd1 O1B 2.222(6)
Cd1 N9A 2.298(5)	Cd1 O2B 2.248(3)	Cd1 O1B 2.222(6)
Cd1 O1B 2.325(5)	Cd1 N9A 2.273(3)	Cd1 O1D 2.255(7)
Cd1 O2W 2.326(5)	Cd1 O2 2.298(4)	Cd1 O1D 2.255(7)
Cd1 N4A 2.367(6)	Cd1 N1A 2.529(3)	Cd1 N1A 2.424(9)
Cd1 N2A 2.372(6)	Cd1 N4A 2.648(3)	Cd1 N1A 2.424(9)
Cd1 Cd2 3.4730(8)	Cd2 O1 2.257(2)	Cd2 O2B 2.254(7)
Cd2 O1 2.229(5)	Cd2 O1 2.257(2)	Cd2 N9A 2.288(8)
Cd2 O3B 2.263(5)	Cd2 O1B 2.324(3)	Cd2 N2A 2.333(8)
Cd2 O1W 2.280(5)	Cd2 N7B 2.327(3)	Cd2 O2D 2.389(6)
Cd2 O1 2.284(5)	Cd2 N3A 2.351(3)	Cd2 O11B 2.409(6)
Cd2 O1B 2.354(5)	Cd2 N2A 2.378(3)	Cd2 O1D 2.454(6)
Cd2 N1A 2.394(6)		Cd2 C3D 2.757(9)
Cd2 Cd2 3.4390(10)		Cd3 O1W 2.231(7)
Cd2 Cd1 3.4730(8)		Cd3 O12B 2.319(7)
		Cd3 O1C 2.319(6)
		Cd3 O1C 2.321(7)
		Cd3 N3A 2.355(8)
		Cd3 O11B 2.384(7)
		Cd3 O2C 2.541(6)
		Cd3 C10B 2.699(10)

Table S2. Selected Bond Angles (Å) for compound **1**, **2** and **3**

1	2	3
O1 Cd1 N9A 86.81(18)	O1 Cd1 O2B 88.47(10)	O1B Cd1 O1B 180.0(4)
O1 Cd1 O1B 75.98(16)	O1 Cd1 N9A 170.11(10)	O1B Cd1 O1D 89.1(2)
N9A Cd1 O1B 161.05(18)	O2B Cd1 N9A 92.50(11)	O1B Cd1 O1D 90.9(2)
O1 Cd1 O2W 120.44(17)	O1 Cd1 O2 89.93(15)	O1B Cd1 O1D 90.9(2)
N9A Cd1 O2W 89.68(18)	O2B Cd1 O2 165.02(18)	O1B Cd1 O1D 89.1(2)
O1B Cd1 O2W 92.21(16)	N9A Cd1 O2 91.63(16)	O1D Cd1 O1D 180.0
O1 Cd1 N4A 159.01(18)	O1 Cd1 N1A 95.42(8)	O1B Cd1 N1A 90.4(2)
N9A Cd1 N4A 102.0(2)	O2B Cd1 N1A 79.29(11)	O1B Cd1 N1A 89.6(2)
O1B Cd1 N4A 96.91(18)	N9A Cd1 N1A 94.43(10)	O1D Cd1 N1A 84.8(2)
O2W Cd1 N4A 79.06(18)	O2 Cd1 N1A 86.04(17)	O1D Cd1 N1A 95.2(2)
O1 Cd1 N2A 79.99(18)	O1 Cd1 N4A 85.23(9)	O1B Cd1 N1A 89.6(2)
N9A Cd1 N2A 99.6(2)	O2B Cd1 N4A 93.66(11)	O1B Cd1 N1A 90.4(2)
O1B Cd1 N2A 85.35(19)	N9A Cd1 N4A 84.88(10)	O1D Cd1 N1A 95.2(2)
O2W Cd1 N2A 158.21(19)	O2 Cd1 N4A 101.05(18)	O1D Cd1 N1A 84.8(2)
N4A Cd1 N2A 79.8(2)	N1A Cd1 N4A 172.89(10)	N1A Cd1 N1A 180.0(4)
O1 Cd1 Cd2 40.55(11)	O1 Cd2 O1 162.71(5)	O2B Cd2 N9A 87.3(3)
N9A Cd1 Cd2 124.46(14)	O1 Cd2 O1B 80.54(10)	O2B Cd2 N2A 102.3(3)
O1B Cd1 Cd2 42.41(12)	O1 Cd2 O1B 83.81(10)	N9A Cd2 N2A 162.0(3)
O2W Cd1 Cd2 126.98(12)	O1 Cd2 N7B 109.73(10)	O2B Cd2 O2D 125.4(2)
N4A Cd1 Cd2 122.77(14)	O1 Cd2 N7B 86.63(10)	N9A Cd2 O2D 88.4(3)
N2A Cd1 Cd2 62.59(15)	O1B Cd2 N7B 168.30(11)	N2A Cd2 O2D 98.0(3)
O1 Cd2 O3B 89.60(17)	O1 Cd2 N3A 81.53(10)	O2B Cd2 O11B 83.0(2)
O1 Cd2 O1W 99.98(17)	O1 Cd2 N3A 91.80(10)	N9A Cd2 O11B 83.0(3)
O3B Cd2 O1W 88.25(18)	O1B Cd2 N3A 92.17(11)	N2A Cd2 O11B 83.1(2)
O1 Cd2 O1 80.72(18)	N7B Cd2 N3A 94.87(12)	O2D Cd2 O11B 150.0(2)
O3B Cd2 O1 103.47(17)	O1 Cd2 N2A 92.70(10)	O2B Cd2 O1D 78.7(2)
O1W Cd2 O1 168.27(17)	O1 Cd2 N2A 92.07(10)	N9A Cd2 O1D 115.0(3)
O1 Cd2 O1B 95.74(16)	O1B Cd2 N2A 80.99(11)	N2A Cd2 O1D 82.1(2)
O3B Cd2 O1B 174.32(17)	N7B Cd2 N2A 92.66(11)	O2D Cd2 O1D 54.7(2)
O1W Cd2 O1B 92.71(17)	N3A Cd2 N2A 171.73(11)	O11B Cd2 O1D 153.4(2)
O1 Cd2 O1B 75.59(16)		O2B Cd2 C3D 102.4(3)
O1 Cd2 N1A 163.40(18)		N9A Cd2 C3D 101.6(3)
O3B Cd2 N1A 89.40(19)		N2A Cd2 C3D 91.3(3)
O1W Cd2 N1A 96.55(19)		O2D Cd2 C3D 26.8(2)
O1 Cd2 N1A 83.41(18)		O11B Cd2 C3D 173.0(3)
O1B Cd2 N1A 84.93(18)		O1D Cd2 C3D 27.9(2)
O1 Cd2 Cd2 40.96(12)		O1W Cd3 O12B 92.3(3)
O3B Cd2 Cd2 98.64(13)		O1W Cd3 O1C 86.0(2)
O1W Cd2 Cd2 139.70(13)		O12B Cd3 O1C 174.8(2)
O1 Cd2 Cd2 39.76(12)		O1W Cd3 O1C 95.6(3)
O1B Cd2 Cd2 84.23(11)		O12B Cd3 O1C 97.5(2)
N1A Cd2 Cd2 123.01(14)		O1C Cd3 O1C 77.8(2)
O1 Cd2 Cd1 105.18(12)		O1W Cd3 N3A 174.7(3)
O3B Cd2 Cd1 134.69(12)		O12B Cd3 N3A 92.7(3)
O1W Cd2 Cd1 129.00(12)		O1C Cd3 N3A 89.2(2)
O1 Cd2 Cd1 40.76(11)		O1C Cd3 N3A 85.6(3)
O1B Cd2 Cd1 41.75(11)		O1W Cd3 O11B 93.8(3)
N1A Cd2 Cd1 64.66(14)		O12B Cd3 O11B 56.0(2)
Cd2 Cd2 Cd1 70.528(19)		O1C Cd3 O11B 129.0(2)
		O1C Cd3 O11B 152.2(2)
		N3A Cd3 O11B 87.5(2)
		O1W Cd3 O2C 99.9(2)
		O12B Cd3 O2C 131.5(2)
		O1C Cd3 O2C 53.7(2)
		O1C Cd3 O2C 127.3(2)
		N3A Cd3 O2C 75.4(2)
		O11B Cd3 O2C 76.4(2)
		O1W Cd3 C10B 93.1(3)
		O12B Cd3 C10B 27.5(3)
		O1C Cd3 C10B 157.4(3)
		O1C Cd3 C10B 124.6(3)
		N3A Cd3 C10B 90.4(3)
		O11B Cd3 C10B 28.5(3)
		O2C Cd3 C10B 104.5(3)

2. Luminescence Properties.

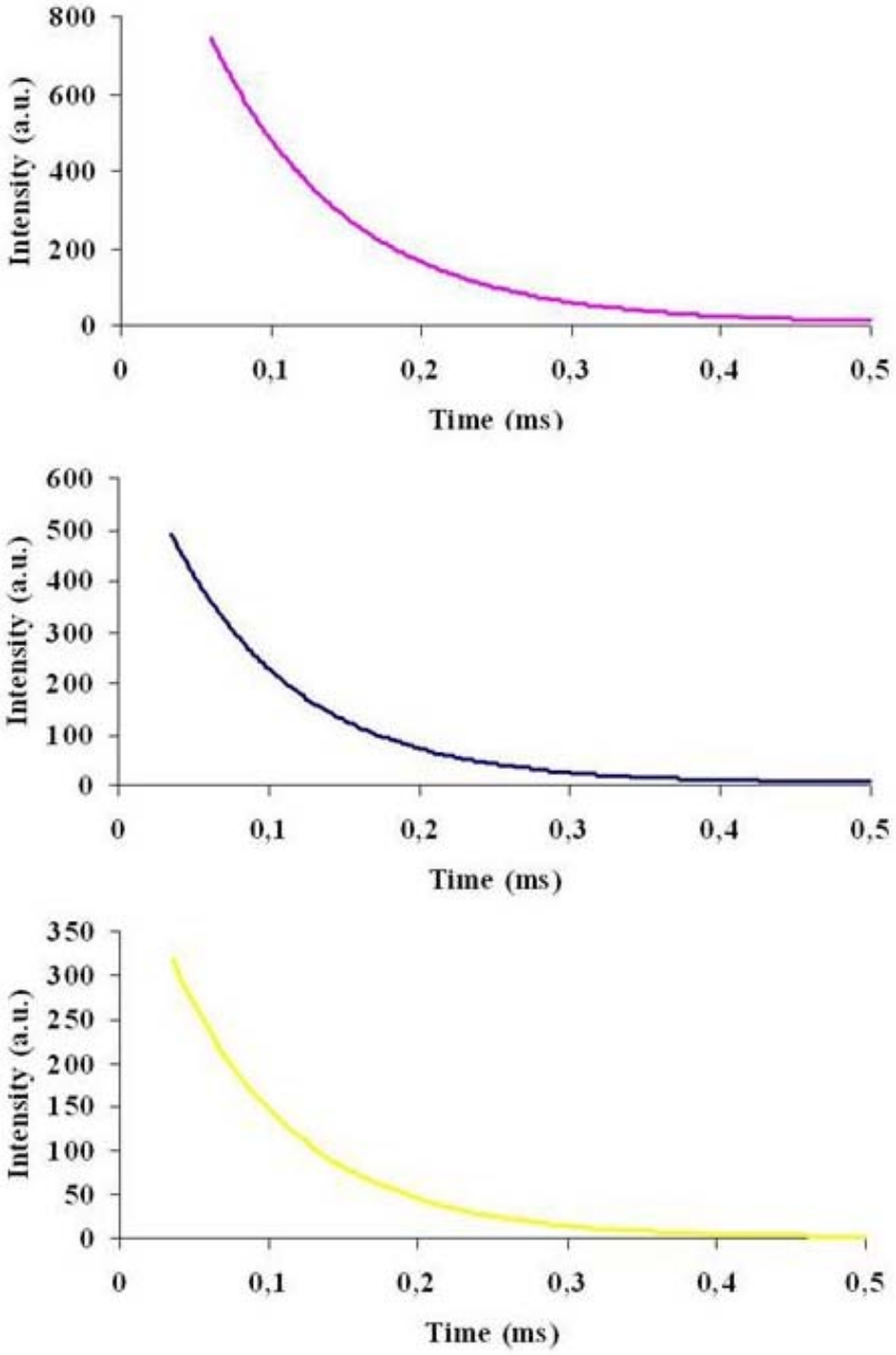

Figure S1. Decay time of **1** (pink), **2** (blue) and **3** (yellow) in solid state.

3. N_2-Adsorption-Desorption Isotherm.

N_2 gas adsorption-desorption isotherm was performed using a Micromeritics ASAP 2020 analyzer degassing the sample at 90ºC during 6 hours prior to the adpsortion experiments.

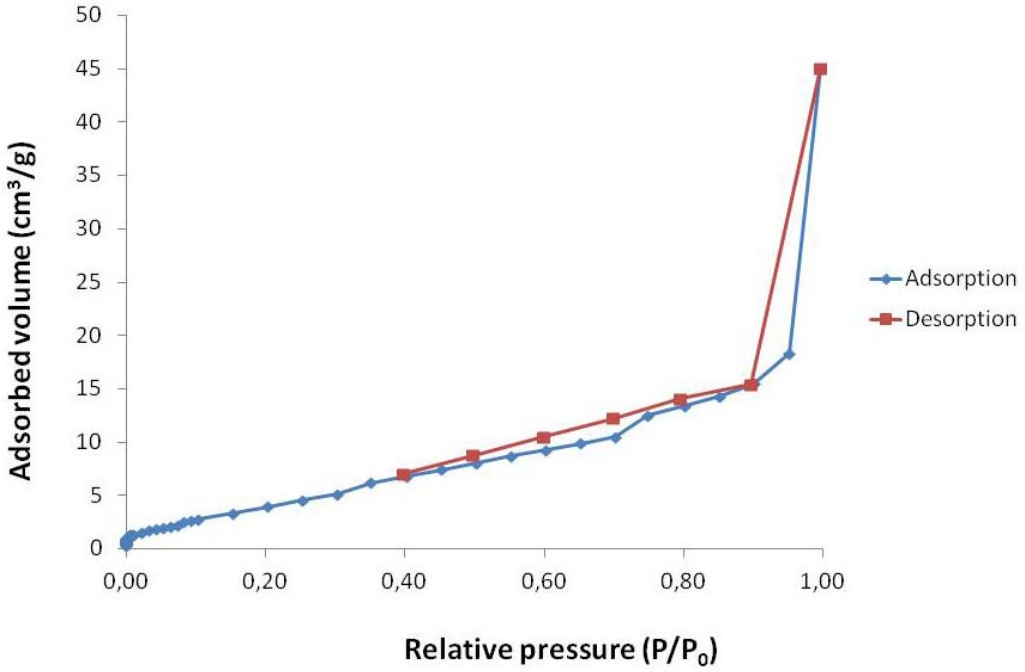

Figure S2. Experimental analysis of **3**.

Dalton Transaction

Dynamic Article Links ►

Cite this: DOI: 10.1039/c0xx00000x

www.rsc.org/xxxxxx

Communication

Blue-Green Photoluminescence of the First Examples of Metal-Organic-Frameworks with Two Novel Tetrazolatephenyl Acetic Acid Derivatives.

Antonio J. Calahorro,[a] Piero Macchi,[b,*] Alfonso Salinas-Castillo[c] and Antonio Rodríguez-Diéguez[a,*]

Received (in XXX, XXX) Xth XXXXXXXXX 20XX, Accepted Xth XXXXXXXXX 20XX

DOI: 10.1039/b000000x

We report on the synthesis of two new Zn Metal-Organic-Frameworks with 1,3-tetrazolatephenyl-acetic and 1,4-tetrazolatephenyl-acetic spacers obtained *in situ* by hydrothermal routes. These three-dimensional structures exhibit an intense blue-green long lifetime photoluminescence emissions at room temperature in the solid state. To the best of our knowledge, this is the first time that coordination compounds have been synthesized with these ligands.

Metal-Organic Framework materials currently represent an area of enormous interest owing not only to the need of developing new functional materials but also of elucidating their topologies and their potential applications.[1] Recently, the design and study of Zn-based MOF has evolved enormously[2] because of their interesting structures and in particular their potential applications in areas such as luminescence,[3] gas adsorption,[4] sensing, and optical storage.[5] These materials are commonly prepared through a bottom-up approach, using solvothermal methods, connecting ions with the appropriate bridging ligands. Still, there is a great interest in the design of new bridging ligands that will allow the preparation of novel MOFs. In the last years, we and others have described different metal coordination polymers based on tetrazolate with interesting topologies synthesized by *in situ* Demko-Sharpless cycloaddition reactions of organonitriles and sodium azide.[6] Recently, we have designed and prepared novel coordination polymers with different pyrimidine derivative ligands, with interesting luminescent properties.[7] Moreover, we have shown the use of hydrothemal syntheses to generate *in situ* new ligands and construct novel three-dimensional coordination polymers.[8] Following our work, we have designed, by hydrothermal routes, two new multidentate bridging anionic ligands derivatives of tetrazol-phenyl-acetic acid (H_2tzbaa), 3-tetrazolatephenyl acetic and 4-tetrazolatephenyl acetic linkers, which contain one carboxylate group and one tetrazolate ring with a methylene-benzene group in the middle of the spacer. Thanks to its extended aromaticity and to the presence of poly-heterosubstituted penta- and hexa-atomic rings, H_2tzbaa is a good candidate for enhanced emissive properties, tunable, in principle, by coordination to different metals or environments.

Here, we report on the synthesis , the crystal structure and the luminescence properties of the first examples of 3D-MOFs $[Zn(1,3\text{-tzbaa})]_n$ (**1**) and $[Zn(1,4\text{-tzbaa})]_n$ (**2**) with the new multidentate derivative anionic tzbaa^{2-} ligands, shown in scheme I, demonstrating the potential of this new linkers to construct novel MOFs. To the best of our knowledge, these are the first examples of MOFs with these derivative ligands, investigated here for the first time. There is only one biological study on 1,4-H_2tzbaa, used as inhibitor for the Syk C-Terminal SH2 Domain in biomedical area.[9]

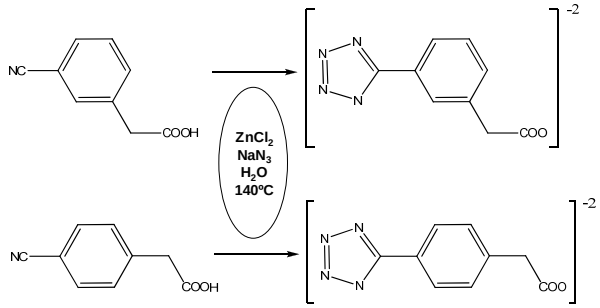

Scheme I. Preparation of the anionic $(1,3\text{-tzbaa})^{2-}$ (up) and $(1,4\text{-tzbaa})^{2-}$ (down) ligands by hydrothermal routes.

Hydrothermal reactions of zinc chloride (1 mmol) with the appropriate 3-cyanophenyl acetic acid or 4-cyanophenyl acetic acid (1 mmol) and sodium azide (3 mmol) in water (10 ml) at 160 ºC for 12 h followed by cooling to room temperature over 3 h yields prismatic yellow and colourless crystals of **1** (in 65% yield) and **2** (in 39% yield), respectively.[10] The crystal structures were determined by single crystal X-ray crystallography.[11]

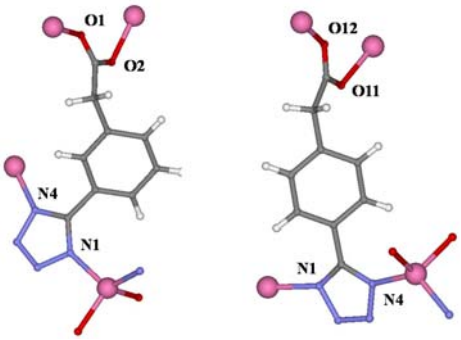

Figure 1. A view of the coordination mode of the ligands $(1,3\text{-tzbaa})^{2-}$ and $(1,4\text{-tzbaa})^{2-}$ for **1**(left) and **2** (right), respectively.

Both MOFs crystallize in the orthorhombic system and crystal class mm2, though not in the same space group ($Pna2_1$ and $Pca2_1$ for **1** and **2**, respectively). Both structures are three-dimensional, built from tetrahedral Zn^{2+} connectors coordinated to four $(tzbaa)^{2-}$ linkers. The biding sites of $(tzbaa)^{2-}$ are two oxygen of the carboxylate group and two nitrogen atoms (N1 and N4) of the tetrazole ring. The two isomers produce different supramolecular structures, because **2** is characterized by large rings of 3 linkers and 3 connectors (Figure 2, right), producing apparent channels (in reality not available for guest molecules) along ***b*** and therefore perpendicular to the 2_1 helix.

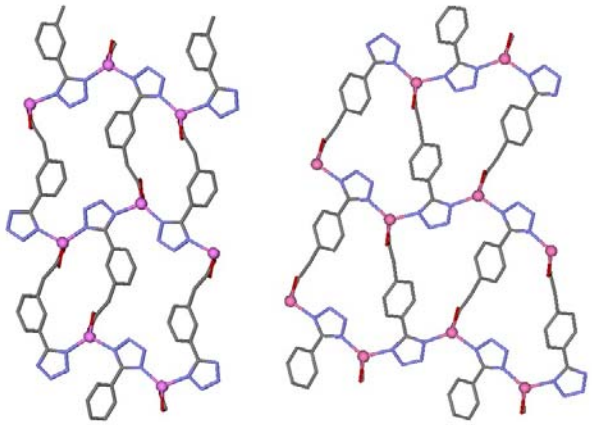

Figure 2. A view of the rings formed in the structures for **1**(left) and **2** (right), respectively.

These rings are formed by two long edges (Zn-tetrazole-carboxylate-Zn) and a shorter one (Zn-tetrazole-Zn). The rings are interconnected forming 8 member rings (4 connectors and 4 linkers) perpendicular to ***a***, with shorter edges (Zn-tetrazole-Zn or Zn-carboxylate-Zn).

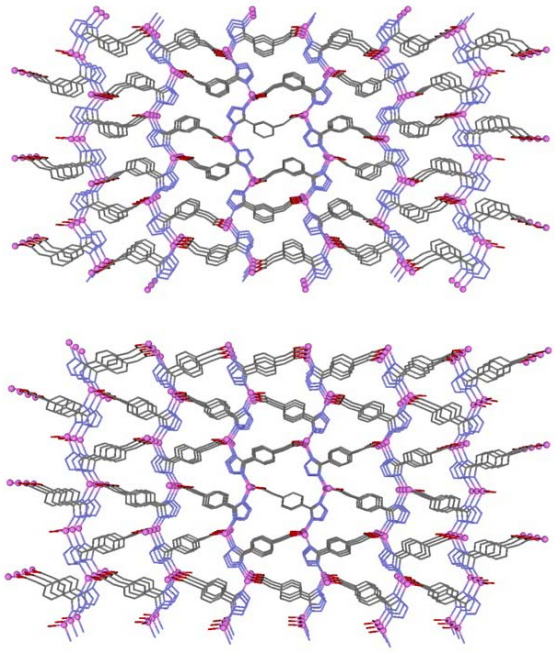

Figure 3. Packings of **1** (top) and **2** (bottom) along *c* and *b* axes, respectively.

The structure of **1** instead is more complex (Figure 2, left), having two different cycles (4 connectors + 4 linkers and 2 connectors + 2 linkers respectively) which form apparent channels along the helical axis ***c***. This different structure is due to the more asymmetric shape of 1,3-tzbaa. 8-member rings similar to those of **2** are perpendicular to ***b.*** In Figure 3, the two packings are shown.

The emission spectra of **1** and **2** in the solid state at room temperature are shown in Figure 3. Broad intense emission bands are observed, centred about λ = 449 and 479 nm, respectively, upon excitation at λ = 350 nm. The emissions in complexes **1** and **2** are assigned to intraligand $\pi \rightarrow \pi^*$ transitions.

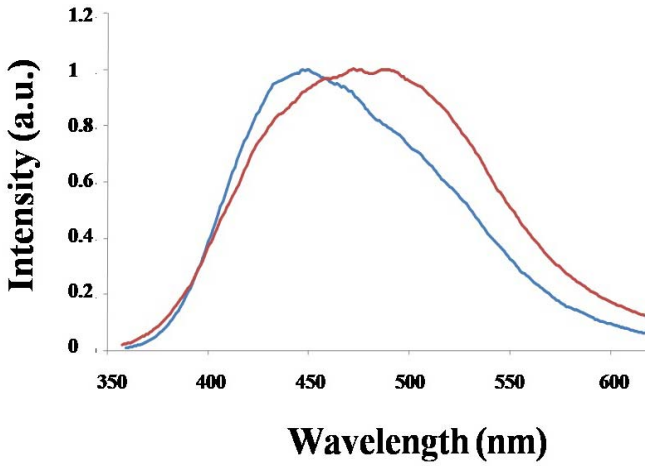

Figure 4. The emission spectra of **1** (blue) and **2** (red) after excitation at 350 nm in solid state at room temperature.

The similarity of emissions for **1** and **2** is in agreement with the explanation, which indicates that ligand-centered π–π^* excitation is responsible for emissions. In contrast with Zn complexes of 5-aliphatic tetrazolates that usually show emissions in the range of 390–420 nm,[12] energetic emissions in **1** and **2** possibly come from the conjugation of tetrazolate and phenyl-carboxylate groups. The decay curves were fitted to mono exponential function: $I = I_0 + A_1 \exp(-t/\tau)$, where I and I_0 are the luminescent intensities at time t and 0, τ is defined as the luminescent lifetime. For this function, the best fit of the experimental luminescence intensities to the above equation led to the lifetimes of 0.084 ms and 0.098 ms for **1** and **2**, respectively.

We have succeeded in synthesising the first metal-organic-frameworks with the 1,3-tetrazolatephenyl-acetic and 1,4-tetrazolatephenyl-acetic spacer ligands. These compounds show fascinating structures with intense blue-green photoluminescence emission at room temperature in the solid state. To the best of our knowledge, this is the first time that coordination compounds have been synthesized with these new multidentate ligands.

This work was supported by the Junta de Andalucía (FQM-

4228) (A.J. Calahorro for a predoctoral grant) and by the Swiss National Science Foundation (Project Nr. 141271).

Notes and references

a Departamento de Química Inorgánica, Universidad de Granada, Avda Fuentenueva s/n, 18071, Granada, Spain. email: antonio5@ugr.es
b Departament of Chemistry and Biochemistry, University of Bern, Friestrasse 3, CH3012, Bern, Switzerland. email: piero.macchi@dcb.unibe.ch.
c Departamento de Química Analítica, Universidad de Granada18071, Granada, Spain.

† CCDC 930950 and 930951 contain the supplementary crystallographic data for this paper. These data can be obtained free of charge from The Cambridge Crystallographic Data Centre via www.ccdc.cam.ac.uk/data_request/cif.

1.- (a) H. Xu, X. Rao, J. Gao, J. Yu, Z. Wang, Z. Dou, Y. Cui, Y. Yang, B. Chen and G. Qian, *Chem.Commun.*, 2012, **48**, 7377-7379. (b) J.L.C. Rowsell, O.M. Yaghi, *J. Am. Chem. Soc.* 2006, **128**, 1304. (c) S.H. Jhung, J.-H. Lee, A.K. Cheetham, G. Ferey, J.S. Chang, *J. Catal.* 2006, **239,** 97. (d) M. Hong, *Cryst. Growth Des.* 2007, **7,** 10. (e) A. Vertova, I Cucchi, P. Fermo, F. Porta, D.M. Proserpio, S. Rondinini, *Electrochim. Acta* 2007, **52,** 2603. (f) M. M. Wanderley, C. Wang, C.-D. Wu and W. Lin, *J. Am. Chem. Soc*, 2012, **134**, 9050-9053. (g) P. Kar, R. Haldar, C. J. Gomez-Garcia and A. Ghosh, *Inorg. Chem.*, 2012, **51**, 4265-4273. (h) S.T. Hyde, O. Delgado-Friedrichs, S.J. Ramsden, V. Robins, *Solid State,* 2006, 740.

2.- (a) F.A. Almeida Paz, J. Klinowski, *Chem. Commun*., 2003, 1484. (b) V. Colombo, C. Montoro, A. Maspero, G. Palmisano, N. Masciocchi, S. Galli, E. Barea and J. A. R. Navarro, *J. Am. Chem. Soc*, 2012, **134**, 12830-12843 (c) D.-L. Long, A.J. Blake, N.R. Champness, C. Wilson, M. Schröder, *Angew. Chem. Int. Ed*., 2001, **40**, 2444. (d) L.G. Westin, M. Kritikos, A. Caneschi, *Chem. Commun*., 2003, 1012. (e) B.-Q. Ma, D.-S. Zhang, S. Gao, T.-Z. Jin, C.-H. Yan, G.-X. Xu, *Angew. Chem. Int. Ed.*, 2000, **39**, 3644. (f) J. Seo, C. Bonneau, R. Matsuda, M. Takata and S. Kitagawa, *J. Am. Chem. Soc*, 2011, **133**, 9005-9013.

3.- (a) D.T. de Lill, A. de Bettencourt-Dias, C.L. Cahill, *Inorg. Chem*., 2007, **46**, 3960. (b) K. Lunstroot, K. Driesen, P. Nockemann, C. Gorller-Walrand, K. Binnemans, S. Bellayer, J. Le Bideau, A. Vioux, *Chem. Mater*., 2006, **18**, 5711. (c) R. Shunmugam, G.N. Tew, *J. Am. Chem. Soc*., 2005, **127**, 13567. (d) N.L. Rosi, J. Kim, M. Eddaoudi, B.L. Chen, M. O'Keeffe, O.M. Yaghi, *J. Am. Chem. Soc*., 2005, **127**, 1504. (e) M. Ji, X. Lan, Z. Han, C. Hao and J. Qiu, *Inorg. Chem.*, 2012, **51**, 12389-12394. (f) Y. Yang, P. Du, J.-F. Ma, W.-Q. Kan, B. Liu and J. Yang, *Crystal Growth & Design*, 2011, **11**, 5540-5553. (g) F. Tong, Z.-G. Sun, K. Chen, Y.-Y. Zhu, W.-N. Wang, C.-Q. Jiao, C.-L. Wang and C. Li, *Dalton Trans.*, 2011, **40**, 5059-5065.

4.- (a) L. Pan, K.M. Adams, H.E. Hernandez, X. Wang, C. Zheng, Y. Hattori, K. Kaneko, *J. Am. Chem. Soc*., 2003, **125**, 3062. (b) Q.-G. Zhai, Q. Lin, T. Wu, L. Wang, S.-T. Zheng, X. Bu and P. Feng, *Chemistry of Materials*, 2012, **24**, 2624-2626. (c) W. Morris, N. He, K. G. Ray, P. Klonowski, H. Furukawa, I. N. Daniels, Y. A. Houndonougbo, M. Asta, O. M. Yaghi and B. B. Laird, *Journal of Physical Chemistry C*, 2012, **116**, 24084-24090 (d) P.-Q. Liao, D.-D. Zhou, A.-X. Zhu, L. Jiang, R.-B. Lin, J.-P. Zhang and X.-M. Chen, *J. Am. Chem. Soc*, 2012, **134**, 17380-17383. (e) P. Cui, Y.-G. Ma, H.-H. Li, B. Zhao, J.-R. Li, P. Cheng, P. B. Balbuena and H.-C. Zhou, *J. Am. Chem. Soc*, 2012, **134**, 18892-18895.

5.- (a) K. Kuriki, Y. Koike, Y. Okamoto, *Chem. Rev*., 2002, **102**, 2347. (b) C.L. Cahill, D.T. de Lill, M. Frisch, *Cryst. Eng. Comm.*, 2007, **9**, 15. (c) J.C.G. Bünzli, C. Piguet, *Chem. Soc. Rev*., 2005, **34**, 1048. (d) A.Y. Robin, K.M. Fromm, *Coord. Chem. Rev.*, 2006, **250**, 2127. (e) G. Lu and J. T. Hupp, *J. Am. Chem. Soc*, 2010, **132**, 7832-7833. (f) R. Gheorghe, P. Cucos, M. Andruh, J.P. Costes, B. Donnadieu, S. Shova, *Chem. Eur. J*., 2005, **12**, 187. (g) B. Gole, A. K. Bar and P. S. Mukherjee, *Chem Commun*, 2011, **47**, 12137-12139.

6.- (a) A. Rodríguez-Diéguez, R. Kivekäs, E. Colacio, *ChemComm*, 2005, 5228; (b) A. Rodríguez-Diéguez and E. Colacio, *ChemComm*, 2006, 4140; (c) Z. P. Demko and K. B. Sharpless, *J. Org. Chem.*, 2001, **66**, 7945.

7.- (a) A Rodríguez-Diéguez, A. Salinas-Castillo, S. Galli, N. Masciocchi, J. M. Gutiérrez-Zorrilla, P. Vitoria and E. Colacio, Dalton Trans. (2007) 1821. (b) J.M. Seco, M. de Araujo-Farias, N.M. Bach, A.B. Caballero, A. Salinas-Castillo and A. Rodríguez-Diéguez, *InorgChimActa*, 2010, 363, 3194.

8.- (a) A. Rodríguez-Diéguez, J. Cano, R. Kivekäs, A. Debdoubi, E. Colacio, *Inorg. Chem.* 2007, **46**, 2503. A. Rodríguez-Diéguez, J.M. Seco and E. Colacio, *Eur.J.Inorg.Chem*., 2012, 203; (b) A. Rodríguez-Diéguez, A. Salinas-Castillo, A. Sironi, J.M. Seco and E. Colacio, *CrystEngComm*, 2010, **12**, 1876. ; (c) A.J. Calahorro, D. Fairen-Jiménez, A. Salinas-Castillo, M.E. López-Viseras and A. Rodríguez-Diéguez, *Polyhedron*, 2013, *doi.org/10.1016/j.poly. 2012.09.018.*

9.- T. Niimi, M. Orita, M. Okazawa-Igarashi, H. Sakashita, K. Kikuchi, E. Ball, A. Ichikawa, Y. Yamagiwa, S. Sakamoto, A. Tanaka, S. Tsukamoto and S. Fujita, *J.Med.Chem*, **2001**, *44*, 4737-4740.

10.- **Preparation of [Zn(1,3-tzbaa)]$_n$ (1).** A mixture of $ZnCl_2$ (0.136 g, 1 mmol), 3-cyanophenyl acetic acid (0.161 g, 1 mmol), sodium azide (0.195 mg, 3 mmol) and distilled water (10 mL) was sealed in a Teflon-lined acid digestion autoclave and heated at 160 ºC under autogenous pressure. After 12 h of heating, the reaction vessel was slowly cooled down to room temperature during a period of about 3 h. Yellow crystals of the compound under study were obtained. Yield: 65%, based on Zn. Anal. calcd $C_9H_6N_4O_2Zn$: C 40.37, H 2.24, N 20.93. Found: C 40.78, H 2.81, N 21.29. IR/cm^{-1}: 3421 (s), 2921 (m), 2850 (w), 1536 (s), 1385 (s), 1209 (m), 1077 (m), 813 (m), 773 (m), 742 (s), 684 (s). **Preparation of [Zn(1,4-tzbaa)]$_n$ (2).** A mixture of $ZnCl_2$ (0.136 g, 1 mmol), 4-cyanophenyl acetic acid (0.161 g, 1 mmol), sodium azide (0.195 mg, 3 mmol) and distilled water (10 mL) was sealed in a Teflon-lined acid digestion autoclave and heated at 160 ºC under autogenous pressure. After 12 h of heating, the reaction vessel was slowly cooled down to room temperature during a period of about 3 h. Colourless crystals of the compound under study were obtained. Yield: 39%, based on Zn. Anal. calcd $C_9H_6N_4O_2Zn$: C 40.37, H 2.24, N 20.93. Found: C 40.49, H 2.92, N 21.11. IR/cm^{-1}: 3440 (m), 2957 (w), 2910 (w), 1541 (s), 1382 (s), 1212 (m), 1018 (m), 832 (m), 743 (m), 710 (m).

11.- Crystal Data. **1**: $[C_9H_6N_4O_2Zn)]$, M = 267.55, orthorhombic, space group *Pna21*, a = 10.4858(3), b = 18.8309(6), c = 4.8130(2) Å, V = 950.36(6) Å^3, Z = 4, ρ_{calcd} = 1.87 g cm^{-3}, μ(Mo-$K\alpha$) = 2.572 mm^{-1}, R_{int} = 0.0303, T = 293 K, $R1(F_o)$ = 0.0319, ($wR2(F_o^2)$ = 0.0731) with a goodness-of-fit on F^2 1.08. **2**: $[C_9H_6N_4O_2Zn)]$, M = 267.55, orthorhombic, space group *Pca21*, a = 18.5081(5), b = 4.8230(1), c = 10.9635(4) Å, V = 978.65(5) Å^3, Z = 4, ρ_{calcd} = 1.816 g cm^{-3}, μ(Mo-$K\alpha$) = 2.498 mm^{-1}, R_{int} = 0.043, T = 293 K, $R1(F_o)$ = 0.0347, ($wR2(F_o^2)$ = 0.058) with a goodness-of-fit on F^2 1.049. Data were collected by 2θ scans (on a Bruker APEXII diffractometer with graphite-monochromated MoKα radiation (λ = 0.71073 Å). The structures were solved by direct methods and refined on F2 by the SHELX-97 program. CCDC reference numbers are 930950 and 930951.

12.- X.-S. Wang, Y.-Z. Tang, X.-F. Huang, Z.-R. Qu, C.-M. Che, P.W.H. Chan, R.-G. Xiong, *Inorg. Chem*., 2005, **44**, 5278.

SHORT COMMUNICATION

DOI: 10.1002/ejic.200((will be filled in by the editorial staff))

UNIQUE METAL-ORGANIC-FRAMEWORK WITH BASED ON 4'-TETRAZOLATE-4-BIPHENYL CARBOXYLATE SPACER: BLUE-GREEN PHOTOLUMINESCENCE.

Antonio J. Calahorro,[a] Guillermo Zaragoza,[b] Alfonso Salinas-Castillo,[c] Jose M. Seco[d] and Antonio Rodríguez-Diéguez[a,*]

Keywords: Metal Organic Framework / Hydrothermal / Lanthanide / squarate / oxalate

We have been successful in the synthesis of the first Metal-Organic-Frameworks with the novel 4'-tetrazolate-4-biphenyl carboxylate Spacer. We report the formation *in situ* of cadmium MOF by hydrothermal routes. The compound is a three-dimensional structure with small channels that shows an intense blue-green photoluminescence emission at room temperature in the solid state. To the best our knowledge, this is the first time that a coordination compound has been synthesized with this ligand.

[a] Departamento de Química Inorgánica, Universidad de Granada, 18071, Granada, Spain. Tel: 0034958240442; E-mail: antonio5@ugr.es
[b] Unidad de Rayos X; RIAIDT Edificio CACTUS, Universidad de Santiago de Compostela, 15782 Santiago de Compostela, Spain.
[c] Departamento de Química Analítica, Universidad de Granada18071, Granada, Spain.
[d] Departamento de Química Aplicada, Facultad de Ciencias Químicas de San Sebastián, UPV/EHU, 20018 San Sebastián (Spain).

Introduction

The growth of Metal-Organic Framework materials is an area of intense current interest owing to the need not only to develop various functional materials but also to elucidate the topologies as a consequence of their potential uses in many applications.[1] Recently, the design and study of Cd-based MOF has evolved enormously[2] because of their interesting structures and potential applications in areas such as luminescence,[3] gas adsorption,[4] sensing, and optical storage.[5] These materials are commonly prepared through a bottom-up approach, using solvothermal methods, connecting ions with the appropriate bridging ligands. Still, there is a great interest in the design of new bridging ligands that will allow the preparation of novel MOFs. In the last years, we have designed and prepared novel coordination polymers with different pyrimidine derivates ligands, with interesting luminescent properties[6] synthesized by in-situ Demko-Sharpless [2+3] cycloaddition reactions of organonitriles and sodium azide. [7] Moreover, we have demonstrated the use of hydrothemal syntheses to generate *in situ* new ligands. [8] Following our work, we have designed and synthesized, by hydrothermal routes, a new multidentate bridging dianionic ligand derivative of 4-tetrazolyl benzene carboxylate and p-mesitylphenyltetrazole, which contain one carboxylate group and one tetrazolate ring with two benzene rings in the middle of the spacer. Thanks to its extended aromaticity and to the presence of poly-heterosubstituded penta- and hexa-atomic rings, 4'-tetrazolate-4-biphenyl carboxylate spacer $(TBPC)^{2-}$ is a good candidate for enhanced emissive properties, tunable, in principle, by coordination to different metals or environments. Here, we report the synthetical, structural and luminescence properties of the first example of 3D-MOFs $[Cd(TBPC)(H_2O)]_n$ (**1**) with the new multidentate $(TBPC)^{2-}$, shown in scheme I, demonstrating the potential of this new linker to construct novel MOFs. To the best of our knowledge, this is the first example of MOFs with this ligand due to it´s the first time that this ligand is synthesized and studied. There are some studies about the 4-tetrazolyl benzene carboxylate and p-mesitylphenyltetrazole in which ligand show fascinating luminescence properties and interesting applications (ie OLEDs). [9]

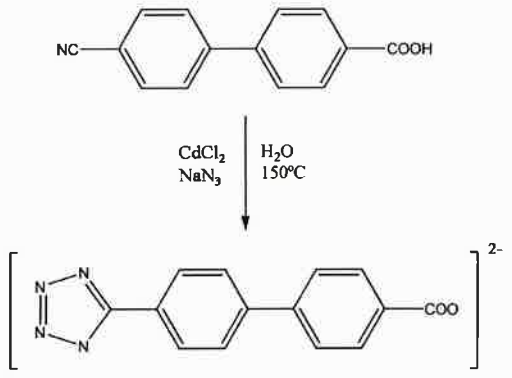

Scheme I. Preparation *in situ* of the anionic $(TBPC)^{2-}$ ligand by hydrothermal routes.

Results and Discussion

Hydrothermal reaction of cadmium chloride (1 mmol) with the appropriate 4'-cyano-4-biphenyl carboxylic acid (1 mmol) and sodium azide (3 mmol) in water (10 ml) at 150 °C for 12 h followed by cooling to room temperature over 3 h yields prismatic colourless crystals of **1** (in 65% yield). The crystal structure was determined by single crystal X-ray crystallography. [10] Compound **1** crystallizes in the monoclinic space group $P2_1/c$. The 3D-MOF structure can be described as ditetrazolate doble-bridged Cd(II)

dimers connected by $(TBPC)^{2-}$ ligands (Figure 1).

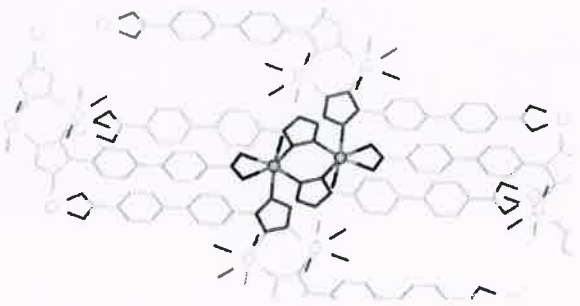

Figure 1. View of the metal environment and coordination mode of the tetrazolate group for **1**. Hydrogen atoms have been omitted for clarity. Colour code N = blue, O = red, C = grey, Cd = yellow.

These dimers are formed by two cadmium atoms bridged through nitrogen atoms N3 and N4 from tetrazolate group, and are united to others dimers through N1 atom of the same tetrazolate ring. Dimers form a dihedral angle of 87.68° and generate cationic (4,4) layers formed by square units (Figure 2).

Figure 2. View down the *bc* plane of cationic (4,4) layers in compound **1**. Hydrogen atoms have been omitted for clarity.

Within the dinuclear Cd_2 units, each cadmium atom adopts a very distorted octahedral coordination geometry in which has a CdN_3O_3 environment in *fac* disposition. The distortion of the Cd^{II} coordination polyhedron is mainly due to the small bite angle of the carboxylate group pertaining to $(TBPC)^{2-}$ ligand. The Cd atom is coordinated to three nitrogen atoms pertaining to three different tetrazolate groups (N1, N3 and N4), two oxygen atoms (O1 and O2) belonging to one carboxylate group from $(TBPC)^{2-}$ ligand and one water molecule. Cd-N distances are in the ranges 2.292(8)-2.365(7) Å, whereas Cd-O distances have values of 2.187(6), 2.515(6) and 2.314(7) Å, for O1, O2 and O3, respectively. *cis* and *trans* angles of metal environment are in the ranges 55.5(2)-104.7(3)° and 150.1(2)-169.8(2), respectively, highlighting the small bite angle of the carboxylate group (55.5(2)°) and *cis* N–M–N angles are in the ranges 87.2(3)-104.7(3).

Within the sheets formed by dimers, the intradimer Cd···Cd separation through the tetrazolate ring (N3 and N4) is 4.138(3) Å, whereas the interdimer shortest Cd···Cd distances through the N1 are 6.354 (3) and 6.755(3) Å. Within these square-grid-like sheets parallel to *bc* plane, the Cd···Cd distances through the diagonal are 7.329 and 10.799 Å. These sheets are bridged by $(TBPC)^{2-}$ linker and this distance is 12.906 Å. With respect to $(TBPC)^{2-}$ spacer, whereas the carboxylate group and the two benzenes are almost coplanar (dihedral angle of 3.77 and 5.42°), the dihedral angle between the tetrazolate group and the adjacent benzene ring is 66.68°. It should be noted that a similar tetra-chelating bridging mode in which tetrazolate ring coordinates through N1, N3 and N4 atoms and the two oxygen atoms pertaining to one carboxylate group coordinates to one metal atom has been only previously reported for the compound $[Cd(cptta)(H_2O)]$ (H_2cptta = 5-(4′-carboxy-phenyl)tetrazole) with a shorter different ligand.[11]

As above, the structure can be described as sheets, formed by ditetrazolate doble-bridged Cd(II) dimers, propagating along *bc* plane, and are bridged by the aromatic skeleton of the $(TBPC)^{2-}$ linker in *a* direction generating a interesting 3D-MOF (Figure 3).

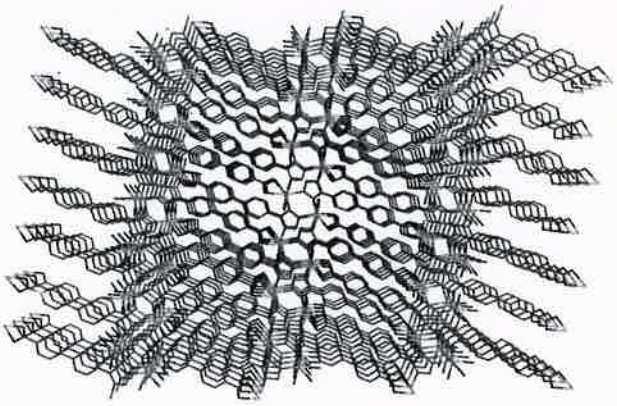

Figure 3. View down the *b* axis of the structure in the three-dimensional network. Hydrogen atoms have been omitted for clarity.

Luminescence properties occupies a special ranking among the most studied properties of materials containing aromatic molecules, in molecular crystals, organic polymers, coordination compounds or even donor–acceptor pairs, due to the potential applications of visible light emitters[12] in a number of technologically advanced fields. Thanks to its extended aromaticity and to the presence of polyheterosubstituded hexa- and penta-atomic rings, $(TBPC)^{2-}$ is a good candidate for enhanced emissive properties, tunable, in principle, by coordination to different metals or environments.

The excitation and emission spectra of compound **1** in solid state at room temperature are shown in in Figure 4. The emission spectrum of **1** exhibited broad intense emission bands centred about 405, 420 and 447 nm, respectively, upon excitation at 315 nm. The emission in complex **1** is assigned to intraligand π–π* tr

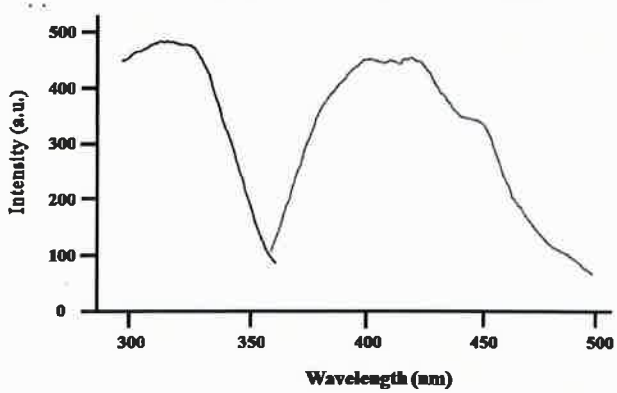

Figure 4. Excitation (blue) and emission (pink) spectra of compound **1** at room temperature in the solid state. Horizontal axis: wavelength (nm); vertical axis: intensity (a.u.).

The similarity of emissions for **1** to other compounds[13] is in agreement with the explanation, which indicates that ligand-centered $\pi-\pi^*$ excitation is responsible for emissions. In contrast with Cd complexes of 5-aliphatic tetrazolates that usually show emissions in the range of 420–530 nm,[14] lower energetic emissions in **1** possibly come from the conjugation of tetrazolate and phenyl-carboxylate groups.

Conclusions

Therefore, we have been successful in the synthesis of the first metal-organic-framework with the novel 4'-tetrazolate-4-biphenyl carboxylate spacer. This compound shows a interesting structure with intense blue-green photoluminescence emission at room temperature in the solid state. To the best our knowledge, this is the first time that a coordination compound has been synthesized with this new multidentate ligand.

Experimental Section

Materials: All analytical reagents were purchased from commercial sources and used without further purification.

Physical Measurements: Elemental analyses were carried out at the "Centro de Instrumentación Científica" (University of Granada) on a Fisons-Carlo Erba analyzer model EA 1108. The IR spectra on powdered samples were recorded with a ThermoNicolet IR200FTIR instrument by using KBr pellets.

Single-Crystal Structures Determination.

Suitable crystals of **1** was mounted on glass fiber and used for data collection. Data were collected with a Bruker AXS APEX CCD area detector equipped with graphite monochromated Mo Kα radiation (λ = 0.71073 Å) by applying the ω-scan method. The data were processed with APEX2[14] and corrected for absorption using SADABS.[15] The structures were solved by direct methods using SIR97,[16] revealing positions of all non-hydrogen atoms. These atoms were refined on F^2 by a full matrix least-squares procedure using anisotropic displacement parameters.[17] All hydrogen atoms were located in difference Fourier maps and included as fixed contributions riding on attached atoms with isotropic thermal displacement parameters 1.2 times those of the respective atom. Crystallographic data (excluding structure factors) for the reported structure have been deposited with the Cambridge Crystallographic Data Centre as supplementary publication No. CCDC 926617. Copies of the data can be obtained free of charge upon application to CCDC, 12 Union Road, Cambridge CB2 1EZ, U.K. (fax, (+44)1223 336-033; e-mail, deposit@ ccdc.cam.ac.uk).

Preparation of $[Cd(TBPC)(H_2O)]_n$ (1).
A mixture of $CdCl_2$ (0.183 g, 1 mmol), 4'-cyano-4-biphenyl carboxylic acid (0.223 g, 1 mmol), sodium azide (0.195 mg, 3 mmol) and distilled water (10 mL) was sealed in a Teflon-lined acid digestion autoclave and heated at 150 °C under autogenous pressure. After 12 h of heating, the reaction vessel was slowly cooled down to room temperature during a period of about 3 h. Colourless crystals of the compound under study were obtained. Yield: 65%, based on Cd. Anal. calcd $C_{14}H_{10}N_4O_3Cd$: C 42.61, H 2.51, N 14.20. Found: C 42.78, H 2.71, N 14.09. IR/cm^{-1}: 3403 (m), 3132 (s), 1587 (m), 1526 (m), 1458 (w), 1399 (s), 1251 (w), 832 (m), 785 (m), 689 (m).

Acknowledgments

This work was supported by the MEC of Spain (Project CTQ2011-24478) and the Junta de Andalucía (FQM-4228) (A.J. Calahorro for a predoctoral grant).

[1] (a) A. C. Sudik, A. P. Cote, A. G. Wong-Foy, M. O'Keeffe, O.M. Yaghi, *Angew. Chem. Int. Ed.* **2006**, *45*, 2528-2533; (b) A. Kondo, H. Noguchi, H. Kajiro, L. Carlucci, P. Mercandelli, D. M. Proserpio, H. Tanaka, K. Kaneko, H. Kanoh, *J. Phys. Chem. B* **2006**, *110*, 25565-25567; (c) J. L. C. Rowsell, O. M. Yaghi, *J. Am. Chem. Soc.* **2006**, *128*, 1304-1315; (d) S. H. Jhung, J. H. Lee, A. K. Cheetham, G. Ferey, J. S. Chang, *J. Catal.* **2006**, *239*, 97-104; (e) M. Hong, *Cryst. Growth & Design* **2007**, *7*, 10-14; (f) A. *Vertova, I* Cucchi, P. Fermo, F. Porta, D. M. Proserpio, S. Rondinini, *Electrochim. Acta* **2007**, *52*, 2603-2611; (g) C. Janiak, *Dalton Trans.* **2003**, *14*, 2781-2804; (h) D. Braga, M. Polito, D. D'Addario, F. Grepioni, *Cryst. Growth & Design* **2004**, *4*, 1109-1112.

[2] (a) Q. R. Fang, D. Q. Yuan, J. Sculley, W. G. Lu, H. C. Zhou, *Chem.Commun.* **2012**, *48*, 254-256; (b) E. J. Kyprianidou, G. S. Papaefstathiou, M. J. Manos, A. J. Tasiopoulos, *CrystEngComm.* 2012, *14*, 8368-8373; (c) D. Sun, Z. H. Yan, Y. K. Deng, S. Yuan, L. Wang, D. F. Sun, *CrystEngComm.* **2012**, *14*, 7856-7860; (d) N. Wang, J. G. Ma,W. Shi, P. Cheng, *CrystEngComm.* **2012**, *14*, 5198-5202; (e) M. D. Zhang, C. M. Di, L. Qin, Q. X. Yang, Y. Z. Li, Z. J. Guo, H. G. Zheng, *CrystEngComm.* **2013**, *15*, 227-230; (f) Z. Zhang, L. Zhang, L. Wojtas, P. Nugent, M. Eddaoudi, M. J. Zaworotko, *J. Am. Chem. Soc.* **2012**, *134*, 924-927; (g) T. Zhao, X. Jing, J. Wang, D. Wang, G. Li, Q. Huo, Y. Liu, *Cryst. Growth & Design* **2012**, *12*, 5456-5461; (h) D. C. Zhong, W. X. Zhang, F. L. Cao, L. Jiang, T. B. Lu, *ChemComm.* **2011**, *47*, 1204-1206; (i) D. F. Sava, T. B. Kravtsov, F. Nouar, L. Wojtas, J. F. Eubank, M. Eddaoudi, *J. Am. Chem. Soc.* **2008**, *130*, 3768-3770.

[3] (a) C. X. Chen, Q. K. Liu, J. P. Ma, Y. B. Dong, *Journal of Materials Chemistry* **2012**, *22*, 9027; (b) F. Guo, F. Wang, H. Yang, X. Zhang, J. Zhang, *Inorg.Chem.* **2012**, *51*, 9677; (c) L. J. Li,X. L. Wang, K. Z. Shao, Z. M. Su, *Inorg.Chem.Comm.* **2012**, *26*, 42; (d) T. W. Tseng, T. T. Luo, S. Y. Chen, C. C. Su, K. M. Chi, K. L. Lu, *Crystal Growth & Design* **2013**, *13*, 510; (e) J. J. Wang, T. L. Hu, X. H. Bu, *CrystEngComm.* **2011**, *13*, 5152; (f) K. A. White, D. A. Chengelis, K. A. Gogick, J. Stehman, N. L. Rosi, S. Petoud, *J. Am. Chem. Soc.* **2009**, *131*, 18069; (g) Y. Yang, P. Du, J. F. Ma, W. Q. Kan, B. Liu, J. Yang, *Cryst. Growth & Design* **2011**, *11*, 5540; (h) X. Zhou, B. Li, G. Li, Z. Qi, Z. Shi, S. Feng, *CrystEngComm.* **2012**, *14*, 4664.

[4] (a) Q. R. Fang, D. Q. Yuan, J. Sculley, W. G. Lu, H. C. Zhou, *Chem. Commun.* **2012**, *48*, 254; (b) Q. R. Fang, G. S. Zhu, Z. Jin, M. Xue, X. Wei, D. J. Wang, S. L. Qiu, *Angew. Chem. Int. Ed.* **2006**, *45*, 6126; (c) L. Hu, P. Zhang, Q. Chen, H. Zhong, X. Hu, X. Zheng, Y. Wang, N. Yan, *Cryst. Growth & Design* **2012**, *12*, 2257; (d) D. F. Sava, V. C. Kravtsov, F. Nouar, L. Wojtas, J. F. Eubank, M. Eddaoudi, *J. Am. Chem. Soc.* **2008**, *130*, 3768; (e) M. Xue, G. Zhu, Y. Li, X. Zhao, Z. Jin, E. Kang, S. Qiu, *Cryst. Growth & Design* **2008**, *8*, 2478; (f) D. C. Zhong, W. X. Zhang, F. L. Cao, L. Jiang, T. B. Lu, *Chem. Commun.* **2011**, *47*, 1204.

[5] (a) S. M. Chen, T. T. Lian, *Inorg. Chem. Comm.* **2011**, *14*, 447; (b) Z. Jin, H. Zhao, D. Yang, X. Yao, G. Zhu, *Inorg. Chem. Comm.* **2012**, *25*, 74; (c) M. M. Wanderley, C. Wang, C. D. Wu, W. Lin, *J. Am. Chem. Soc.* **2012**, *134*, 9050.

[6] (a) A. Rodríguez-Diéguez, R. Kivekäs, E. Colacio, *Chem. Commun.* **2005**, 5228; (b) A. Rodríguez-Diéguez, E. Colacio, *Chem. Commun.* **2006**, 4140; (c) A Rodríguez-Diéguez, A. Salinas-Castillo, S. Galli, N. Masciocchi, J. M. Gutiérrez-Zorrilla, P. Vitoria, E. Colacio, *Dalton Trans.* **2007**, 1821; (d) A. Rodríguez-Diéguez, M. A. Palacios, E. Colacio, *Dalton Trans.* **2008**, 2887; (e) A. Rodríguez-Diéguez, J. Cano, R. Kivekäs, A. Debdoubi, E. Colacio, *Inorg. Chem.* **2007**, *46*, 2503; (f) J. Suárez-Varela, A. J. Mota, H. Aouryaghal, J. Cano, A. Rodríguez-Diéguez, D. Luneau, E. Colacio, *Inorg. Chem.* **2007**, *47*, 8143; (g) A. Rodríguez-Diéguez, A. Salinas-Castillo, J. M. Seco, E. Colacio, *CrystEngComm.* **2010**, *12*, 1876.

[7] (a) Z. P. Demko, K. B. Sharpless, *Angew. Chem. Int. Ed.* **2002**, *41*, 2110; (b) Z. P. Demko, K. B. Sharpless, *J. Org. Chem.* **2001**, *66*, 7945;

(c) Z. P. Demko, K. B. Sharpless, *Angew. Chem. Int. Ed.* **2002**, *41*, 2113.

[8] (a) A. Rodríguez-Diéguez, J. M. Seco, E. Colacio, *Eur. J. Inorg. Chem.* **2012**, 203; (b) J. M. Seco, M. de Araujo-Farias, N. M. Bach, A. B. Caballero, A. Salinas-Castillo, A. Rodríguez-Diéguez, *Inorg.Chim. Acta* **2010**, *363*, 3194; (c) A. J. Calahorro, D. Fairen-Jiménez, A. Salinas-Castillo, M. E. López-Viseras, A. Rodríguez-Diéguez, *Polyhedron* 2013, *doi.org/10.1016/j.poly. 2012.09.018.*

[9] (a) L. Wang, J. Morales, T. Wu, X. Zhao, W. P. Beyermann, X. Bu, P. Feng, *Chem. Commun.* **2012**, *48*, 7498; (b) Q. Wei, D. Yang, T. E. Larson, T. L. Kinnibrugh, R. Zou, N. J. Henson, T. Timofeeva, H. Xu, Y. Zhao, B. R. Mattes, *J. Mater. Chem.* **2012**, *22*, 10166; (c) P. Venkatakrishnan, P. Natarajan, J. N. Moorthy, Z. Lin, T. J. Chow, *Tetrahedron* **2012**, *68*, 7502.

[10] Crystal Data. 1: $[CdC_{14}H_{10}N_4O_3]$, $M = 394.66$, monoclinic, space group *P21/c*, $a = 16.246(3)$, $b = 7.3291(15)$, $c = 10.799(2)$ Å, $\beta = 99.02(3)$, $V = 1269.9(4)$ Å^3, $Z = 4$, $\rho_{calcd} = 2.064$ g cm^{-3}, μ(Mo-$K\alpha$) = 1.74 mm^{-1}, $R_{int} = 0.0997$, $T = 100$ K, $R1(F_o) = 0.0636$, ($wR2(F_o^2) = 0.1309$), GOF= 1.039. Data were collected by ω and ψ scans on a Bruker APEXII diffractometer with graphite-monochromated MoKα radiation (λ = 0.71073 Å). The structures were solved by direct methods and refined on F^2 by the SHELX-97 program. CCDC reference number is 926617.

[11] T. Jiang, Y. F. Zhao, X. M. Zhang, *Inog. Chem. Comm.* **2007**, *10*, 1194.

[12] U. H. F. Bunz, *Chem. Rev.* **2000**, *100*, 1605.

[13] D. C. Zhong, M. Meng, J. H. Deng, X. Z. Luo, Y. R. Xie, *Inog. Chem. Comm.* **2011**, *14*, 1952.

[14] (a) T. Hu, L. Liu, X. Lv, X. Chen, H. He, F. Dai, G. Zhang, D. Sun, *Polyhedron* **2010**, *29*, 296; (b) Y. Qiu, Y. Li, G. Peng, J. Cai, L. Jin, L. Ma, H. Deng, M. Zeller, S.R. Batten, *Cryst. Growth & Design* **2010**, *10*, 1332; (c) J. Tao, Z. J. Ma, R. B. Huang, L. S Zheng, *Inorg. Chem.* **2004**, *43*, 6133.

[15] *Bruker Apex2*, Bruker AXS Inc, Madison, Wisconsin, USA, 2004.

[16] G. M. Sheldrick, *SADABS, Program for Empirical Adsorption Correction*, Institute for Inorganic Chemistry, University of G¨ ottingen, Germany, 1996.

[17] A. Altomare, M. C. Burla, M. Camilla, G. L. Cascarano, C. Giacovazzo, A. Guagliardi, A. G. G. Moliterni, G. Polidori and R. Spagna, *J. Appl. Crystallogr*, **1999**, *32*, 115.

[18] G. M. Sheldrick, *SHELX97, Program for Crystal Structure Refinement*, University of Göttingen, Göttingen, Germany, 1997.

Entry for the Table of Contents ((Please choose one layout.))

Layout 1:

((Key Topic))

We have been successful in the synthesis of the first Metal-Organic-Frameworks with the novel 4'-tetrazolate-4-biphenyl carboxylate Spacer. The compound is a three-dimensional structure with small channels that shows an intense blue-green photoluminescence emission at room temperature in the solid state. To the best our knowledge, this is the first time that a coordination compound has been synthesized with this ligand.

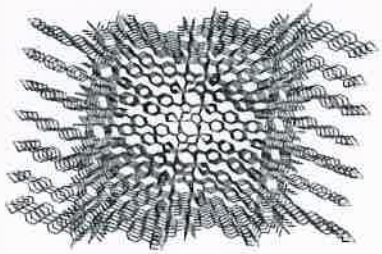

Antonio J. Calahorro, Guillermo Zaragoza, Alfonso Salinas-Castillo, Jose M. Seco and Antonio Rodríguez-Diéguez

UNIQUE METAL-ORGANIC-FRAMEWORK WITH BASED ON 4'-TETRAZOLATE-4-BIPHENYL CARBOXYLATE SPACER: BLUE-GREEN PHOTOLUMINESCENCE.

Keywords: Metal-Organic Framework / Hydrothermal / Photoluminescence